UNIVERSIDADE ESTADUAL DE CAMPINAS
FACULDADE DE ENGENHARIA QUÍMICA
ÁREA DE CONCENTRAÇÃO:
DESENVOLVIMENTO DE PROCESSOS QUÍMICOS

SIMULAÇÃO DE COLUNAS DE DESTILAÇÃO CONVENCIONAL, EXTRATIVA E AZEOTRÓPICA NO PROCESSO DE PRODUÇÃO DE BIOETANOL ATRAVÉS DA MODELAGEM DE NÃO EQUILÍBRIO E DA MODELAGEM DE ESTÁGIOS DE EQUILÍBRIO COM EFICIÊNCIA

Autora: Tassia Lopes Junqueira
Orientador: Prof. Dr. Rubens Maciel Filho
Co-orientadora: Prof.ª Dra. Maria Regina Wolf Maciel

Dissertação de Mestrado apresentada à Faculdade de Engenharia Química como parte dos requisitos exigidos para a obtenção do título de Mestre em Engenharia Química.

Campinas - São Paulo
Março de 2010

FICHA CATALOGRÁFICA ELABORADA PELA
BIBLIOTECA DA ÁREA DE ENGENHARIA E ARQUITETURA - BAE - UNICAMP

Junqueira, Tassia Lopes
J968s Simulação de colunas de destilação convencional, extrativa e azeotrópica no processo de produção de bioetanol através da modelagem de não equilíbrio e da modelagem de estágios de equilíbrio com eficiência / Tassia Lopes Junqueira. --Campinas, SP: [s.n.], 2010.

Orientadores: Rubens Maciel Filho, Maria Regina Wolf Maciel.
Dissertação de Mestrado - Universidade Estadual de Campinas, Faculdade de Engenharia Química.

1. Bioetanol. 2. Separação (Tecnologia). 3. Destilação - Modelos matemáticos. 4. Termodinâmica de sistemas em não-equilíbrio. 5. Simulação por computador. I. Maciel Filho, Rubens. II. Maciel, Maria Regina Wolf. III. Universidade Estadual de Campinas. Faculdade de Engenharia Química. IV. Título.

Título em Inglês: Simulation of conventional, extractive and azeotropic distillation for bioethanol production process using nonequilibrium model and equilibrium stage model with efficiency
Palavras-chave em Inglês: Bioethanol, Separation (Technology), Distillation - Mathematical models, Non-equilibrium thermodynamics, Computer simulation
Área de concentração: Desenvolvimento de Processos Químicos
Titulação: Mestre em Engenharia Química
Banca examinadora: Antonio Maria Francisco Luiz Jose Bonomi, Carlos Eduardo Vaz Rossell, Mario Eusébio Torres Alvarez
Data da defesa: 02/03/2010
Programa de Pós Graduação: Engenharia Química

Dissertação de Mestrado defendida por Tassia Lopes Junqueira e aprovada em 02 de março de 2010 pela banca examinadora constituída pelos doutores:

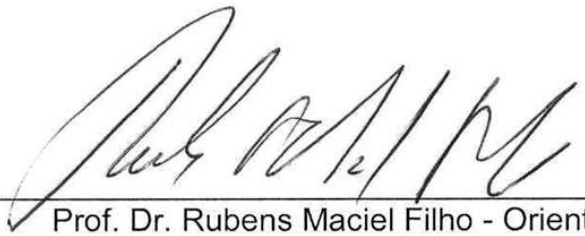

Prof. Dr. Rubens Maciel Filho - Orientador

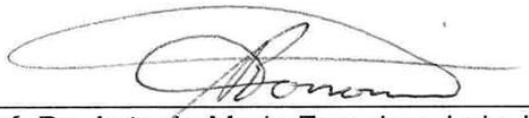

Prof. Dr. Antonio Maria Francisco Luiz Jose Bonomi

Prof. Dr. Carlos Eduardo Vaz Rossell

Dr. Mario Eusébio Torres Alvarez

Este exemplar corresponde à versão final da Dissertação de Mestrado em Engenharia Química.

Prof. Dr. Rubens Maciel Filho

Aos meus pais, Roberto e Mara,
pelo amor, compreensão e incentivo,
dedico este trabalho.

Agradecimentos

É difícil demonstrar com palavras toda a gratidão que sinto por todos aqueles que estiveram ao meu lado ao longo desta etapa tão importante da minha vida, seja para suporte ao meu trabalho, seja para incentivo pessoal. Agradeço verdadeiramente a todos. Em especial, meus agradecimentos:

A Deus que me guiou e me iluminou para seguir em frente independente de qualquer dificuldade.

Aos meus pais, Roberto e Mara, por acreditarem em minha capacidade e investirem em mim amor, tempo e esforços. À minha mãe agradeço ainda por me ouvir incansavelmente, ajudando-me em cada decisão.

Aos meus irmãos, João Gustavo, Roberta e Maira, por todo o apoio e carinho.

Ao meu namorado Raphael, pelo amor, incentivo e paciência e por estar sempre ao meu lado.

Aos professores Rubens Maciel Filho e Maria Regina Wolf Maciel, pela orientação, incentivo, dedicação e amizade ao longo deste trabalho.

Aos meus amigos, Carlos e Cecilia, pela amizade e nossos inesquecíveis almoços.

À Marina pela ajuda no desenvolvimento deste trabalho e pela grande amizade.

Ao Daniel pelas proveitosas discussões e por estar sempre disposto a ajudar. E aos funcionários do CTC pelas colaborações a este trabalho.

À Usina da Pedra e seus funcionários pela recepção e dados fornecidos para a execução deste trabalho.

Aos colegas do LOPCA/LDPS e à Cristiane e à Mara do LDPC.

Aos funcionários e professores da Faculdade de Engenharia Química da Unicamp.

À FAPESP pelo apoio financeiro.

“Nunca duvide que um pequeno grupo de
pessoas determinadas possa mudar o mundo.
De fato, foi sempre assim que o mundo mudou”
Margaret Mead

“Se você acha que pode fazê-lo, isto é confiança.
Se você o fizer, isto é competência"
Ken Blanchard

Resumo

No Brasil, o bioetanol é usado para substituir a gasolina, compondo uma porcentagem desta ou sendo usado como combustível alternativo. Esta tendência de substituição dos combustíveis fósseis vem se fortalecendo em âmbito global, sendo necessárias, portanto, alternativas e propostas que viabilizem o aumento da produção de forma economicamente e ambientalmente sustentável. Neste contexto, a otimização energética do processo de separação do bioetanol visa à disponibilização de bagaço de cana-de-açúcar, usado como combustível na geração de vapor de processo, para a produção de bioetanol através do processo de hidrólise. Para tanto, inovações ao processo são essenciais e melhoramento na representação de modelos torna-se necessário para estudos e avaliações.

Neste trabalho, simulações da etapa de destilação para a produção de álcool hidratado assim como da etapa de desidratação do bioetanol foram realizadas utilizando o simulador Aspen Plus®. Visando um estudo dentro de um cenário mais realista, a modelagem de estágios de não equilíbrio foi utilizada para prever o comportamento das colunas de destilação envolvidas. Além disso, o uso da correlação de Barros e Wolf para a determinação de eficiência na modelagem de estágios de equilíbrio em colunas de destilação foi avaliado.

A comparação entre as modelagens de estágios de equilíbrio e não equilíbrio para as destilações convencional e extrativa indicou que a associação da correlação de eficiência de Barros e Wolf à modelagem de estágios de equilíbrio fornece predições satisfatórias tendo como referência a modelagem de estágios de não-equilíbrio. Para a destilação azeotrópica, o estudo de formação de duas fases líquidas na coluna foi realizado, indicando que os parâmetros de processo, como posição de alimentação, possuem influência significativa.

O estudo da fermentação extrativa a vácuo, como configuração alternativa às etapas de fermentação e concentração, revelou seu potencial para redução do consumo de energia na etapa de destilação subseqüente, sendo uma alternativa viável para intensificação de processos.

Palavras-chave: Bioetanol, Separação, Destilação, Não-equilíbrio, Simulação

Abstract

In Brazil, bioethanol is used to replace gasoline, being a percentage of this or used as an alternative fuel. This trend of replacing fossil fuels has gained strength globally, necessitating, therefore, alternatives and proposals to enable the increase of production in an economically and environmentally sustainable way. In this context, the energy optimization of the bioethanol separation aims the provision of sugarcane bagasse, used as fuel in process steam generation, for bioethanol production through the hydrolysis process. Consequently, innovations to the process are essential and improvement in the representation of models is required for studies and evaluations.

In this work, simulations of the distillation step for the production of hydrous bioethanol and the bioethanol dehydration were performed using the simulator Aspen Plus®. In order to study a more realistic scenario, nonequilibrium stage model was used to predict the behavior of the involved distillation columns. Furthermore, the use of Barros and Wolf correlation for the determination of efficiency in equilibrium stage model for distillation columns was evaluated.

The comparison between equilibrium and nonequilibrium stage models for conventional and extractive distillation processes indicated that the association between Barros and Wolf efficiency correlation and equilibrium stage model provides satisfactory predictions considering the nonequilibrium stage model as reference. For azeotropic distillation, formation of two liquid phases inside the column was studied, indicating that process parameters, such as feed position, have significant influence.

The study of vacuum extractive fermentation, as an alternative configuration to fermentation and concentration steps, showed its potential for reducing energy consumption in the subsequent distillation step, and it seems a viable alternative to process intensification.

Keywords: Bioethanol, Separation, Distillation, Nonequilibrium, Simulation

Sumário

Lista de Figuras

Lista de Tabelas

Nomenclatura

Letras Latinas

D	Difusividade, [m^2 s^{-1}]
i	Indica o estágio
I	Interface
j	Indica o componente
k	Condutividade térmica, [W m^{-1} K^{-1}]
L	Fase líquida
T	Temperatura, [ºC]
V	Fase vapor
x	Fração molar na fase líquida
y	Fração molar na fase vapor

Letras Gregas

μ	Viscosidade, [Pa s]
η	Eficiência de Murphree
ρ	Massa específica, [kg m^{-3}]

Siglas, Abreviações e Definições

AEAC/AE	Álcool etílico anidro carburante
AEHC/HE	Álcool etílico hidratado carburante
CFD	Fluidodinâmica Computacional
comp	Componente
Cp	Capacidade calorífica, [J $kmol^{-1}$ K^{-1}]

EC	Coluna de Destilação Extrativa
Eff	Eficiência
HMF	5-hydroxymethyl-furfural
HOC	Correlação de Hayden-O'Connell
HyPol	Polímeros altamente ramificados
IL	Líquidos iônicos
MEG / EG	Monoetilenoglicol
MW	Massa molecular, [kg $kmol^{-1}$]
nc	Número de componentes
NRTL	*Non-Random Two-Liquid*, modelo para o cálculo de coeficiente de atividade
RC	Coluna de recuperação de solvente
UNIFAC	*UNIQUAC Functional-group Activity Coefficient*, método de cálculo de coeficiente de atividade
UNIQUAC	*Universal Quasi-Chemical*, modelo para o cálculo de coeficiente de atividade
VLE	Equilíbrio líquido-vapor

Capítulo 1
Introdução e Objetivos

1.1. Introdução

Devido às atuais preocupações acerca do aquecimento global e aos novos contratos internacionais de produção de bioetanol, espera-se que a indústria alcooleira seja um dos propulsores da economia brasileira nos próximos anos. Embora a produção em grande escala deste combustível já dure mais de 30 anos, melhorias no processo devem ser buscadas para que o Brasil não perca a posição que ocupa no cenário mundial com relação à produção de bioetanol (segundo maior produtor mundial e maior exportador).

Além disso, a introdução dos veículos com motores bicombustíveis na frota brasileira aumentou consideravelmente a demanda de álcool combustível. Neste contexto, dois grandes desafios foram originados: manter os preços competitivos frente à gasolina e motivar os produtores de álcool e açúcar a priorizar a produção de bioetanol e assim manter o estoque deste e, consequentemente, os preços atraentes no momento da escolha do combustível a ser abastecido.

Dessa forma, para atender à demanda nacional e mundial, o Brasil necessita aumentar a sua produção de bioetanol e também diminuir os custos de produção. Diferentemente dos Estados Unidos, o Brasil possui grande potencial para atingir estes objetivos, uma vez que, além de utilizar a matéria-prima mais eficiente (cana-de-açúcar), apresenta excesso de bagaço e palha. Estes subprodutos podem ser utilizados na produção de vapor e energia elétrica através da queima em caldeiras, permitindo que as usinas sejam auto-suficientes em energia elétrica e, nos casos de utilização de sistemas eficientes de cogeração, vendam energia elétrica às concessionárias.

Outra vantagem competitiva do país é sua grande disponibilidade de áreas apropriadas para o cultivo de cana-de-açúcar, sendo possível a expansão agrícola sem afetar áreas ambientalmente preservadas e sem ocorrer competição com a agricultura de alimentos.

Adicionalmente, novos desenvolvimentos no processo de produção de bioetanol como a viabilização da hidrólise de materiais lignocelulósicos (por exemplo, o bagaço e a palha da cana) para produção de álcool de segunda geração e novas rotas de produção como a conversão de gás de síntese em bioetanol vêm sendo investigados no país.

Vale ressaltar que, independentemente da rota utilizada para a obtenção de bioetanol, o bioetanol é obtido em baixas concentrações, geralmente diluído em água e co-produtos, sendo assim as etapas de concentração e desidratação são de grande importância no processo de produção de bioetanol. Com esta finalidade são comumente empregadas colunas de destilação, cujas variáveis operacionais influenciam fortemente no consumo de vapor de processo. Como consequência da redução no consumo de vapor, menos bagaço de cana-de-açúcar precisa ser queimado a fim de fornecer energia à planta, aumentando, portanto, a quantidade de bagaço disponível para a cogeração de energia elétrica e para o processo de produção de álcool de segunda geração, que possibilita o aumento de produção sem acrescer a área plantada.

Além da aplicação como combustível, o bioetanol também pode ser utilizado como matéria-prima na produção de diferentes produtos químicos produzidos normalmente a partir de derivados de petróleo, como o eteno. O aumento nos preços do petróleo motiva também o desenvolvimento de rotas de produção alternativas para este e outros petroquímicos básicos, sendo a alcoolquímica uma alternativa cada vez mais atraente (Dias, 2008).

1.2. Objetivos

Diante da variada gama de utilização do bioetanol, o aumento da produção, sem acrescer proporcionalmente as áreas de cultivo, é um grande desafio. Portanto, a melhoria da eficiência do processo de produção de bioetanol é essencial e o estudo de cada etapa do processo é necessário.

Neste contexto, o objetivo geral deste trabalho é a simulação das etapas de concentração e desidratação do processo de produção de bioetanol, de forma mais realista possível, através do simulador Aspen Plus®. Para tanto, a

modelagem de estágios de não equilíbrio é empregada e sua comparação à modelagem de estágios de equilíbrio serve como base para o estabelecimento de uma metodologia mais confiável para prever a eficiência de estágio.

Assim, foram determinados os seguintes objetivos específicos:

- definição do modelo termodinâmico mais representativo do sistema;
- simulação dos processos de destilação convencional e extrativa utilizando a modelagem de estágios de equilíbrio, aplicação da correlação de eficiência e modelagem de estágios de não equilíbrio;
- simulação da destilação azeotrópica visando à diminuição da região de duas fases líquidas no interior da coluna;
- proposição de configuração alternativa para o processo de destilação.

1.3. Estrutura da Dissertação

Esta dissertação é dividida em 11 capítulos da seguinte forma:

No Capítulo 2, a revisão da literatura é apresentada, sendo salientada a importância do bioetanol como combustível e apresentada a descrição do processo de produção de bioetanol. São também abordadas as modelagens para colunas de destilação bem como os conceitos e correlações de eficiência.

No Capítulo 3 é apresentada uma revisão dos processos de separação atualmente empregados no processo de produção de bioetanol bem como dos recentes desenvolvimentos nesta área.

A caracterização termodinâmica do sistema é apresentada no Capítulo 4. Neste capítulo são avaliados modelos de coeficiente de atividade para a fase líquida através da comparação com dados experimentais de equilíbrio líquido-vapor e líquido-líquido dos binários presentes no sistema.

Resultados das simulações utilizando modelagens de estágios de equilíbrio, não equilíbrio e equilíbrio com eficiência são apresentados e comparados no Capítulo 5 para o processo de destilação convencional empregado para a produção de álcool hidratado.

No Capítulo 6, modelagens de estágios de equilíbrio, não equilíbrio e equilíbrio com eficiência são aplicadas para a simulação do processo de destilação extrativa com monoetilenoglicol.

No Capítulo 7, simulações em conjunto das destilações convencional e extrativa utilizando modelagem de estágios de equilíbrio e aplicação de correlações de eficiência são apresentadas.

No Capítulo 8, diferentes configurações do processo de destilação azeotrópica com cicloexano são avaliadas e otimizadas a fim de minimizar a formação de duas fases líquidas na coluna, as perdas de produto e a demanda energética.

Alternativas para as etapas de fermentação e destilação são apresentadas no Capítulo 9. São apresentadas simulações do processo alternativo de fermentação acoplado a diferentes configurações de destilação (convencional, duplo e triplo efeito).

Análise geral dos resultados apresentados nesta dissertação é realizada no Capítulo 10, de forma a comparar os diferentes processos estudados.

Finalmente, no Capítulo 11 são apresentadas as conclusões obtidas neste trabalho bem como sugestões para trabalhos futuros.

Nesta dissertação de mestrado, o desenvolvimento dos capítulos apresenta-se através de trabalhos submetidos, aceitos e/ou publicados em anais de congressos, além de artigos a serem submetidos a periódicos.

Capítulo 2
Revisão da Literatura

2.1. Etanol Combustível

O uso de energia renovável tem sido visto como uma solução para as questões relacionadas à poluição atmosférica e à escassez dos combustíveis fósseis. Dessa forma, a conversão de biomassa em biocombustíveis representa uma importante opção para aproveitamento de um recurso alternativo de energia e para a redução da emissão de gases poluentes, principalmente de gás carbônico.

Atualmente, dois tipos de biocombustíveis são produzidos em larga escala: bioetanol e biodiesel. A maior parte do bioetanol é produzida a partir de milho nos Estados Unidos e de cana-de-açúcar no Brasil, enquanto menores quantidades são obtidas na Europa tendo como matéria-prima o trigo e a beterraba. O biodiesel é predominantemente produzido a partir de óleo de canola na Europa, de palma na Ásia e de soja no Brasil (Goldemberg, 2008).

A adição de bioetanol à gasolina eleva o teor de oxigênio desta e, consequentemente, permite uma melhor oxidação dos hidrocarbonetos e reduz a quantidade de gases poluentes liberados para a atmosfera (Alzate e Toro, 2006). Além disso, o bioetanol pode ser usado em substituição à gasolina, sendo que sua combustão gera emissões de hidrocarbonetos menos tóxicas do que as da gasolina, pois possuem menor reatividade atmosférica (Goldemberg et al., 2008a).

A fim de avaliar as vantagens em substituir a gasolina por bioetanol, alguns estudos apresentam a análise do ciclo de vida do bioetanol. Balanços de energia e de emissões de gases do efeito estufa mostraram-se bastante favoráveis para o bioetanol derivado de cana-de-açúcar produzido no Brasil, mesmo quando este é exportado para outros países (Goldemberg et al., 2008a).

No Brasil, o incentivo à produção de bioetanol iniciou-se na década de 70. Com o Proálcool, programa de forte cunho estatal, o país tornou-se o maior produtor de bioetanol do mundo até início de 2000, quando os Estados Unidos ultrapassaram o Brasil. Isto porque com o objetivo primário de reduzir a dependência estrangeira de derivados de petróleo e diminuir a emissão de gases

responsáveis pelo efeito estufa, os Estados Unidos impulsionaram de forma expressiva o mercado mundial de bioetanol. No entanto, o Brasil continua sendo o maior exportador mundial, uma vez que sua produção gera excedentes que podem ser direcionados a outros países e também por possuir os menores custos de produção (Souza, 2006).

Basicamente, o álcool combustível pode ser utilizado em duas formas: anidro e hidratado; ambos são combustíveis usados em veículos de passeio e comerciais leves, mas diferem quanto a sua forma de utilização. O álcool anidro, ou álcool etílico anidro carburante (AEAC), é praticamente puro, com um teor alcoólico entre 99,3 e 99,8 %. É utilizado como um aditivo que aumenta o teor de oxigenados na gasolina. No Brasil, a porcentagem de álcool anidro na mistura pode variar entre 20 e 25 %. O álcool hidratado, ou álcool etílico hidratado carburante (AEHC), com teor entre 92,6 e 93,8 % em massa de etanol (BRASIL, 2005), pode ser utilizado diretamente em motores movidos a álcool ou bicombustíveis (*flex-fuel*). Os veículos com motores flexíveis foram introduzidos no mercado em março de 2003 e permitem o abastecimento, na sua totalidade, com álcool hidratado ou gasolina, ou ainda, com qualquer teor de mistura desses combustíveis (Scandiffio, 2005).

A Figura 2.1 apresenta a produção de álcool combustível no Brasil nos últimos dez anos, utilizando dados fornecidos por MAPA (2009).

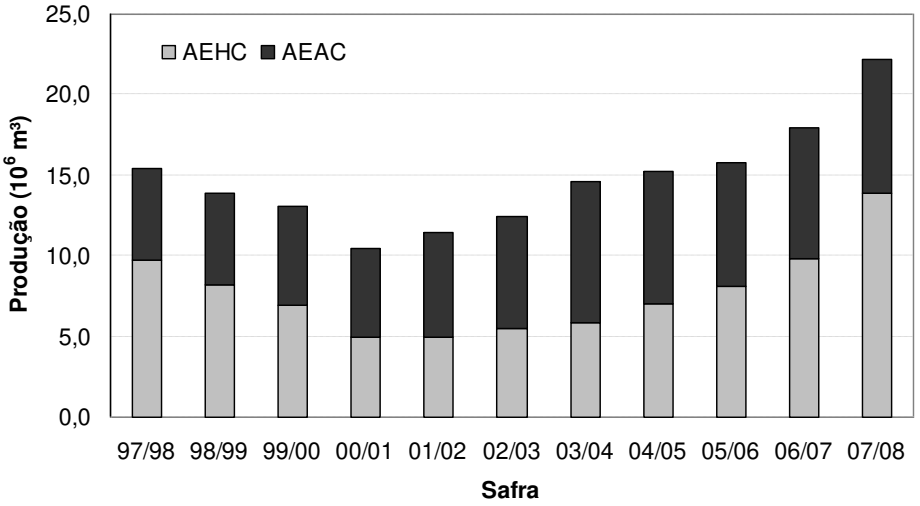

Figura 2.1. Produção brasileira de etanol combustível entre as safras de 1997/98 e 2007/08.

Observa-se que, a partir de 2003, em decorrência do lançamento dos veículos *flex-fuel,* a produção de álcool hidratado tem aumentado significativamente, superando a produção de álcool anidro desde 2005/06. A produção total de álcool na safra de 2007/08, máxima no período compreendido, foi de 22,2 milhões de metros cúbicos.

Além do grande potencial como combustível, o bioetanol possui diversas aplicações nos setores farmacêutico, alimentício e químico, entre outros. A partir de bioetanol é possível obter acetaldeído de alta qualidade, ácido acético, acetato de etila, etileno e, a partir destes, uma grande variedade de produtos químicos, incluindo polímeros (Rivera et al., 2008). Dessa forma, a utilização do bioetanol como matéria-prima na produção de diferentes produtos químicos, produzidos normalmente a partir de derivados do petróleo, surge como uma alternativa cada vez mais atraente, principalmente por ser uma tecnologia sustentável, seguindo a tendência da Engenharia Verde (*Green Process Engineering*).

2.2. Processo de Obtenção do Bioetanol

No Brasil, a matéria-prima empregada para a produção de bioetanol é a cana-de-açúcar. Altamente eficiente e com baixo custo, o bioetanol de cana-de-açúcar é uma das melhores opções para mitigar as emissões de gases de efeito estufa decorrentes da queima de combustíveis fósseis (Goldemberg et al., 2008b). Além disso, a cogeração de energia a partir do bagaço de cana permite que as usinas sejam auto-suficientes em energia térmica e elétrica, além da possibilidade de venda da eletricidade excedente (Ensinas, 2008).

Alternativamente ao uso do caldo de cana-de-açúcar, podem ser utilizados para a produção de bioetanol outros recursos biológicos, como cultivos ricos em energia (como o milho) ou de biomassa lignocelulósica, os quais requerem o condicionamento ou pré-tratamento da matéria-prima para que os organismos de fermentação convertam esta em etanol (Cardona e Sánchez, 2007). A chamada biomassa lignocelulósica inclui resíduos agriculturais, agroindustriais, industriais (processamento de alimentos e outros) e resíduos sólidos municipais. Dessa forma, é uma matéria-prima bastante abundante, presente em materiais como:

bagaço de cana-de-açúcar, lascas de madeira, serragem, resíduos de papéis e capim (Alzate e Toro, 2006).

A utilização do bagaço de cana como matéria-prima tem como vantagem sua disponibilidade nas usinas e o aproveitamento de parte da infra-estrutura já existente nestas (fermentação e separação). O bagaço da cana-de-açúcar é composto principalmente pelos polímeros de carboidratos lignina (cerca de 20 %), celulose (40 %) e hemicelulose (38 %) (IPT, 2000). Para a produção de bioetanol é necessário transformar os polímeros em carboidratos fermentescíveis. A fração hemicelulósica é facilmente convertida a pentoses e hexoses, mas no caso da celulose é necessário realizar um tratamento prévio (Zaldivar et al., 2001), utilizando-se um solvente para dissolver a lignina, permitindo assim a conversão da celulose a hexoses utilizando catalisadores ácidos (hidrólise ácida) ou enzimáticos (hidrólise enzimática). A hidrólise do bagaço permite o aumento significativo da produção de bioetanol sem o aumento da área plantada de cana-de-açúcar.

O processo de produção de bioetanol anidro é apresentado através de diagrama de blocos na Figura 2.2, extraído de Dias (2008), que realizou a simulação da produção de bioetanol a partir do caldo e do bagaço da cana-de-açúcar, visando o levantamento do consumo de energia destes processos.

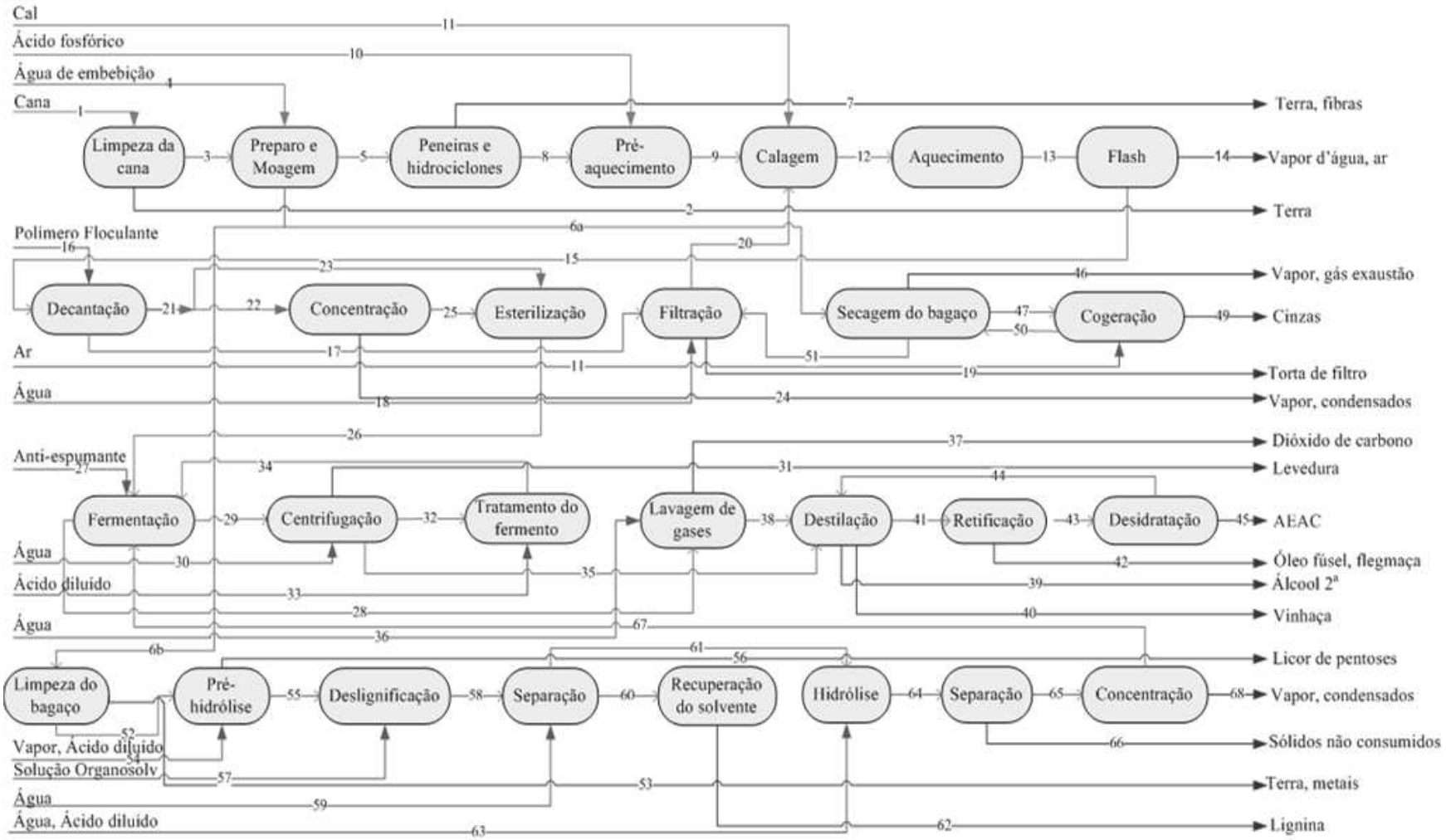

Figura 2.2. Diagrama de blocos do processo de produção de etanol anidro a partir do caldo e do bagaço da cana-de-açúcar (Dias, 2008).

Dentre as etapas indicadas na Figura 2.2, neste trabalho são abordadas a fermentação, a destilação e a desidratação, cujas descrições são apresentadas a seguir.

2.2.1. Fermentação

A fermentação alcoólica consiste em uma série de reações químicas catalisadas por um microorganismo, a levedura *Saccharomyces cerevisiae*. Essa levedura é um aeróbio facultativo, isto é, pode se ajustar metabolicamente a condições de aerobiose e anaerobiose. Enquanto porções de açúcar são transformadas em biomassa (reprodução celular), H_2O e CO_2 em condições aeróbias, a maior parte é convertida em etanol e CO_2 em condições anaeróbias (Lima et al., 2001). O produto da fermentação, denominado vinho, deve conter entre 8 e 12 % (em massa) de etanol. Para obter um vinho final de graduação elevada, é necessária uma fermentação estável com fermento ativo, livre de inibição, infecção e floculação. Além disso, tem-se que a temperatura em que é conduzida a fermentação representa uma etapa crítica do processo fermentativo, pois temperaturas elevadas afetam o comportamento da levedura e diminuem o teor alcoólico do vinho (Dias, 2008).

Os vinhos geralmente contêm impurezas de natureza gasosa (principalmente CO_2), sólidas (células de levedura, bactérias contaminantes, sais minerais, açúcares não-fermentados e outras impurezas) e líquidas (álcool amílico, isoamílico, propílico, isobutílico, glicerol, aldeídos, ácidos, furfural, ésteres e ácidos orgânicos).

Simplificadamente, pode-se assumir a conversão de sacarose em glicose e frutose (Equação 2.1) e a posterior conversão destes açúcares redutores em etanol e gás carbônico (Equação 2.2). Além disso, a formação de co-produtos como ácido acético e glicerol pode ser descrita pela Equação 2.3 (Franceschin et al., 2008).

$$C_{12}H_{22}O_{11} + H_2O \rightarrow 2\ C_6H_{12}O_6 \qquad (2.1)$$

$$C_6H_{12}O_6 \rightarrow 2\ C_2H_5OH + 2\ CO_2 \qquad (2.2)$$

$$2\ C_6H_{12}O_6 + H_2O \rightarrow C_2H_4O_2 + 2\ C_3H_8O_3 + C_2H_5OH + 2\ CO_2 \qquad (2.3)$$

2.2.2. Destilação

A destilação consiste na separação, mediante vaporização, de misturas líquidas de substâncias voláteis miscíveis nos seus componentes individuais, ou em grupos de componentes. A sua integração com outros processos, como a pervaporação, e a possibilidade de se trabalhar com altas quantidades de forma contínua tornam o processo de separação por destilação o preferido nas indústrias químicas e petroquímicas. Além disso, o uso da destilação proporciona um considerável aumento no valor agregado dos produtos e possibilita o cumprimento das exigências cada vez mais restritas do mercado, quer seja em termos econômicos, quer seja na minimização da geração de poluentes (Noriler, 2003). Apesar dos significantes avanços de processos alternativos de separação, como a peneira molecular, a destilação ainda é operação mais utilizada, especialmente devido à sua flexibilidade e à possibilidade de trabalhar com altas vazões sem necessitar de procedimentos de regeneração que trazem complicações adicionais em escala industrial.

No caso da indústria sucroalcooleira, a separação do sistema etanol-água é objetivo de grande interesse. Este sistema constitui uma mistura não ideal, pois os seus componentes formam um azeótropo com composição molar de aproximadamente 89 % etanol e 11 % água a 1 atm (Vasconcelos, 1999). Vale ressaltar que azeótropo é uma mistura de componentes que possui a mesma concentração nas fases líquida e vapor no equilíbrio, não sendo possível a separação dos componentes por destilação convencional.

Dessa forma, tem-se que na unidade de destilação é utilizado um processo de destilação convencional que realiza a concentração da mistura até pontos próximos do azeótropo (entre 92,6 e 93,8 %, em massa).

A configuração normalmente empregada nas usinas brasileiras inclui 5 colunas: A, A1, D, B e B1, sendo a coluna A conhecida como coluna de esgotamento do vinho, A1 de epuração do vinho e D de concentração de álcool de segunda. No álcool de segunda, concentram-se os componentes mais voláteis, conhecidos como produtos de cabeça, sendo necessária a sua retirada a fim de evitar a contaminação do álcool hidratado. Estas três colunas formam o que é

chamado de conjunto de destilação, enquanto a coluna B (de retificação) e a coluna B1 (de esgotamento) compõem o conjunto de retificação, onde é obtido o AEHC através da concentração das flegmas vapor e líquida retiradas das colunas A e D, respectivamente (Meirelles, 2006). O esquema simplificado desta configuração é apresentado na Figura 2.3.

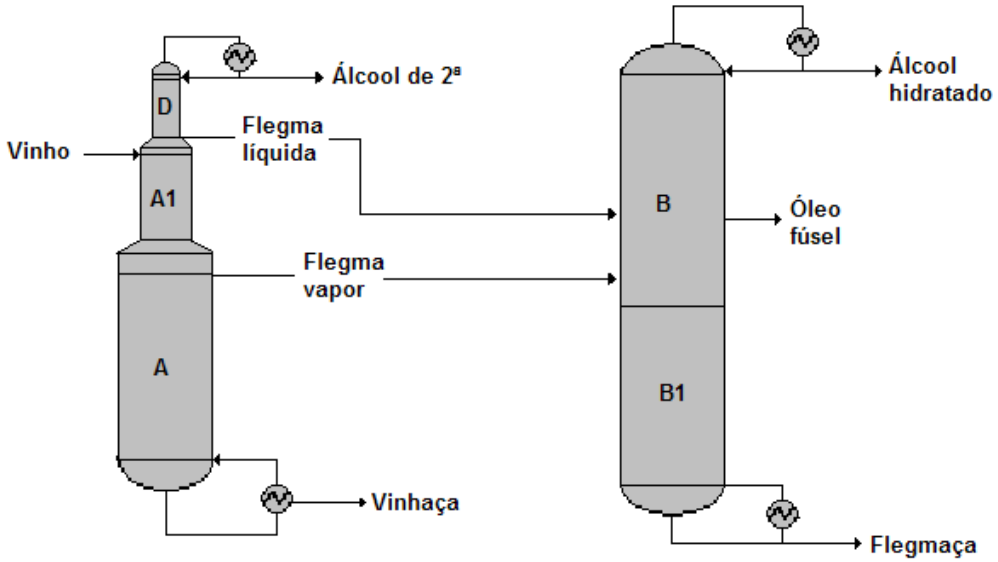

Figura 2.3. Configuração usual da destilação no processo de produção de bioetanol.

Como se pode observar na Figura 2.3, a alimentação do vinho é realizada no topo da coluna A1, cuja função é eliminar substâncias mais voláteis e gases contaminantes. O vapor produzido nesta coluna é encaminhado ao fundo da coluna D, e o produto de fundo desce diretamente à coluna A.

Na coluna A, o produto de fundo da coluna A1 é esgotado no fundo, produzindo a vinhaça, que é rica em água e deve possuir teor alcoólico menor do que 0,02 %. Na coluna A, próximo ao topo também há uma retirada lateral na fase vapor, denominada flegma vapor, que é encaminhada ao conjunto de retificação.

A coluna D recupera em seu topo os componentes mais voláteis, formando o álcool de segunda, enquanto no fundo é obtida a flegma líquida, a qual também é alimentada ao conjunto de retificação.

No conjunto de retificação, formado pelas colunas B e B1 de mesmo diâmetro, as flegmas líquida e vapor são concentradas, sendo o álcool hidratado

produzido no topo. Em alguns casos, quando há componentes mais voláteis do que o etanol no topo, é usual realizar-se a retirada de AEHC na fase vapor presente no primeiro prato. No fundo da coluna B1, obtém-se a flegmaça, que é uma mistura com alto teor de água e deve conter no máximo 0,02 % etanol (base mássica). Na coluna B ainda pode-se retirar óleo fúsel que é composto por alcoóis de cadeia longa como o álcool isoamílico.

Vale ressaltar que esta configuração é utilizada há muitos anos e não foi originalmente projetada para este processo, mas adaptada para a produção de álcool combustível. Sendo assim, configurações otimizadas e mais adequadas a este processo são utilizadas em algumas destilarias.

2.2.3. Desidratação

Para a finalidade de produzir álcool anidro, álcool hidratado é concentrado a pelo menos 99,3 % de etanol (em massa), sendo, portanto, necessários processos complementares à destilação convencional, uma vez que esta, devido ao azeótropo formado, não é capaz de obter a mistura etanol-água na especificação desejada. Dessa forma, processos de desidratação tais como destilação azeotrópica com cicloexano, destilação extrativa com monoetilenoglicol e adsorção em peneiras moleculares são comumente empregados na indústria alcooleira.

Destilação azeotrópica

A destilação azeotrópica (ou azeotrópica heterogênea) consiste na adição de um terceiro componente, chamado componente de arraste, com a finalidade de formar um novo azeótropo com um ou mais dos componentes presentes inicialmente na mistura. O novo azeótropo formado deve ser heterogêneo, de modo a provocar a formação de duas fases líquidas após condensação da corrente de vapor. O novo azeótropo formado é retirado no topo (azeótropo de mínimo) ou no fundo (azeótropo de máximo) da coluna, enquanto um dos componentes da mistura original é obtido puro na outra extremidade da coluna. Uma segunda coluna deve ser utilizada para recuperação do componente de arraste (Brito, 1997).

Durante muitos anos, foi utilizado o benzeno como componente de arraste na separação do sistema etanol-água (Ito, 2002). Entretanto, como o benzeno é um composto potencialmente cancerígeno, sua utilização foi proibida. Atualmente, a maior parte das usinas que utilizavam o processo de destilação azeotrópica com benzeno como componente de arraste utiliza o cicloexano, sendo possível a utilização da infra-estrutura existente.

Uma das possíveis configurações da destilação azeotrópica é ilustrada pela Figura 2.4.

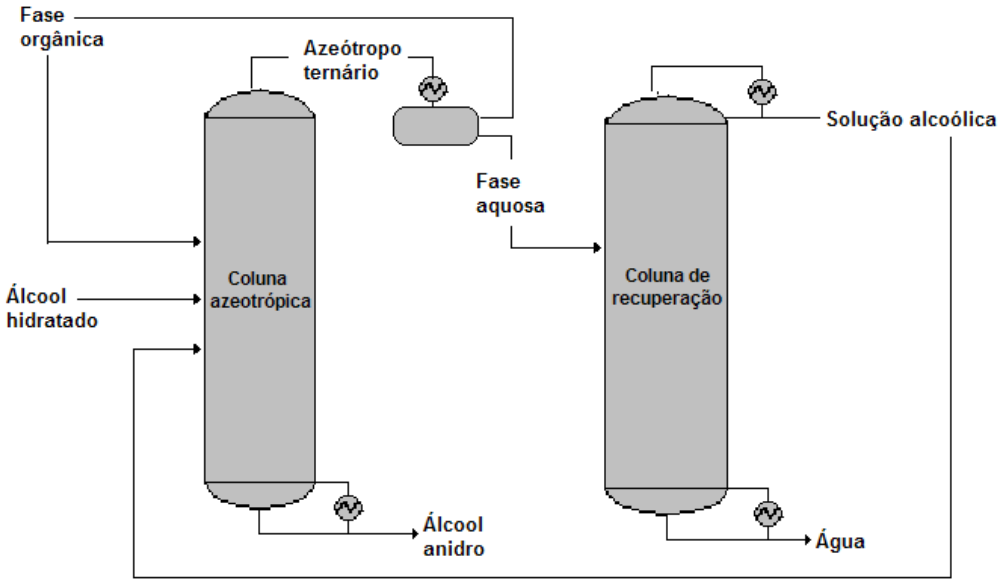

Figura 2.4. Configuração da destilação azeotrópica para produção de bioetanol anidro (adaptado de Vasconcelos, 1999).

Na primeira coluna, álcool anidro é produzido no fundo, enquanto uma mistura azeotrópica de etanol, água e cicloexano sai no topo da coluna. Esta mistura é condensada e resfriada e, então, é alimentada em um decantador, no qual ocorre a formação de duas fases líquidas: orgânica e aquosa. A fase orgânica, rica em cicloexano, é reciclada para a primeira coluna, enquanto a aquosa é encaminhada à coluna de recuperação. Nesta coluna, água é recuperada no fundo, enquanto a solução alcoólica, obtida no topo, é realimentada na coluna azeotrópica. Em alguns casos, é necessária a reposição do componente de arraste, devido a perdas de cicloexano no álcool anidro.

Outras configurações podem ser encontradas na literatura como, por exemplo, a configuração descrita por Meirelles (2006) e Mortaheb e Kosuge (2004). Na configuração reportada por Meirelles (2006), usualmente encontrada nas usinas brasileiras, parte da mistura azeotrópica ternária condensada é realimentada na coluna azeotrópica e a solução alcoólica é reciclada para o decantador. A adaptação sugerida por Mortaheb e Kosuge (2004) é o reciclo de uma fração da fase aquosa obtida no decantador para a coluna azeotrópica. No caso da destilação azeotrópica, a existência de diversas configurações é justificada pela necessidade de modificações no processo a fim de diminuir sua instabilidade, a qual é causada pela presença de duas fases líquidas no interior da coluna e pela multiplicidade de estados estacionários.

Destilação extrativa

Na destilação extrativa (ou azeotrópica homogênea), um terceiro componente, o solvente, é adicionado à mistura original azeotrópica de modo a alterar a volatilidade relativa dos componentes da mistura modificando, portanto, o equilíbrio líquido-vapor dos componentes originais, através, primordialmente, da mudança dos coeficientes de atividade dos componentes. Neste processo, não deve haver separação da mistura em duas fases líquidas (Ito, 2002, Brito, 1997). Sendo assim, o processo completo de destilação extrativa envolve a coluna extrativa e a coluna de recuperação do solvente. O solvente comumente empregado para a separação do sistema etanol-água é o monoetilenoglicol (MEG). Vale ressaltar que o bioglicerol, obtido como co-produto na produção de biodiesel, tem sido estudado como solvente alternativo, visto que é renovável e apresenta grande disponibilidade no mercado devido à crescente produção de biodiesel (Dias, 2008).

A configuração usual da destilação extrativa é mostrada na Figura 2.5.

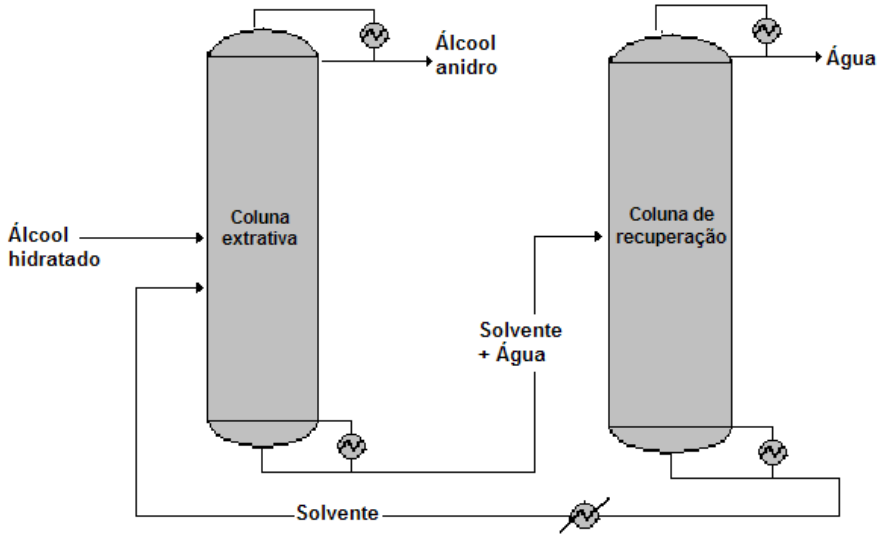

Figura 2.5. Configuração usual da destilação extrativa.

Na primeira coluna, o álcool anidro é produzido no topo, enquanto no fundo, solvente e água são recuperados e destinados à segunda coluna. Na coluna de recuperação, água é recuperada no topo, enquanto no fundo uma corrente rica em solvente é obtida e reciclada para a primeira coluna. Em caso de perdas de solvente, reposição deste pode ser implementada. Uma configuração alternativa foi proposta por Brito (1997), em que apenas uma coluna é empregada, sendo água obtida através de uma saída lateral, o bioetanol anidro produzido no topo e o solvente recuperado no fundo.

Adsorção em peneiras moleculares

No processo de desidratação de etanol por meio de adsorção em peneiras moleculares, um leito de zeólitas é utilizado para adsorver a água presente no bioetanol hidratado, de modo a produzir bioetanol anidro. O diâmetro nominal das zeólitas empregadas no processo de desidratação de etanol é de 3 Å, com o objetivo de promover a adsorção das moléculas de água, que têm diâmetro da ordem de 2,8 Å, separando-a do etanol, de diâmetro de 4,4 Å (Huang et al., 2008).

A configuração utilizada pelas biorrefinarias brasileiras inclui três leitos adsorventes que operam em ciclos: enquanto a adsorção ocorre em dois leitos, o outro está em regeneração (remoção da água acumulada). A alimentação das peneiras é feita com bioetanol hidratado na fase vapor e uma bomba de vácuo é

empregada para promover a regeneração do leito. A solução aquosa recuperada durante a regeneração é reciclada à etapa de destilação, uma vez que contém significativa quantidade de etanol.

As vantagens deste processo são a produção de álcool anidro de alta qualidade, sem contaminação por solventes e menor consumo energético quando comparado a processos baseados em destilação (Dias, 2008). No entanto, as peneiras moleculares possuem elevado custo de investimento, uma vez que as zeólitas não são produzidas no Brasil, sendo necessariamente importadas (Meirelles, 2006).

2.3. Modelagem de Colunas de Destilação

A destilação é um dos processos de separação mais frequentemente encontrados nas indústrias químicas e petroquímicas. Neste contexto, a simulação de processos constitui uma importante ferramenta para o entendimento e a predição do comportamento das colunas de destilação nos processos industriais. Em geral, as ferramentas computacionais disponíveis para este fim são baseadas no conceito idealizado de estágios de equilíbrio.

2.3.1. Modelagem de Estágio de Equilíbrio

O modelo de estágios de equilíbrio é bem conhecido (King, 1980; Henley e Seader, 1981; Holland, 1981) e supõe que as correntes – líquida e vapor – que deixam um estágio em particular estão em equilíbrio termodinâmico. Neste modelo, são resolvidas equações conhecidas como MESH (*Mass, Equilibrium, Summation, Heat*) que consistem em balanço de massa por componente, equações para equilíbrio de fases, operações de somatório e balanço de energia.

Todavia, em uma operação real, os estágios raramente, ou mesmo nunca, operam em equilíbrio apesar das tentativas para se atingir essa condição através de um projeto apropriado e da escolha de condições adequadas de operação. O meio usual de se considerar o desvio do equilíbrio é a incorporação do conceito de eficiência nas relações de equilíbrio (Krishnamurthy e Taylor, 1985).

Conceitos de Eficiência

Algumas revisões foram publicadas a respeito dos diversos conceitos de eficiência (Pescarini, 1996; Barros, 1997; Soares, 2000). De acordo com estas, encontram-se, a seguir, os principais conceitos de eficiência existentes.

A eficiência global de colunas de destilação foi definida por Lewis (1922) como a relação entre o número de estágios teóricos e o número de estágios reais necessários para uma dada separação. Entretanto, as limitações do ponto de vista prático e matemático tornam pouco realista a sua aplicação aos processos de destilação por considerar a uniformidade da eficiência para todos os estágios.

Murphree (1925) definiu a eficiência de estágio, relacionando o comportamento de um estágio real com o de um estágio ideal mediante o grau de contato entre líquido e vapor, admitindo-se que o líquido esteja completamente misturado no prato. Na prática, as eficiências para a fase vapor e para a fase líquida conduzem geralmente a valores numéricos diferentes para o mesmo estágio real. Em geral, a literatura dedica extensiva aplicação à fase vapor (Soares, 2000). A eficiência de Murphree de vapor no prato é definida pela Equação 2.4.

$$\eta_{i,j} = \frac{y_{i,j} - y_{i+1,j}}{y^{*}_{i,j} - y_{i+1,j}} \qquad (2.4)$$

onde η é a eficiência, *i* é o estágio, *j* é o componente, y é a fração molar na fase vapor e asterisco (*) denota equilíbrio. No entanto, a eficiência de Murphree de prato para separações multicomponente é difícil de prever. Em alguns casos, os valores de eficiência estão além dos limites comuns de 0 e 1, esperados para sistemas binários (Taylor and Krishna, 1993).

A definição de eficiência de Murphree no ponto, desenvolvida por West et al. (1952), apresenta melhores resultados nos estudos de desenvolvimento de predição e correlação da eficiência. A eficiência de Murphree de vapor no ponto usa a concentração do componente na fase vapor em equilíbrio com o líquido no ponto considerado.

As eficiências de Colburn (1936), de Nord (1946), de Hausen (1953), de Standart (1965) e de Holland (1981), entre outras, são conhecidas como

eficiências de Murphree modificadas, isto porque todas são definidas como uma relação entre frações molares, como é o caso da eficiência de Murphree original (Pescarini, 1996).

Não pertencente a esta classe, existe a eficiência de vaporização definida por Holland e McMahon (1970). Neste contexto, Medina et al. (1978) utilizaram o conceito de eficiência de vaporização na destilação binária e, posteriormente, estenderam o conceito para processos multicomponentes. O conceito de eficiência de vaporização foi considerado falho na descrição do comportamento das fases em um prato de destilação devido às limitações matemáticas, pois se observou que a eficiência de vaporização não zera, sempre tende a um valor finito e positivo mesmo em situações onde não ocorre separação (Barros, 1997).

Resumindo, existem diversas definições de eficiência e não há consenso sobre qual a melhor definição, contudo, os conceitos de eficiência desenvolvidos por Lewis e Murphree são os mais utilizados (Pescarini, 1996). Além da indefinição com relação ao conceito de eficiência, outra dificuldade é com relação à estimativa de valores para eficiência. A proposição de eficiência constante ao longo da coluna pode gerar resultados não confiáveis, sendo necessária uma correlação que calcule valores de eficiência considerando fundamentos teóricos.

Correlações de Eficiência

A maioria das correlações empíricas e semi-empíricas desenvolvidas até hoje tem aplicações restritas, pois as principais variáveis envolvidas no processo de transferência de massa e calor não são consideradas. Outras possuem um bom fundamento teórico, mas são complexas uma vez que dependem de variáveis dificilmente correlacionáveis. A seguir são apresentadas as principais correlações existentes.

A primeira correlação usada para o cálculo da eficiência foi proposta por Drickamer e Bradford (1943) e posteriormente foi modificada por O'Connell (1946) que estendeu sua faixa de operação para colunas fracionadoras. A correlação apresentada por O'Connell foi melhorada por Chu (1951) que incluiu outros fatores na correlação empírica, tais como a relação entre as vazões de líquido e de vapor

dentro da coluna e relações geométricas do borbulhador e do prato (Pescarini, 1999).

No entanto, foi com o estudo publicado pela AIChE (1958) que se lançou as bases para um entendimento mais profundo do problema. O método de predição, inicialmente desenvolvido para campânulas, envolvia a estimativa de número de unidades de transferência nas fases líquida e vapor, combinando estes para obter valores de eficiência de ponto (Rousseau, 1987).

Gomes (1995), utilizando a correlação de O'Connell, desenvolveu uma metodologia para o cálculo da eficiência de estágios na indústria.

Barros e Wolf-Maciel (1996) desenvolveram uma nova correlação, mais realista, para o cálculo da eficiência nas colunas de destilação. A correlação de Barros e Wolf foi obtida através do ajuste de parâmetros de mistura que variam com a eficiência, sendo que diferentes equações foram formuladas para a destilação convencional e a extrativa. Equações 2.5 e 2.6 apresentam a correlação de Barros e Wolf para o cálculo de eficiência (Eff) para um prato *i* empregadas na destilação convencional e na extrativa, respectivamente.

$$\mathrm{Eff(i)} = 38{,}5309\left[\frac{\mathrm{k(i)}\rho\mathrm{(i)D(i)MW(i)}}{\mathrm{Cp(i)}\mu^2\mathrm{(i)}}\right]^{-0{,}04516} \tag{2.5}$$

$$\mathrm{Eff(i)} = 19{,}37272\left[\frac{\mathrm{k(i)}\rho\mathrm{(i)D(i)MW(i)}}{\mathrm{Cp(i)}\mu^2\mathrm{(i)}}\right]^{-0{,}109588} \tag{2.6}$$

Nestas correlações são utilizadas as seguintes propriedades da mistura na fase líquida: condutividade térmica (k), massa específica (ρ), difusividade (D), massa molecular (MW), capacidade calorífica (Cp) e viscosidade (μ). Estas correlações podem também ser aplicadas para o cálculo de eficiência de componente no prato – Eff (i,j) – sendo necessário apenas substituir os parâmetros da mistura pelos dos componentes puros (j) na fase líquida.

Muitas vezes, a eficiência de estágio por ser função de propriedades físicas, características geométricas e condições de operação, somente pode ter suas conclusões extrapoladas se todas as condições forem iguais às do caso estudado (Pescarini et al., 1996). Além disso, devido às imprecisões e às incertezas

causadas ao se trabalhar com o conceito de eficiência na modelagem de estágios de equilíbrio, surgiu a necessidade de modelagens mais realistas, utilizando métodos matemáticos mais rigorosos que levassem em conta a transferência simultânea de massa e energia, como as modelagens de estágios de não equilíbrio, que eliminam completamente o conceito de eficiência.

2.3.2. Modelagem de Estágio de Não equilíbrio

O modelo de estágios de não equilíbrio, também conhecido como modelo baseado na taxa, foi desenvolvido por Krishnamurthy e Taylor (1985) e no Brasil por Barros (1997) e Pescarini (1996).

Krishnamurthy e Taylor (1985) publicaram artigos descrevendo o modelo de estágio de não equilíbrio para processos de separação multicomponente. Neste modelo, assume-se que o prato está em equilíbrio mecânico (igualdade de pressão). As equações de conservação são escritas para cada fase independentemente e resolvidas juntamente com as equações de transporte que descrevem as transferências de massa e energia em misturas multicomponentes. O equilíbrio termodinâmico é assumido somente na interface. As funções que descrevem os processos físicos no prato são: balanço material para componente na fase vapor, na fase líquida e na interface, balanço de entalpia na fase vapor, na fase líquida e na interface, relações de equilíbrio na interface e equações de somatório na interface.

Esta abordagem proposta por Krishnamurthy e Taylor (1985), tornou-se modelo para a modelagem e simulação no estado estacionário e dinâmico de equipamentos de separação, principalmente devido à disponibilidade de sistemas computacionais eficientes. Com esta modelagem é possível simular a destilação e absorção como operações baseadas na taxa de transferência de massa ao invés simulá-las como processos de equilíbrio (Higler et al., 2004).

Eckert e Vaněk (2001) afirmam que o conceito de não equilíbrio é certamente superior ao conceito de estágio de equilíbrio, o qual usa vários tipos de correções para se ajustar ao desempenho real do equipamento de separação. No entanto, uma desvantagem em relação à modelagem de estágios de equilíbrio, como mencionado por Taylor e Krishna (1993), é o número de parâmetros do

equipamento para dimensionamento do prato que devem ser normalmente especificados e somente assim os coeficientes de transferência de massa podem ser estimados corretamente. Parâmetros reais de projeto da coluna, como diâmetro da coluna, tipo de prato, altura do vertedor, devem ser conhecidos para obter um resultado consistente. Além disso, os fluxos são importantes na modelagem de não equilíbrio, porque, em colunas reais, os fluxos afetam tanto os coeficientes de transferência de massa como a hidráulica do prato. Uma especificação de fluxo inapropriada pode resultar em inundação ou arraste do liquido através dos furos no prato (Lee e Dudukovic, 1998).

A modelagem de estágios de não equilíbrio pode ainda ser empregada na destilação reativa, incluindo-se os termos de reação química no modelo baseado na taxa, assim como apresentado por Lee e Dudukovic (1998).

Higler et al. (2004) estudaram a destilação trifásica através da modelagem de não equilíbrio. Incorporado ao algoritmo, há uma avaliação da estabilidade da fase líquida e o cálculo da divisão de fase para avaliar a estabilidade termodinâmica de todas as fases presentes na coluna de destilação a cada iteração. A partir deste estudo, concluíram que a introdução de uma segunda fase de equilíbrio pode ter uma forte influência, positiva ou negativa, no comportamento da transferência de massa. Além disso, através da modelagem de estágios de não equilíbrio, demonstraram que as eficiências de Murphree dos componentes tendem a ser menores e mais variáveis na região de duas fases líquidas do que na região de uma única fase líquida.

Outra forma de obter resultados mais realistas foi estudada por Noriler (2007), que aplicou um modelo microscópico multifásico baseado na conservação de quantidade de movimento, calor e massa, de forma a prever perfis de velocidade, fração volumétrica, pressão, temperatura e concentração em um prato perfurado de uma coluna de destilação. Através de técnicas de CFD (Fluidodinâmica Computacional), Noriler (2007) avaliou o desempenho de pratos de destilação e obteve eficiência de 64,16 % para o sistema etanol/água.

Capítulo 3
Processos Eficientes de Separação Etanol – Água

3.1. Introdução

A separação etanol-água é uma etapa bastante crítica do processo de produção de bioetanol, uma vez que este é obtido inicialmente a baixas concentrações e deve ser purificado a fim de ser utilizado como combustível puro ou adicionado à gasolina. Além disso, a formação de azeótropo entre estes componentes na composição 95,6 % de etanol (em massa) a 1 atm impossibilita o uso da destilação convencional para a obtenção do bioetanol anidro (99,5 %).

Consequentemente, este processo envolve diversas operações bem como considerável consumo de energia e de solventes. Assim, com a finalidade de aumentar a sustentabilidade da produção de bioetanol, o estudo de processos alternativos de separação baseados em agentes ambientalmente amigáveis e com baixo consumo de energia é de grande importância.

Neste contexto, uma revisão dos processos de separação atualmente empregados bem como dos recentes desenvolvimentos nesta área é apresentada neste capítulo. Dentre as novas tecnologias, destacam-se destilação extrativa com polímeros altamente ramificados (HyPol) e líquidos iônicos (IL), pervaporação, adsorção, processos híbridos, entre outras.

Dessa forma, são descritas e avaliadas novas configurações de processo incluindo as etapas de fermentação, destilação e desidratação assim como são propostas reformulações ao processo convencional com intuito de reduzir o consumo de energia e a geração de resíduos.

O desenvolvimento deste capítulo é apresentado a seguir no trabalho *"Improving sustainability of bioethanol production: efficient ethanol – water separation processes"* publicado nos anais do *5th Dubrovnik Conference on Sustainable Development of Energy, Water and Environment Systems.*

3.2. Improving sustainability of bioethanol production: efficient ethanol – water separation processes

ABSTRACT

In this work a review of the current situation of ethanol-water separation in Brazil for anhydrous bioethanol production is carried out, as well as a study of alternative and more efficient separation processes and/or agents, in order to aid the evaluation and proposition of more appropriate process configurations. A description of alternative dehydration and extractive fermentation processes that may be employed in bioethanol production is presented in this work. This work offers ground to support the choice of new enterprises as well as the reformulation of existing processes, aiming reduction of energy consumption and residue generation during bioethanol production, thus improving its sustainability.

INTRODUCTION

Ethanol has been increasingly viewed as the most important alternative to fossil fuels, in order to promote reduction of greenhouse gases emissions and to reduce dependence on oil, which is mainly available on the most politically unstable areas in the world. Bioethanol is produced from fermentation of sugars, either from sucrose or starch containing materials, such as sugarcane and corn, or from lignocellulosic materials, like sugarcane bagasse, straw and harvest residues (Balat et al., 2008). Regardless of the chosen bioethanol production process and raw material, a product purification step will be necessary in order to produce anhydrous bioethanol, which may be used as a fuel in a mixture with gasoline.

Ordinary fermentation processes produce a wine of low concentration (usually from 7 to 10 wt% ethanol, depending on process parameters), which contains water, ethanol and components derived from the raw material or from fermentation parallel reactions. In a conventional biorefinery, a series of distillation and rectification columns operating under near-atmospheric pressures is employed to purify the wine (Ensinas et al., 2007). This process is characterized by a large consumption of energy on column reboilers, accounting for an important fraction of the energy

consumption of the process (Ensinas et al., 2007; Gu et al., 2007). Because water and ethanol form an azeotrope with 95.6 wt% ethanol at 1 atm, conventional distillation can not achieve the separation required to produce anhydrous bioethanol, and alternative separation processes are necessary.

Brazil has been producing ethanol on a large scale basis for more than 30 years. The most usual process for ethanol dehydration employed in this period was azeotropic distillation with benzene, which has been replaced by cyclohexane for the past decade due to safety concerns (Gomis et al., 2005). Up to this day, it remains the most common dehydration method, followed by extractive distillation with monoethyleneglycol (MEG) and adsorption onto molecular sieves, which have been used since the 2001 and 1999 harvest seasons, respectively. In spite of being the most common dehydration process, azeotropic distillation with cyclohexane presents several disadvantages, such as high energy consumption on columns reboilers, use of a harmful, flammable, toxic and fossil separation agent (Rivière and Marlair, 2009) and product contamination with solvent. Extractive distillation with MEG requires less energy, but it is also based on a fossil and harmful separating agent. Adsorption onto molecular sieves, on the other hand, is the most environmental friendly commercial process available: no toxic or fossil separating agent is used, final product is not contaminated and energy consumption is relatively small (Simo et al., 2008).

In order to improve bioethanol production sustainability, alternative separation processes based on eco-friendly separating agents, with low energy consumption and allowing the production of high quality anhydrous bioethanol are required. In this work a review of the current and possible separation processes related to ethanol recovery from the wine and dehydration is carried out, in order to aid the evaluation and proposition of more appropriate process configurations.

CONVENTIONAL DISTILLATION

Nowadays, fermentation wine (7 – 10 wt% ethanol) is fed to a conventional distillation system in order to produce hydrous bioethanol (around 93 wt% ethanol), which can be used as a fuel in ethanol-driven or flex-fuel engines, which correspond to the majority of the Brazilian new light-duty fleet. Over 86 % of the light-duty vehicles sold

in 2007 in Brazil may run on 100 % hydrous ethanol fuel (Cerqueira Leite et al., 2009).

In a typical industrial scale process, as depicted in Figure 3.1, a series of distillation (A, A1 and D, located above one another) and rectification columns (B and B1) are employed to produce hydrous bioethanol (around 93 wt% ethanol). In the distillation columns, wine is pre-concentrated up to 50 wt% ethanol, producing phlegms in both liquid and vapour phases, as well as vinasse in the bottom and 2nd grade ethanol in the top. Phlegms are fed to rectification columns, in which hydrous ethanol bioethanol is obtained in the top, as well as fusel oil as side draws and phlegmasse as bottom product. All columns work under pressures around atmospheric. This process usually demands a large amount of energy, thus thermal integration can be employed to reduce high utilities consumption (Sobočan and Glavič, 2000).

Improvements on distillation: multiple effect operation

Multiple effect operation of the distillation and rectification columns allows a significant reduction on energy consumption of the bioethanol production process, since condensers and reboilers of the different columns may be thermally integrated. Several column arrangements are possible; one of them is the double effect distillation, in which columns configuration are similar to that of the conventional distillation, but the distillation columns operate under vacuum (19 – 25 kPa), while rectification columns operate under atmospheric pressure (101 – 135 kPa). In this way, different temperature levels are observed between column A reboiler and column B condenser, allowing thermal integration of these equipments and consequently reducing energy consumption on the distillation stage.

Another possible configuration is the triple effect distillation, in which the liquid phlegm stream produced on column D may be split in two: one of them is fed to a rectification column operating under nearly atmospheric pressure (70 – 80 kPa) and the other is fed to a rectification column which operates under relatively high pressure (240 – 250 kPa). This way, only the reboiler of the high pressure column requires energy to be supplied, and the other reboilers work with thermal integration with the

other condensers. The overall energy consumption may be quite smaller than that of the conventional distillation column.

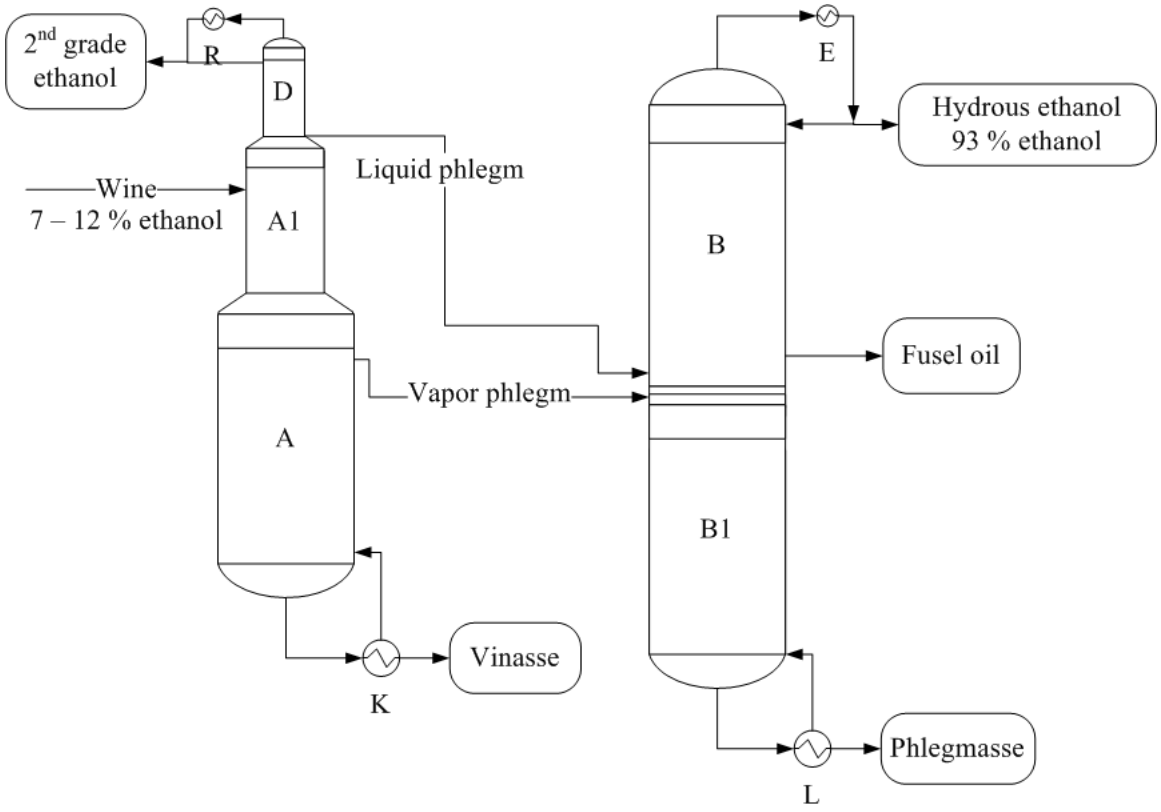

Figure 3.1. Configuration of the conventional distillation process.

DEHYDRATION PROCESSES

In order to produce anhydrous bioethanol, which is used as fuel in a mixture with gasoline around the world, alternative separation processes are required, since water and ethanol form an azeotrope with 95.6 wt% ethanol at 1 atm. In this section a description of the most common dehydration processes in Brazil is made, as well as of those that are yet to be employed commercially on ethanol separation.

Azeotropic Distillation

In the conventional configuration of the heterogeneous azeotropic distillation process for anhydrous bioethanol production, two distillation columns are used: azeotropic and recovery. Hydrous ethanol and entrainer are fed in the azeotropic column, where anhydrous ethanol is produced on the bottom and a minimum boiling ternary azeotrope formed between ethanol, water and entrainer is produced on the top. The

ternary azeotrope is heterogeneous, and the two liquid phases are separated in a decanter. The light phase contains most of the entrainer and is recycled to the azeotropic column, while the aqueous phase is fed to the recovery column where ethanol and eventually entrainer are recovered (Mortaheb and Kosuge, 2004). The stream containing ethanol recovered may be recycled to the azeotropic column or fed to the conventional distillation column, in order to reduce ethanol losses.

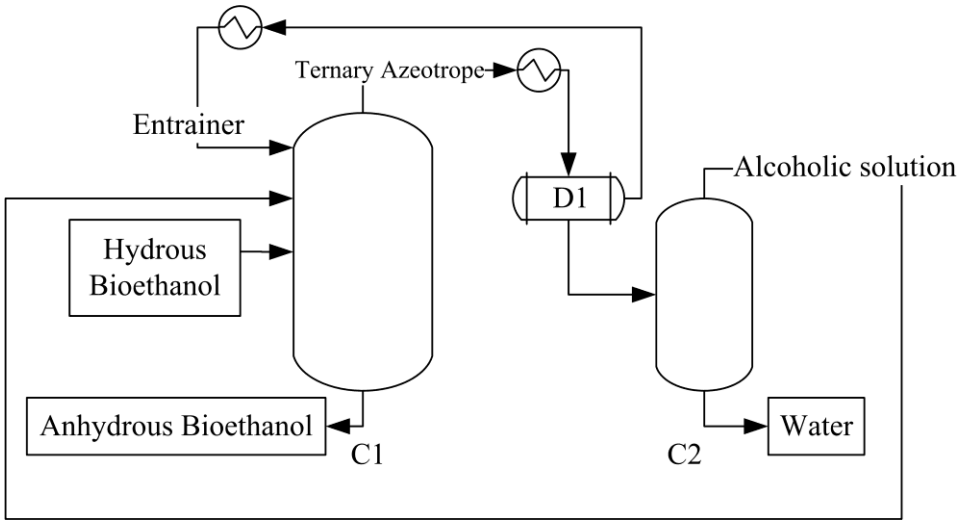

Figure 3.2. Configuration of the azeotropic distillation process for anhydrous bioethanol production. C1: azeotropic column; D1: decanter; C2: recovery column.

Benzene was the most common entrainer employed in anhydrous bioethanol production, but due to its carcinogenic characteristics, it has been replaced by cyclohexane for the last decade (Gomis et al., 2005). However, cyclohexane also presents disadvantages, since it is a harmful, flammable, toxic and fossil separation agent (Rivière and Marlair, 2009). Besides, azeotropic distillation with cyclohexane requires high energy consumption in the column reboilers and anhydrous bioethanol is frequently contaminated by entrainer.

An alternative to cyclohexane as an entrainer in azeotropic distillation process is n-heptane: traces of this entrainer will not decrease the quality of the final product (anhydrous bioethanol) when it is used in a mixture with gasoline, since n-heptane is one of the main components of gasoline itself (Gomis et al., 2006).

Extractive Distillation

In extractive distillation, also known as homogeneous azeotropic distillation, a separating agent, called solvent or entrainer, is added to the azeotropic mixture in order to alter the relative volatility of the components in the original mixture.

In the conventional extractive distillation process, solvent is fed to the first column (extractive column), above the azeotropic feed. Anhydrous ethanol is produced on the top of the extractive column, while in the bottom a mixture containing solvent and water is obtained. The solvent is recovered in a second column (recovery column), cooled and recycled to the extractive column (Huang et al., 2008).

An alternative configuration for this process makes use of a single column. On its top, anhydrous ethanol is produced, while pure solvent is recovered on the bottom. By means of a side draw of water in vapour phase located a few stages above the bottom, pure water is obtained (Brito et al., 1997). Configuration of conventional and alternative extractive distillation process is depicted in Fig. 3.3.

Meirelles et al. (1992) demonstrated that monoethyleneglycol (MEG) is an efficient solvent for anhydrous bioethanol production by extractive distillation. This process was first employed in industrial scale in Brazil in the 2001 sugarcane harvest season, and is today one of the most common processes along with azeotropic distillation with cyclohexane and adsorption onto molecular sieves.

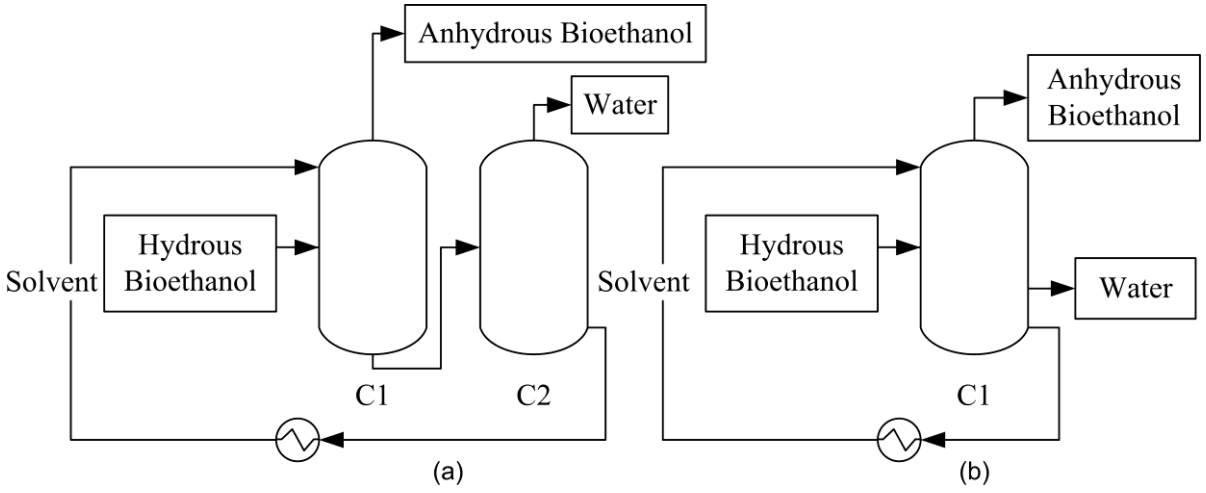

Figure 3.3. Configuration of conventional (a) and alternative (b) extractive distillation process for anhydrous bioethanol production. C1: extractive column; C2: recovery column.

The solvent most used in industry for the separation of ethanol - water mixtures is MEG, which is fossil and toxic. The use of bioglycerol – by-product of biodiesel production – as a substitute of MEG has been encouraged due to its availability and low price. Besides, bioglycerol is not harmful to humans or the environment, thus can be safely used to produce anhydrous ethanol for use in food or pharmaceutical industries (Dias et al., 2008).

Novel separating agents for the extractive distillation process, ionic liquids (IL) and hyperbranched polymers (HyPol) have been studied for the past few years with great interest (Huang et al., 2008; García-Miaja et al., 2008; Pereiro and Rodríguez, 2008; Seiler et al., 2004).

Ionic liquids (IL), usually a mixture of organic cation and inorganic anion, possess several characteristics that make them suitable agents for the separation of the ethanol-water azeotrope in extractive distillation processes, such as low viscosity, thermal stability, good solubility and low corrosiveness (Huang et al., 2008). Since those properties can be customized, IL appear superior to many conventional entrainers and extractive solvents (Seiler et al., 2004).

Hyperbranched polymers (HyPol) are highly branched macromolecules with a large number of functional groups. Their properties, such as remarkable selectivity and capacity, low viscosity and thermal stability, make them suitable agents for extractive distillation process (Huang et al., 2008). Since their polarity can be adjusted by their functional end groups, suitable solvents can be designed for specific operations (Seiler et al., 2004).

Some of the advantages of the IL and HyPol reside on the fact that they do not contaminate the final product (anhydrous bioethanol), since they are not volatile, and because the entrainer recovery process does not require distillation columns (Huang et al., 2008), a stripping column working with air may be used to promote entrainer regeneration, as depicted in Figure 3.4.

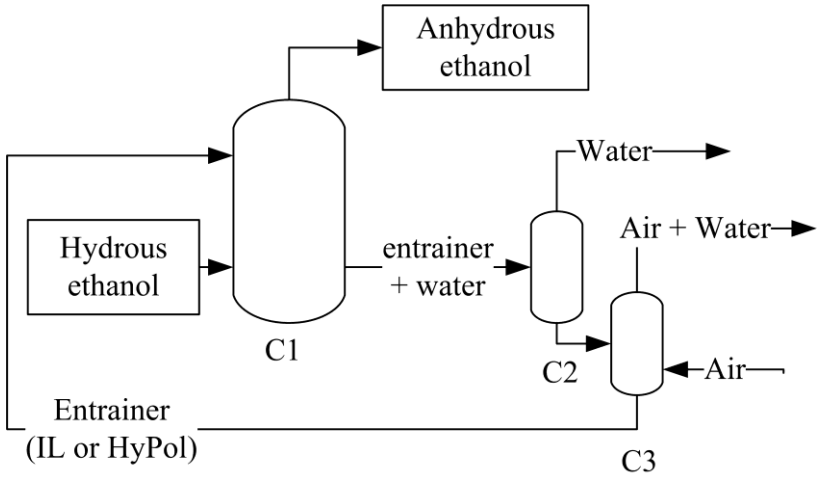

Figure 3.4: Example of extractive distillation process configuration with non-volatile entrainers Ionic Liquid (IL) or low-viscosity Hyperbranched Polymers (HyPol); C1: main column, C2: flash, C3: stripping column (adapted from Seiler, 2006).

Adsorption

Adsorption involves the transfer and resulting equilibrium distribution of one or more solutes between a fluid phase and particles (Perry et al., 1997). Usually, inorganic adsorbents are employed, such as molecular sieves, lithium chloride, silica gel and activated alumina. Besides, Huang et al. (2008) also report the use of bio-based adsorbents, such as cornmeal, cracked corn, starch, corn cobs, wheat straw, bagasse, cellulose, hemicellulose, wood chips and other grains, which are biodegradable and derived from renewable resources (Al-Asheh et al., 2004).

In the ethanol dehydration process by adsorption onto molecular sieves, a fixed bed packed with zeolites is employed in order to adsorb water present in hydrous ethanol, producing anhydrous ethanol. 3A zeolite molecular sieves are generally used in this process, which corresponds to a nominal pore size of 3 Angstroms (0.30 nm). In view of their small diameter (0.28 nm), the water molecules can easily penetrate the structural zeolite canals, while most of the ethanol molecules (0.44 nm) are simultaneously excluded (Carmo and Gubulin, 2002).

Brazilian biorefineries configuration of the dehydration process by adsorption includes three adsorbent beds in a cyclic operation: one of them is regenerating (water accumulated in adsorbent is removed) while in the others adsorption is carried out. Hydrous ethanol on vapour phase (about 93 wt%) is fed to the molecular sieves

bed. A vacuum pump is used to promote regeneration of the bed and the aqueous solution recovered is recycled to the distillation stage, since it contains a large amount of ethanol. The configuration of the adsorption process for anhydrous bioethanol production used in Brazil is depicted in Figure 3.5.

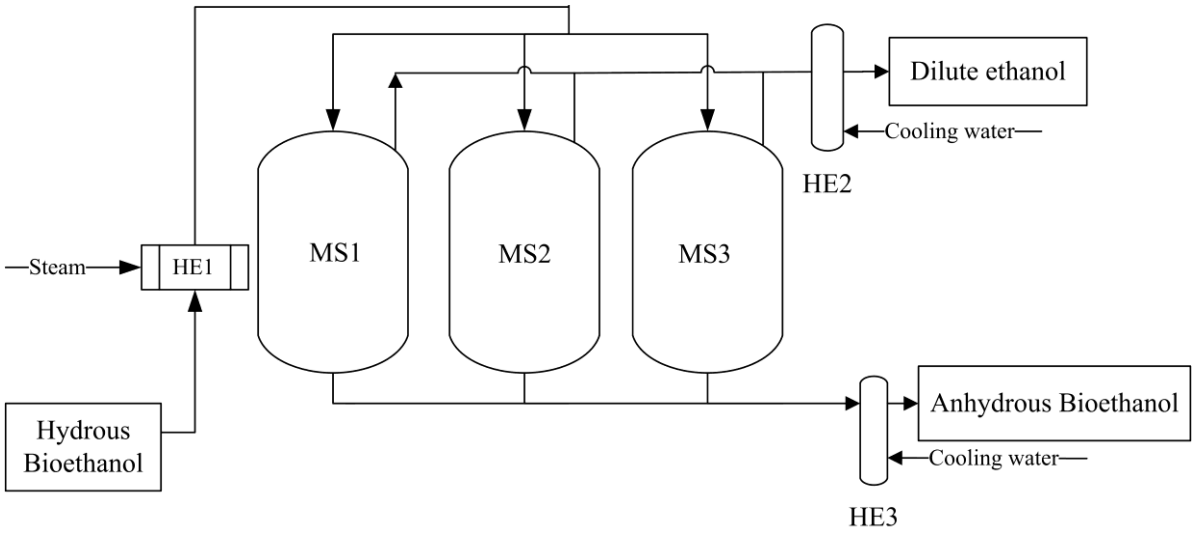

Figure 3.5. Configuration of the adsorption onto molecular sieves process for anhydrous bioethanol production. HE1: superheater; HE2, HE3: condensers; MS1: regenerating molecular sieves bed; MS2, MS3: molecular sieves beds.

Adsorption using molecular sieves allows the production of high purity ethanol without contamination by solvent; besides, it requires less energy when compared to distillation-based processes, given that only one vaporization step is necessary. However, a barrier to its use by Brazilian biorefineries is the high investment cost, since zeolites are not produced in Brazil; this problem may be completely surpassed when bio-based adsorbents become viable.

One of the most important characteristics of the configuration of the adsorption process employed in Brazil is that hydrous ethanol is produced in the distillation columns as a liquid and fed to the molecular sieves beds as a superheated vapour, thus energy is required to promote its vaporization; because hydrous ethanol must be fed to the beds at around 3 bar, it is easier to raise the pressure of the liquid phase ethanol and then to vaporize it, instead of compressing hydrous ethanol vapours obtained directly from the distillation columns. As a result, there is an increase on the steam consumption of the process. Another disadvantage is the high vacuum

required to bed regeneration due to the strong zeolites-water interaction (Huang et al., 2008).

Electromagnetic as well as mechanical waves have been studied as regeneration methods for loaded adsorbents; Reuβ et al. (2002) has studied the use of microwaves to enhance desorption, which strongly depends on the electromagnetic properties of adsorbent and solvents adsorbed. Their work included experiments with ethanol/acetone, ethanol/toluene and ethanol/water systems and their results showed that polar components, such as ethanol and water, present enhanced desorption.

Pervaporation

Pervaporation is a membrane process in which a phase change from liquid to vapour occurs. In this process, the feed mixture is a liquid and one component in the mixture permeate preferentially through the membrane and evaporate as a result of the partial pressure on the permeate side being held lower than the saturation vapour pressure. The driving force is controlled by applying a vacuum or occasionally with a sweep gas on the permeate side. Pervaporation membranes are chosen for high selectivity, and the permeate is often highly purified (Perry et al., 1997; Coulson et al., 2002). Configuration of the pervaporation process for anhydrous bioethanol production is represented in Figure 3.6.

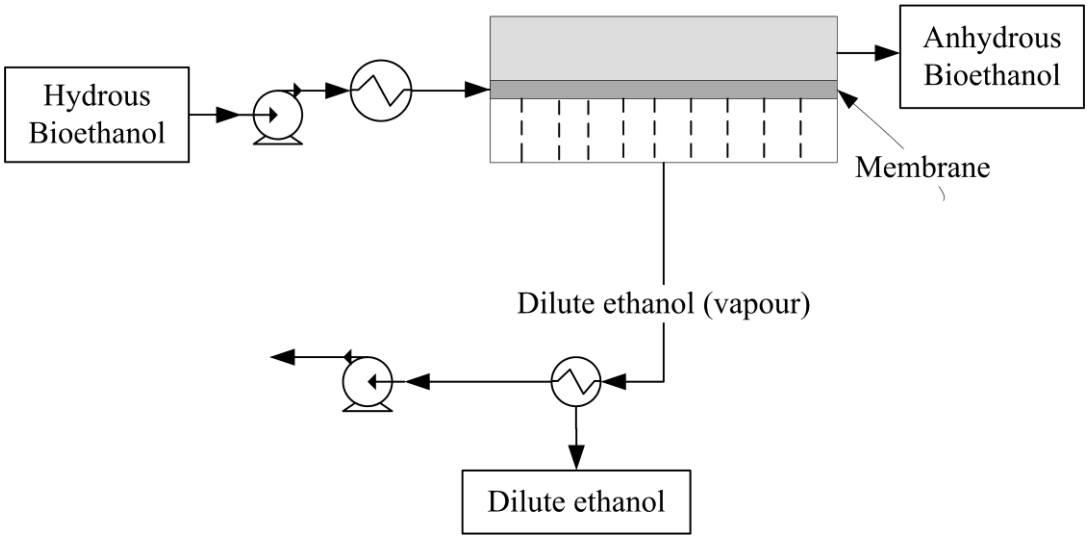

Figure 3.6. Configuration of the pervaporation process for anhydrous bioethanol production.

It is possible to use the pervaporation system to concentrate the mixture obtained after fermentation, which is a dilute ethanol solution, as well as to concentrate hydrous ethanol obtained after distillation of the fermentation broth. Nevertheless, fermentation broth components may impact pervaporation membranes and modules. Vane (2005) reports several works available in the literature which evaluate the impacts of broth components on membranes, such as suspended solids and yeast cells, which may potentially accumulate in modules, blocking flow path and membrane surface, and glucose, which decreases water and ethanol fluxes. These problems would be diminished in the case where pervaporation is employed only as a method for ethanol dehydration, since those undesired broth components are removed in the vinasse.

In order to reduce the fouling potential of solids in the fermentor broth, a pre-pervaporation solid–liquid separation device may be employed, thus allowing the use of the full range of pervaporation module options. In fact, the simplest situation would be one in which the pervaporation modules are able to accept the fermentation broth as delivered from the fermentor (including solids) and the broth contains no temperature-sensitive components or they are no longer necessary in the process. However, the addition of any separation device to the system adds capital and operating costs (Vane, 2005).

Ultrasonic Separation

Ultrasonic separation consists of the fragmentation of a liquid layer to form a fine droplet mist by high frequency ultrasonic atomization and it has been applied to a range of industrial applications such as fine chemical manufacturing, pharmaceutical production, and food processing (Suzuki et al., 2006).

In this context, Sato et al. (2001) have shown that pure ethanol can be obtained through ultrasonic atomization of ethanol-water solutions with several concentrations at relatively low temperature (10 ºC). Since the enrichment ratio provided by this technique is much higher than that expected for the vapour in equilibrium with the original mixture and the required energy is much smaller than that required for liquid vaporization, ultrasonic separation has the potential to become an alternative to distillation (Yano et al., 2007).

Suzuki et al. (2006) conducted experiments in batch and continuous feed processing systems and observed that ethanol concentration of the mist and the ethanol collection rate were significantly increased and maintained constant in the continuous feed system, which is explained by the low variation in the ethanol feed concentration and constant liquid level in the separation vessel.

HYBRID PROCESSES

Hybrid separation processes combine two or more of the techniques described above, as well as fermentation processes, in order to create optimized processes and increase their efficiency.

Pervaporation/vapour permeation coupled with distillation

One of the most promising approaches consist of integrated pervaporation and distillation systems (Szitkai et al., 2002), on which the pervaporation module may be located at the final stage of dehydration, to produce anhydrous bioethanol, or immediately after the fermentation process, substituting the distillation and rectification columns in order to produce hydrous bioethanol, or part of a hybrid system using other dehydration methods (29).

For the ethanol – water system, Pressly and Ng (1998) evaluated the influence of different feed concentrations in the costs and observed that the lowest concentration studied (0.1 mol fraction ethanol) presented the highest scaled break-even cost overall. Therefore, the configuration that employs pervaporation after distillation is more economically attractive, since its pervaporation module is fed with a mixture of high concentration.

Szitkai et al. (2002) describe a system with a distillation column, which purifies the crude ethanol inlet, and a succeeding network of pervaporation membrane modules. The top product of the column is fed to the first section of the membrane train. In each membrane section the retentate is collected and fed to a heat exchanger for re-heating. There is a vacuum pump at the permeate side of the membrane system. The permeate is withdrawn as a product stream and/or recycled to the column feed. Results showed that total permeate recycling is more economical, when compared to partial recycling.

Pervaporation coupling with distillation is a potential alternative, since pervaporation alone will rarely be economical due to the purity required nowadays in production and the limitation on flux given by the activity as the driving force of the pervaporation process (Lipnizki et al., 1999).

Another similar option is to feed hydrous ethanol vapours obtained in conventional distillation directly to a vapour permeation membrane system (Sato et al., 2008), what does not require the total condensation of the rectification column top product (hydrous bioethanol), thus decreasing water consumption in the bioethanol production process. Sato et al. (2008) successfully produced anhydrous bioethanol (over 99.6 wt%) with NaA zeolite membranes, by coupling conventional distillation, where hydrous bioethanol (88 wt% ethanol) is produced, and two membrane modules for vapour permeation.

Coupled Fermentation/Pervaporation

Accumulation of ethanol in the fermentation broths can lead to a decrease in ethanol productivity due to low activity of the biocatalyst, which is known as product inhibition. Therefore, the removal of ethanol from the fermentation reactor is indispensable and a possible solution is the pervaporation with ethanol-selective hydrophobic membranes, which allows ethanol to be continuously removed from the fermentation system and simultaneously concentrated (Ikegami et al., 1997).

O'Brien and Craig (1996) studied a conventional yeast fermentation coupled to a flat-plate membrane pervaporation unit using a commercially available polydimethylsiloxane membrane. A concentrated dextrose was fed to the system and, as a result, an enriched ethanol stream (20-23 wt% ethanol) was continuously recovered from the fermentation broth and a level of 4-6 wt% ethanol was maintained in the fermentation reactor.

Ikegami et al. (1997) also investigated the performance of a coupled fermentation/pervaporation process, but using silicalite membranes. They observed a 20 % increase in an average glucose consumption rate as compared with that without the pervaporation unit. In addition, ethanol concentrations in the permeate reached 85 % (v/v).

Liquid-Liquid Extraction-Fermentation Hybrid

Liquid–liquid extraction combined with fermentation is also employed to remove ethanol and other inhibitory compounds, causing an increase in the ethanol yield (Huang et al., 2008).

Minier and Goma (1981) proposed the coupling of plug flow reactor and liquid-liquid extraction with n-dodecanol as a solvent. Alcoholic fermentations on glucose syrup at 35 °C using *Saccharomyces cerevisiae* was carried out and the results showed that ethanol productivity was multiplied by 5 and a solution of 407 g/L of glucose, considered a highly concentrated feed, was totally fermented.

Gyamerah and Glover (1996) constructed a continuous pilot plant for fermentation production of ethanol, using liquid-liquid extraction to remove the product and with recycle of the fermented broth raffinate. The plant was fed with glucose concentrations in the range 10.0-45.8 wt%, n-dodecanol – used as a solvent – and immobilised yeast to overcome the problem of emulsification. It was observed that for a feed glucose concentration of 45.8 wt%, the aqueous purge was equivalent to 2.8 m^3 of effluent per m^3 of ethanol produced and represented a 78 % reduction in the volume of the aqueous purge compared with using a feed containing 10 wt% glucose.

Continuous fermentation coupled with vacuum flash chamber

Silva et al. (1999) studied the technical viability and the dynamic response of the continuous extractive alcoholic fermentation, which consists of a fermentation reactor coupled with an extractive vacuum flash chamber. Results showed that the temperature could be maintained at desirable levels without using heat exchangers for the temperature control, besides the partial removal of ethanol increased significantly the productivity.

In this context, experiments conducted by Atala (2004) using *Saccharomyces cerevisiae* and concentrated sugarcane molasses, containing up to 330 g/l of sugar, showed that an alcoholic solution of 50 °GL can be obtained. Furthermore, the fermentation reactor operated with concentrations of ethanol at 5 °GL, which is a weakly inhibitory value for the yeast of the process.

CONCLUSION

Novel separations processes have been proposed for ethanol purification and dehydration in order to substitute or assist distillation-based processes.

In order to replace azeotropic and extractive distillation, the most used process for ethanol dehydration in Brazilian biorefineries, adsorption, pervaporation and ultrasonic separation seem to be better alternatives regarding energy consumption and use of eco-friendly separation agents, along with the substitution of fossil-derived solvents in azeotropic and extractive distillation by renewable or less pollutant ones.

Besides, hybrid process such as pervaporation/distillation and integrated fermentation and separation processes may improve the efficiency of the bioethanol production process: by coupling different processes, each process may be employed on its optimum conditions, thus combining their individual advantages.

However, the use of these new processes or solvents faces many barriers in Brazil. One of them is the fact that the Brazilian bioethanol industry is very traditionalist, and new technologies usually take longer to be employed in bioethanol production than in other sectors of the industry. The high capital cost of these new technologies is also an obstacle to the replacement of old processes, especially because several equipments and separating agents are produced abroad.

Improvements on the fermentation step may also improve bioethanol production sustainability when regarding the purification step. Integrated fermentation and separation process, like extractive fermentative processes, allow the continuous removal of ethanol from the fermentor, in order to prevent product inhibition on yeast cells, thus a more concentrated substrate can be supplied to fermentation reactor. Therefore, a wine of higher ethanol concentration can be obtained and, consequently, volumes of residue generated are diminished, as well as energy consumption in the purification step.

It is of fundamental importance to decrease both energy consumption and residue generation on the bioethanol production process. Integration of different fermentation and separation processes, thermal integration of distillation columns, use of less energy-intensive dehydration systems and of more efficient separating agents, as described in this work, are essential to achieve those goals.

3.3. Comentários e Conclusões

Neste capítulo, foram apresentados os processos usuais de separação para a concentração e desidratação do etanol bem como novos processos que possam auxiliar ou substituir processos baseados na destilação.

A avaliação das alternativas indicou que os processos de adsorção, pervaporação e separação ultrassônica são alternativas atraentes para a desidratação do etanol bem como a utilização de agentes de separação ambientalmente amigáveis na destilação extrativa.

Além disso, o uso de processos híbridos como pervaporação/destilação e da fermentação integrada a outros processos de separação podem aumentar a eficiência do processo de separação, uma vez que a combinação dos processos permite utilizar cada um destes em suas condições ótimas.

Por fim, apresenta-se, através da Tabela 3.1, um resumo das aplicações, vantagens e desvantagens de cada processo apresentado na seção 3.2.

Tabela 3.1. Comparação entre os processos apresentados.

Processo	Aplicação	Vantagem	Desvantagem
Destilação múltiplo efeito	Concentração	Redução no consumo de energia/ Menor quantidade de trocadores de calor	Uso de diferentes níveis de pressão pode requerer o emprego de compressores
Destilação Azeotrópica com Cicloexano	Desidratação	Uso da infra-estrutura já existente nas usinas	Uso de agente de separação fóssil e tóxico / Alto consumo energético / Processo de operação complexa
Destilação Azeotrópica com n-Heptano	Desidratação	Pode aproveitar infra-estrutura existente nas usinas / Contaminação por solvente não afeta a qualidade do produto a ser adicionado à gasolina	Uso de agente de separação fóssil e tóxico / Alto consumo energético / Processo de operação complexa
Destilação Extrativa com MEG	Desidratação	Menor consumo de energia comparada à destilação azeotrópica	Uso de agente de separação fóssil e tóxico
Destilação Extrativa com Glicerol	Desidratação	Menor consumo de energia comparado à destilação azeotrópica / Baixo custo do solvente / Solvente não-tóxico e de origem renovável	Decomposição do glicerol (altas temperaturas) gera substância tóxica
Destilação Extrativa com IL/HyPol	Desidratação	Menor consumo de energia / Os solventes podem ser customizados para a separação desejada / Baixa volatilidade permite recuperação sem uso de destilação	IL que possui ânion halogenado é caro e apresenta baixa estabilidade, pode formar substância tóxica e corrosiva
Adsorção em peneiras moleculares	Desidratação	Não apresenta contaminação por solvente / Necessita menos energia do que os processos de destilação	Necessidade de regeneração do leito / Reciclo de solução alcoólica à etapa de concentração / Alto custo das zeólitas (importação)
Pervaporação	Concentração / desidratação	Menor consumo de energia	Presença de sólidos no vinho pode inviabilizar a etapa de concentração / Fluxo limitado
Separação Ultrassônica	Concentração / desidratação	Menor consumo de energia	-
Pervaporação/ Destilação	Concentração / desidratação	Menor consumo de energia comparado à destilação / O acoplamento pode permitir utilizar ambos os processos em suas condições ótimas	-
Fermentação/ Pervaporação	Fermentação/ concentração	Aumento da taxa de reação / Produção de vinho mais concentrado	Presença de sólidos no vinho pode inviabilizar a etapa de concentração
Fermentação/ Extração líquido-líquido	Fermentação/ concentração	Aumento da taxa de reação / Produção de vinho mais concentrado	-
Fermentação extrativa a vácuo	Fermentação/ concentração	Produção de vinho mais concentrado / Dispensa o uso de trocador de calor na fermentação	-

Capítulo 4
Caracterização Termodinâmica

4.1. Introdução

No processo de produção de bioetanol, há uma grande variedade de componentes devido à formação de subprodutos e à ocorrência de reações paralelas na etapa de fermentação. Condições do processo fermentativo, tais como temperatura, pH e concentração de açúcares, influenciam significativamente a composição do vinho produzido. A qualidade da matéria-prima e do fermento utilizados, teor alcoólico do meio, aditivos químicos, tipo do processo fermentativo (batelada ou contínuo) também podem afetar o comportamento da levedura e, consequentemente, induzir à formação de outros compostos.

Portanto, além de etanol e água, podem ser encontrados açúcares, outros alcoóis, ácidos orgânicos, acetaldeído, acetona e glicerol. Considerando-se a produção de bioetanol de 2ª geração, tem-se que a hidrólise do bagaço de cana-de-açúcar pode também gerar furfural, 5-hidroxi-metil-furfural (HMF) e pentose.

Com relação ao processo de desidratação do etanol, a destilação azeotrópica com cicloexano e a destilação extrativa com monoetilenoglicol também são baseadas no equilíbrio de fases, sendo importante também a consideração destes componentes na caracterização do sistema.

A caracterização do sistema é essencial para entender o comportamento dos componentes nas colunas de destilação, portanto a utilização de modelos termodinâmicos apropriados para representar o sistema é de grande importância na simulação de processos.

Com o intuito de avaliar a acurácia dos modelos termodinâmicos presentes no banco de dados do simulador Aspen Plus®, foram pesquisados na literatura dados experimentais de equilíbrio para os binários presentes no sistema. Em seguida, estes dados foram comparados com os resultados fornecidos pelo simulador utilizando os modelos de coeficientes de atividade UNIQUAC (*Universal Quasi-Chemical*) e NRTL (*Non-Random Two Liquid*).

Realizou-se também a análise de diagramas T-x-y e y-x a fim de observar a ocorrência de não-idealidades, como azeotropia, miscibilidade parcial e baixa e alta volatilidade relativa.

Na Tabela 4.1 são apresentados os componentes considerados na análise dos modelos termodinâmicos bem como as respectivas temperaturas de ebulição estimadas pelo simulador Aspen Plus®.

Tabela 4.1. Temperaturas de ebulição dos componentes envolvidos no processo de produção de bioetanol a pressão atmosférica.

Componente	**Temperatura de ebulição (ºC)**
Acetaldeído	21,1
Acetona	56,1
Metanol	64,5
Acetato de Etila	77,2
Etanol	78,3
Cicloexano	80,8
n-Propanol	97,2
Água	100,0
Isobutanol	107,7
n-Butanol	117,7
Ácido Acético	118,0
Álcool Isoamílico	130,9
Furfural	161,4
Monoetilenoglicol	197,1
Glicerol	287,7
Glicose	343,8
Sacarose	477,7

O desenvolvimento deste capítulo é apresentado a seguir no trabalho intitulado *"Phase equilibrium data for binary mixtures in bioethanol production - evaluation of thermodynamic models adequacy"* a ser submetido a periódico internacional.

4.2. Phase equilibrium data for binary mixtures in bioethanol production - evaluation of thermodynamic models adequacy

ABSTRACT

One of the most important tools used to evaluate new technologies and alternative processes is the process simulation software. In order to appropriately represent the thermodynamic properties of a system, thermodynamic models employed must be consistent with experimental phase equilibrium data.

In bioethanol production, a large number of components are found due to the complexity of the raw material and to the generation of a number of products during fermentation reactions, thus increasing complexity of the thermodynamic representation of the bioethanol production process. The purification step is mainly based on distillation process, and as such it is strongly dependent on vapor-liquid or vapor-liquid-liquid equilibrium.

In this work a phase equilibrium study of components found in bioethanol production was carried out using results predicted by Aspen Plus® and experimental data available in the literature. Several deviations from ideal behaviour were observed for many binary systems.

INTRODUCTION

Improvements on bioethanol production process have been increasingly investigated, mainly due to climate change and predicted depletion of fossil resources. One of the most important tools used to study process alternatives and to evaluate their impacts on process yields, energy consumption and costs is the process simulation software. Nevertheless, the simulation must employ the appropriate thermodynamic models to properly predict process behavior (Cardona and Sánchez, 2007). The thermodynamic models provided in the databanks also determine the efficiency of simulation packages (Abderafi and Bounahmidi, 1994).

The reliable knowledge of the thermophysical properties of the pure compounds and their binary and higher mixtures is essential for the design and optimization of chemical processes. Considering specially the separation processes, the reliable knowledge of the phase equilibrium behaviour of the

systems considered is of special importance (Gmehling, 2009).

A large number of components are found in the bioethanol production process due to fermentation by-products and parallel reactions. Process fermentation conditions, such as temperature, pH and sugars concentration, significantly influence the composition of the wine produced. Ethanol and water are the main components found in wine; however, methanol, propanol, isobutanol, isoamyl alcohol, acetaldehyde, acetone, acetic and succinic acids, ethyl acetate, glycerol, glucose and sucrose are also present in low concentrations. Considering the production of 2nd generation bioethanol, furfural, 5-hydroxymethyl-furfural and pentose might be present as well, depending on the chosen hydrolysis process.

In addition, in the purification process, extractive distillation with monoethyleneglycol as solvent and azeotropic distillation with cyclohexane as entrainer can be employed in order to obtain anhydrous bioethanol. These operations are based on the phase equilibrium, so a previous detailed study about these component interactions is necessary to understand columns behaviour and to predict more accurate results.

For instance, Faúndez and Valderrama (2004) analyzed binaries of ethanol and water with congeners through calculation of deviations between predicted and experimental temperatures and vapor mole fractions. NRTL model, PSRK equation of state and UNIFAC method were considered in this evaluation and it was observed that NRTL model suitably represents the system. However, sugars and entrainers employed in ethanol dehydration were not taken into account in their work.

In this work, a phase equilibrium study was carried out using results predicted by Aspen Plus® and experimental data available in the literature. Non-Random Two-Liquid (NRTL) and Universal Quasi-Chemical (UNIQUAC) thermodynamic models for calculation of the activity coefficient on the liquid phase were employed and compared to experimental data, in order to evaluate if they represent the system behaviours appropriately. Furthermore, non-ideal behaviours were evaluated in order to understand the interaction between components in the mixture.

DATA AVAILABLE IN THE LITERATURE

The first step to evaluate the relevant data consisted on selecting the most important components present on bioethanol production. Those include besides water and ethanol, sugarcane components, such as glucose and sucrose, by-products generated during fermentation reactions, such as other alcohols, organic acids, acetaldehyde, acetone, and glycerol, as well as components that may be generated on 2nd generation bioethanol production, like furfural, 5-hydroxymethyl-furfural (HMF) and pentose.

Secondly, an extensive research was carried out to determine which binaries are available in the literature. The first sources consulted were the DECHEMA equilibrium data collections (Gmehling et al., 1982a-c; Gmehling et al., 1981; Gmehling, 1993); data for binary pairs not available in those sources were searched for in journals. Data for most of the pairs containing water or ethanol was obtained. On Table 4.2 the references for each binary pair is depicted.

Table 4.2. Sources for the binary pairs equilibrium data.

Component	1	2	3	4	5	6	7	8	9	10	11	12	13	14	15
1- Ethanol															
2- Water	2,10														
3- Methanol	2,10	10													
4- Propanol		4	3												
5- Isobutanol	2	4	3												
6- n-Butanol		4	3		3										
7-Isoamyl alcohol	2,16				3										
8- Acetaldehyde	12	12,4	3			3									
9-Acetone	8,6		15					6							
10- Acetic acid	2	4	17				11	6							
11- Ethyl acetate	2	5				5	16			18					
12- Glycerol	7	4,7,9	7	7		7									
13- Glucose		1													
14- Sucrose		1													
15- Furfural	13	6							6	14	6				

[1] Abderafi & Bounahmidi (1994)
[2] Gmehling et al. (1982a)
[3] Gmehling et al. (1982b)
[4] Gmehling et al. (1981)
[5] Gmehling et al. (1982c)
[6] Gmehling (1993)
[7] Oliveira et al. (2009)
[8] Lee & Hu (1995)
[9] Chen & Thompson (1970)
[10] Christensen (1998)
[11] Lee et al. (2000)
[12] d'Avila & Silva (1970)
[13] Wisniak & Polishuk (1999)
[14] Fele & Grilc (2003)
[15] Tu et al. (1997)
[16] Sanz & Gmehling (2008)
[17] Arlt (1999)
[18] Kato (1988)

The next step consisted of plotting experimental data along with that predicted using NRTL and UNIQUAC models with the Aspen Plus® process simulator. A large number of plots was generated, for instance, a T-x-y diagram for the ethanol – water system is shown on Figure 4.1 to provide an example of what was done for all the binaries cited in Table 4.2.

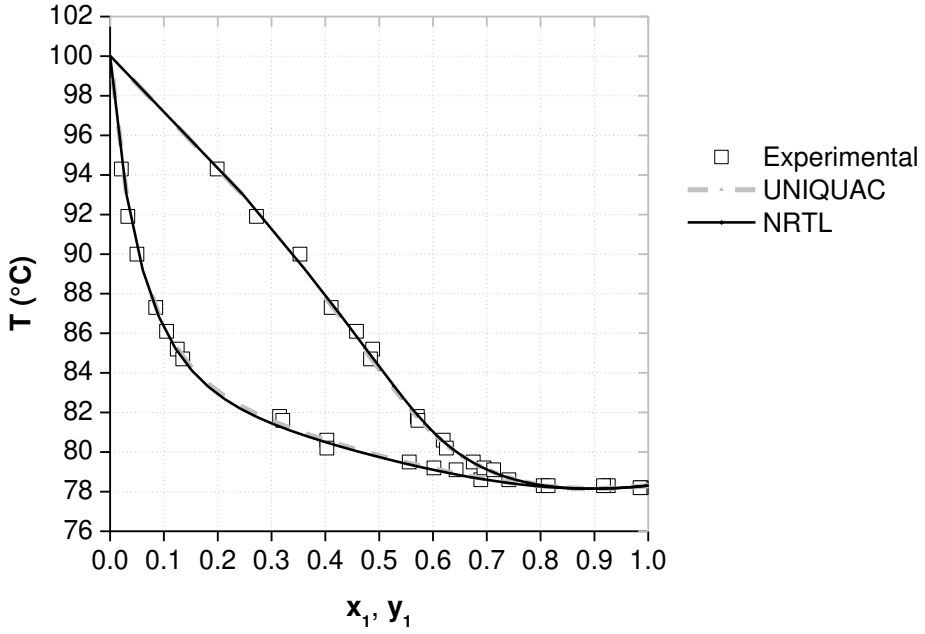

Figure 4.1. T-x-y diagram for the ethanol (1) - water (2) system, at 760 mm Hg.

Thus, it is possible to evaluate if the two models employed for calculation of the activity coefficient on the liquid phase (NRTL and UNIQUAC) are in agreement with experimental data. In the case of ethanol and water, both models represent appropriately the system behavior, including the azeotrope.

Most of the systems were suitably represented by both NRTL and UNIQUAC models, with a few systems being represented better by NRTL and some by none. Table 4.3 summarizes the results of the comparison between experimental data and the thermodynamic models, indicating the model that better represents each binary.

Table 4.3. Representative model for each binary.

Component	1	2	3	4	5	6	7	8	9	10	11
1- Ethanol											
2- Water	Both										
3- Methanol	Both	Both									
4- Propanol		Both	Both								
5- Isobutanol	Both	Both	Both								
6- n-Butanol		Both	Both		Both						
7-Isoamyl alcohol	Both				Both						
8- Acetaldehyde	Both	Both	Both			Both					
9-Acetone	Both		Both					Both			
10- Acetic acid	Both	Both	Both				NRTL	Both			
11-Ethyl acetate	Both	Both				Both	Both			Both	
12- Glycerol	Both	None	Both	Both		Both					
13- Glucose		None									
14- Sucrose		None									
15- Furfural	Both	Both							Both	NRTL	Both

Binary interaction parameters available in the process simulator were checked, since a collection of built-in binary parameters for the activity coefficient models (NRTL and UNIQUAC) are available in Aspen Plus® database, as well as some equation-of-state (EOS) models and Henry's law, different databank parameters are available (Aspen Plus Help, 2000). For instance, these comprise VLE-IG (NRTL and UNIQUAC models with ideal gas vapor EOS), VLE-HOC (Wilson, NRTL and UNIQUAC models with Hayden-O'Connell vapor EOS), VLE-LIT (NRTL and UNIQUAC models with ideal gas vapor EOS, obtained from the literature). Even though on the majority of the cases the appropriate databank is automatically chosen, in some situations parameters retrieved from VLE-HOC represented the process behavior more accurately. This was the case in the parameters containing acetic acid, as an example.

The most significant deviation of the experimental data was verified in the binary pairs containing water and sugar (sucrose and glucose), for which both NRTL and UNIQUAC models predicted the boiling point temperature in accordance with experimental data (Abderafi and Bounahmidi, 1994) only for solutions with low sugar content (less than 10 %). However, different works predicting binary or

thermodynamic data for sugar systems are available in the literature (Abderafi and Bounahmidi, 1999; Peres and Macedo, 1997) using UNIFAC or other property methods. For example, T-x diagram for the binary water-sucrose is shown in Figure 4.2. From this figure, it is observed that UNIQUAC provided a slightly better prediction, since its curve coincides with experimental data until 20 % (mole basis).

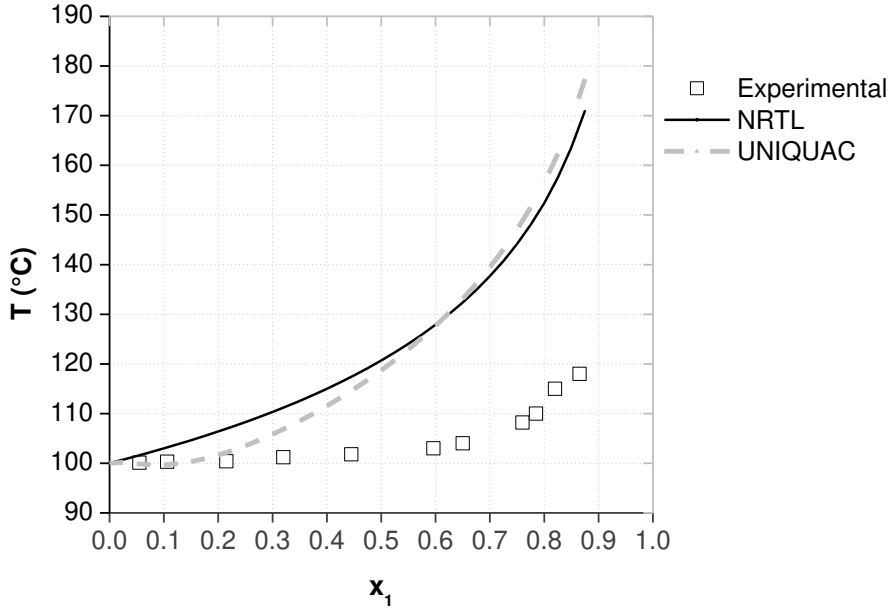

Figure 4.2. T-x diagram for the sucrose (1) - water (2) system, at 760 mm Hg.

In addition, for the pairs acetic acid – furfural or isoamyl alcohol, only the NRTL model (with VLE-HOC parameters) suitably represented experimental data. For instance, T-x-y diagram for acetic acid – furfural is depicted in Figure 4.3. In this case, prediction of the system behavior given by UNIQUAC model was erroneous, since it forecasted an azeotrope between acetic acid and furfural that does not exist in practice as shown by experimental data (Fele and Grilc, 2003).

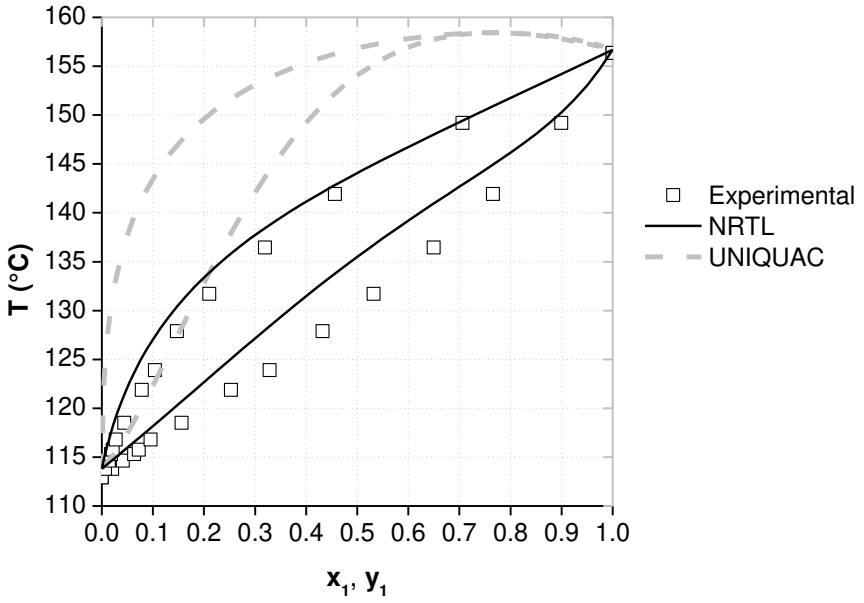

Figure 4.3. T-x-y diagram for the acetic acid (1) - furfural (2) system, at 667 mmHg.

For water-glycerol system, NRTL and UNIQUAC provided a correct representation only for the liquid phase as can be seen in Figure 4.4.

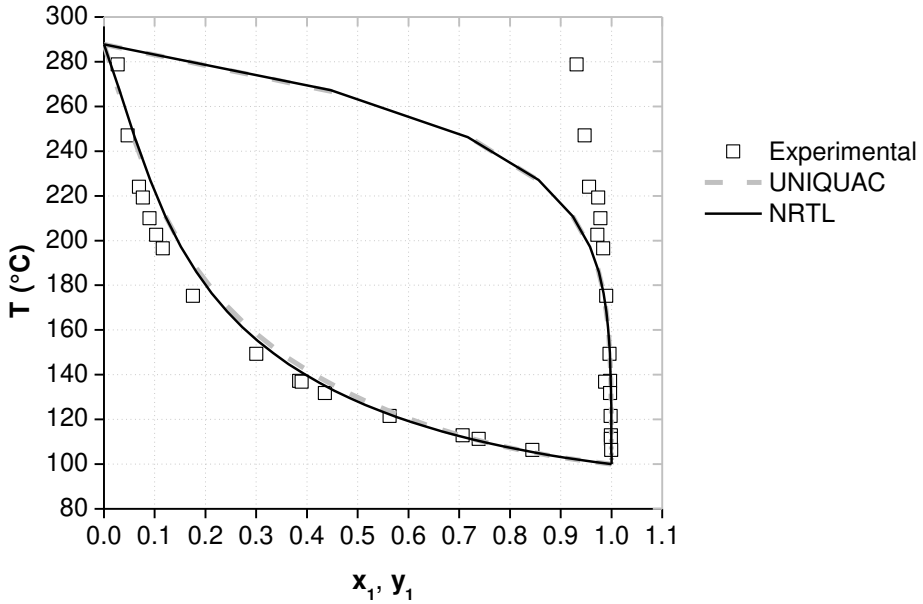

Figure 4.4. T-x-y diagram for the water (1) - glycerol (2) system, at 760 mm Hg.

In spite of the mentioned divergences, NRTL equation yields the best overall results for the binary mixtures investigated in this work. However, UNIQUAC also provides satisfactory predictions for the main binaries present in the mixture.

Regarding system behavior, several deviations from ideality were verified, such as low and high relative volatility, azeotropes and the formation of two liquid phases. These characteristics are assembled in Table 4.4.

Table 4.4. Behavior of selected binary pairs.

Behavior	**Binary Pairs**				
Azeotrope	Ethanol - Water	Ethyl acetate - Water	Water - Propanol	n-Butanol - Water	Isobutanol - Water
	Isoamyl alcohol - Acetic acid	Acetone - Methanol	Water - Furfural	Ethyl acetate - Ethanol	
Two liquid phases	Water – Propanol	n-Butanol - Water	Isobutanol - Water	Ethyl acetate - Water	Water - Furfural
Low relative volatility	Ethanol - Methanol	Acetone - Ethanol	Acetone- Methanol	Ethyl acetate - Ethanol	
	Isobutanol – Butanol	Isobutanol – Isoamyl alcohol	Acetic acid - Isoamyl alcohol	Ethanol - Isobutanol	
	Acetaldehyde – Acetone	Ethanol - Acetic acid	Acetic acid - Water	Acetic acid - furfural	
High relative volatility	Glycerol - Ethanol	Glycerol - Water	Glycerol - Methanol	Glycerol - Propanol	
	n-Butanol - Acetaldehyde	Furfural - Ethanol	Water - Acetaldehyde		

DATA NOT AVAILABLE IN THE LITERATURE

Vapor-liquid equilibrium (VLE) data was not found in the literature for several pairs encountered among the components studied in this work. For some reactive systems, such as those present in alcohol – acid systems, experimental data are found only for low temperatures, on which esterification reactions are very slow (Arlt, 1999), thus special equipment is needed to acquire VLE data. Arlt (1999) developed an apparatus to acquire data for such systems (e.g., methanol – acetic acid), but only data for the liquid phase was obtained due to problems in determining vapor phase composition. For several pairs, only experimental data for the liquid phase and either the boiling temperature or vapor phase composition were obtained and, in these situations, the data available was plotted and compared in different diagrams, such as x-y diagrams. This was the case for some of the glycerol-containing pairs, for instance.

Data for binary pairs containing either HMF (5-hydroxymethyl-furfural) or pentose were not found in the literature. HMF is an important by-product of cellulose hydrolysis derived from glucose decomposition, but it is not available on the process simulator database. It would be important to gather that data and to make this component available in the database of Aspen Plus®.

Data for binary pairs involving succinic acid were not found as well. Even though its concentration remains at low levels during bioethanol production process, succinic acid is a very important carboxylic acid produced during alcoholic fermentation. Thus, experimental equilibrium data for this component is important as well.

DEHYDRATION COMPONENTS

A separate study was carried out to verify equilibrium data for components present on the dehydration operations. The most frequently employed distillation-based separation processes (extractive distillation with monoethyleneglycol, MEG, and azeotropic distillation with cyclohexane) were considered. Since those processes use hydrous ethanol produced on the distillation columns, only ethanol, water and entrainer (monoethyleneglycol and cyclohexane) are considered.

Since a heterogeneous azeotrope is formed between water, ethanol and cyclohexane, a ternary diagram for the liquid-liquid equilibrium between those components was made (Gomis et al., 2005), besides the individual binary pair for VLE data. It was verified that both models represent the ternary liquid-liquid equilibrium of the system appropriately; the ternary diagram is depicted in Figure 4.5.

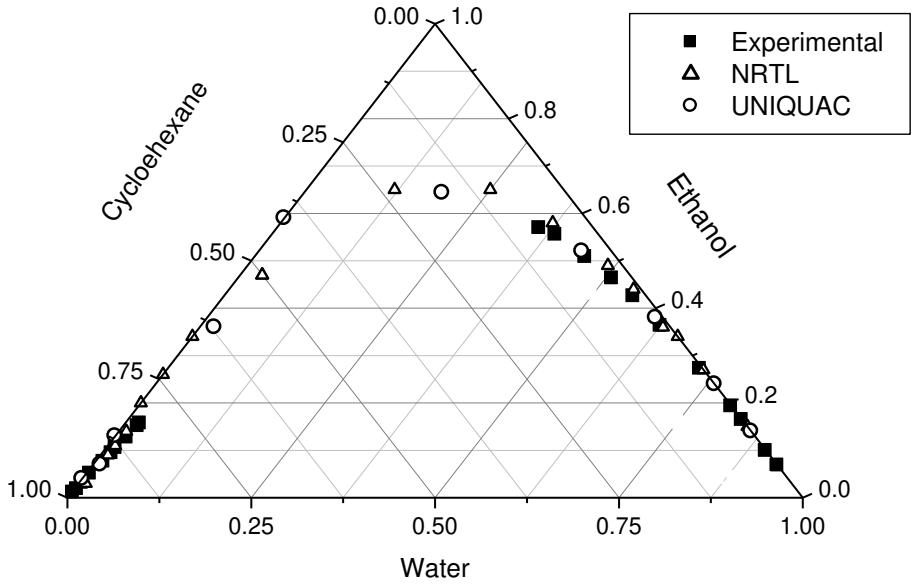

Figure 4.5. Ternary diagram for the ethanol – water - cyclohexane system, at 760 mmHg and 35 ºC.

Data for the binary system ethanol – MEG (Gmehling et al., 1982a) and water – MEG (Gmehling et al., 1981) are illustrated in Figures 4.6 and 4.7. NRTL and UNIQUAC provided the same predictions and appropriately represented the system, except for liquid phase in the T-x-y diagram for binary water – MEG.

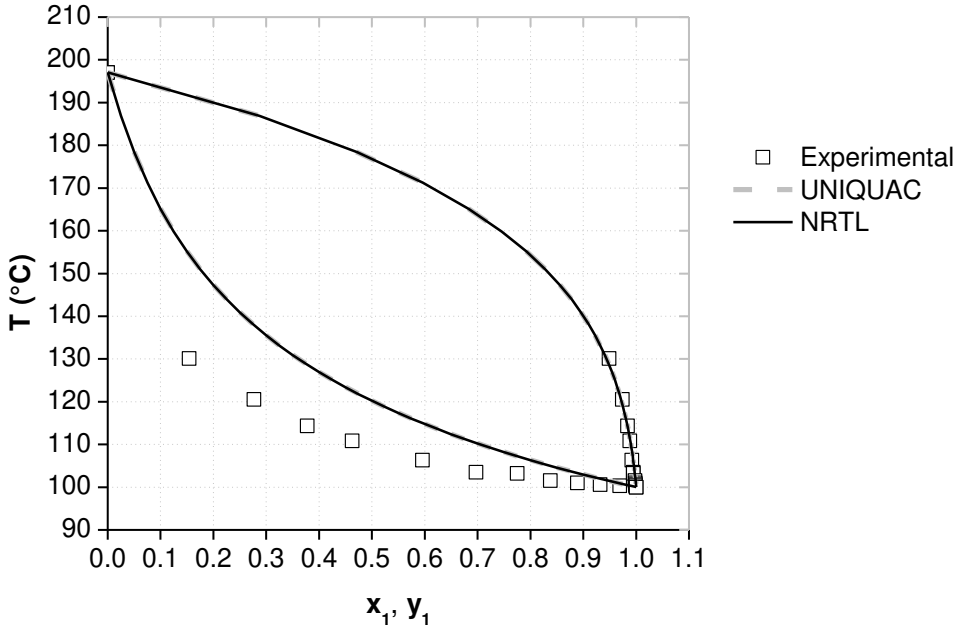

Figure 4.6. T-x-y diagram for the water (1) – MEG (2) system, at 760 mmHg.

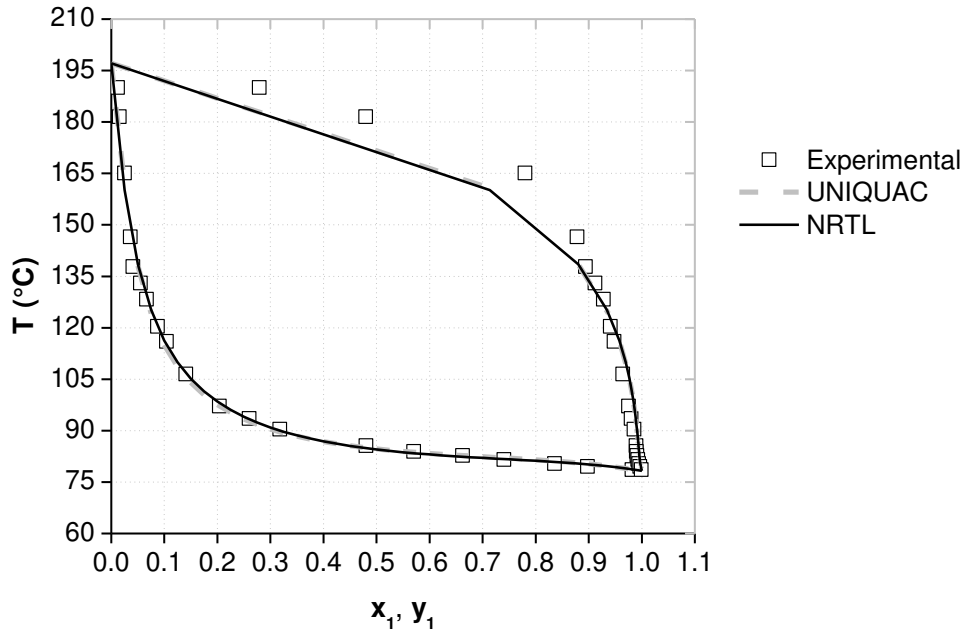

Figure 4.7. T-x-y diagram for the ethanol (1) – MEG (2) system, at 760 mmHg.

CONCLUSIONS

Experimental data for binary systems present in bioethanol production process were gathered in this work and compared to estimated data using process simulator Aspen Plus® and the models for calculation of the activity coefficient on the liquid phase NRTL and UNIQUAC. T-x-y and y-x diagrams were obtained and evaluated for all binaries found in the bioethanol production process, and it was observed that the mixtures have a highly non-ideal behaviour, since azeotropes, low and high relative volatility, partial miscibility were predicted for some binaries.

It was found that data for the most important compounds present during ethanol distillation, on which vapor-liquid equilibrium is of upmost importance, were in accordance with experimental data. Only a few binary pairs between components present in low concentrations in the distillation stage, such as fermentation by-products and sugars, were not represented by the studied models appropriately.

This work assembles the data available in the literature and establishes NRTL and UNIQUAC as suitable models for predicting phase equilibrium in the bioethanol production process. Besides, a complete analysis of all binaries, as

showed in this work, has not been published yet and will assist the development of other studies in this area. This study also revealed that equilibrium data are not available for several pairs of components (e.g., 5-hydroxymethyl-furfural, pentose, succinic acid), emphasizing the need of further experiments regarding compounds present in bioethanol production and their phase equilibrium.

4.3. Comentários e Conclusões

A comparação dos dados experimentais com os resultados do simulador Aspen Plus® permitiu observar que os modelos UNIQUAC e NRTL predizem satisfatoriamente o equilíbrio neste sistema, sendo que o NRTL apresentou resultados ligeiramente superiores ao UNIQUAC. Observou-se ainda a necessidade de se considerar a não-idealidade da fase vapor sendo empregada a correlação de Hayden-O'Connell para a predição da dimerização do ácido acético nesta fase.

Verificou-se também a ausência de dados experimentais para diversos pares, principalmente para os que incluem componentes gerados no processo de produção de álcool de segunda geração.

Os resultados mostraram ainda que o sistema é bastante não ideal, visto que foram verificadas ocorrências de azeotropia, baixa e alta volatilidade relativa, formação de duas fases líquidas entre os componentes.

Considerando-se os resultados obtidos neste capítulo, optou-se por adotar o modelo NRTL-HOC neste trabalho, com o qual foram calculados os dados de equilíbrios sob a forma de diagramas y-x para a pressão atmosférica apresentados no Apêndice. Vale ressaltar que as curvas de equilíbrio representam a interação binária entre os componentes, uma vez que o equilíbrio pode ser alterado pelo fato do sistema ser multicomponente. Dessa forma, os diagramas foram empregados apenas para estimar o comportamento dos componentes na coluna.

Capítulo 5
Avaliação dos Métodos de Cálculo para a Destilação Convencional na Produção de Bioetanol

5.1. Introdução

Neste capítulo é apresentada a avaliação da etapa de destilação empregada para a concentração do vinho com a finalidade de produzir bioetanol hidratado (93 % em massa).

O processo de destilação apresenta considerável consumo de energia, a qual é provida através da geração de vapor por meio da queima de bagaço. Como afirmado anteriormente, o bagaço pode ser utilizado para a cogeração de eletricidade ou para a produção de bioetanol através da hidrólise, portanto a redução no consumo de vapor é desejável a fim de aumentar os excedentes de bagaço. Por esta razão, a simulação do processo de destilação deve ser a mais representativa possível a fim de que as propostas de otimização avaliadas através desta possam ser implementadas em uma planta real.

No entanto, simuladores de processos usualmente utilizam a modelagem de estágios de equilíbrio para realizar os cálculos das colunas de destilação. Útil para estimativas iniciais e comparação entre configurações alternativas, esta modelagem é baseada no conceito idealizado de estágios teóricos, embora na prática essa suposição seja raramente aplicável. Com o intuito de considerar os desvios do equilíbrio, a modelagem de estágios de equilíbrio pode incorporar eficiências em seus cálculos.

Para obtenção de estimativas mais realistas, é indicado o uso da modelagem de estágios de não equilíbrio, o qual considera as equações de transporte que descrevem os fenômenos de transferência de massa e energia e assume que o equilíbrio ocorre apenas na interface líquido-vapor.

Neste trabalho, utilizando-se como base a composição média do vinho delevedurado apresentada por Dias (2008) bem como a configuração das colunas de destilação também fornecida por esta autora, foram realizadas simulações do

processo de destilação através de diferentes métodos de cálculos. Foram consideradas as modelagens de estágios de equilíbrio e de não equilíbrio bem como a aplicação da correlação de Barros e Wolf para a determinação das eficiências de prato e componente. A modelagem de estágios de não equilíbrio, por ser mais rigorosa, foi utilizada como base para a avaliação dos resultados.

O desenvolvimento deste capítulo é apresentado a seguir no artigo intitulado *"Bioethanol Production Process: assessment of different calculation methods for conventional distillation"* a ser submetido a periódico internacional.

5.2. Bioethanol Production Process: assessment of different calculation methods for conventional distillation

ABSTRACT

Distillation operation requires a significant amount of energy and, consequently, it represents a considerable contribution to the bioethanol production costs. This is a motivation to carry out extensive studies so that there exist incentive to simulate this unit operation as representative as possible and the use of nonequilibrium stage model is usually recommended since it is a rigorous calculation method. However, most models available for simulation of multicomponent separation processes are based on the idealized concept of equilibrium or theoretical stages. In order to take into account the deviation from equilibrium, a usual alternative is the consideration of efficiencies in the equilibrium stage model, thus the estimation method of these efficiencies has considerable effects in the simulation results. In this work, Barros & Wolf efficiency correlations for plate and component were evaluated through comparison with nonequilibrium stage model for hydrous bioethanol production process. It was observed that plate efficiencies are around 50 % and component efficiency is very sensitive to component properties. A satisfactory agreement was achieved when results were compared to those obtained using nonequilibrium stage model. Besides, constant efficiencies were also assessed, showing that an efficiency of 70 % as global efficiency is a reasonable estimative for this process.

INTRODUCTION

Bioethanol has been increasingly used as substitute or additive to gasoline, since it is a renewable fuel and its combustion discharges less greenhouse gases when compared to fossil-derived fuels. In Brazil, second largest producer in the world, it is typically produced through fermentation of sugars derived from sugarcane.

In order to be used as a fuel, wine obtained from fermentation process must be concentrated to about 93 wt% of ethanol (hydrous bioethanol), which requires distillation process. Besides, for bioethanol being used as gasoline additive, further processes are necessary, since water and ethanol form an azeotrope with 95.6 wt% ethanol at 1 atm. Thus, conventional distillation cannot reach anhydrous bioethanol specification (approximately 99.5 wt%). Azeotropic distillation with cyclohexane as entrainer, extractive distillation with monoethyleneglycol as solvent and adsorption onto molecular sieves are possible and usual alternatives for bioethanol dehydration.

In view of the fact that distillation operations require a significant amount of energy and have a great importance in bioethanol production, the simulation of this unit operation has to be as representative as possible. However, most available models for separation process simulation are based on the idealized concept of equilibrium or theoretical stages, although, in practice, columns rarely operate under thermodynamic equilibrium conditions. To take into account the deviations from equilibrium, an efficiency value can be introduced in the calculations. In fact, predictions can be more accurate if a nonequilibrium stage model is considered; nevertheless the calculations are quite complex, thus taking more computational time, which is not desirable in advanced control applications. Besides, design parameters are needed in order to perform these calculations.

Nonequilibrium stage model of multicomponent separation processes was first described by Krishnamurthy and Taylor (1985); their results showed that equilibrium and nonequilibrium stage model provided predictions quite different from each other. In the nonequilibrium stage model, conservation equations are

written for each phase independently and solved together with transport equations that describe mass and energy transfers in multicomponent mixtures; also it is assumed that equilibrium occurs only in the vapor-liquid interface. Besides, in this way, the empirical correcting factors, such as efficiencies used in the equilibrium model, are no longer necessary (Pescarini et al., 1996).

Several works have been developed regarding comparison between nonequilibrium stage model and experimental data. For instance, Springer et al. (2002) realized experiments in a bubble cap distillation column with the system water – ethanol – methylacetate and showed that the predictions of nonequilibrium stage model present considerably better agreement with experimental data than those of the equilibrium stage model. In addition, Repke et al. (2004) carried out the validation of the developed nonequilibrium stage model in a pilot packed column and concluded that nonequilibrium stage model describes the experimental data with a good accuracy.

Equilibrium stage model with efficiency can supply accurate results provided that efficiencies are estimated properly. In this context, the Barros & Wolf efficiency correlation can be used to calculate plate efficiencies for conventional distillation columns (Wolf-Maciel et al., 2001). This correlation was obtained based on techniques of factorial design and it is dependent on the properties of the mixture, such as thermal conductivity, density, heat capacity and diffusivity, which vary with efficiency. This correlation was evaluated for some systems by comparison with results given by nonequilibrium stage model and experimental data and it was observed that equilibrium stage model with Barros and Wolf correlation for efficiency can represent a real non- ideal process.

In this work, simulations of distillation process in bioethanol production were carried out in Aspen Plus®, considering equilibrium stage model with constant plate efficiency, with Barros & Wolf efficiency correlation and nonequilibrium stage model.

PROCESS SIMULATION

Initial Information

The distillation process simulated was based on the traditional Brazilian biorefineries configuration employed to produce hydrous bioethanol.

Usual configuration consists of a series of distillation and rectification columns as depicted in Figure 5.1. Wine, produced in the fermentation stage, is fed to column A1. Column D is responsible for removing volatile contaminants at the top, while a large amount of water (stillage or vinasse) is obtained in the bottom of column A. Vapor phlegm produced near to the top of column A and liquid phlegm obtained at the bottom of column D are sent to rectification columns. The task of the rectification consists on the concentration of the phlegm streams from 40-50 wt% to 93 wt% ethanol (hydrous bioethanol).

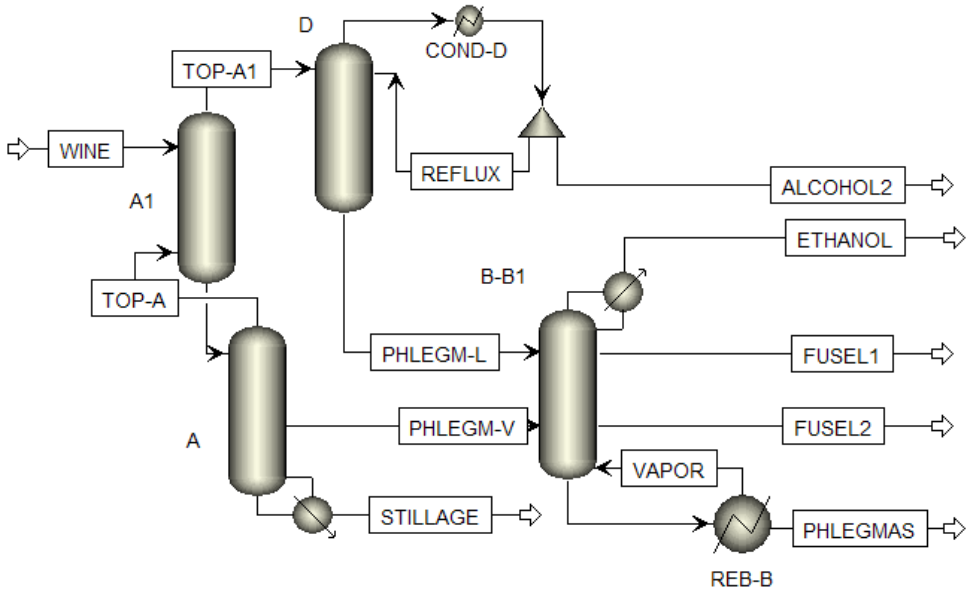

Figure 5.1. Configuration of the simulated process.

In Table 5.1, columns conditions and specifications are summarized. Stages numbering is initiated in the top stage or condenser, when it is present and coupled reboiler, as in column A, is considered the last stage. The distillation stage was simulated considering a wine flow rate of 207 t/h, based on a distillation unit employed in a Brazilian biorefinery.

Table 5.1. Distillation columns conditions and specifications

Column A	
Number of stages	19
Feed stage	1
Top pressure (kPa)	139.3
Bottom pressure (kPa)	152.5
PHLEGM-V withdrawal stage	2 (vapor phase)
PHLEGM-V rate (kg/h)	30000
Distillate rate (kg/h)	12750
Column A1	
Number of stages	8
Feed stage: WINE	1
TOP-A	8
Top pressure (kPa)	136.3
Bottom pressure (kPa)	139.3
Column D	
Number of stages	6
Feed stage: REFLUX	1
TOP-A1	6
Top pressure (kPa)	133.8
Bottom pressure (kPa)	136.3
Column B-B1	
Number of stages	46
Feed stage: PHLEGM-L	22
PHLEGM-V	22
VAPOR	46
Top pressure (kPa)	116.0
Bottom pressure (kPa)	135.7
FUSEL withdrawal stages	21 and 45 (liquid phase)
FUSEL rates (kg/h)	500 and 300
Distillate rate (kg/h)	16100

Wine composition, also proceeding from biorefinery data, is given in Table 5.2. This data showed that other components, such as acetaldehyde, acetone, acetal, n-propanol, isobutanol, n-butanol and acetic acid, are also present in the wine; however they represent less than 0.1 % in the composition and were disregarded in this work.

Table 5.2. Composition of wine fed to distillation process.

Component	Mass fraction
Water	0.920
Ethanol	0.073
Glycerol	0.004
Isoamyl alcohol	0.002
Glucose	0.001

Simulation Procedure

The adequacy of thermodynamic models to represent the system was evaluated by comparison between vapor-liquid and vapor-liquid-liquid equilibrium results given by Aspen Plus® and available experimental data (Gmehling and Onken, 1977). Aspen Plus® simulator supplies binary parameters from its databank and uses them automatically. Results showed that NRTL model for the activity coefficient provides very accurate predictions. For this reason, it was used to calculate these coefficients for the liquid phase.

Three different approaches were used in the simulation of this distillation process regarding to column calculations: equilibrium model with constant plate efficiencies (100, 85, 70 and 55 %), equilibrium model with Barros & Wolf efficiency correlation for plate and component and nonequilibrium model. All simulations considered condenser and reboiler as an equilibrium stage.

Configuration of the distillation process and specifications of the columns were the same for all approaches. In all simulations, condenser and reboiler were considered as equilibrium stages.

Nonequilibrium stage model simulation (NEQ)

In the nonequilibrium stage model, which is a more rigorous calculation, the RateFrac™ model was employed. This model calculates the product of the binary mass transfer coefficients and interfacial areas using the correlations developed by Gerster and co-workers (1958); the vapor phase and liquid phase heat transfer coefficients are determined using the Chilton-Colburn analogy. In general, these quantities depend on column diameter and operating parameters. Tray type was defined as bubble cap and column diameter was calculated based on the approach of flooding on the stage where it is most critical (Aspen Technology, 2001).

Parameters used in calculations, such as vapor and liquid flows, densities, viscosities, surface tension of liquid, vapor and liquid phase binary diffusion coefficients, are all estimated through equations present in Aspen Plus®.

Equilibrium stage model simulation with constant efficiency (EQ)

In order to perform equilibrium stage model simulations, RadFrac™ model in Aspen Plus® software is used, which performs calculation using the MESH equations (mass, equilibrium, summation and heat). In this case, number of stages and feed inlet positions are specified together with the specification given in Table 5.1. Efficiencies were inserted as Murphree efficiency and were considered the same for all stages: 100, 85, 70 and 55 % in cases EQ100, EQ85, EQ70 and EQ55, respectively.

Equilibrium stage model simulation with Barros & Wolf efficiency correlation (Eff)

For these simulations, column distillation model is also RadFrac™ (equilibrium calculation). In this case, number of stages and feed inlet positions are specified as well as the efficiencies calculated through Barros & Wolf correlation (Equation 5.1), which are included as Murphree efficiencies (Barros, 1997).

$$Eff(i) = 38.5309\left[\frac{k(i)\rho(i)D(i)MW(i)}{Cp(i)\mu^2(i)}\right]^{-0.04516} \qquad (5.1)$$

In Equation 5.1, Eff(i) is the plate efficiency (Eff-plate) described as a function of the following mixture properties in each stage (i): thermal conductivity (k), density (ρ), diffusivity (D), molecular weight (MW), heat capacity (Cp) and viscosity (μ). These properties are calculated for all stages in the distillation columns using Aspen Plus®. For component efficiencies (Eff-comp), instead of mixture properties in the plate, individual component properties are considered in Equation 5.1.

The determination of these efficiencies is an iterative method, since the first simulation is carried out using an efficiency of 100 %, then the calculated properties are used to predict efficiencies through Barros & Wolf correlation. Subsequently, these efficiencies are inserted in the simulation and the properties are recalculated, thus new efficiencies values are obtained. This procedure is repeated until the difference between two consecutive efficiency iterations reaches

a level of tolerance below 1.10^{-4}. Generally, three iterations are enough to determine efficiencies within the specified tolerance.

RESULTS AND DISCUSSION

Sidestream Withdrawal

Since fusel oil has a significant commercial value, its recovery is essential to the process. Fusel oil (FUSEL stream) consists of heavy alcohols, such as isoamyl alcohol. The fusel oil withdrawal position was determined by analysing isoamyl alcohol mass fraction in liquid phase using equilibrium model as base case. Column B-B1 composition profiles can be seen in Figure 5.2.

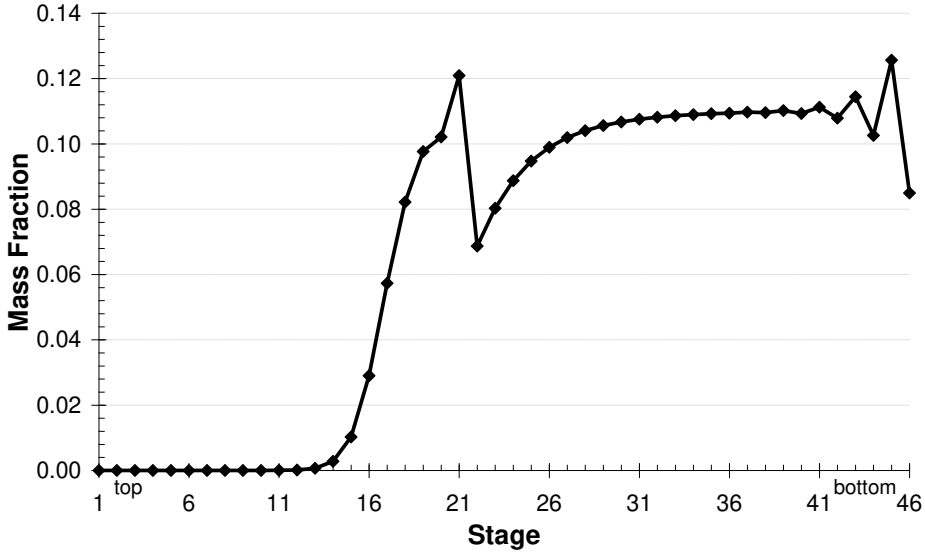

Figure 5.2. Isoamyl alcohol mass fraction profile in column B-B1 for equilibrium model simulation.

From Figure 5.2 can be observed that stages 21 and 45 present the highest mass fractions of isoamyl alcohol, thus sidestreams were withdrawn from these stages.

Nonequilibrium Stage Model

Simulation using nonequilibrium stage model presented more convergence problems and took more time to provide results when compared to other models, which was expected since it takes into account more equations. For instance, equilibrium calculation solves 2nc+1 equations for each stage while nonequilibrium

solves 5nc+3 equations, where nc is the number of components (Pescarini et al., 1996), consequently, 11 and 28 equations, respectively, per stage in the situation considered in this work.

Since nonequilibrium stage model takes into account mass and energy transfer phenomena, it is more rigorous and complex than equilibrium stage model. In addition, predictions given by nonequilibrium model are usually more accurate when compared to experimental results (Repke et al., 2004; Springer et al., 2002). For these reasons, it will be used to evaluate other calculation approaches considered in this work.

Main stream results obtained with nonequilibrium stage model are shown in Table 5.3.

Table 5.3. Main stream results given by nonequilibrium model.

Stream	STILLAGE	PHLEGMAS	ETHANOL	FUSEL1	FUSEL2
Temperature (°C)	111.9	106.0	81.7	93.1	100.9
Mass Flow (kg/h)	175347.2	14693.2	16100.0	500.0	300.0
Water (wt%)	99.4	98.8	7.0	48.3	62.2
Glucose (wt%)	0.1	-	-	-	-
Ethanol (wt%)	-	-	93.0	25.0	0.2
Glycerol (wt%)	0.5	-	-	-	-
Isoamyl alcohol (wt%)	-	1.1	0	26.7	37.6

From Table 5.3, it can be inferred that hydrous bioethanol production was 16.1 t//h and its concentration was around 93 wt% ethanol. Stillage and phlegmasse (“STILLAGE and “PHLEGMAS” in Figure 5.1) do not present ethanol and are basically water. Besides, fusel oil streams – “FUSEL1” and “FUSEL2” – have a considerably amount of isoamyl alcohol as desired in this process.

Although all columns were simulated using nonequilibrium stage model, in this work, column B-B1 is used to summarize the results of this study. Column B-B1 has larger number of stages and, as a result, it is the most influenced column in this process, concerned with the objectives of this work. Temperature profile is given in Figure 5.3.

It can be observed that liquid and interface temperature profiles obtained in the NEQ model were coincident, indicating that there is no resistance to energy transfer between interface and liquid phase. However, vapor temperatures

calculated by NEQ slightly diverged from the other temperatures, which means that vapor phase controls energy transfer in the system.

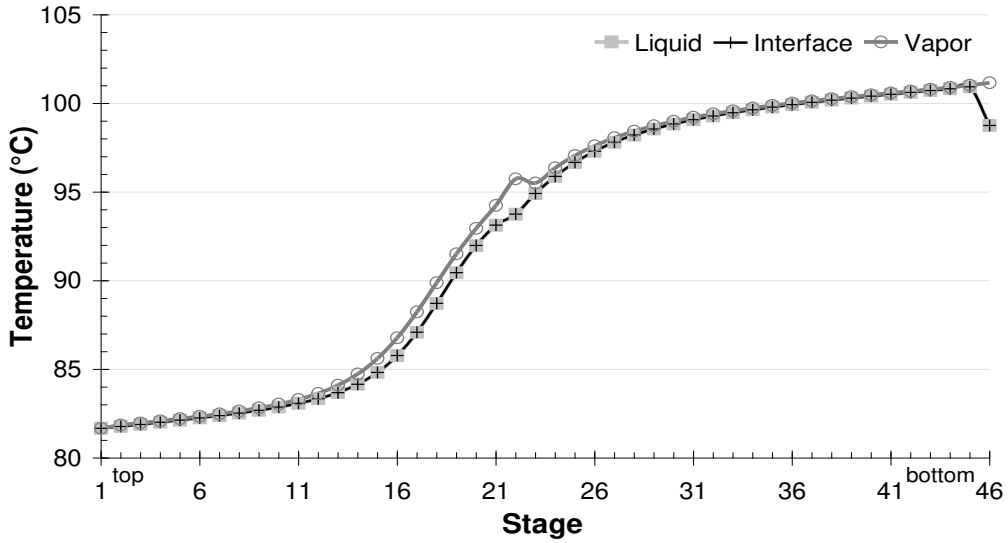

Figure 5.3. Temperature profile for column B-B1 using nonequilibrium stage model.

Equilibrium Stage Model with Constant Efficiency

Simulations considering equilibrium stage model with constant plate efficiencies were carried out in order to evaluate whether a constant efficiency can provide predictions similar to nonequilibrium stage model. Temperature profile, depicted in Figure 5.4, was used to illustrate the comparison between these models.

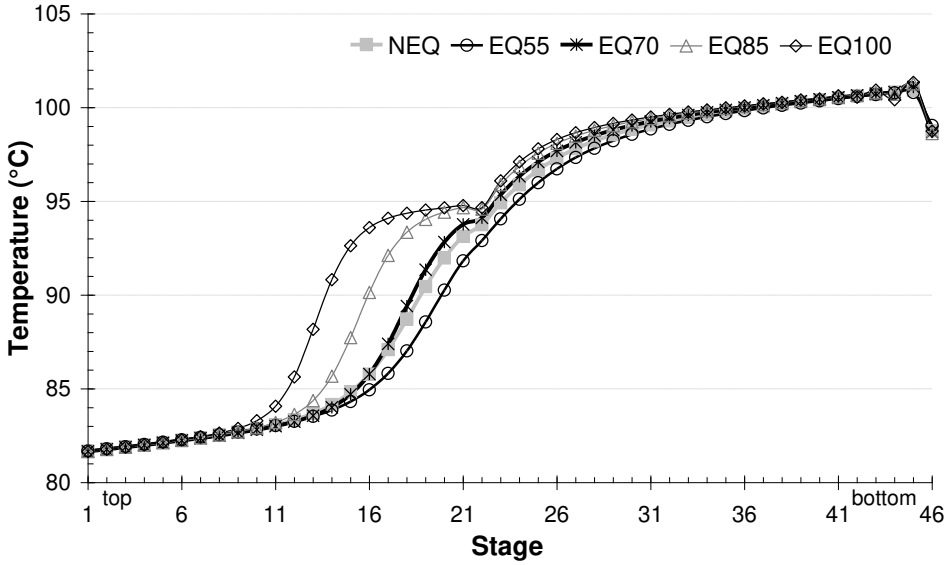

Figure 5.4. Temperature profile using equilibrium stage model with constant plate efficiencies and nonequilibrium stage model.

It can be inferred from Figure 5.4 that the curve given by EQ100 (ideal situation) considerably deviates from the one given by NEQ. Besides, analyzing temperatures given by equilibrium model with constant plate efficiency (EQ55, EQ70 and EQ85), it can be observed that temperatures are higher for the superior values of efficiency, since this cases are closer to the ideal situation, hence it follows that energy transfer is not as restrictive as in nonequilibrium model. Among simulations considering plate efficiency, taking NEQ simulation as base, EQ70 predicted better results since its curve is the closest to NEQ along the entire column. Therefore, efficiency of 70 % is a reasonable value for efficiency in this process.

Concerning energy requirements, Figure 5.5 presents the comparison between cases studied. It is important to emphasize that, in this process, energy consumption is the amount of energy required in the reboilers of columns A and B-B1, which, in practice, is provided through heat exchange between process steam and the bottom product to be evaporated.

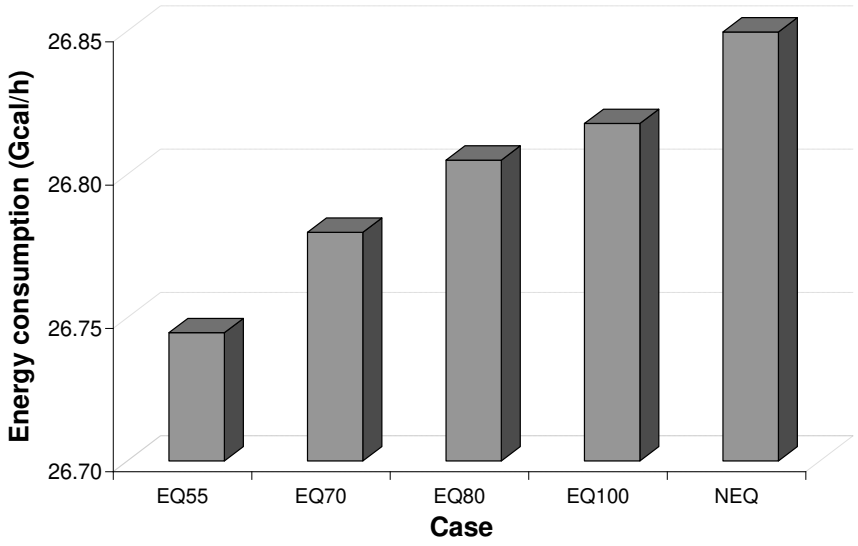

Figure 5.5. Comparison between energy demand of distillation process using equilibrium stage model with constant plate efficiencies and nonequilibrium stage model.

Analyzing Figure 5.5, it was observed that energy consumptions presented not significant variations, since the values were between 26.7 and 26.9 Gcal/h. Besides, it can be verified that the energy consumption increases with the

efficiency. At first, it can seem contradictory, given that, for a fixed number of stages, lower efficiencies require higher reflux rates and, consequently, larger energy requirements if the product specification is the same. However, in this case, product specification was not fixed, but the column parameters were. Therefore, this behavior can be associated to the stage temperatures, which also increases with efficiency as shown in Figure 5.4.

Equilibrium Stage Model with Barros & Wolf Efficiency Correlation

Values obtained for plate and component efficiency across column B-B1 are displayed on Figure 5.6. Water, ethanol, and isoamyl alcohol efficiencies are between 0.45 and 0.60, whereas glycerol presents higher efficiencies, around 0.7, and glucose efficiencies vary between 1.2 and 1.7. These results indicate that efficiency is higher for low-volatile components, which also present high viscosity and are mostly found in liquid phase inside the column. Plate efficiencies are situated between water and ethanol efficiencies, since these components are found in higher concentration in column B-B1, presenting values around 0.50.

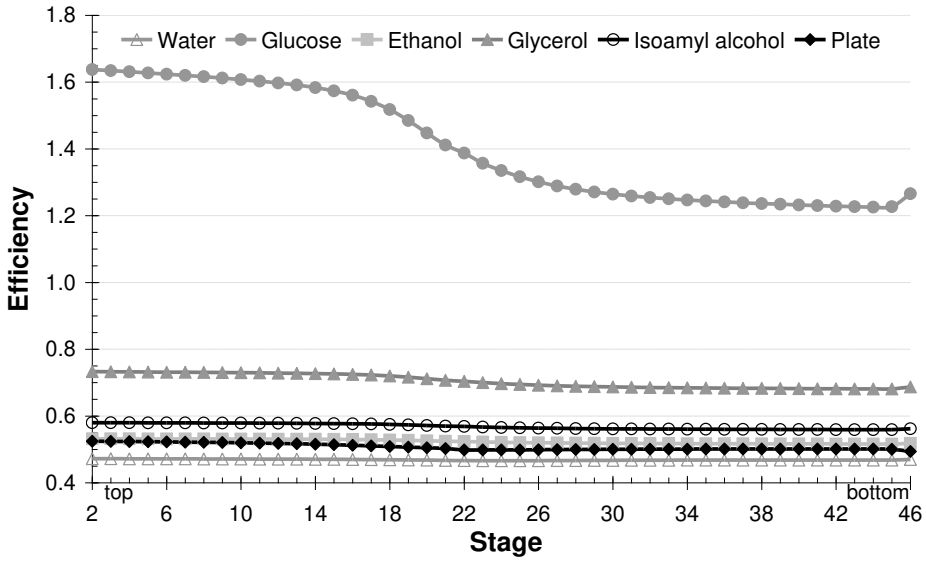

Figure 5.6. Efficiency profile in column B-B1.

Temperature profiles for equilibrium stage model with Barros & Wolf efficiency correlation for plate and component and nonequilibrium stage model are illustrated in Figure 5.7.

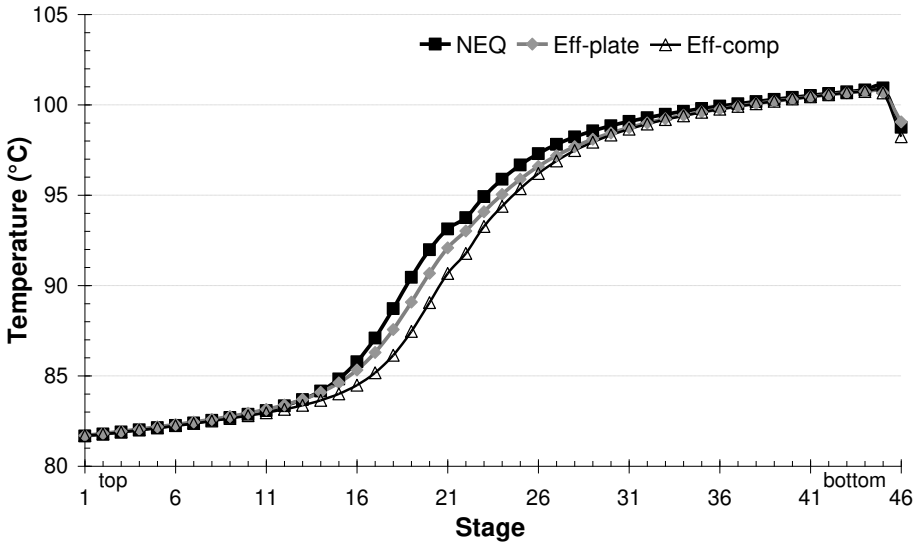

Figure 5.7. Temperature profile using equilibrium model with Barros & Wolf efficiency correlation for plate and component and nonequilibrium stage model.

Equilibrium stage model with Barros & Wolf correlation efficiency provided reasonable temperature values when compared to nonequilibrium stage model; moreover curve generated considering plate efficiency was closest to that given by nonequilibrium stage model.

Energy requirements for equilibrium model with Barros & Wolf efficiency correlation for plate (Eff-plate) and component (Eff-comp) were also evaluated and comparison with nonequilibrium model results is shown in Figure 5.8 In this case, it can be noticed that energy consumptions were not significantly different from results of nonequilibrium stage model, and simulation using plate efficiency presented more similar results than that using component efficiency.

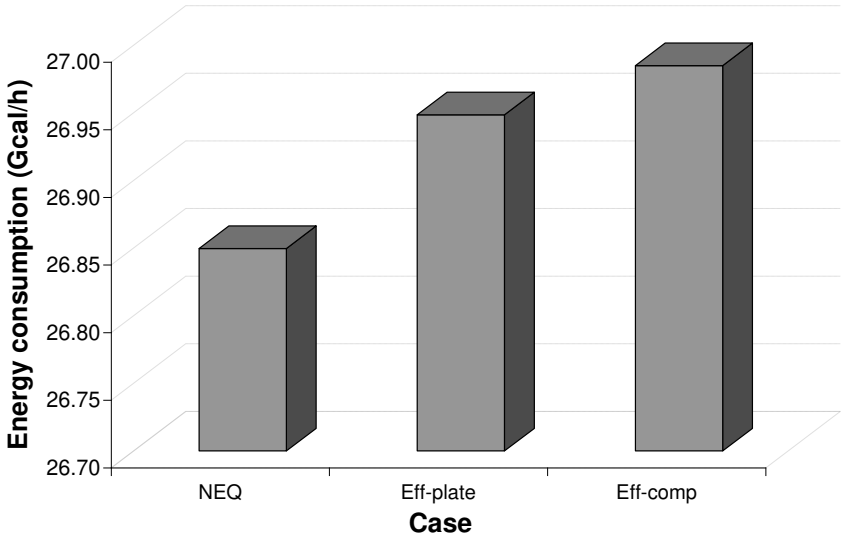

Figure 5.8. Comparison between energy demand of distillation process using equilibrium model with Barros & Wolf efficiency correlation for plate and component and nonequilibrium model.

The superiority of plate efficiency over component efficiency to predict temperatures and energy consumptions can be explained by the fact that plate efficiencies take into account mixture properties while component efficiencies use only individual properties. The effect of the mixture in the plate is essential to column behaviour; consequently, a correlation that uses its properties is generally more accurate.

Summary of Results

Comparison between results given by equilibrium stage model (efficiency of 100 %), equilibrium model with Barros & Wolf correlation efficiency for plate and component and nonequilibrium model is presented through composition profiles (vapor and liquid) depicted in Figures 5.9 and 5.10. In order to simplify the analysis of composition profiles, only water and ethanol mole fraction are shown, since they present higher concentration inside the column.

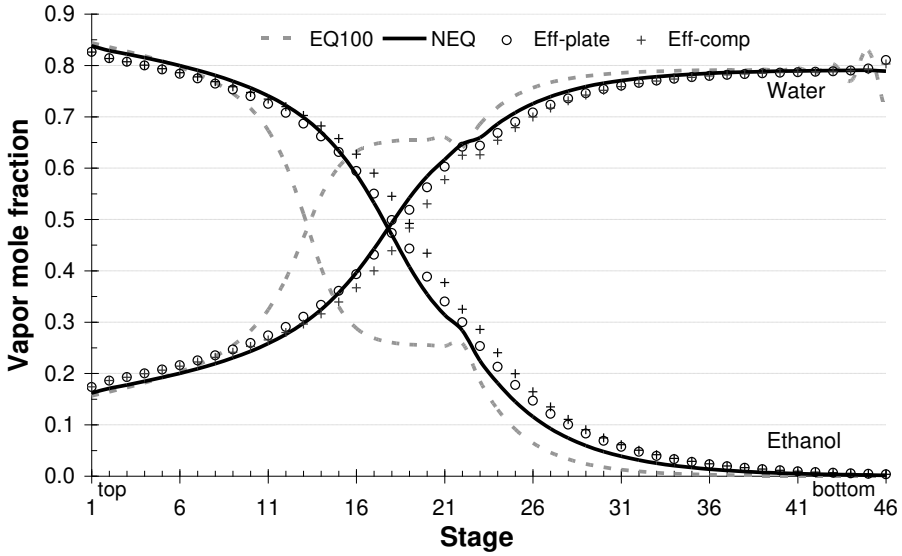

Figure 5.9. Composition profile for vapor phase considering equilibrium model with efficiency of 100 %, with efficiency estimated by Barros & Wolf correlation and nonequilibrium stage model.

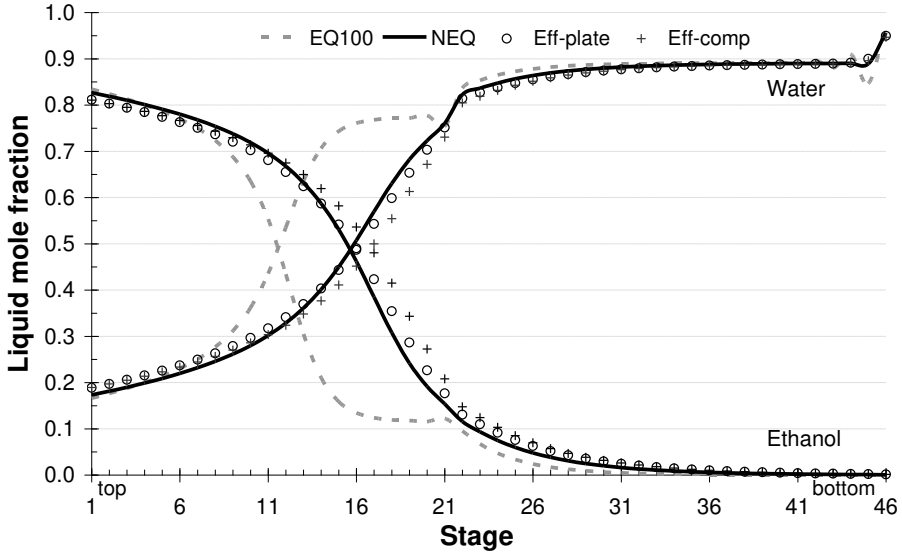

Figure 5.10. Composition profile for liquid phase considering equilibrium model with efficiency of 100 %, with efficiency estimated by Barros & Wolf correlation and nonequilibrium model.

From examination of Figures 5.9 and 5.10, it is possible to observe that equilibrium stage model with Barros and Wolf efficiency correlations (Eff-plate and

Eff-comp) provides a composition profile more accurate taking nonequilibrium model as base.

Energy demand was also compared and results are shown in Table 5.4.

Table 5.4. Comparison between energy requirements.

Case	Energy consumption (Gcal/h)	Relative Difference (%)
Nonequilibrium model	26.85	-
Equilibrium model with Barros & Wolf correlation plate efficiency	26.95	0.37
Equilibrium model with Barros & Wolf correlation component efficiency	26.98	0.50
Equilibrium model (ideal situation)	26.82	- 0.12

Although equilibrium stage model showed results more similar to nonequilibrium regarding energy requirements, relative differences between results are not significant, since they are less than 1 %. Besides, it can be seen that equilibrium stage model calculates slightly lower energy consumption when compared with other calculation methods, because it assumes that vapor and liquid phases leave stages in equilibrium. Once mass and energy transfers or efficiency are considered, as in nonequilibrium stage model and equilibrium stage model with efficiency, more stages and energy are required to achieve the same separation.

CONCLUSIONS

Simulations of bioethanol production process were carried out considering equilibrium with constant efficiency, with plate and component correlation efficiency and nonequilibrium stage models. Literature review showed that nonequilibrium stage model predicts results in good agreement with experimental results, however, further studies including experiments are recommended to validate nonequilibrium stage model for bioethanol production process. In this work, nonequilibrium stage model was used as base to evaluate equilibrium stage model with efficiency.

In the nonequilibrium stage model, liquid, vapor and interface temperature profiles were analysed; liquid phase and interface temperatures were coincident,

while vapor phase presented a deviation from interface temperatures, which means that the liquid phase presents no resistance to energy transfer and the vapor phase controls this process.

Results obtained considering equilibrium model with constant plate efficiency indicated that efficiency of 70 % is a good estimative for this process, since a satisfactory agreement was achieved between temperature profiles. Equilibrium model with efficiency of 100 % presented significant deviations in temperature profile as well as in composition profiles.

Plate efficiencies determined through Barros & Wolf efficiency correlation are around 50 % and component efficiencies are found in a range between 0.4 and 1.7, presenting higher values for low-volatile components. Simulation results with equilibrium stage model with plate and component efficiency, determined by Barros and Wolf correlation, showed a good agreement with results predicted by the nonequilibrium stage model.

Energy requirements were evaluated for equilibrium model with efficiency of 100 %, with plate and component efficiency and nonequilibrium model and it can be concluded that there is no considerable difference between the predicted values.

5.3. Comentários e Conclusões

Neste capítulo foram avaliadas diferentes abordagens para o cálculo de colunas de destilação empregadas no processo de produção de bioetanol.

A modelagem de estágios de equilíbrio forneceu perfis de temperatura para as fases líquida e vapor e também para a interface. Observou-se que a fase líquida e a interface apresentam curvas coincidentes, enquanto a curva relativa à fase vapor distancia-se destas. Desta forma, pode-se afirmar que a fase líquida não oferece resistência à transferência de energia e a fase vapor controla este processo.

A comparação entre a modelagem de equilíbrio com eficiência constante com a modelagem de não equilíbrio indicou que eficiência de 70 % é uma estimativa razoável para este processo. No entanto, eficiências de prato

calculadas pela correlação de Barros e Wolf mantiveram-se em torno de 50 % e as eficiências de componente variaram entre 40 e 170 %, sendo maiores para componentes de baixa volatilidade. Resultados preditos utilizando a modelagem de estágios de equilíbrio com eficiências determinadas pela correlação de Barros e Wolf apresentaram concordância satisfatória quando comparada à modelagem de não equilíbrio.

Vale ressaltar que o processo de concentração do etanol é composto por colunas de destilação e retificação, possuindo múltiplas alimentações e saídas laterais. Além disso, a consideração de um sistema multicomponente bem como a interação entre as colunas através de reciclos tornam a aplicação da correlação de eficiência mais complexa.

Capítulo 6
Avaliação dos Métodos de Cálculo para a Destilação Extrativa na Produção de Bioetanol

6.1. Introdução

Com a finalidade de ser misturado à gasolina, bioetanol deve ser desidratado de forma a atingir a especificação de 99,5 % etanol (em massa). Assim, o bioetanol hidratado produzido através da destilação convencional deve ser submetido a processos posteriores de separação que sejam capazes de obter bioetanol com concentração de etanol maior que a do azeótropo (95,6 %). No Brasil, dentre os processos de desidratação destacam-se a destilação azeotrópica com cicloexano e a destilação extrativa com monoetilenoglicol. Apesar de a destilação azeotrópica ser a mais utilizada atualmente, tem-se que a destilação extrativa é superior no que se refere à facilidade de operação e ao consumo de vapor de processo, o qual é consideravelmente menor neste último processo.

Assim como para a destilação convencional, os cálculos para a destilação extrativa podem ser realizados utilizando modelagens de estágios de equilíbrio e de não equilíbrio bem como podem ser inseridos valores de eficiência de prato e componente. Neste contexto, considerando-se como alimentação o produto da destilação descrita na seção 5.2, foram realizadas simulações do processo de destilação extrativa com monoetilenoglicol considerando os diferentes métodos. Além disso, o uso da correlação de eficiência de Barros e Wolf para destilação extrativa foi avaliado através de comparação com a modelagem de não equilíbrio.

O desenvolvimento deste capítulo é apresentado a seguir no artigo intitulado *"Simulation of extractive distillation process in bioethanol production using equilibrium stage model with efficiency and nonequilibrium stage model"* a ser submetido a periódico internacional.

6.2. Simulation of extractive distillation process in bioethanol production using equilibrium stage model with efficiency and nonequilibrium stage model

ABSTRACT

In view of the increasing environmental concern, the use of renewable and less pollutant energy sources has been encouraged. In this context, bioethanol has been used as fuel in the anhydrous form, blended with gasoline. In this work, simulations of extractive distillation process in anhydrous bioethanol production were carried out in Aspen Plus® using nonequilibrium stage model and equilibrium stage model with Barros & Wolf efficiency correlations for plate and component. Equilibrium stage model with plate efficiency determined through Barros & Wolf efficiency correlation showed a satisfactory agreement with results predicted by nonequilibrium stage model for anhydrous bioethanol production process.

INTRODUCTION

Recently, global concern about climate change has motivated the use of alternative forms of energy all over the world. In the transportation sector, more specifically, bioethanol and biodiesel have been increasingly used as substitutes of gasoline and diesel, respectively.

Bioethanol is mainly produced from fermentation of sugars, which generates wine containing about 7-12 wt% ethanol. In order to be used as a gasoline additive, wine must be concentrated at least to 99.5 wt% ethanol. Initially, conventional distillation is employed to concentrate wine up to 93 wt%, which is near the azeotropic composition (95.6 wt% of ethanol). Subsequently, further operations are required to produce anhydrous bioethanol, such as azeotropic distillation with cyclohexane and extractive distillation with ethyleneglycol (EG).

In spite of being the most common dehydration process, azeotropic distillation with cyclohexane presents several disadvantages, such as high energy consumption on columns reboilers, use of a harmful, flammable, toxic and fossil separation agent

(Rivière and Marlair, 2009) and product contamination with solvent, besides its operation is quite complex due to formation of two liquid phases in some of internal plates (Junqueira et al., 2009). Although extractive distillation with EG also makes use of a fossil and harmful separating agent, it is still advantageous since it requires less energy and it is easier to operate.

For any distillation-based process, it is essential to ensure appropriate design of distillation columns to guarantee that the separation desired is achieved, otherwise it can have considerable environmental and economic implications. In order to design a column, number of stages and operational conditions are required; in this context, simulation softwares are useful tools. However, simulation accuracy deeply relies on the type of model used for calculations. Most available simulation softwares are based on the equilibrium stage model (EQ) calculations, which is an idealized model that assumes the achievement of thermodynamic equilibrium between the contacting phases. In practice, the contact time between the vapor and liquid phases is not long enough for equilibrium to be established. In this context, it is, therefore, desirable to consider the deviation from equilibrium through introduction of efficiency. Another possible alternative is the use of nonequilibrium stage model (NEQ), also called rate-based. This type of model, though complicated relative to the equilibrium model, it provides a realistic estimate of the distillation column performance without incorporating efficiency factors.

In this work, simulations of bioethanol dehydration process through extractive distillation with ethyleneglycol were carried out in Aspen Plus®. Nonequilibrium stage model and equilibrium stage model with application of an efficiency correlation were used to perform calculations.

EXTRACTIVE DISTILLATION PROCESS

Extractive distillation, also known as homogeneous azeotropic distillation, is commonly used to separate nonideal mixtures with close boiling point or azeotropes. In this process, a heavy boiling solvent is added to the system to be separated, which alters the volatility of the component in the original mixture. New azeotropes must not be formed and the solvent must be completely miscible in the mixture, in other words,

it must not form a second liquid phase as in heterogeneous azeotropic distillation (Dias et al. 2009a; Reis et al., 2006).

In the conventional configuration employed in bioethanol production process, solvent and the water-ethanol mixture (HE, hydrous ethanol) are fed to the first column (extractive column). Anhydrous ethanol is produced on the top of the extractive column, while in the bottom a mixture containing solvent and water is obtained. The solvent is recovered in a second column (recovery column), cooled and recycled to the extractive column (Huang et al., 2008).

Meirelles et al. (1992) demonstrated that ethyleneglycol (EG) is an efficient solvent for anhydrous bioethanol production by extractive distillation. This process was first employed in industrial scale in Brazil in the 2001 sugarcane harvest season, and is today one of the most common processes for ethanol dehydration.

Comparing with conventional distillation process, extractive distillation has larger number of degrees of freedom. In a simple distillation setup, these degrees of freedom are the reflux ratios and the number of stages of the distillation columns. For extractive distillation, the solvent choice and the solvent flow rate comprise additional degrees of freedom (Kossack et al, 2007).

NONEQUILIBRIUM STAGE MODEL

The development of the rigorous nonequilibrium stage model, described by Krishnamurthy and Taylor (1985), considers each phase to be separated by an interface through which heat and mass transfer occur. Consequently, conservation equations are written for each phase independently and solved together with transport equations that describe mass and energy transfers in multicomponent mixtures; also it is assumed that equilibrium occurs only in the vapor-liquid interface (Pescarini et al., 1996).

While the nonequilibrium model is more rigorous, it can also become more difficult to implement for dynamic simulations, optimization and control. In addition, some parameters of the model such as the mass transfer coefficients may be difficult to estimate accurately (Pradhan and Kannan, 2005).

Pradhan and Kannan (2005) analyzed extractive distillation process through nonequilibrium stage model and concluded that purity in the distillate is significant

lower than that predicted by equilibrium stage model. Additionally, it was observed that the idealized model requires fewer stages to achieve the same purity obtained using the rate-based model.

Nava and Krishna (2004) examined the influence of interphase mass transfer on the composition trajectories in extractive distillation. They highlighted the need of adopting nonequilibrium stage model in this process, since their results showed the superiority of NEQ over equilibrium stage model regarding prediction of column composition trajectories.

Castillo and Towler (1998) also studied the influence of mass transfer in the extractive distillation by analysis of residue-curve maps. The authors noticed that NEQ affects the curvature of boundaries and, occasionally, EQ might allow design of distillation sequence that is unfeasible once mass transfer is taken into account. In these cases, not even the overdesign, which can include extra trays or additional reflux, can overcome this miscalculation.

Nonequilibrium stage model has been incorporated into the commercially available software Aspen Plus® through the package RateFrac™. This model calculates the product of the binary mass transfer coefficients and interfacial areas using the correlations developed by Gerster and co-workers (1958); the vapor and liquid phase heat transfer coefficients are determined using the Chilton-Colburn analogy. In general, these quantities depend on column diameter and operating parameters. Parameters used in calculations, such as vapor and liquid flows, densities, viscosities, surface tension of liquid, vapor and liquid phase binary diffusion coefficients, are all estimated through well known equations included in Aspen Plus® (Aspen Technology, 2001).

EFFICIENCY CORRELATIONS

As stated previously, through equilibrium stage model is not possible to predict accurately extractive distillation since heat and mass transfer mechanisms must be taken into account. Towards this end, an alternative way to correct this weakness is the application of efficiency correlations.

In this context, efficiency correlations for plate and component in conventional and extractive distillations were evaluated (Barros, 1997; Wolf-Maciel et al., 2001;

Reis et al., 2006). These correlations, known as Barros and Wolf efficiency correlation, were obtained based on techniques of factorial design and present the relation between efficiency and the properties of the mixture, such as thermal conductivity, density, heat capacity and diffusivity, which vary with efficiency.

Barros and Wolf plate correlation and the component efficiency correlation for conventional (Equations 6.1 and 6.2) and extractive distillation (Equations 6.3 and 6.4) are displayed below.

$$Eff(i) = 38.5309\left[\frac{k(i)\rho(i)D(i)MW(i)}{Cp(i)\mu^2(i)}\right]^{-0.04516} \tag{6.1}$$

$$Eff(i,j) = 38.5309\left[\frac{k(i,j)\rho(i,j)D(i,j)MW(j)}{Cp(i,j)\mu^2(i,j)}\right]^{-0.04516} \tag{6.2}$$

$$Eff(i) = 19.37272\left[\frac{k(i)\rho(i)D(i)MW(i)}{Cp(i)\mu^2(i)}\right]^{-0.109588} \tag{6.3}$$

$$Eff(i,j) = 19.37272\left[\frac{k(i,j)\rho(i,j)D(i,j)MW(j)}{Cp(i,j)\mu^2(i,j)}\right]^{-0.109588} \tag{6.4}$$

In these equations, Eff(i) is the plate efficiency in plate *i* and Eff(i,j) is the efficiency of component *j* on plate *i*. The equations are function of thermal conductivity (k), density (ρ), diffusivity (D), molecular weight (MW), heat capacity (Cp) and viscosity (μ). For calculation of plate efficiencies, properties of the mixture in the plate are considered, whereas for component efficiency, the pure component properties in the plate are used.

Reis et al. (2006) performed calculations using a computational program in Fortran language to simulate extractive distillation columns using equilibrium stage model. In this program, a subroutine to calculate efficiency through Barros and Wolf correlations was included. The simulation results were compared to those calculated using NEQ and also with experimental data of a pilot-scale extractive distillation column. A satisfactory agreement was achieved, showing that the efficiency correlations are reliable and applicable to extractive distillation process.

In Aspen Plus®, calculations of equilibrium stage model are realized through RadFrac™ model. This model allows the inclusion of Murphree efficiencies and vaporization efficiencies for plate and components (Aspen Technology, 2001).

SIMULATION PROCEDURE

For calculations, NRTL model was used for the estimation of activity coefficients and vapor phase was considered ideal. Configuration of the distillation process to produce anhydrous bioethanol (AE) is depicted in Figure 6.1. Column specifications are given in Table 6.1. All simulations considered the same configuration and columns specifications, besides condenser and reboiler were considered as equilibrium stages for all calculation approaches.

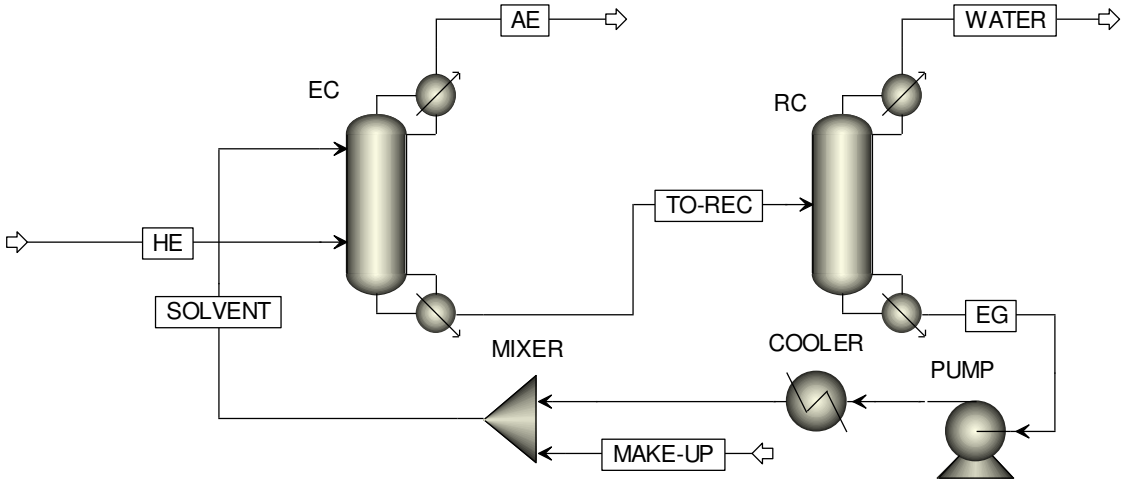

Figure 6.1. Configuration of extractive distillation process with ethyleneglycol.

Table 6.1. Specifications in the extractive and recovery columns (mass basis).

Specification	Extractive Column	Recovery Column
Number of Stages	32	18
Pressure (kPa)	101.3	50
Feed Position	Solvent 3 HE 24	9
Condenser Type	Partial	Partial
Solvent to Feed Ratio	0.62	-
Reflux Ratio	1.05	0.38
Distillate Rate (kg/h)	15051	-
Bottoms Rate (kg/h)	-	9984.0

Firstly, simulations were performed using nonequilibrium stage model, which makes use of RateFrac™ model in Aspen Plus®, with the purpose of obtaining anhydrous bioethanol (99.5 wt% ethanol). Tray type was defined as bubble cap and column diameter was calculated based on the approach of flooding on the stage where it is most critical.

Secondly, calculations considering equilibrium stage model (RadFrac™) were carried out without addition of efficiency values, which means an efficiency of 100 % (ideal situation). Finally, in order to include efficiency in equilibrium calculations, properties were retrieved from the previous simulation and used to calculate the initial values of efficiency through Barros and Wolf efficiency correlation. For the extractive column it was employed the correlation for extractive distillation, while for the recovery column it was used the correlation for conventional distillation. Subsequently, these efficiencies were inserted in the simulation as Murphree efficiencies and the properties were recalculated, thus obtaining new efficiencies values. This procedure was repeated until the difference between two consecutive efficiency iterations reached a level of tolerance below 1.10^{-4}. Generally, three iterations are enough to determine efficiencies within the specified tolerance. The procedures for plate and component efficiency are similar, except for the equation used.

RESULTS AND DISCUSSION

Tables 6.2 to 6.5 present the main stream results for the different approaches considered in this study.

Table 6.2. Main stream results using nonequilibrium stage model.

Stream	AE	SOLVENT	WATER	TO-REC
Temperature (°C)	78.4	110	82.2	139
Pressure (bar)	1.0	1.0	0.5	1.0
Mass Flow (kg/h)	15051	9989.0	1054.0	11038
Ethanol (wt%)	99.5	-	-	-
Water (wt%)	0.5	-	99.8	9.5
Ethyleneglycol (wt%)	-	100	0.2	90.5

Table 6.3. Main stream results using equilibrium stage model.

Stream	AE	SOLVENT	WATER	TO-REC
Temperature (°C)	78.3	110	83.5	139.1
Pressure (bar)	1.0	1.0	0.5	1.0
Mass Flow (kg/h)	15051	9989.0	1054.0	11038
Ethanol (wt%)	99.5	-	-	-
Water (wt%)	0.5	-	99.6	9.5
Ethyleneglycol (wt%)	-	100	0.4	90.5

Table 6.4. Main stream results using equilibrium stage model with plate efficiency.

Stream	AE	SOLVENT	WATER	TO-REC
Temperature (°C)	78.4	110	82.0	138
Pressure (bar)	1.0	1.0	0.5	1.0
Mass Flow (kg/h)	15051	9989.0	1054.0	11038
Ethanol (wt%)	99.4	-	1.3	0.1
Water (wt%)	0.6	-	98.5	9.4
Ethyleneglycol (wt%)	-	100	0.1	90.5

Table 6.5. Main stream results using equilibrium stage model with component efficiency.

Stream	AE	SOLVENT	WATER	TO-REC
Temperature (°C)	78.3	110	81.9	135
Pressure (bar)	1.0	1.0	0.5	1.0
Mass Flow (kg/h)	15051	9989.0	1054.0	11038
Ethanol (wt%)	99.0	-	7.3	0.7
Water (wt%)	1.0	-	92.5	8.8
Ethyleneglycol (wt%)	-	100	0.2	90.5

From analysis of main stream results, it is possible to observe that NEQ, EQ and EQ with plate efficiency are in better agreement regarding stream temperatures than the simulation with component efficiency. Concerning stream composition, EQ and simulation with plate efficiency provided satisfactory results when compared to NEQ. EQ with component efficiency did not present reasonable results probably due to lack of mixture properties in the equation that can lead to miscalculations. Although EQ is an idealized model, it provided reasonable prediction when compared to NEQ, which can be explained by the large number of stages due to the demanding specification (93 wt% ethanol). In other words, if

number of stages were determined to achieve separation considering EQ, NEQ results would be quite different since it requires a larger number of stages to perform the same separation.

Energy requirements were also evaluated and comparison between results for all approaches is displayed in Table 6.6.

Table 6.6. Energy requirements for all calculation methods.

Calculation Method	Energy Requirement (Gcal/h)			
	NEQ	EQ	EQ with Plate Efficiency	EQ with Component Efficiency
Condenser-EC	-3.26	-3.22	-3.25	-3.26
Reboiler-EC	2.91	2.87	2.89	2.91
Condenser-RC	-0.21	-0.22	-0.21	-0.20
Reboiler-RC	0.99	1.00	0.98	0.98

Energy requirements predicted by different models were quite similar, with EQ presenting the larger deviations, which was expected since this model does not take into account mass and heat transfer mechanisms.

In order to analyze column profiles, results of extractive and recovery columns are presented apart from each other.

Extractive Column (EC)

Plate and component efficiencies determined by Barros and Wolf correlation for extractive distillation are shown in Figure 6.2. It can be observed that efficiencies are between 0.30 and 0.60, presenting disturbances in solvent and azeotropic feed positions (stages 3 and 24). Plate efficiencies are located between component efficiencies and water presents lowest efficiency values and EG the largest ones. These observations are in accordance with results obtained by Reis et al. (2006).

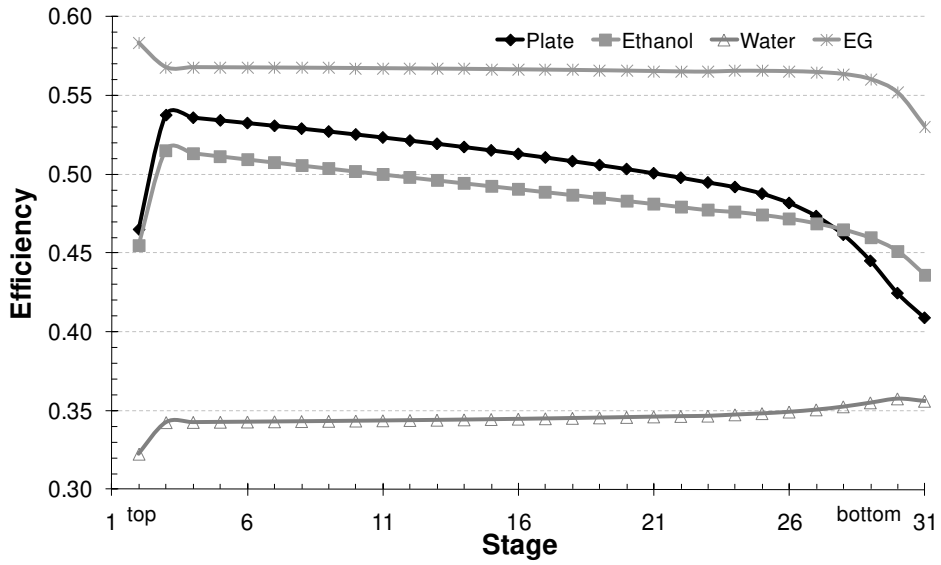

Figure 6.2. Efficiency profiles obtained in the extractive column.

Temperature profiles are illustrated in Figure 6.3. EQ with component efficiency was omitted in the comparison since it presented a poor performance when compared to NEQ results. Besides, an extra curve would make more difficult the visualization of the profiles.

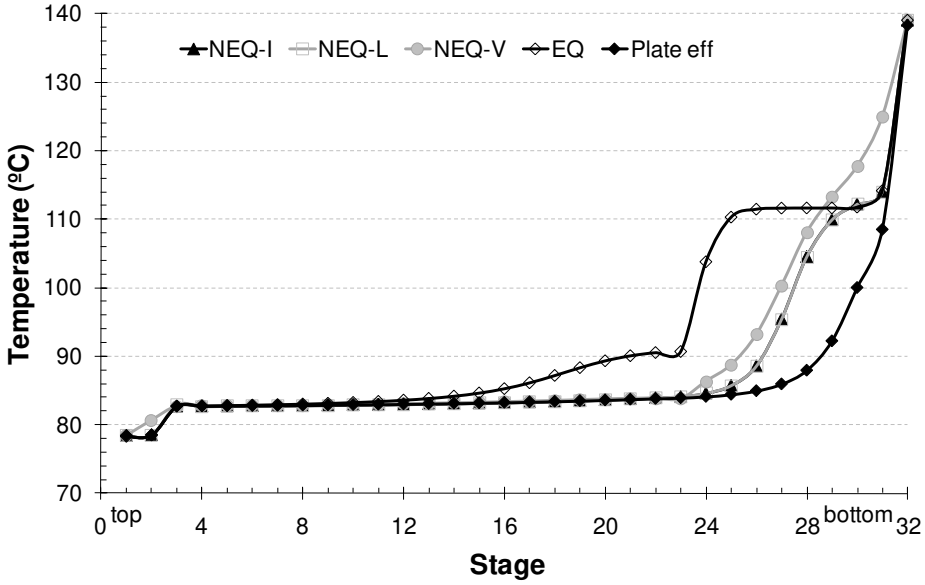

Figure 6.3. Temperature profiles in extractive column.

From Figure 6.3, it can be inferred that liquid and interface temperature profiles are practically identical, whereas vapor phase temperature profile is

different, which means that there is no resistance to energy transfer between interface and liquid phase, while vapor phase controls energy transfer in the system. Therefore, it can be concluded that the supposition of equality of all temperatures as considered in the equilibrium stage model is not a reasonable approximation for this system.

Although none of equilibrium stage model presented a satisfactory agreement with NEQ as shown in Figure 6.3, EQ with plate efficiency provided prediction with smaller deviations as well as a behavior more similar to NEQ than the idealized equilibrium stage model.

In respect to composition profile, vapor mole fractions along the column are given in Figure 6.4. Ethyleneglycol mole fraction was omitted from this profile since its values were normally around zero. Analyzing the curve given by EQ, it can be seem that the last stages have no function since the composition does not vary between stages 25 and 31, which means that the column is overdesigned for the equilibrium situation. Therefore, curves predicted by EQ and NEQ have the same initial and final values, although the curves follow different tendencies.

On the other hand, EQ with plate efficiency presented tendency analogous to that of the NEQ. In addition, vapor mole fraction predicted by EQ with plate efficiency also presented coincident values in the top and bottom of the column when compared to NEQ.

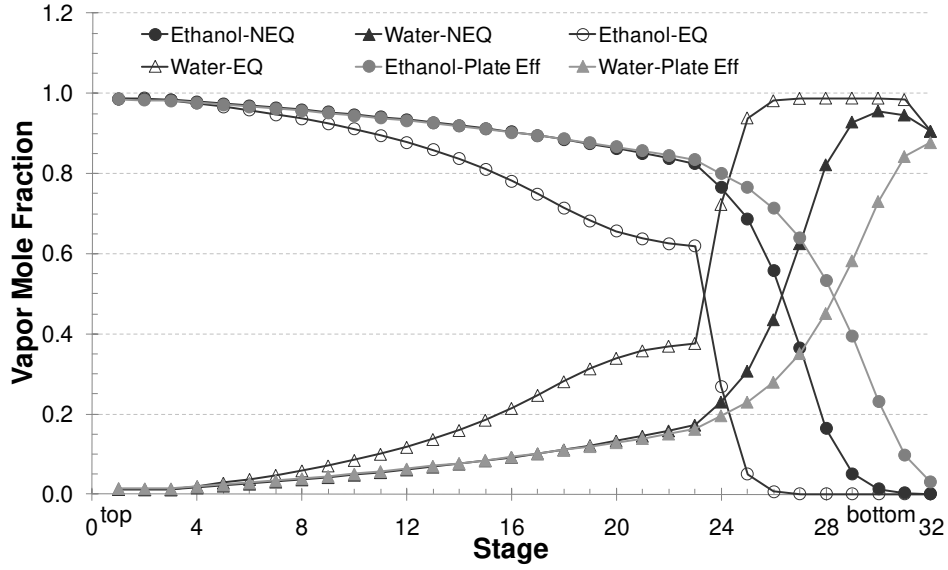

Figure 6.4. Composition profiles for vapor phase in extractive column.

Recovery Column (RC)

Plate and component efficiencies determined by Barros and Wolf correlation for conventional distillation are shown in Figure 6.5. Component efficiency range is between 0.45 and 0.60, whereas plate efficiency oscillates around 0.53. Once more, water has the lowest efficiencies and EG the largest ones.

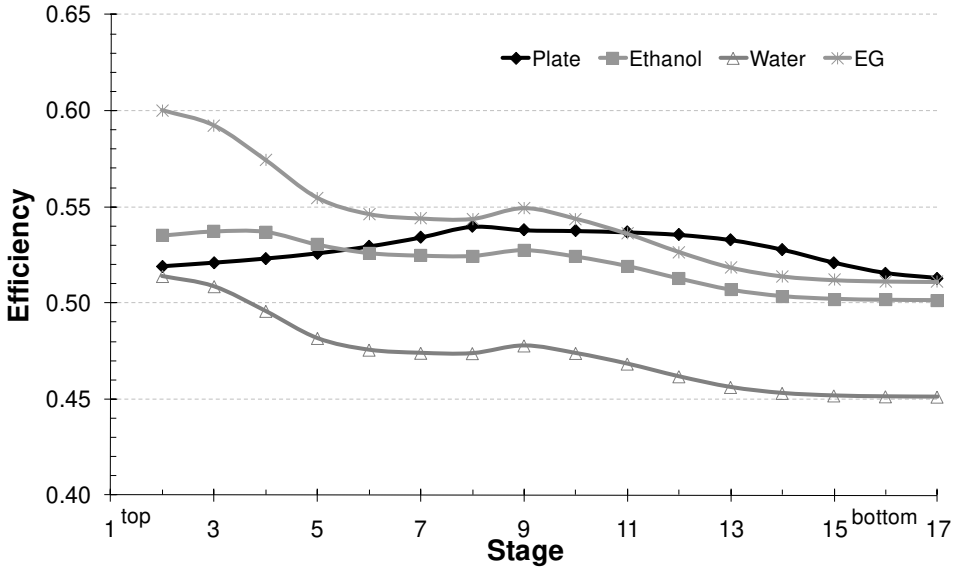

Figure 6.5. Efficiency profiles obtained in the recovery column.

Temperature profiles are depicted in Figure 6.6. The same conclusions with regard to heat transfer resistance can be drawn from vapor, interface and liquid profiles given by NEQ. Though the curve predicted by EQ with plate efficiency (Plate-eff in Figure 6.6) does not have the same behavior as NEQ, the curves are coincident in the top stages and below the feed stage (stage 9). At the same time, EQ only synchronizes with NEQ in the first and final stages. Therefore, the superiority of EQ with efficiency over the idealized model is clearly established.

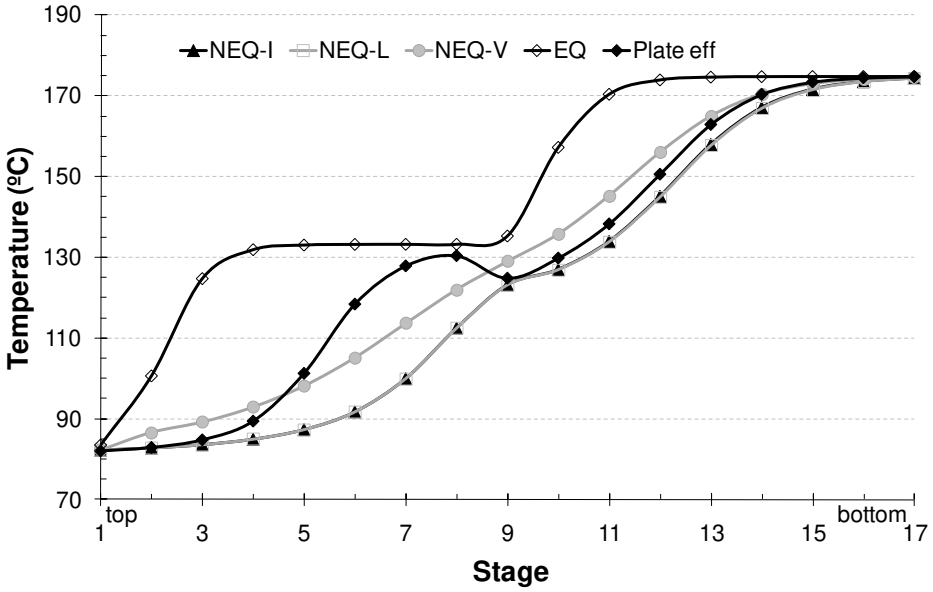

Figure 6.6. Temperature profiles in recovery column.

Composition profile in vapor phase is exhibited in Figure 6.7. Ethanol mole fraction was omitted from this profile since its values were commonly around zero. Results provided by EQ with plate efficiency are noticeably closer to NEQ predictions. Comparing to NEQ, EQ calculates values quite different for almost all stages, except for top and bottom stages.

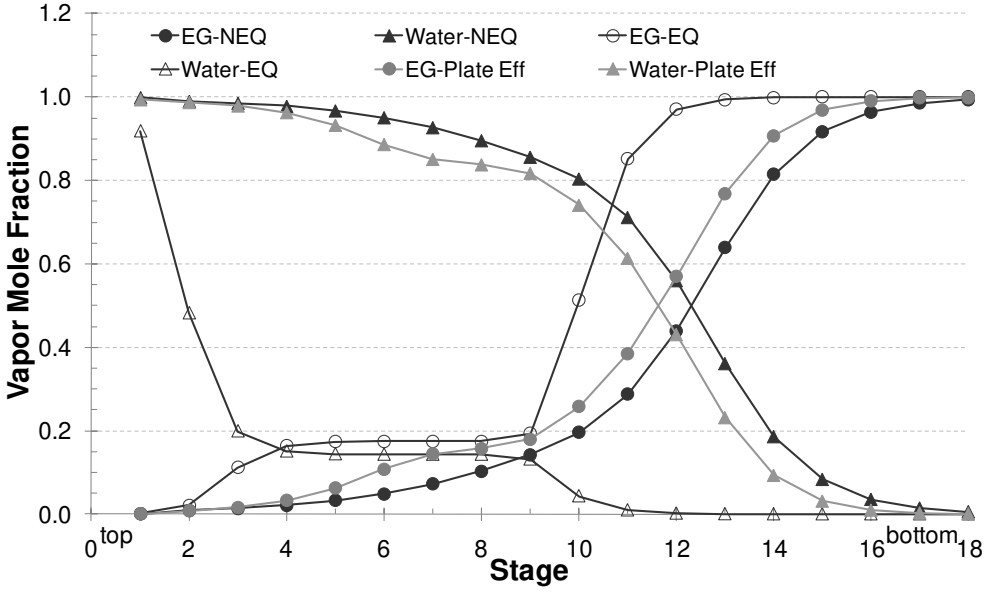

Figure 6.7. Composition profiles for vapor phase in recovery column.

CONCLUDING REMARKS

Extractive distillation process consists of an extractive distillation and a conventional distillation column that is responsible for solvent recovery. In this work, Barros and Wolf efficiency correlations for plate and component developed for these two processes were evaluated through comparison to nonequilibrium stage model. Results showed that the addition of plate efficiencies improved the predictions of equilibrium stage model. However, the consideration of component efficiencies did not seem to be accurate.

Temperature profiles showed that temperatures of vapor phase differ from those of interface and liquid phase; hence vapor phase controls the heat transfer in the process. Besides, it confirms that the assumption of equal temperatures for both phases, as stated in EQ, is not reasonable.

In summary, this study reconciles efficiency correlations and equilibrium stage model calculations performed by the commercially available software Aspen Plus®. Although this software also comprises a nonequilibrium stage model, it requires the knowledge of some design properties; additionally, computational time for nonequilibrium stage model calculations is significantly high as well as its complexity, leading to convergence problems, which are not desirable in online control applications. The use of efficiency correlation has the objective of simplify the calculations when compared to NEQ and, at the same time, increase accuracy of predictions in comparison to the idealized equilibrium stage model.

6.3. Comentários e Conclusões

Este capítulo apresentou o processo de destilação extrativa, incluindo a coluna de destilação extrativa e a coluna de destilação convencional empregada na recuperação de solvente.

A aplicação das correlações de eficiência de Barros e Wolf para prato e componente foi avaliada através da comparação com os resultados preditos pelo modelo de estágios de não equilíbrio. A incorporação de eficiências de prato aumentou a acurácia da predição do modelo de estágio de equilíbrio, enquanto as

simulações considerando as eficiências de componente não apresentaram resultados satisfatórios.

Observou-se ainda que as simulações utilizando a modelagem de não equilíbrio requerem o conhecimento de alguns dados de projeto, além de maior tempo para a realização dos cálculos. A complexidade deste modelo assim como aumenta a acurácia das predições também induz a problemas de convergência, dessa forma não é aconselhável para aplicações em controle *online*.

Capítulo 7
Simulação do Processo de Produção de Bioetanol usando Correlações de Eficiência para Destilação Convencional e Extrativa

7.1. Introdução

Assim como apresentado nos capítulos anteriores, a simulação das etapas de concentração e desidratação é de grande importância no processo de produção de bioetanol. Para essas etapas, foram avaliadas as correlações de eficiência de Barros e Wolf para as destilações convencional e extrativa.

Neste capítulo, as etapas de concentração e desidratação são analisadas em conjunto para avaliar o efeito da introdução da eficiência de prato nos cálculos da modelagem de estágios de equilíbrio.

O desenvolvimento deste capítulo é apresentado a seguir no trabalho intitulado *"Simulation of Anhydrous Bioethanol Production Process using Efficiency Correlations for Conventional and Extractive Distillation"* submetido ao *9th Distillation & Absorption Conference* - DA 2010.

7.2. Simulation of Anhydrous Bioethanol Production Process using Efficiency Correlations for Conventional and Extractive Distillation

ABSTRACT

In this work, simulations of the complete separation process in anhydrous bioethanol production were carried out in Aspen Plus®. This process comprises distillation and rectification columns as well as an extractive column. Equilibrium stage model and Barros & Wolf efficiency correlations were used to perform the calculations. Efficiency profiles were obtained for all columns showing that efficiency values significantly vary along the columns. Influence of the introduction of efficiencies was evaluated through comparison with equilibrium stage model

(ideal process). Results pointed out that energy requirements are not significantly higher when efficiencies are taken into account; however stream results and temperature profiles were quite different from each other. This reveals that is necessary to consider efficiency changes along the column if reliable predictions are to be made.

INTRODUCTION

Bioethanol plays an important role in the sustainable development, since it is a renewable fuel and originates less pollutant gases when compared to fossil-derived fuels. In this context, bioethanol can be used as substitute or in a mixture with gasoline. In Brazil, it is typically produced through fermentation of sugars derived from sugarcane and the separation step to obtain anhydrous bioethanol has a significant impact on the product cost.

In Brazilian biorefineries, wine obtained from fermentation stage is concentrated by means of a set of distillation and rectification columns, on which hydrous bioethanol (93 wt%) is obtained. Subsequently, due to the azeotrope formed by ethanol and water (95.6 wt% ethanol at 1 atm), dehydration processes are required to obtain anhydrous bioethanol (99.5 wt%) and the most usual process, nowadays in large scale industrial units, is the azeotropic distillation with cyclohexane, followed by extractive distillation with ethylene glycol (EG). Compared to azeotropic distillation, extractive distillation requires less energy and is easier to operate, since it does not present two liquid phases inside the column.

Due to the fact that distillation operations demand a significant amount of energy and have a great importance in bioethanol production, the simulation of this unit operation has to be as representative as possible. In fact, reliable simulations allow the study of the distillation columns behavior and the optimization of the process, so the results can be put into practice in real facilities.

Usually, simulations of distillation process consider the equilibrium stage model, although, in practice, columns rarely operate under thermodynamic equilibrium conditions. For this reason, consideration of efficiencies can be quite useful, provided that they are estimated properly. Among the available correlations, the Barros & Wolf efficiency correlations – obtained through adjustment of the

mixture properties, such as thermal conductivity, density, heat capacity and diffusivity – can be used to calculate efficiencies for conventional and extractive distillations (Reis et al., 2006; Wolf-Maciel et al., 2001).

In this work, simulations of the complete separation process for bioethanol production was carried out in Aspen Plus® considering the equilibrium stage model and the efficiency values obtained through Barros & Wolf efficiency correlations. The purpose of this work is to analyze the influence of incorporating efficiency in the column calculations.

PROCESS DESCRIPTION

Hydrous Bioethanol Production

In order to produce hydrous bioethanol, most Brazilian biorefineries employ the configuration depicted in Figure 7.1, which consists of a series of distillation and rectification columns. Initially, the wine produced in the fermentation stage is fed to column A1 originating the top and bottom products that are sent to column D and A, respectively. Column D is responsible for removing volatile contaminants at the top, whereas column A removes large amounts of water (stillage or vinasse) in the bottom. Vapor phlegm produced near to the top of column A and liquid phlegm obtained at the bottom of column D are sent to rectification columns (column B-B1). The task of the rectification section is to concentrate the phlegm streams from 40-50 wt% to 93 wt% ethanol (hydrous bioethanol, “HE”). Sidestreams are withdrawn from column B-B1 and correspond to fusel oil, which is mainly characterized by isoamyl alcohol presence.

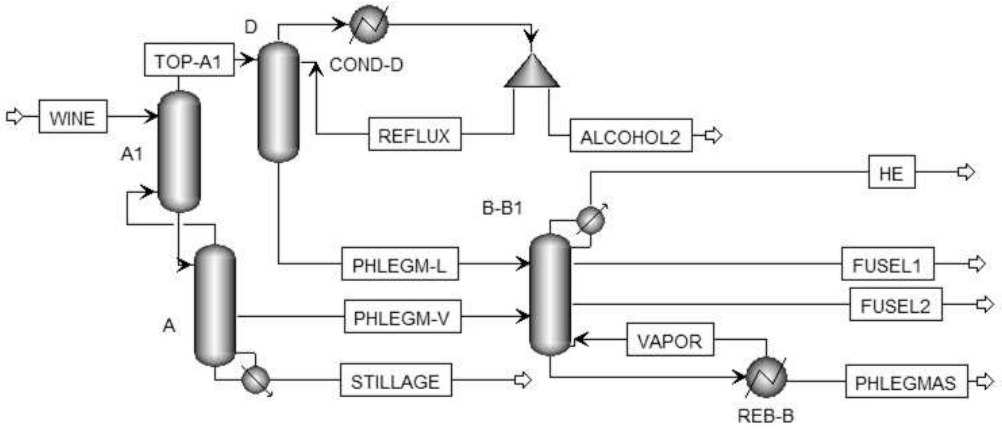

Figure 7.1. Configuration of the conventional distillation process.

Anhydrous Bioethanol Production

In this work, the extractive distillation process was considered as the method to separate the azeotropic mixture in order to produce anhydrous bioethanol. Extractive distillation, also known as homogeneous azeotropic distillation, is commonly used to separate nonideal mixtures with close boiling point or azeotropes. In this process, a heavy boiling solvent is added to the system to be separated, which alters the volatility of the component in the original mixture. Care has to be taken in the choice of the solvent since new azeotropes must not be formed and the solvent must be completely miscible in the mixture, in other words, it must not form a second liquid phase as in heterogeneous azeotropic distillation (Reis et al., 2006; Dias et al., 2009a). The conventional configuration employed in bioethanol production process is shown in Figure 7.2.

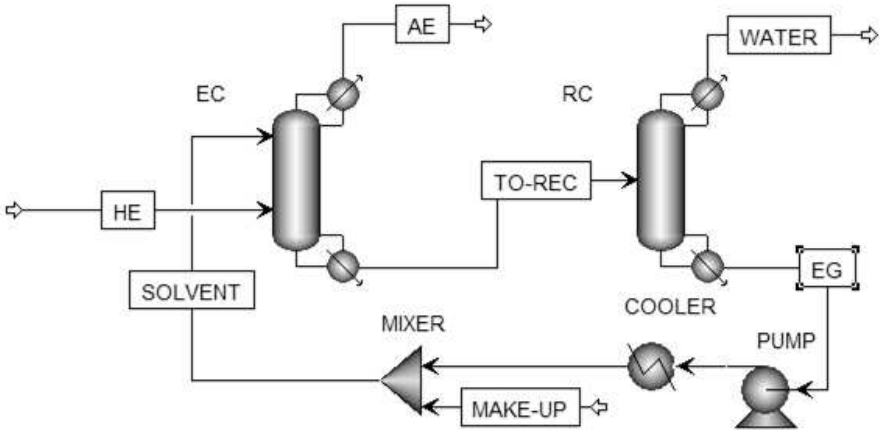

Figure 7.2. Configuration of extractive distillation process.

As can be seen in Figure 7.2, solvent is fed to the first column (extractive column, “EC”), above the azeotropic feed. Anhydrous ethanol is produced on the top of the extractive column, while in the bottom a mixture containing solvent and water is obtained. The solvent is recovered in a second column (recovery column, “RC”), which is operated under vacuum (0.5 bar), then cooled and recycled to the first column.

EFFICIENCY CORRELATIONS

Several works have shown the deviations of the equilibrium stage model results from experimental data (Springer et al., 2002; Repke et al., 2004; Nava and Krishna, 2004). In order to correct this weakness, efficiency can be introduced in the equilibrium calculations.

For instance, efficiency correlations were developed by Barros (1997) based on techniques of factorial design. These correlations, known as Barros & Wolf efficiency correlations, were proposed for conventional (Equation 7.1) and extractive (Equation 7.2) distillations.

$$Eff(i) = 38.5309\left[\frac{k(i)\rho(i)D(i)MW(i)}{Cp(i)\mu^2(i)}\right]^{-0.04516} \quad (7.1)$$

$$Eff(i) = 19.37272\left[\frac{k(i)\rho(i)D(i)MW(i)}{Cp(i)\mu^2(i)}\right]^{-0.109588} \quad (7.2)$$

In Equations 7.1 and 7.2, Eff (i) is the plate efficiency, which is a function of the following properties of the mixture: thermal conductivity (k), density (ρ), diffusivity (D), molecular weight (MW), heat capacity (Cp) and viscosity (μ).

Wolf-Maciel and collaborators (2001) evaluated the performance of the Barros & Wolf efficiency correlation for a conventional distillation column using ethanol-water system. Comparison with nonequilibrium stage model and experimental data were carried out and a satisfactory agreement was achieved, validating the use of Barros & Wolf efficiency correlation. Similarly, Reis and coauthors (2006) validated Barros & Wolf efficiency correlation for extractive distillation columns.

SIMULATION PROCEDURE

For calculations, NRTL model was used for the estimation of activity coefficients and vapor phase was considered ideal, since previous work about thermodynamic characterization has showed the adequacy of this model.

Typical industrial compositions of wine and hydrous bioethanol were considered the same for both approaches and are shown in Table 7.1. Additionally,

configurations of the conventional and extractive distillation processes used in the simulations are those depicted in Figures 7.1 and 7.2, respectively. Column specifications are given in Table 7.2 and 7.3. Stages numbering initiates from the top stage or condenser, when it is present and coupled reboiler is considered the last stage.

Correlation for conventional columns (Equation 7.1) was used to determine plate efficiency in the rectification and distillation columns employed in the concentration of wine and in the solvent recovery column, whereas correlation for extractive distillation (Equation 7.2) was used only for the ethanol dehydration column. Condenser and reboiler were considered as equilibrium stages for both calculation approaches.

The procedure to determine and include efficiencies in the calculation procedure was an iterative method. First, simulations considering equilibrium stage model were carried out in Aspen Plus® without the addition of efficiency values, which means an efficiency of 100 % (ideal situation). Subsequently, mixture properties were retrieved from the previous simulation and used to calculate the initial values of efficiency through Barros & Wolf efficiency correlation. These efficiencies were inserted in the simulation as Murphree efficiencies and the properties were recalculated, thus obtaining new efficiencies values. This procedure was repeated until the difference between two consecutive efficiency iterations reached a level of tolerance below 1.10^{-4}.

Table 7.1. Composition of the streams fed to the process.

	Wine	**Hydrous bioethanol**
Water (wt%)	92.0	7.0
Ethanol (wt%)	7.3	93.0
Glycerol (wt%)	0.4	-
Isoamyl alcohol (wt%)	0.2	-
Glucose (wt%)	0.1	-
Mass Flow (t/h)	207.0	16.1

Table 7.2. Column specifications in bioethanol production process.

	Column A	Column A1	Column D	Column B-B1
Number of stages	19	8	6	46
Feed stage	1	1 (WINE) 8 (TOP-A)	1 (REFLUX) 6 (TOP-A1)	22 (PHLEGM-L) 22 (PHLEGM-V)
Sidestream rate (kg/h)	PHLEGM-V 30000 (2^V)	-	-	500 (FUSEL1 - 21^L) 300 (FUSEL2 - 45^L)
Distillate rate (kg/h)	12750			16100

Number in parenthesis shows the withdrawal stage. Superscript denotes the phase, L for liquid and V for vapor.

Table 7.3 Specifications in the extractive and recovery columns (mass basis).

	Extractive Column	Recovery Column
Number of Stages	32	18
Feed Position	3 (SOLVENT) and 24 (HE)	9
Solvent to Feed Ratio	0.62	-
Reflux Ratio	1.05	0.38
Distillate Rate (kg/h)	15051	-
Bottoms Rate (kg/h)	-	9984.0

RESULTS AND DISCUSSION

Efficiency profiles were generated for all columns employed in the complete process and can be seen in Figure 7.3. It was observed quite different profile for each column. Generally, efficiencies were around 50 % and varied along the columns, except for column A1, which presented constant values.

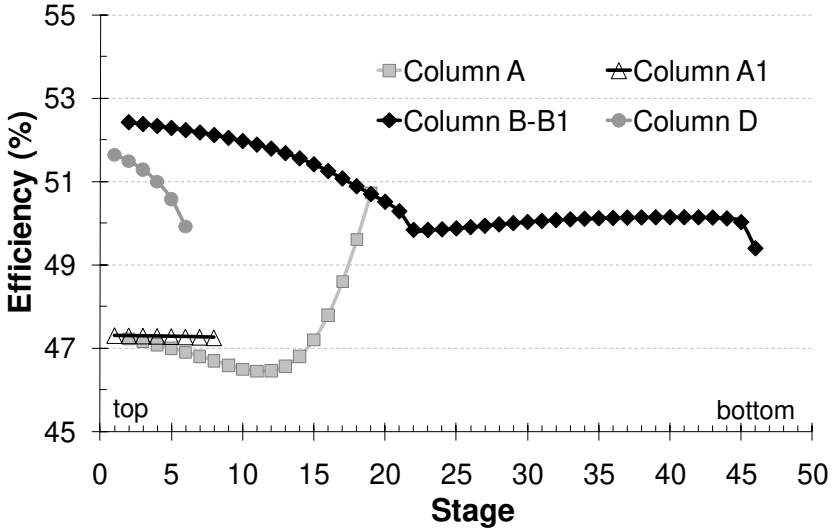

Figure 7.3. Efficiency profiles obtained in the columns.

Results of main streams are compared through Tables 7.4 and 7.5. It can be inferred that ethanol contents in hydrous ethanol (HE) and in anhydrous ethanol (AE) are lower when efficiency is taken into account; moreover there is ethanol loss in phlegmasse (PHLEGMAS) and water streams. Stillage and solvent results were the same for both approaches.

Table 7.4. Stream results for hydrous bioethanol production.

	Equilibrium Stage Model (Ideal)			**Equilibrium Stage Model with Efficiency**		
	STILLAGE	**PHLEGMAS**	**HE**	**STILLAGE**	**PHLEGMAS**	**HE**
Temperature (°C)	111.9	107.0	81.7	111.9	105.6	81.7
Mass Flow (kg/h)	175418	14622	16100	175240	14800	16100
Water (wt%)	99.4	99.4	6.8	99.4	98.6	7.6
Glucose (wt%)	0.1	-	-	0.1	-	-
Ethanol (wt%)	-	-	93.2	-	0.1	92.4
Glycerol (wt%)	0.5	-	-	0.5	-	-
Isoamyl alcohol (wt%)	-	0.6	-	-	1.3	-

Table 7.5 Stream results for anhydrous bioethanol production.

	Equilibrium Stage Model (Ideal)			**Equilibrium Stage Model with Efficiency**		
	AE	**SOLVENT**	**WATER**	**AE**	**SOLVENT**	**WATER**
Temperature (°C)	78.3	110	83.5	78.4	110	82.0
Pressure (bar)	1.013	1.013	0.5	1.0	1.0	0.5
Mass Flow (kg/h)	15051	9989	1054	15051	9989.0	1054.0
Ethanol (wt%)	99.5	-	-	99.4	-	1.3
Water (wt%)	0.5	-	99.6	0.6	-	98.5
Ethylene glycol (wt%)	-	100	0.4	-	100	0.1

Comparison of temperature profiles in column B-B1 is illustrated in Figure 7.4. This column was chosen since it has a larger number of stages and, as a result, it is the most influenced column in this process, concerned with the objectives of this work. It was observed that the curves significantly detach from each other between stages 11 and 31, besides the fact that equilibrium stage model (EQ) presents the highest temperature values. This fact can be explained by the assumption that there is enough contact time between the phases to achieve thermal equilibrium. Another observation is that EQ is more sensible to column operation, since the profile presents a disturbance in the feed position (stage 22).

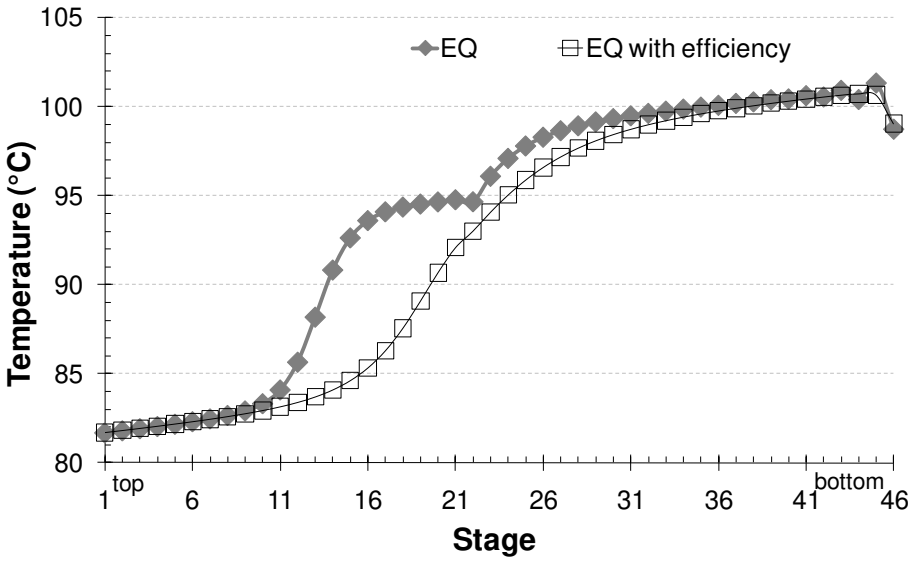

Figure 7.4. Temperature profile for column B-B1.

Temperature profile is also shown for the extractive column in Figure 7.5. Similarly to column B-B1, curves are coincident in the top and bottom stages. There is also a disturbance in the solvent feed position (stage 24) predicted by EQ.

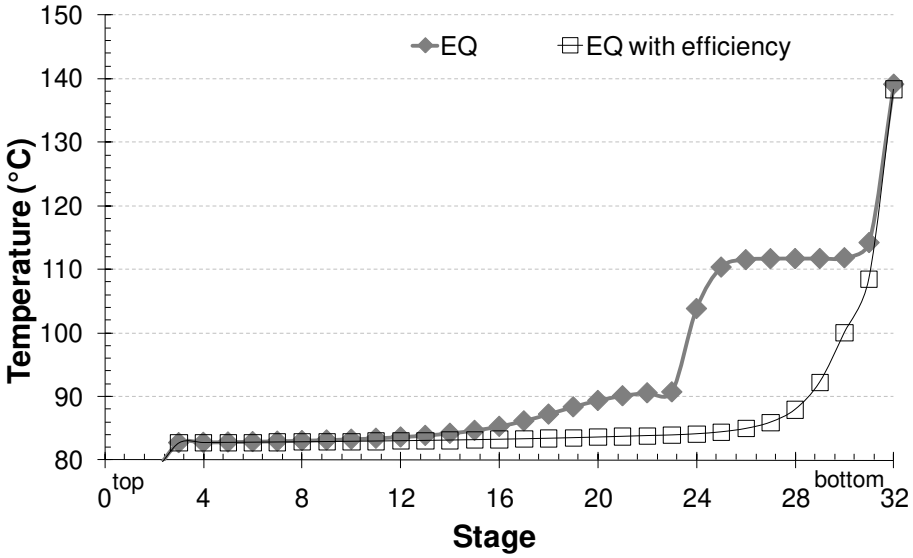

Figure 7.5. Temperature profile for the extractive column (EC).

Finally, energy requirements for concentration and dehydration processes were evaluated. The first process demanded 26.82 and 26.95 Gcal/h for EQ and EQ with efficiency, respectively. The dehydration process required 3.87 and 3.88 Gcal/h. Therefore, differences in the required energies were not considerable

between the calculation methods. However, energy requirements in the concentration process revealed to be significantly higher than in dehydration. Larger flows are the main responsible for this difference.

CONCLUSIONS

This work has shown the complete separation process in the anhydrous bioethanol production. This is an important step in the product production with a significant impact on the costs. Contrasting to other published works, this study considered other components in wine composition as well as all columns included in the process. Solvent recovery column is usually disregarded and concentration process is usually simplified using a single column. Therefore, simulations were more complex and detailed so that a more deep study can be carried out.

The introduction of efficiencies is important to diminish the consequences of the idealized assumptions of equilibrium stage model. In the simulated process, efficiencies varied along the columns, oscillating around 50 %.

Results showed significant differences in respect to stream results and temperature profiles, although energy requirements were not so influenced by the inclusion of efficiency. The concentration process revealed to be the main responsible for energy demand in the anhydrous bioethanol production process, particularly due to the large flows involved.

7.3. Comentários e Conclusões

Neste capítulo, o processo de separação completo empregado na produção de bioetanol anidro foi simulado. Diferentemente de outros trabalhos publicados, este estudo considerou co-produtos da fermentação na composição do vinho. A configuração composta por um conjunto de colunas de retificação e destilação usualmente empregada nas biorrefinarias foi considerada bem como o processo de destilação extrativa completo, ou seja, incluindo também a coluna de recuperação de solvente.

Nos processos baseados em destilação, tem-se que a introdução de eficiências diminui as implicações da suposição de equilíbrio entre as fases líquida

e vapor que deixam cada estágio. Para todo o processo de separação, os valores de eficiência variaram ao longo das colunas, no entanto, permaneceram em torno de 50 %.

A comparação entre os resultados da modelagem de equilíbrio sem e com a introdução de eficiência revelou diferenças significativas no que se refere à composição e condições das correntes de saída e aos perfis de temperatura, entretanto o consumo de energia nos refervedores das colunas não apresentou diferença significativa com a inclusão das eficiências.

Comparando-se a demanda de energia nas etapas de concentração e desidratação do bioetanol, tem-se que a etapa de concentração requer mais energia, principalmente por envolver correntes de processo com maiores vazões.

Capítulo 8
Simulação da Destilação Azeotrópica no Processo de Produção de Bioetanol Anidro

8.1. Introdução

Sendo o processo de desidratação mais utilizado nas biorrefinarias brasileiras, a destilação azeotrópica com cicloexano é caracterizada pelo alto consumo de vapor de processo e pela complexidade de operação decorrente da formação de duas fases líquidas no interior da coluna.

A formação de duas fases líquidas na coluna de destilação influencia a transferência de massa do processo, afetando a eficiência deste (Higler et al., 2004). Neste capítulo, o processo de destilação azeotrópica foi simulado através do software Aspen Plus® utilizando a modelagem de estágios de equilíbrio. A formação de duas fases líquidas no interior da coluna azeotrópica foi analisada e, com o intuito de diminuir esse fenômeno, foram estudadas diferentes configurações de processo bem como variações nas condições de operação.

Considerou-se que a alimentação do processo é bioetanol hidratado com a mesma composição indicada na seção 5.2. O objetivo da simulação foi a produção de bioetanol anidro (99,5 % em massa).

O desenvolvimento deste capítulo é descrito a seguir no trabalho intitulado "*Simulation of the azeotropic distillation for anhydrous bioethanol production: study on the formation of a second liquid phase*", publicado no periódico *Computer Aided Chemical Engineering*, v. 27, p. 1143-1148 (2009), decorrente da participação no *10th International Symposium on Process Systems Engineering* (PSE'09).

8.2. Simulation of the azeotropic distillation for anhydrous bioethanol production: study on the formation of a second liquid phase

ABSTRACT

Bioethanol is produced from fermentation of sugars, what produces a dilute solution (around 10 wt% ethanol). Because water and ethanol form an azeotrope with concentration of 95.6 wt% ethanol at 1 atm, an alternative separation process such as azeotropic distillation must be employed to produce anhydrous bioethanol, which can be used in a mixture with gasoline. In this work, simulations of three different configurations of the azeotropic distillation process with cyclohexane for anhydrous bioethanol production were carried out using software Aspen Plus. Process parameters were optimized in order to decrease the formation of a second liquid phase inside the column. Ethanol and entrainer losses as well as energy demand were evaluated.

INTRODUCTION

Climate change and the consequent need to diminish greenhouse gases emissions have encouraged the use of bioethanol in a mixture with or as a replacement of gasoline. In order to be used in a mixture with gasoline, ethanol produced from fermentation of sugars, obtained at a concentration of about 10 wt% ethanol, must be concentrated to at least 99.3 %. Since ethanol and water form an azeotrope with 95.6 wt% ethanol at 1 atm, conventional distillation can not achieve the necessary separation that meets product specification. The main processes employed for anhydrous bioethanol production are azeotropic and extractive distillation and adsorption on molecular sieves.

In the conventional configuration of the heterogeneous azeotropic distillation process for anhydrous bioethanol production, two distillation columns are used: the azeotropic one and the recovery unit. Hydrous ethanol and entrainer are fed in the azeotropic column, where anhydrous ethanol is produced on the bottom and a minimum boiling ternary azeotrope formed between ethanol, water and entrainer is produced on the top. The ternary azeotrope is heterogeneous, and the two liquid

phases are separated in a decanter. The light phase contains most of the entrainer and is recycled to the azeotropic column, while the aqueous phase is fed to the recovery column where ethanol and eventually entrainer are recovered. The stream containing ethanol recovered may be recycled to the azeotropic column, in order to reduce ethanol losses.

Benzene was the most common entrainer employed in anhydrous bioethanol production, but due to its carcinogenic characteristics cyclohexane is most frequently used nowadays. The azeotropic distillation process with cyclohexane is the most common method for anhydrous bioethanol production employed in Brazil, which is the second largest ethanol producer in the world. This process is characterized by high steam consumption on column reboilers, as well as high entrainer losses on the product. In other words, the separation step for obtaining anhydrous ethanol has a significant impact on the final product price, so that it is worthwhile to investigate procedures and alternatives to improve the process economy and performance. Simulation is an attractive tool to evaluate the process since it is not suitable to use large scale units to do so.

Simulation of the azeotropic distillation process is often complex and extremely sensitive to project parameters and specifications, mainly because of the formation of a second liquid phase inside the azeotropic column, which influences the mass transfer behaviour: column efficiencies between 25 and 50 % are not uncommon when a second liquid phase is present (Higler et al., 2004).

In this work simulations of the azeotropic distillation process with cyclohexane for anhydrous bioethanol production were carried out using software Aspen Plus. Simulation of different process configurations were carried out, and the main parameters evaluated were the formation of the second liquid phase inside the column, the separation of the ternary azeotrope during settling, entrainer losses on the anhydrous bioethanol and energy consumption on column reboilers.

Heterogeneous azeotropic distillation

Heterogeneous azeotropic distillation is widely employed in industry as a separation process for azeotropic or close-boiling mixtures, for which conventional distillation can not achieve the necessary separation. In this process, a third

component, called entrainer, is added to the binary mixture, producing a heterogeneous azeotrope with one or both components of the original mixture. In the separation of a binary azeotropic mixture, the new azeotrope produces a more favorable azeotropic pattern for the desired separation. Even though the formation of a second liquid phase simplifies entrainer recovery and the recycle process, it may affect column performance and, consequently, decrease efficiency. Different process configurations can lead to a decreased formation of a second liquid phase, without compromising anhydrous bioethanol production.

Simulation of the azeotropic distillation process

Three different configurations of the azeotropic distillation process with cyclohexane for anhydrous bioethanol production were simulated using software Aspen Plus. NRTL was the model used for calculation of the activity coefficient on the liquid phase. Approximately 500 m^3/day of anhydrous bioethanol (99.5 wt% ethanol) are produced on each case, from 16,100 kg/h (521 m^3/day) of hydrous bioethanol (93 wt% ethanol).

Configuration 1

The first configuration of the process is depicted in Figure 8.1. In this case, hydrous bioethanol is mixed with the recycle stream of the recovery column and fed to the azeotropic column. Entrainer is comprised by the organic phase obtained in the decanter and a solvent make-up stream. Anhydrous bioethanol is produced on the bottom of the azeotropic column, and the ternary azeotrope in the top. After cooling, the ternary azeotrope splits into two liquid phases in the decanter. The aqueous phase is fed to the recovery column, producing pure water on the bottom.

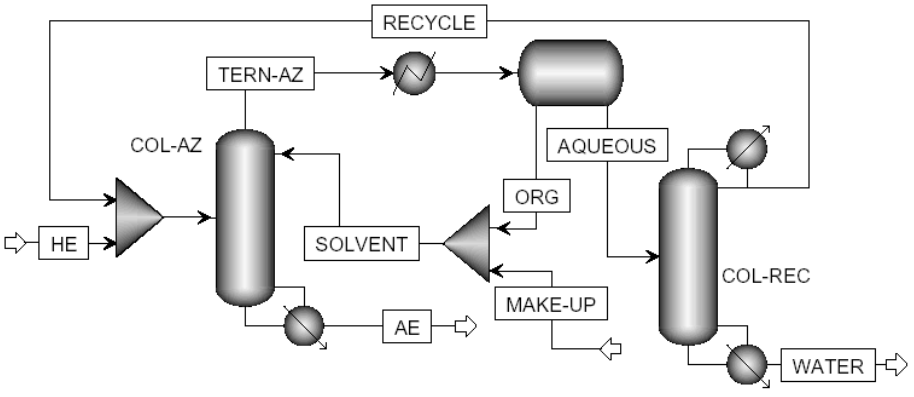

Figure 8.1. First configuration of the azeotropic distillation process.

Configuration 2

The main difference between this configuration and the first one is the withdrawn of a fraction of the aqueous phase obtained in the decanter and its mixture with the hydrous ethanol and recycle stream, which are fed to the azeotropic column (Mortaheb and Kosuge, 2004). Configuration 2 of the azeotropic distillation process is displayed in Figure 8.2.

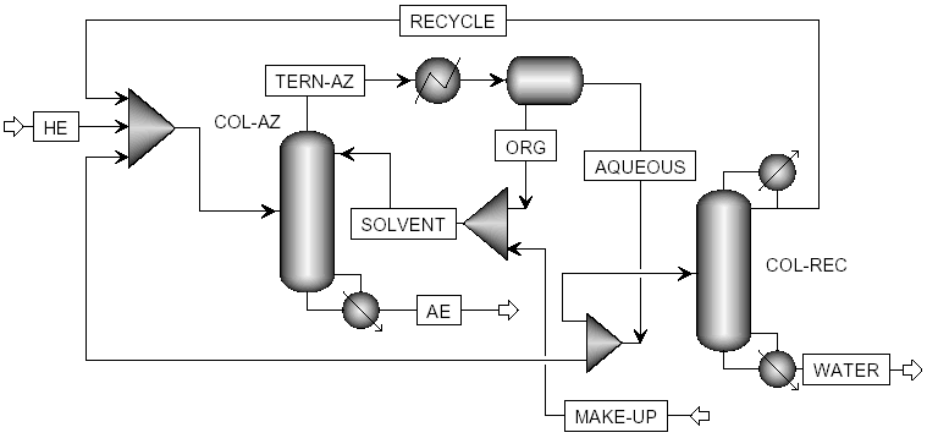

Figure 8.2. Second configuration of the azeotropic distillation process.

Configuration 3

In the third configuration part of the ternary azeotrope is condensed and mixed with hydrous ethanol, being subsequently fed to the azeotropic column. In this configuration the top product of the recovery column is not recycled to the azeotropic column, but to the decanter. This configuration is depicted in Figure 8.3.

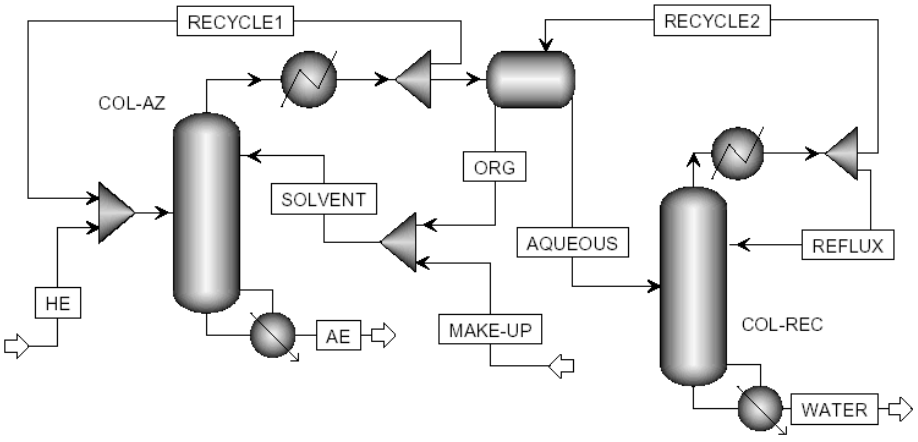

Figure 8.3. Third configuration of the azeotropic distillation process.

Simulation parameters

Columns parameters are displayed in Table 8.1. Stage numbering initiates in the top stage or attached condenser and reboiler is considered the last stage.

Table 8.1. Process parameters for each configuration.

	Configuration 1	Configuration 2	Configuration 3
COL-AZ number of stages	31	31	31
Feed inlet stage – COL-AZ	18	20	20
Solvent inlet stage	1	1	1
COL-REC number of stages	25	22	17
Feed inlet stage – COL-REC	13	13	13
Decanter temperature (°C)	50	50	50

Simulation results and discussion

Main streams results

The characteristics of process stream differ for each configuration. Results are presented in Tables 8.2 through 8.4.

Table 8.2. Composition of the main streams for the first configuration.

Stream	AE	MAKE-UP	ORG	AQUEOUS	WATER
Temperature (ºC)	78.2	50.0	50.0	50.0	100.0
Flow (kg/h)	15063.6	16.8	42501.6	19524.1	1053.5
Ethanol (wt%)	99.5	0.0	4.7	71.2	0.0
Water (wt%)	0.4	0.0	0.1	10.8	100.0
Cyclohexane (wt%)	0.1	100.0	95.2	18.0	0.0

Table 8.3. Composition of the main streams for the second configuration.

Stream	AE	MAKE-UP	ORG	AQUEOUS	WATER
Temperature (ºC)	78.2	50.0	50.0	50.0	100.0
Flow (kg/h)	15064.4	21.0	50274.1	22813.3	1057.3
Ethanol (wt%)	99.5	0.0	4.6	71.5	0.0
Water (wt%)	0.4	0.0	0.1	11.3	100.0
Cyclohexane (wt%)	0.1	100.0	95.3	17.2	0.0

Table 8.4. Composition of the main streams for the third configuration.

Stream	AE	MAKE-UP	ORG	AQUEOUS	WATER
Temperature (ºC)	78.1	50.0	50.0	50.0	78.6
Flow (kg/h)	8395.4	16.8	22877.5	31880.6	7722.0
Ethanol (wt%)	99.5	0.0	5.2	67.6	85.9
Water (wt%)	0.3	0.0	0.1	7.5	14.1
Cyclohexane (wt%)	0.2	100.0	94.7	24.9	0.0

Streams obtained in the decanter (AQUEOUS and ORG) have different compositions on each studied configuration. Configurations 1 and 2 showed similar results, while configuration 3 had a higher concentration of solvent in the aqueous phase. Due to this contamination, recovery column behaviour was significantly affected and "WATER" stream has a high concentration of ethanol (85.9 wt%), so it must be recycled to the previous distillation stage, where hydrous bioethanol is produced.

Energy consumption and entrainer and ethanol losses

Different process parameters affect ethanol and entrainer losses, as well as energy consumption on column reboilers. The results for these parameters are given in Table 8.5.

Table 8.5. Ethanol and entrainer losses and energy consumption on column reboilers for each configuration.

	Configuration 1	Configuration 2	Configuration 3
Ethanol losses (%)*	0.00	0.00	44.26
Entrainer losses (%)**	0.04	0.03	0.07
Reboilers energy (kJ/kg AE)	5588	5828	7235

* Considering the amount of ethanol in the "HE" stream

** Considering the amount of cyclohexane that is fed to the azeotropic column

The "WATER" stream on the third configuration has a very high concentration of ethanol, thus ethanol losses on this configuration are significant. The recycle of this stream to the conventional distillation column would allow ethanol recovery at the expense of an increase in energy consumption of the process, which already has the largest energy consumption on column reboilers.

Configurations 1 and 2, on the other hand, present low ethanol and entrainer losses, as well as a relatively low energy consumption.

Formation of the second liquid phase inside the azeotropic column

Similar liquid flow profiles were observed in the azeotropic column. The profiles for each configuration are represented in Figures 8.4 through 8.6.

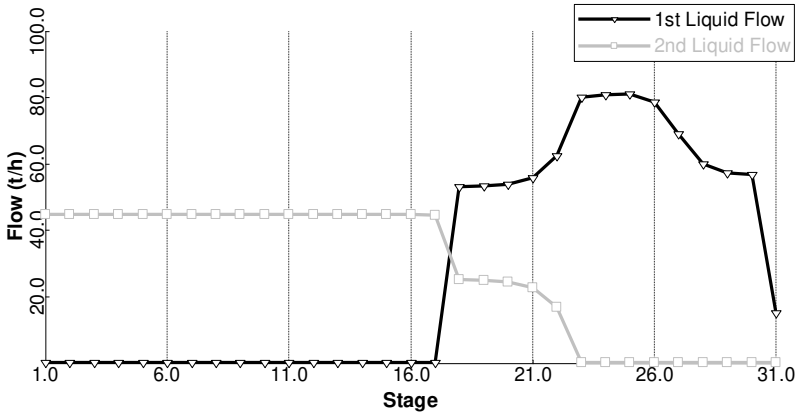

Figure 8.4. Liquid flow profile in the azeotropic column for configuration 1.

Changes in column parameters, such as feed inlet position in the azeotropic column, greatly influence the formation of a second liquid phase. For the first configuration, the feed inlet stage in the azeotropic column (18) is the one that first presents two liquid phases. The same occurs for the other configurations. The feed inlet stage is the last one that allows column convergence; on the other hand, if the feed stage is located near the top of the column, two liquid phases are present in this region too. This means that the feed inlet stage in the azeotropic column has to be defined with caution, since it impacts unit behavior and performance.

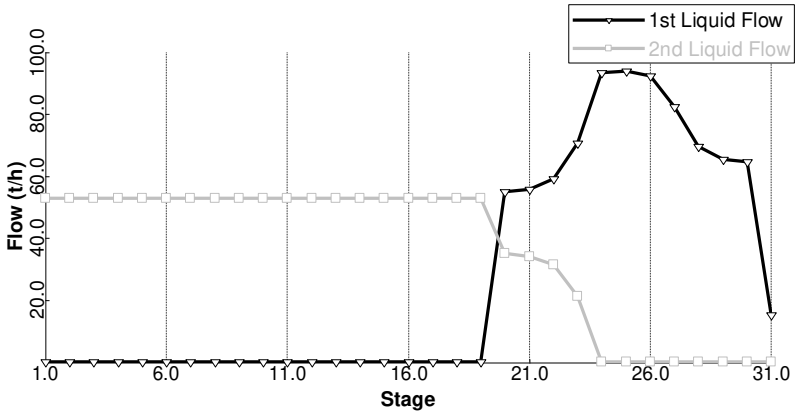

Figure 8.5. Liquid flow profile in the azeotropic column for configuration 2.

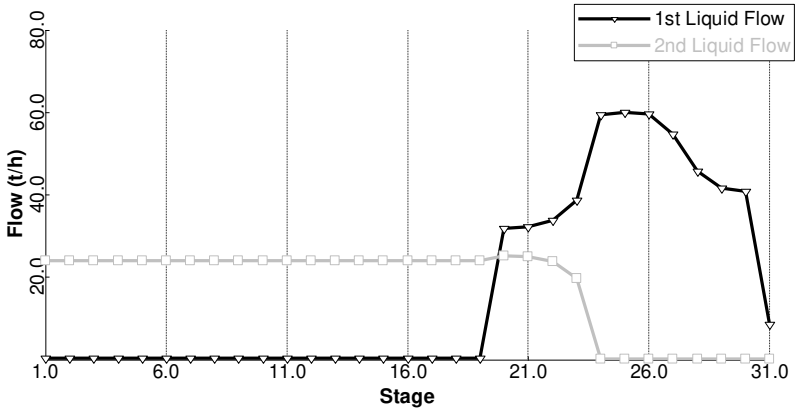

Figure 8.6. Liquid flow profile in the azeotropic column for configuration 3.

CONCLUSIONS

Simulations of the azeotropic distillation process with cyclohexane for anhydrous bioethanol production were carried out for three different process configurations. Simulations focus was on decrease of the formation of a second liquid phase inside the azeotropic column, what has significant impacts on process performance. It was observed that changes in process parameters, such as feed inlet stage, greatly influence the formation of the second liquid phase. Configuration 1 presented the best results, considering energy consumption on columns reboilers, ethanol and entrainer losses and product contamination with entrainer.

8.3. Comentários e Conclusões

Neste capítulo, foram apresentadas três configurações alternativas para o processo de destilação azeotrópica. As simulações tiveram como objetivo a diminuição da formação de duas fases líquidas no interior da coluna azeotrópica, uma vez que este fenômeno possui efeitos significativos no desempenho da coluna. Observou-se que a mudança de parâmetros de processo, como posição de alimentação na coluna, influencia consideravelmente a formação da segunda fase líquida. Além disso, a definição do equipamento para o qual a corrente de topo da coluna de recuperação retorna apresentou significativa importância. Na configuração 1, que apresentou os melhores resultados no que se refere à demanda de energia e às perdas de etanol e solvente, esta corrente é reciclada para a coluna azeotrópica.

Capítulo 9

Simulação do Processo de Extração Fermentativa a Vácuo e Análise do Impacto na Etapa de Destilação

9.1. Introdução

Como mostrado na seção 3.2, como alternativa para o processo fermentativo, Silva et al. (1999) e Atala (2004) estudaram a fermentação extrativa a vácuo, que consiste em um processo fermentativo contínuo acoplado a um evaporador a vácuo do tipo *flash*. Esta configuração permite que uma maior quantidade de substrato seja adicionada ao reator, produzindo um vinho mais concentrado. Consequentemente, a destilação deste vinho produz menores volumes de resíduos como a vinhaça. Adicionalmente, tem-se a diminuição da demanda de energia térmica do processo de destilação.

Neste capítulo, esta configuração alternativa em conjunto com a destilação foi estudada a fim de se avaliar o processo, principalmente quanto à energia requerida. Outra alteração do processo foi a realização da integração energética no processo de destilação (destilação duplo e triplo efeito).

O desenvolvimento deste capítulo é apresentado a seguir, no trabalho intitulado "*Evaluation of an extractive fermentation process coupled with a vacuum flash chamber and the subsequent distillation for bioethanol production*" a ser submetido a periódico internacional.

9.2. Evaluation of an extractive fermentation process coupled with a vacuum flash chamber and the subsequent distillation for bioethanol production

ABSTRACT

An alternative to the conventional fed-batch fermentation process for bioethanol production, the extractive fermentation process coupled with a vacuum flash chamber, is evaluated in this work through process simulation. In the alternative process, ethanol produced is continuously removed from the fermentation medium,

thus decreasing inhibitory effects on yeast cells and producing a wine of higher ethanol content, which leads to decreased energy consumption and residue generation on the subsequent distillation step, where wine purification takes place. Different configurations of the distillation system (conventional, double and triple effect) for hydrous bioethanol (93 wt%) production are integrated to the studied fermentation process, providing resources that allow the comparison of different process configurations and their impacts on bioethanol losses, energy consumption and residue generation.

INTRODUCTION

The efficient production of renewable fuels is one of the most significant challenges faced by humanity, in a scenario of predicted depletion of fossil resources, increase on energy demand and climate change (Dodić et al., 2009; Saxena, 2009). Bioethanol has been acknowledged as the best viable alternative to fossil fuels in the immediate future (Walter et al., 2008), offering environmental and long-term economic advantages over fossil fuels (Cheng and Wang, 2008). Even though bioethanol has been produced in a large scale basis in countries like Brazil for more than twenty years, process improvements are still possible.

Considering the entire bioethanol production process from sugarcane, the fermentation step, on which sugars are converted into ethanol by yeasts, is responsible for the majority of the sugar losses: yeast cells are inhibited by product (ethanol), substrate (sugars) and biomass (yeast cells), and fermentation yields are limited due to cells growth, rising temperature (Rivera et al., 2006) and byproducts formation during parallel fermentation reactions (Bai et al., 2008). One of the main alternatives to increase fermentation yields by minimizing inhibition by product is the removal of ethanol from fermentation media, based on vacuum fermentation (Ramalingham and Finn, 1977; Cysewski and Wilke, 1978), on pervaporation techniques (Christen et al., 1990; Thongsukmak and Sirkar, 2009), on liquid-liquid extraction (Daugulis et al., 1991; Chen and Wang, 2008) and on the integration of a flash to the process (Ishida and Shimizu, 1996; Maiorella et al., 1984; Silva et al., 1999; Costa et al., 2001). The fermentation system coupled with a vacuum flash chamber seems to be the most adequate process for industrial application in

Brazil, due to its ease of operation and low cost (Silva et al., 1999). In this process, ethanol is continuously removed from the fermentation media, simultaneously to its production, allowing ethanol concentration in the reactor to remain at low levels (5 °GL), which presents low inhibitory effects on yeast cells. In addition, wine obtained in the flash chamber presents higher ethanol concentration (around 50 °GL), what reduces energy consumption and ethanol losses on the subsequent distillation step (Atala, 2004). As a consequence of the reduction on energy consumption, less sugarcane bagasse need to be burnt in boilers to provide energy to supply the plant; thus, larger amounts of bagasse may be available for the hydrolysis process when 2nd generation ethanol production takes place.

After fermentation is achieved, wine is concentrated on a series of distillation and rectification columns, producing hydrous bioethanol (around 95 °GL). Since wine produced in conventional fermentation processes contains between 7 and 10 °GL, the distillation process must be re-evaluated in order to efficiently purify the product derived from vacuum flash fermentation.

In this work simulations of both conventional and extractive fermentation process coupled with a vacuum flash chamber, associated with different configurations of the subsequent distillation step were carried out using the process simulation software Aspen Plus®. Conventional, double and triple effect distillation systems were simulated; energy consumption, ethanol losses and residue generation were evaluated on each case.

METHODOLOGY

Simulation of fermentation and distillation processes was carried out using software Aspen Plus®. The Non-Random Two Liquid model for calculation of the activity coefficient of the liquid phase and Hayden-O'Connell equation-of-state for calculation of the vapor phase (NRTL-HOC) were employed for estimation of thermodynamic properties. An extensive study of the thermodynamic behavior of binary pairs present on the distillation columns for bioethanol purification was previously carried out, and it was verified that the NRTL-HOC model represents the system suitably.

In order to define the best operating conditions of the vacuum extractive fermentation process, which allow significant reduction on energy consumption as well as on ethanol and sugar losses, the main parameters of the flash chamber (pressure and temperature) and the amount of wine recycled to the reactor were carefully evaluated through several simulations. The evaluated parameters define the phase separation in the flash chamber, and therefore the amount of ethanol recovered in the system. This analysis is of crucial importance on the current development stage of the technology. The results of the optimum configuration of the extractive fermentation coupled with a flash chamber are then compared to those obtained in the conventional fermentation process employed in the Brazilian ethanol industry.

Different combinations between conventional and alternative (extractive fermentation coupled with a vacuum flash chamber) fermentation processes and conventional, double and triple effect distillation columns were carried out. A throughout description of the studied processes is given below.

Conventional fermentation process

The simulation of the conventional fermentation process, represented in Figure 9.1, is based on the configurations employed in the industry, on which a substrate of relatively low concentration (around 150 g/L sucrose, which corresponds to 15 wt% sucrose) is fed to the fermentation reactor. Fermentation reactions are comprised by sucrose hydrolysis, producing glucose and fructose (equation 9.1, with conversion equal to 99 %), conversion of 99.5 % of reducing sugars into ethanol and carbon dioxide (equation 9.2) and conversion of the remaining reducing sugars into byproducts (acetic acid and glycerol), ethanol and carbon dioxide, as shown in equation 9.3 (Franceschin et al., 2006).

$$C_{12}H_{22}O_{11} + H_2O \rightarrow 2\ C_6H_{12}O_6 \quad (9.1)$$

$$C_6H_{12}O_6 \rightarrow 2\ C_2H_5OH + 2CO_2 \quad (9.2)$$

$$2\ C_6H_{12}O_6 + H_2O \rightarrow C_2H_4O_2 + 2C_3H_8O_3 + C_2H_5OH + 2CO_2 \quad (9.3)$$

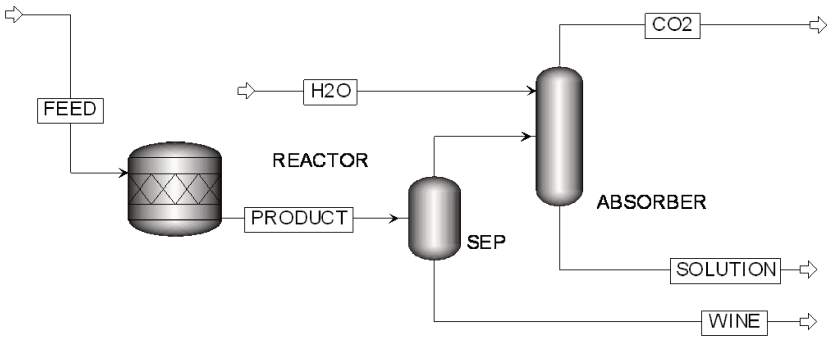

Figure 9.1. Configuration of the conventional fermentation process.

A stoichiometric reactor model was used to simulate the fermentation reactor. The three reactions cited above occur in series, and the heat of reaction was set to 1200 kJ/kg of ethanol (Kwiatkowski et al., 2006).

Fermentation is usually carried out in Brazilian industries under temperatures around 33 °C, since higher temperatures disable yeast cells, decreasing fermentation yields (Rivera et al., 2006). Because fermentation reactions are exothermic, a heat exchanger must be employed in the conventional fermentation reactor in order to keep suitable temperatures. In addition, ethanol content in fermentation reactors must be maintained between 7 and 10 °GL to prevent inhibitory effects.

Two products are obtained after fermentation: wine and fermentation gases. Gases are fed to an absorber column in order to recover evaporated ethanol, on which an alcoholic solution and carbon dioxide are obtained. Due to low substrate concentration and yeast inhibition, ethanol content of the wine produced in conventional fermentation is relatively low (around 8 wt%). In the product purification step, a series of distillation and rectification columns is employed to produce hydrous ethanol, with an ethanol content close to that of the azeotropic point (95.6 wt%).

Extractive fermentation process coupled with a vacuum flash chamber

The main objective of the fermentation process is to obtain high concentration of ethanol in the wine, which is desirable to achieve low energy consumption on the subsequent distillation stage as well as complete consumption

of sugars in the fermentation media, but restrictions in the fermentation conditions, such as product inhibition, must be taken into consideration.

In the extractive fermentation process coupled with a vacuum flash chamber, ethanol produced during fermentation reactions (reactions 1, 2 and 3 cited above) is continuously removed from the fermentation media, thus allowing the use of higher concentration substrate (around 400 g/L). The removal of ethanol simultaneously with its production allows the ethanol content of the reactor to remain at low levels (around 8 wt%), and so the same conversion parameters for the conventional fermentation reactions were adopted. The product is continuously removed from the reactor and after a purge is made to remove low-volatile products, it is fed to a vacuum flash chamber producing an ethanol-rich vapor phase and a liquid phase. While the vapor phase comprises the wine, which is sent to the purification step, the liquid phase is recycled to the reactor; since the temperature of the vacuum flash chamber is relatively low, the recycle of the liquid stream maintains the fermentation reactor at the required temperatures (around 30 °C) without the need of external heat exchangers. Wine produced in the flash chamber contains approximately 30 wt% ethanol, thus less energy is required to produce hydrous ethanol and the amount of residue generated in the distillation step is much smaller than the one produced during concentration of wine from conventional fermentation. Configuration of the extractive fermentation process coupled with a vacuum flash chamber is depicted in Figure 9.2.

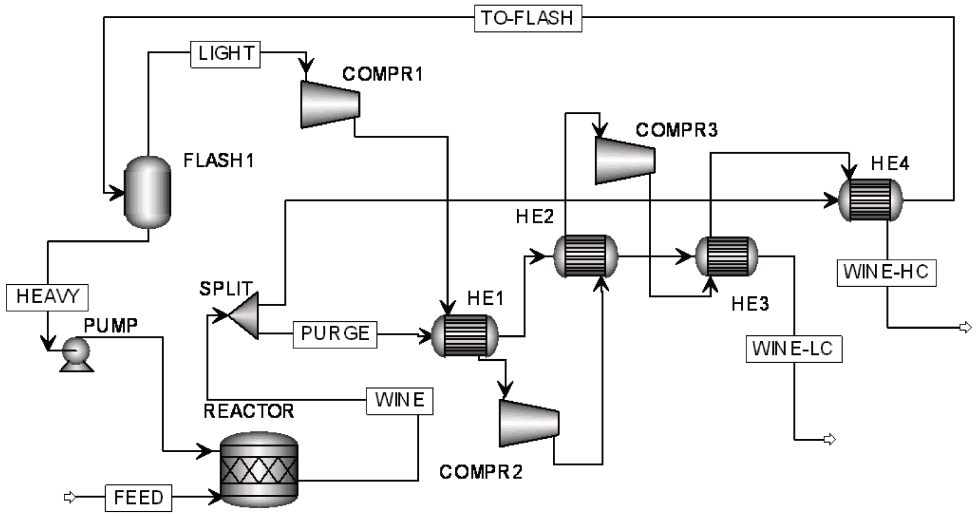

Figure 9.2. Configuration of the vacuum extractive fermentative process.

Differently from the conventional fermentation process, in the vacuum extractive fermentation process, two streams are obtained: “WINE-HC” (30 wt% ethanol) and “WINE-LC” (8 wt% ethanol). Since the flash chamber operates under vacuum, it is necessary to raise the pressure of the “LIGHT” stream using a series of compressors before feeding it to the conventional distillation columns, which are operated under atmospheric pressure. Since compression generates heat, the compressed vapor has to be cooled, so the “PURGE” stream was used to exchange heat with the compressed stream. In addition, the compressed stream was used to heat up the stream that feeds the flash chamber up to around 32 °C.

Distillation

Concentration of the wine is achieved using a series of distillation and rectification columns in order to produce hydrous bioethanol, which contains around 93 wt% ethanol. In the conventional fermentation process, an ethanol-rich stream (”WINE”) and an alcoholic solution from the absorber, named “SOLUTION”, are produced. Whereas in the alternative process, two other streams are obtained: “WINE-HC” and “WINE-LC”, comprised by flash vapour phase and a mixture of a reactor purge. Thus, the distillation columns for each case may have different configurations, due to the characteristics of the feed streams.

Conventional distillation

The conventional distillation system simulated in this work is based on the configuration commonly employed in the industry: the distillation section is comprised by three columns located in the top of each other: A (18 stages), A1 (8 stages) and D (6 stages), and rectification takes place in column B (50 stages); all columns operate under atmospheric pressures.

In this process, the feed streams are fed to the distillation columns, on which stillage (residue), phlegms (ethanol-rich streams, containing around 40 – 50 wt% ethanol), second grade ethanol (a mixture with high ethanol and volatiles content) and gases (mainly CO_2) are produced; liquid phlegm is a bottom product of column D and vapour phlegm is produced near the top of column A. Phlegms are fed to the rectification columns, producing hydrous ethanol in the top and phlegmasse in the

bottom. Configuration of the conventional distillation columns is depicted in Figure 9.3. This simulation was taken as base for the alternative configurations.

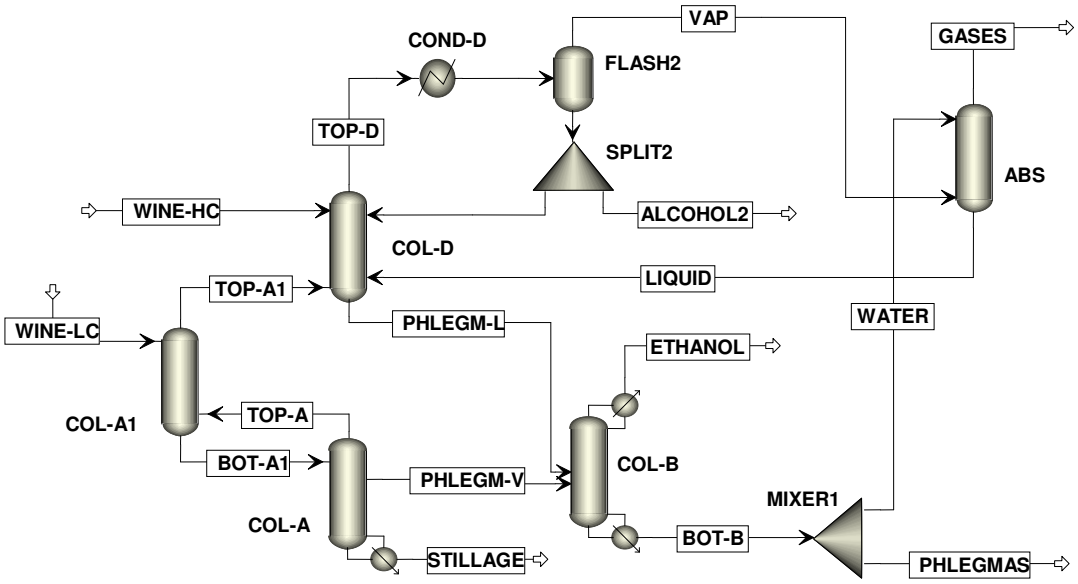

Figure 9.3. Configuration of the conventional distillation process.

When wine is produced in the extractive fermentation process, 3 compressors must be employed in series, since the operating pressure of the flash chamber is very low (around 0.07 bar) and that of the distillation columns is atmospheric. When conventional fermentation is employed, no compressors are necessary.

Double effect distillation

The double effect process is similar to the conventional configuration, but the distillation columns operate under vacuum (19 – 25 kPa), while rectification columns operate under atmospheric pressure (101 – 135 kPa). In this way, different temperature levels are observed between column A reboiler and column B condenser (65 and 78 °C, respectively), allowing thermal integration of these equipments and consequently reducing energy consumption on the distillation stage. However, due to the low pressure of column D, large amounts of ethanol are lost on the “GASES” stream, produced at the top of this column; thus, an absorber was employed to recover some of the ethanol vaporized on top of column D, and a fraction of “PHLEGMAS” stream (bottom stream of the rectification column

containing 99.9 % of water) is used to wash the gases. Configuration of this process applied to the alternative fermentation is depicted in Figure 9.4.

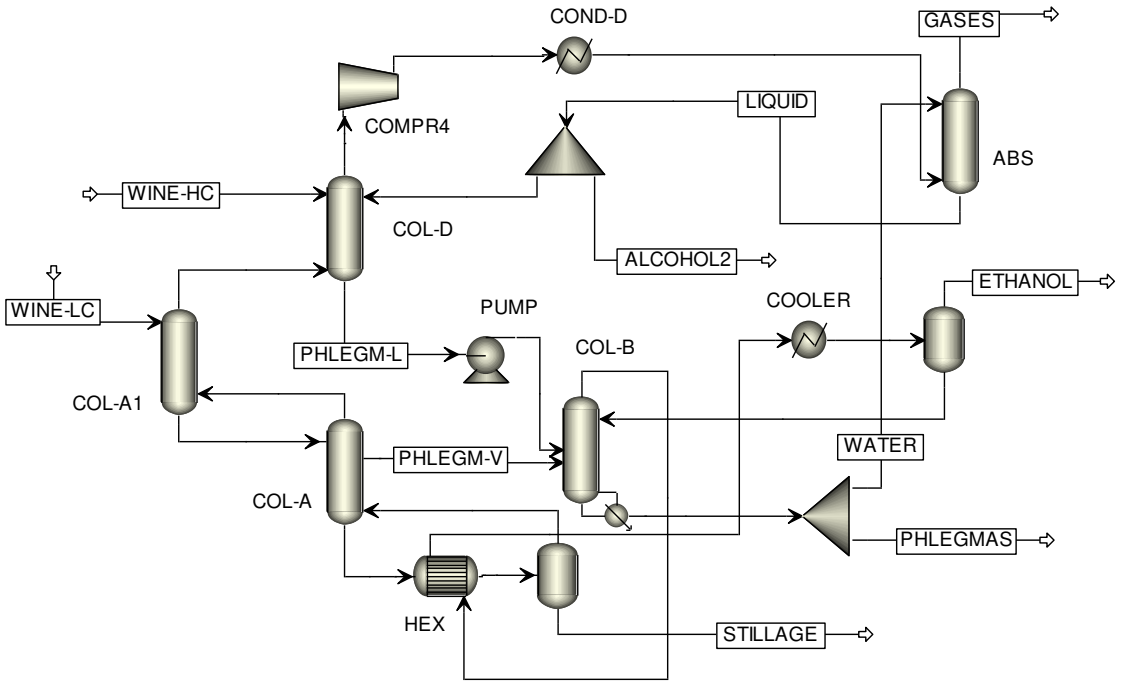

Figure 9.4. Configuration of the double effect distillation process.

Since the operating pressures of the distillation columns in this case are lower than those of the conventional distillation, only one compressor must be used to raise the pressure of the flash vapour phase when the extractive fermentation process is employed. However, in the distillation step, another compressor is necessary to raise the pressure of the top stream of column D it is sent to the absorber column.

Triple effect distillation

In the triple effect configuration, the distillation columns operate under vacuum (19 – 25 kPa), and the liquid phlegm stream produced on column D is split in two: one of them is fed to a rectification column operating under nearly atmospheric pressure (column “B”, 70 – 80 kPa) and the other is fed to a rectification column which operates under relatively high pressure (column “B-P”, 240 – 250 kPa). As in the double effect distillation, top product of column D is washed with phlegmasse in an absorber column in order to recover ethanol.

Thermal integration between columns reboilers and condensers are possible, as depicted on Figure 9.5.

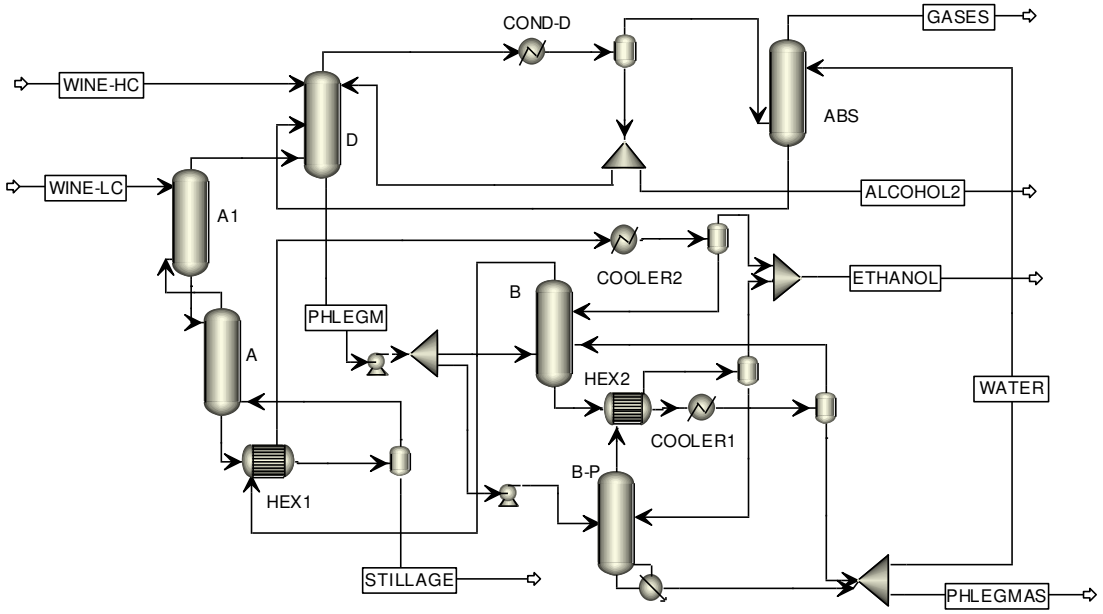

Figure 9.5. Configuration of the triple effect distillation.

RESULTS

Extractive fermentation coupled with a vacuum flash chamber

A preliminary study considering just a flash chamber was carried out. Inlet temperature and the vessel pressure were varied in order to analyze the influence on the outlet temperature and on the ethanol mass fraction of the vapor stream. Results are illustrated in Figure 9.6. It can be observed that pressures below 0.05 bar result in very low temperatures, which is not desirable because the liquid stream will be sent back to the reactor and it can reduce its temperature to less than 28 °C. Moreover, such low pressures are very difficult and expensive to achieve. At the same time, higher pressures lead to lower ethanol content in the vapor phase, which will determine that of the concentrated wine ("WINE-HC"). From Figure 9.6, it can also be verified that lower inlet temperatures result in lower ethanol mass fractions and outlet temperatures.

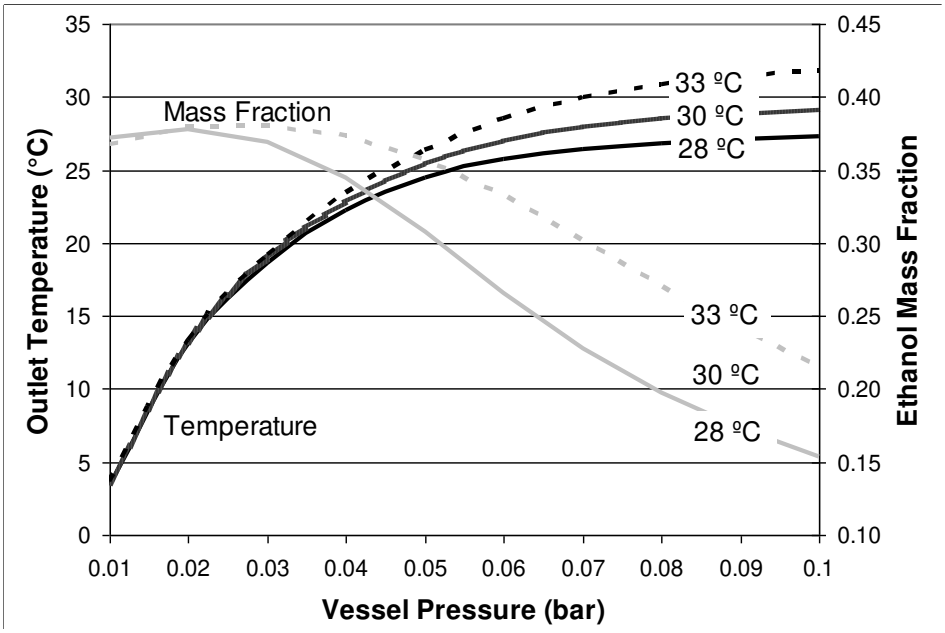

Figure 9.6. Analysis of the flash chamber conditions: outlet temperature of the flash chamber and ethanol content of the flash vapor phase for different vessel pressures.

For these reasons, further simulations considering vessel pressures of 0.05 and 0.07 bar and different inlet temperatures in the complete vacuum extractive fermentative process, similar to the illustration depicted in Figure 9.2, were carried out. In these simulations, a heater was used instead of HE4 to heat the mixture that is fed to the flash chamber, so its energy requirement was evaluated. For a vessel pressure of 0.07 bar, inlet temperatures lower than 30 °C lead to extremely high recirculation flows. Ten cases were evaluated and results are given in Table 9.1. In all simulations, the reactor temperature was kept between 28 and 33 °C without any heating or cooling operation; in addition, concentration of ethanol in the reactor was set to 8 wt%. For all cases studied, ethanol mass fraction and mass flow of “WINE-HC” presented no significant variations, and their values remained around 0.3 and 100 kg/h, respectively.

Table 9.1. Results obtained for different inlet temperatures and vessel pressures.

Case	Inlet Temperature (°C)	Vat Pressure (bar)	Reactor Temperature (°C)	TO-FLASH flow (kg/h)	Required Energy (MJ/h)
1	28	0.05	28.0	8679.9	79.9
2	29	0.05	29.0	6957.4	81.3
3	30	0.05	30.0	5807.0	82.6
4	31	0.05	31.0	4954.3	84.0
5	32	0.05	32.0	4341.1	85.2
6	33	0.05	33.0	3887.9	86.8
7	30	0.07	29.9	119683.6	58.8
8	31	0.07	30.2	25083.9	75.9
9	32	0.07	30.6	14170.1	78.3
10	33	0.07	30.9	9972.0	80.1

From Table 9.1, it is observed that the recirculation flow has an important role in the process, since it allows unfavorable conditions, such as higher vessel pressure and lower inlet temperature, to achieve a desirable ethanol mass fraction in the “WINE-HC” stream. From Table 9.1, it is observed that the recirculation flow in case 7 is quite higher than that of the other cases, which would require considerably large equipments. Therefore, this case was disregarded and the five cases that presented the lowest energy consumption were thoroughly evaluated as shown in Figure 9.7.

The selection of the best operating conditions must take into account the energy requirement to raise the temperature of the mixture fed to the reactor, since it influences the operational costs, and the recirculation flow that determines the equipment volume and consequently its costs. As can be seen in Figure 9.6, the case that combines reasonable flow and energy requirement is the case 9, which consists on the inlet temperature of 32 °C and the vessel pressure of 0.07 bar. Therefore, this case was used to evaluate the distillation stage for ethanol purification.

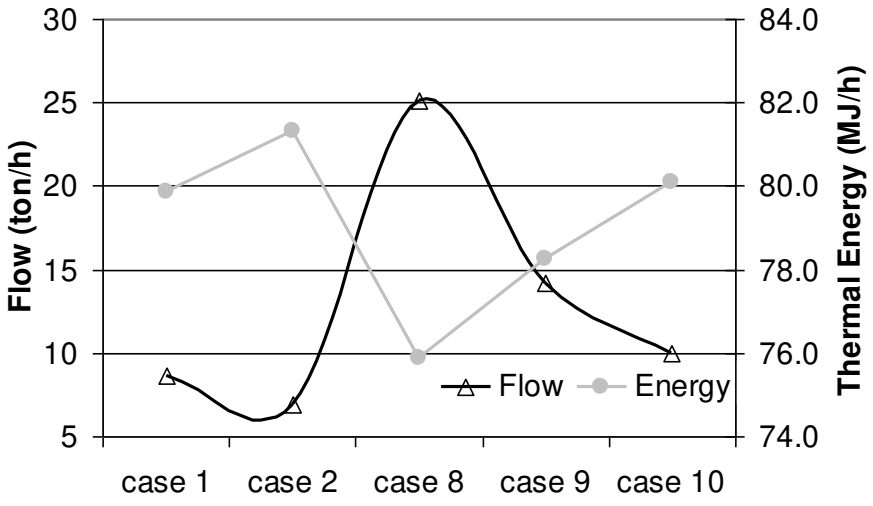

Figure 9.7. Recirculation flow and energy consumption for the main cases.

Concentration of the feed in the extractive fermentation process

Due to the larger concentration of the feed on the extractive fermentation processes (40 wt% sucrose), lower amounts of residue are generated during the purification step. However, when sugarcane juice is used as raw material, it is necessary to raise the concentration of sugars in the feed stream, since concentration of sugars in this solution is equal to around 15 wt%. This is usually done employing multiple effect evaporators (MEE), on which the feed stream is split in two, one of them being concentrated on the MEE until sugars concentration reaches around 65 wt%. Then, this concentrated stream is mixed with the remaining diluted fraction, producing a 40 wt% sucrose solution, suitable to the extractive fermentation process.

Sugarcane juice concentration may be eliminated when molasses, a by-product of sugar refining, are available. This is true in the case of an annexed distillery (a plant on which sugarcane is used to produce both sugar and ethanol), on which sugar molasses are available on site. However, in autonomous distillery, on which all sugarcane processes is diverted for ethanol production, molasses are not promptly available and concentration of juice must be carried out.

Thus, a simulation of the multiple effect evaporation process was carried out, in order to determine the energy required to increase the concentration of the

feed stream. This was done using the process simulator UniSim Design, as described by Dias et al. (2009b). In this simulation, a system comprised by separator, valve and heat exchanger was used to represent the MEE, since the process simulators employed in this work do not have the unit operation that represents this equipment. The simulation was used to calculate the difference between the energy required to concentrate the feed stream for the conventional fermentation process (150 g/L) and that for the extractive fermentation process (400 g/L). Five evaporation stages were considered, requiring approximately 3900 kJ/kg of hydrous ethanol to concentrate the feed in the extractive fermentation process.

Coupled fermentation and distillation processes

Four combinations of the processes described on section 2 were evaluated: one considering the typical industrial configuration found nowadays, and three others based on the extractive fermentation process coupled with a vacuum flash chamber and different configurations of the distillation columns.

In order to represent the typical industrial configuration, conventional fermentation process was simulated along with the conventional distillation process (configuration 1). In this process, wine containing 8 wt% ethanol is fed to the distillation columns, producing hydrous ethanol (93 wt%).

Configurations 2 through 4 are based on the extractive fermentation process coupled with a vacuum flash chamber, with flash parameters equal to those described in section 3.1, and different configurations of the distillation system, as indicated in Table 9.2.

Table 9.2. Items present on each of the studied configurations.

Item	Configuration			
	1	2	3	4
Conventional fermentation	X			
Extractive fermentation coupled with a vacuum flash chamber		X	X	X
Conventional distillation	X	X		
Double-effect distillation			X	
Triple-effect distillation				X

Since ethanol concentration on the product stream obtained on the extractive fermentation are higher than those obtained in conventional fermentation, different flows are observed; in order to properly compare both configurations of the fermentation process, the amount of ethanol that is delivered to the purification step was fixed on all the configurations.

Feed inlet position was optimized for each configuration. Since characteristics of the streams are different on each case, differences in the distillation columns parameters are observed. For instance, the removal of an ethanol-rich stream (phlegm) on the vapour phase from the top of column A, as is the case on the conventional distillation, does not provide reduction on the energy consumption or increase on ethanol recovery on both double and triple effect distillation processes. Thus, ethanol (phlegm) is recovered only on the liquid phase from the top of column D on configurations 3 and 4.

On Table 9.3 the main parameters of the distillation columns are depicted. Stage numbering increases towards the bottom of the column.

Table 9.3**.** Parameters of the distillation columns.

Parameter	**Configuration**			
	1	**2**	**3**	**4**
Number of stages – Column A	19	19	18	18
Number of stages – Column A1	8	8	8	8
Number of stages – Column D	6	6	6	6
Number of stages – Column B,B1	46	50	50	30
Number of stages – Column B-P	-	-	-	35
“WINE-LC” inlet position – Column A1	1	1	1	1
“WINE-HC” inlet position – Column D	-	1	1	1
“PHLEGM-L” inlet position – Column B,B1	24	30	20	24
“PHLEGM-V” inlet position – Column B,B1	36	23	-	-

Energy consumption of the unit operations present on each configuration was evaluated, considering energy demand of thermally integrated units (such as column A reboiler and column B condenser on configuration 2) equal to 0. Electric

energy required to operate compressors was evaluated as well. Results displayed on Table 9.4 include the energy required to concentrate the feed stream containing the sugars, the energy removed from the fermentation reactor, pre-heating of the wine, when is the case, as well as reboilers and condensers duties.

Table 9.4. Energy consumption on each configuration.

Parameter	Configuration			
	1	2	3	4
Heating operations (kJ/kg hydrous ethanol)	10634	7822	7413	6753
Cooling operations (kJ/kg hydrous ethanol)	-7561	-4043	-3404	-1490
Electric energy for compressors (kJ/kg hydrous ethanol)	-	990	853	375

Thus, a reduction on energy consumption is observed from configurations 1 through 4: 26, 30 and 36 % reduction on the heating operations are observed in configurations 2, 3 and 4, respectively, when compared to configuration 1. For the cooling operations, values of 47, 55 and 80 % are observed.

If another sugar-rich stream is available for fermentation, such as molasses in the case of an annexed distillery, there is no need to concentrate the feed prior to the extractive fermentation process. Thus, a decrease on the energy consumption is observed, as shown in Table 9.5:

Table 9.5. Energy consumption on each configuration, for the case of an annexed distillery (use of sugar molasses as raw material).

Parameter	Configuration			
	1	2	3	4
Heating operations (kJ/kg hydrous ethanol)	10634	4013	3493	2885
Cooling operations (kJ/kg hydrous ethanol)	-7561	-4043	-3404	-1490
Electric energy for compressors (kJ/kg hydrous ethanol)		990	853	375

Therefore, in the case of an annexed distillery, the reduction on energy consumption is even more significant, when comparing the alternative process to the conventional fermentation: a decrease of 62, 67 and 73 % on the energy demand of the heating operations are observed in configurations 2, 3 and 4, respectively, when compared to configuration 1. However, sugar molasses could

hardly be enough to provide sugars for bioethanol production, thus sugarcane juice would complement the feed stream. In this case, intermediate values of energy consumption would be observed.

Since feed of the extractive distillation system is more concentrated than that of the conventional fermentation, residue generation during the extractive fermentation process and the subsequent distillation step is considerably smaller.

A similar trend cannot be observed, however, on ethanol losses on each configuration. Due to the fact that the double and triple effect distillation systems work under sub atmospheric pressures, more ethanol is lost on the "GASES" stream than on the situations conventionally employed on the distillation columns (atmospheric pressure).

Flow of the most important process streams and ethanol losses on each configuration are presented in Table 9.6.

Table 9.6. Flow of the main process streams and ethanol losses on each configuration.

Parameter	Configuration			
	1	2	3	4
Hydrous ethanol flow (kg/h)	38.08	38.45	37.36	37.87
Vinasse flow (kg/h)	323.76	42.07	53.69	53.68
Phlegmasse flow (kg/h)	64.96	50.67	36.70	22.11
2nd grade ethanol flow (kg/h)	0.90	0.50	1.27	0.81
Gases flow (kg/h)[(a)]	36.93	37.41	40.09	54.61
Ethanol losses (% of generated during fermentation)	2.24	1.22	4.07	2.69
Fraction of ethanol losses on the gaseous streams (%)[(a)]	0.06	15.90	39.68	43.64

[(a)] Include both gases generated on distillation and gases produced on the absorber column (case 1), where gases released upon fermentation are washed.

Therefore, the case that presented the lowest energy consumption (configuration 4, comprised by extractive fermentation and triple effect distillation) presents ethanol losses similar to those of the conventional fermentation case. Ethanol losses are lowest on configuration 2, where the extractive fermentation process is integrated to conventional distillation columns; however, this case

presents relatively high thermal and electric energy demand, when compared to the other alternative configurations.

Liquid residue generation decreases from around 400 kg/h (configuration 1) to 76 kg/h (configuration 4), yielding a reduction of around 80 %. Due to this large volume, stillage destination is a critical issue. For instance, it can be used in the fields as fertilizers, at the same time irrigating the sugarcane plant; therefore, concentrated stillage is more applicable since it diminishes the risks of underground water contamination. In such case, if an evaporator was employed to reduce the stillage volume in order to produce the same amount of residue as that produced in the alternative process, the difference between energy requirements in configuration 1 in relation to the other configurations would increase considerably, thus reiterating that the alternative fermentation process has potential to decrease energy consumption.

CONCLUSIONS

The combined simulation study of the fermentation and distillation processes for bioethanol production provides important resources that allow the comparison of different process configurations and their impacts on bioethanol losses, energy consumption and residue generation. In this work four process configurations were evaluated, based on conventional and vacuum extractive fermentative processes and conventional, double and triple effect distillation systems for product purification. The optimum configuration regarding energy consumption (the process on which extractive fermentation is integrated to a triple effect distillation system, configuration 4) requires 36 % less thermal energy (heat), when compared to conventional fermentation and distillation processes (configuration 1), the conventional configuration employed in the industry. This figure is considerably greater (73 %) when sugarcane molasses are used as raw material, since there is no need to concentrate the feed (sugars solution) using evaporators for the extractive fermentation process. The optimum configuration also presented ethanol losses similar to the conventionally employed process, presenting as another advantage a reduction of 80 % on residue generation.

The results obtained shown that the alternative fermentation process seems an interesting option to improve bioethanol production, since less energy is required to run the process and less residue is generated.

9.3. Comentários e Conclusões

Este capítulo apresentou a fermentação extrativa a vácuo como alternativa ao processo de fermentação convencional. Otimização do processo alternativo em termos de consumo de vapor de processo foi realizada bem como a avaliação da etapa subsequente de destilação. Por possibilitar o uso de substrato mais concentrado, este processo fermentativo produz vinho mais concentrado e, como consequência, a demanda energética desta etapa em conjunto com a destilação é reduzida.

Este estudo combinado permite analisar as perdas de etanol, consumo de energia e geração de resíduos no processo. Para a destilação também foram propostas reformulações como o uso da destilação duplo e triplo efeito. O processo fermentativo a vácuo acoplado à destilação triplo efeito apresentou os melhores resultados em relação à demanda energética.

Capítulo 10
Análise Geral dos Resultados

10.1. Modelagem de Estágios de Equilíbrio

Neste trabalho, simulações considerando a modelagem de estágios de equilíbrio foram realizadas para as etapas de concentração e desidratação do processo de produção de bioetanol.

A etapa de concentração do etanol consiste em um conjunto de colunas de retificação e destilação cujo objetivo é concentrar o vinho proveniente da fermentação com concentração em torno de 7 a 10 % de etanol em massa até 93 %, produzindo assim o bioetanol hidratado.

Para a desidratação, foram considerados os processos de destilação azeotrópica com cicloexano e de destilação extrativa com monoetilenoglicol. Para ambos os processos, utilizou-se como alimentação o bioetanol hidratado (93 %, em massa) produzido na etapa de destilação e especificou-se a produção de bioetanol anidro com 99,5 % de pureza.

A Tabela 10.1 apresenta as energias requeridas nos refervedores das colunas de destilação para estes três processos. Na prática, essa demanda energética é suprida através do uso de vapor de baixa pressão nos refervedores. No caso da destilação, alternativamente, pode-se utilizar vapor por contato direto via injeção no borbotor no fundo das colunas A e B-B1, dispensando-se assim o uso dos refervedores (Dias, 2008).

Tabela 10.1. Energias requeridas em cada processo.

Processo	Demanda Energética (Gcal/h)
Destilação Convencional	26,8
Destilação Azeotrópica	20,1
Destilação Extrativa	5,5

Observa-se que a destilação convencional necessita de uma grande quantidade de vapor nos refervedores caracterizada pela demanda energética. Neste contexto, a combinação da fermentação extrativa a vácuo com as destilações múltiplo efeito apresentada na seção 9.2 revelou ser bastante

vantajosa, uma vez que uma redução na demanda energética foi observada.

Comparando os processos de desidratação, destilações azeotrópica e extrativa, tem-se que a destilação azeotrópica demanda cerca de 4 vezes mais energia do que a extrativa. Considerando-se como base a produção de bioetanol anidro, tem-se que a destilação extrativa requer aproximadamente 365 kcal/kg de AEAC e a azeotrópica, 1335 kcal/kg de AEAC. Dessa forma, pode-se concluir que a destilação azeotrópica apresenta alto consumo de energia. Com relação à qualidade do bioetanol anidro, observou-se que houve contaminação pelo solvente apenas quando a destilação azeotrópica foi empregada.

10.2. Modelagem de Estágios de Não Equilíbrio

A modelagem de estágios de não equilíbrio (ou governada por taxa), por apresentar método de cálculo mais rigoroso, pode ser usada para prever condições de operação, energia requerida no processo e comportamento das colunas de destilação, fornecendo resultados mais próximos do real, quando comparada à modelagem de estágios de equilíbrio.

Neste trabalho, os processos de destilação convencional e extrativa foram simulados utilizando a modelagem de estágios de não equilíbrio existente no simulador Aspen Plus®. No entanto, não foi possível simular a destilação azeotrópica utilizando esta modelagem devido à limitação do próprio simulador que não permite o equilíbrio vapor-líquido-líquido quando o modelo de não equilíbrio é empregado. Neste caso, a presença das duas fases líquidas no interior da coluna não é considerada, levando a resultados inconsistentes para a destilação azeotrópica.

A modelagem de não equilíbrio para ambos os processos simulados apresentou resultados significativamente diferentes da modelagem de estágios de equilíbrio, no que tange aos perfis de temperatura e composições das correntes calculadas nas simulações. No entanto, variações significativas com relação à demanda energética não foram observadas.

10.3. Aplicação da Correlação de Eficiência

Apesar de a modelagem de estágios de não equilíbrio ser a mais indicada para representar os processos de destilação, esta apresenta elevado tempo de processamento computacional e problemas de convergência, fatores que restringem sua aplicação a controle avançado. Dessa forma, a aplicação de uma correlação de eficiência, como a de Barros e Wolf, possibilita a utilização da modelagem de estágios de equilíbrio, tornando este modelo idealizado mais próximo do real. Assim, este modelo que é mais simples e demanda menor capacidade computacional, pode ser empregado para os cálculos de modo que os desvios do equilíbrio sejam considerados.

Assim como para a modelagem de estágios de não equilíbrio, o processo de destilação azeotrópica não foi simulado utilizando a modelagem de estágios de equilíbrio com eficiência determinada pela correlação de Barros e Wolf. Isto porque no simulador Aspen Plus® não é possível inserir a eficiência de Murphree para cada fase líquida separadamente. Além disso, as correlações desenvolvidas por Barros (1997) são apenas para destilação convencional e extrativa. Portanto, não foi possível estabelecer base para avaliação destas correlações ou ainda de uma nova correlação aplicável à destilação azeotrópica.

Para as destilações convencional e extrativa, as correlações de Barros e Wolf apropriadas para cada caso foram aplicadas para o cálculo de eficiências de prato e componente. Para ambos os processos, os valores de eficiência de prato mantiveram-se em torno de 50 %. Os resultados destas simulações, quando comparados aos gerados pela modelagem de estágios de não equilíbrio, apresentaram satisfatória concordância, exceto para a eficiência de componente para a destilação extrativa. Em geral, as simulações que consideraram a eficiência de prato apresentaram maior concordância com os resultados obtidos através do modelo de estágios de não equilíbrio. Possivelmente, essa observação deve-se ao fato de a correlação de Barros e Wolf ter sido desenvolvida utilizando eficiência de prato e, então, adaptada a de componente. Além disso, a correlação para componente não apresenta propriedades da mistura, apenas as propriedades individuais dos componentes, o que pode levar a erros nas estimativas.

Capítulo 11

Conclusões e Sugestões para Trabalhos Futuros

11.1. Conclusões

A etapa de separação na produção de bioetanol foi abordada neste trabalho através de simulações das destilações convencional, extrativa e azeotrópica bem como de estudo dos recentes desenvolvimentos nesta área, tais como uso de novos agentes de separação e outros processos que auxiliem ou substituam a destilação.

Para a simulação dos processos baseados em destilação, tem-se que o equilíbrio de fases é de considerável importância para o entendimento do processo e para a apropriada representação do sistema. Assim, realizou-se extensiva pesquisa na literatura a fim de obter dados de equilíbrio experimentais para os binários comumente encontrados no processo de separação do bioetanol. A comparação destes dados com os resultados gerados pelo simulador Aspen Plus® utilizando-se os modelos NRTL e UNIQUAC indicou que ambos os modelos são adequados para a representação do sistema. No entanto, o modelo NRTL apresentou desempenho ligeiramente superior ao UNIQUAC, uma vez que suas predições foram mais representativas para um maior número de pares.

Simulações das destilações extrativa e azeotrópica para a desidratação do bioetanol utilizando a modelagem de estágios de equilíbrio indicaram que a destilação azeotrópica apresenta consumo energético cerca de quatro vezes superior ao da destilação extrativa.

Para a destilação azeotrópica, observou-se a formação de duas fases líquidas no interior da coluna. Verificou-se que a região com presença de duas fases líquidas pode ser minimizada através da escolha apropriada do estágio de alimentação na coluna.

Como proposta para diminuição da demanda energética da destilação convencional, estudou-se a fermentação extrativa a vácuo combinada à destilação múltiplo efeito, configuração que permite considerável redução no consumo de energia do processo convencional.

Adicionalmente, simulações considerando a modelagem de estágios de não equilíbrio e as correlações de eficiência de Barros e Wolf aplicadas à modelagem de estágios de equilíbrio foram realizadas para as destilações convencional e extrativa. Os resultados obtidos indicam que a introdução da eficiência de prato nos cálculos aumenta a precisão da modelagem de estágios de equilíbrio quando comparada aos gerados pela modelagem de não equilíbrio. A eficiência de componente mostrou-se menos vantajosa para esta finalidade, porém, possibilitou o entendimento da relação da eficiência com os componentes, sendo observados valores maiores para componentes de baixa volatilidade.

11.2. Sugestões para Trabalhos Futuros

Com esta dissertação de mestrado foi possível verificar diferentes aspectos do processo de separação do bioetanol, bem como diversas oportunidades de pesquisa, apresentadas aqui como sugestões de trabalhos futuros:

- comparação dos resultados das simulações com resultados experimentais obtidos de biorrefinarias;
- aquisição de dados experimentais de equilíbrio líquido-vapor para binários presentes no processo de separação de bioetanol;
- desenvolvimento de sub-rotina em Fortran para a introdução da correlação de eficiência de Barros e Wolf no simulador Aspen Plus®;
- estudo de diferentes composições de vinho, como por exemplo o vinho proveniente da produção de bioetanol de segunda geração;
- estudo do comportamento dinâmico dos processos de destilação e desidratação estudados;
- desenvolvimento de rotina em Fortran para cálculo de coluna de destilação azeotrópica empregando modelagem de estágios de não equilíbrio para proposição de correlação de eficiência adequada para este caso;
- simulação do processo de adsorção com peneiras moleculares, recentemente introduzido em algumas biorrefinarias brasileiras;

- estudo do potencial da aplicação de novos processos de desidratação para produção de bioetanol anidro, tais como destilação extrativa com líquidos iônicos ou polímeros altamente ramificados;
- estudo de processos híbridos como a pervaporação/destilação no processo de produção de bioetanol;
- estudo de outras configurações operacionais nas colunas de destilação como para-destilação, meta-destilação, HIGEE (*High Integrated Graviational*) e HIDIC (*Heat Integrated Distillation Column*) para aplicação na etapa de concentração do bioetanol;
- uso de modelo de reator mais detalhado para a simulação da fermentação extrativa a vácuo;
- simulação de outras alternativas de fermentação extrativa, como a fermentação acoplada à extração líquido-líquido e à pervaporação.

Referências Bibliográficas

ABDERAFI, S., BOUNAHMIDI, T. *Measurement and estimation of vapor-liquid equilibrium for industrial sugar juice using the Peng-Robinson equation of state.* Fluid Phase Equilibria, 162, 225-240, 1999.

ABDERAFI, S., BOUNAHMIDI, T., *Measurement and Modeling of Atmospheric-Pressure Vapor-Liquid-Equilibrium Data for Binary, Ternary and Quaternary Mixtures of Sucrose, Glucose, Fructose and Water Components.* Fluid Phase Equilibria, 93, 337-351, 1994.

AIChE - American Institute of Chemical Engineers, *Bubble Tray Design Manual*. New York, 1958.

AL-ASHEH, S., BANAT, F., AL-LAGTAH, N. *Separation of ethanol-water mixtures using molecular sieves and biobased adsorbents*. Chemical Engineering Research and Design, 82, 855-864, 2004.

ALZATE, C. A. C., TORO, O. J. S. *Energy consumption analysis of integrated flowsheets for production of fuel ethanol from lignocellulosic biomass.* Energy, 31, 2447–2459, 2006.

ARLT, W. *A new apparatus for phase equilibria in reacting mixtures.* Fluid Phase Equilibria, 158–160, 973–977,1999.

ASPEN PLUS Help, Binary Parameter Databanks, 2000.

ASPEN TECHNOLOGY. Aspen Plus 11.1: Unit Operation Models, Cambridge, MA, 2001.

ATALA, D. I. P. *Montagem, instrumentação, controle e desenvolvimento experimental de um processo fermentativo extrativo de produção de etanol.* Tese de Doutorado, Unicamp, Campinas-SP, 2004.

BAI, F.W., ANDERSON, W.A., MOO-YOUNG, M. *Ethanol fermentation technologies from sugar and starch feedstocks,* Biotechnology Advances, 26, 89–105, 2008.

BALAT, M. BALAT, H., ÖZ, C. *Progress in bioethanol processing.* Progress in Energy and Combustion Science, 34, 551–573, 2008.

BARROS, A. A. C. *Desenvolvimento de modelo de estágio de não equilíbrio e proposição de correlações para processos de destilação convencional e extrativa*. Tese de Doutorado, Unicamp, Campinas - SP, 1997.

BARROS, A. A. C., WOLF MACIEL, M. R. *Desenvolvimento de uma correlação para o estudo da eficiência das colunas de destilação*. 11.° Congresso de Engenharia Química, Rio de Janeiro, 271-276, 1996.

BRASIL - Agência Nacional do Petróleo, Gás Natural e Biocombustíveis. *Resolução ANP n^{o} 36, de 06/12/2005*. Publicada no Diário Oficial da União em 07/12/2005.

BRITO, R. P. *Processo de destilação extrativa: modelagem dinâmica, simulação e avaliação de nova configuração.* Tese de Doutorado, Unicamp, Campinas - SP, 1997.

BRITO, R.P., MACIEL M.R.W., MEIRELLES, A.J.A. *New extractive distillation configuration for separating binary azeotropic mixtures*, In: The First European Congress of Chemical Engineering, Italy, 1, 1333-1336, 1997.

CARDONA, C. A., SÁNCHEZ, O. J. *Fuel ethanol production: Process design trends and integration opportunities.* Bioresource Technology, 98, 2415–2457, 2007.

CARMO, M.J., GUBULIN, J.C. *Ethanol-water separation in the PSA Process*. Adsorption, 8, 235-248, 2002.

CASTILLO, F. J. L., TOWLER, G. P. *Influence of multicomponent mass transfer on homogeneous azeotropic distillation*. Chemical Engineering Science, 53, 5, 963-976, 1998.

CERQUEIRA LEITE, R.C., LEAL, M.R.L.V., CORTEZ L.A.B., GRIFFIN, W.M., SCANDIFFIO, M.I.G. *Can Brazil replace 5% of the 2025 gasoline world demand with ethanol?* Energy, 34, 655-661, 2009.

CHEN, D.H.T., THOMPSON, A.R. *Systems Glycerol-Water and Glycerol-Water Saturated with Sodium Chloride.* Journal of Chemical and Engineering Data, 15, 471-474, 1970.

CHENG, H.-C., WANG, F.-S. *Optimal biocompatible solvent design for a two-stage extractive fermentation process with cell recycling.* Computers and Chemical Engineering, 32, 1385–1396, 2008.

CHRISTEN, P., MINER, M., RENON, H. *Ethanol extraction by supported liquid membrane during fermentation.* Biotechnology and Bioengineering, 36, 116 – 123, 1990.

CHRISTENSEN, S.P. *Measurement of dilute mixture vapor-liquid equilibrium data for aqueous solutions of methanol and ethanol with a recirculating still*. Fluid Phase Equilibria, 15, 763–773, 1998.

CHU, J. C. *Plate efficiency correlation in distilling columns and gas absorbers*. J. Appl. Chem., 1(12), 529-541, 1951.

COLBURN, A. P. *Effect of entrainment on plate efficiency in distillation*. Ind. Eng. Chem., 28 (5), 526-530, 1936.

COSTA, A.C., ATALA, D.I.P., MAUGERI F., MACIEL FILHO, R. *Factorial design and simulation for the optimization and determination of control structures for an extractive alcoholic fermentation.* Process Biochemistry, 37, 125 –137, 2001.

COULSON, J. M., RICHARDSON, J. F., HARKER, J. H., BACKHURST, *Coulson and Richardson's Chemical Engineering, Particle Technology and Separation Processes,* Vol. 2, 5th ed., Butterworth-Heinemann, 2002.

CYSEWSKI, G.R., WILKE, C.R. *Process design and economic studies of alternative fermentation methods for the production of ethanol*. Biotechnology and Bioengineering, 20, 1421-1444, 1978.

D'AVILA, S.G., SILVA, R.S.F. *Isothermal vapor-liquid equilibrium data by total pressure method. Systems acetaldehyde-ethanol, acetaldehyde-water, and ethanol-water.* Journal of Chemical and Engineering Data, 15, 421-424, 1970.

DAUGULIS, A.J., AXFORD, D.B., MCLELLAN, P.J. *Economics of ethanol production by extractive fermentation*. Canadian Journal of Chem. Engineering, 69, 488–497, 1991.

DIAS, M. O. S. *Simulação do processo de produção de etanol a partir do açúcar e do bagaço, visando à integração do processo e a maximização da produção de energia e excedentes do bagaço*. Dissertação de mestrado, Unicamp, Campinas - SP, 2008.

DIAS, M. O. S., JUNQUEIRA, T. L., MACIEL FILHO, R., MACIEL, M. R. W., ROSSELL, C. E. V. *Anhydrous bioethanol production using bioglycerol - simulation and optimization of extractive distillation processes.* Computer Aided Chemical Engineering, 26, 519-524, 2009a.

DIAS, M.O.S., ENSINAS, A.V., NEBRA, S.A., MACIEL FILHO,R., ROSSELL, C.E.V., MACIEL, M.R.W. *Production of bioethanol and other bio-based materials from sugarcane bagasse: Integration to conventional bioethanol production process.* Chemical Engineering Research and Design, 87, 1206-1216, 2009b.

DIAS, M.O.S., MATEUS, F.A.D., MACIEL FILHO, R., MACIEL, M.R.W., ROSSELL, C.E.V. *Anhydrous Bioethanol for Fuels and Chemicals - Evaluations of Alternative Distillations and Solvents.* In: 18th European Symposium on Computer Aided Process Engineering (Escape18), Lyon. Amsterdam: Elsevier, 2008.

DODIĆ, S., POPOV, S., DODIĆ, J., RANKOVIĆ, J., ZAVARGO, Z., MUČIBABIĆ, R.J. *Bioethanol production from thick juice as intermediate of sugar beet processing*. Biomass and Bioenergy, 33, 822 – 827, 2009.

DRICKAMER, H. G., BRADFORD, J. R. *Overall plate efficiency of commercial hydrocarbon fractionating columns as a function of viscosity*. Trans. AIChE, 39, 319-360, 1943.

ECKERT, E., VANĚK, T. *Some aspects of rate-based modelling and simulation of three-phase distillation columns.* Computers and Chemical Engineering, 25, 603–612, 2001.

ENSINAS, A. V. *Integração térmica e otimização termoeconômica aplicadas ao processo industrial de produção de açúcar e etanol a partir da cana-de-açúcar.* Tese de Doutorado, Unicamp, Campinas-SP, 2008.

ENSINAS, A.V., NEBRA, S.A. LOZANO, M.A. SERRA, L.M., *Analysis of process steam demand reduction and electricity generation in sugar and ethanol production from sugarcane.* Energy Conversion and Management, 48, 2978–2987, 2007.

FAÚNDEZ, C. A., VALDERRAMA, J. O. *Phase equilibrium modeling in binary mixtures found in wine and must distillation*. Journal of Food Engineering 65, 577–583, 2004.

FELE, L., GRILC, V. *Separation of Furfural from Ternary Mixtures*. Journal of Chemical and Engineering Data 48, 564-570, 2003.

FRANCESCHIN, G., ZAMBONI, A., BEZZO, F., BERTUCCO, A. *Ethanol from corn: a technical and economical assessment based on different scenarios*, Chemical Engineering Research and Design, 86, 488–498, 2008.

GARCÍA-MIAJA, G., TRONCOSO, J., ROMANÍ, L. *Excess properties for binary systems ionic liquid + ethanol: Experimental results and theoretical description using the ERAS model.* Fluid Phase Equilibria, 274, 59–67, 2008.

GERSTER, J. A., HILL, A. B., HOCHGRAF, N. N., ROBINSON, D. G. *Tray Efficiencies in Distillation Columns*. AIChE Research Committee, University Delaware, Newark, 1958.

GMEHLING, J. *Present Status and Potential of Group Contribution Methods for Process Development.* J. Chem. Thermodynamics, 41, 731–747, 2009.

GMEHLING, J. *Vapor-liquid equilibrium data collection - Aldehydes*. DECHEMA, 1993.

GMEHLING, J., ONKEN, U. *Vapor-Liquid Equilibrium Data Collection*. DECHEMA Chemistry Data Series, 1977.

GMEHLING, J., ONKEN, U., ARLT, W. *Vapor-liquid equilibrium data collection. Organic hydroxy compounds: alcohols (supplement 1)*. DECHEMA, 1982a.

GMEHLING, J., ONKEN, U., ARLT, W. *Vapor-liquid equilibrium data collection. Aqueous organic systems (supplement 1)*. DECHEMA, 1981.

GMEHLING, J., ONKEN, WEIDLICH, U. *Vapor-liquid equilibrium data collection. Organic hydroxy compounds: alcohols and phenols (supplement 2)*. DECHEMA, 1982b.

GMEHLING, J., ONKEN, U., GRENZHEUSER, P. *Vapor-liquid equilibrium data collection. Carboxylic acids, anhydrides, esters.* DECHEMA, 1982c.

GOLDEMBERG, J. *The challenge of biofuels*. Energy & Environmental Science, 1, 523–525, 2008.

GOLDEMBERG, J., COELHO, S. T., GUARDABASSI, P. *The sustainability of ethanol production from sugarcane*. Energy Policy, 36, 2086– 2097, 2008a.

GOLDEMBERG, J., NIGRO, F. E. B., COELHO, S. T. *Bioenergia no Estado de São Paulo: Situação atual, Perspectivas, Barreiras e Propostas*. Imprensa Oficial do Estado de São Paulo, 152 p., 2008b.

GOMES, L. G. *Simulação e otimização energética da unidade de processamento de gás natural de Atalaia.* Dissertação de Mestrado, Unicamp, Campinas - SP, 1995.

GOMIS, V., FONT, A., PEDRAZA, R., SAQUETE, M.D. *Isobaric vapor–liquid–liquid equilibrium data for the system water + ethanol + cyclohexane.* Fluid Phase Equilibria*,* 235, 7-10, 2005.

GOMIS, V., FONT, A., SAQUETE, M.D. *Vapour–liquid–liquid and vapour–liquid equilibrium of the system water + ethanol + heptane at 101.3 kPa*. Fluid Phase Equilibria*,* 248, 206–210, 2006.

GU, Z., TAO, Z., XU, N., LI, Y. *Retrofitting of a distillery based on process synthesis.* Energy Conversion and Management, 48, 335-343, 2007.

GYAMERAH, M., GLOVER, J. *Production of ethanol by continuous fermentation and liquid-liquid extraction*. J Chem Tech Biotech, 66 (2), 145-152, 1996.

HAUSEN, H. *The definition of the degree of exchange on rectifying plates for binary and ternary mixtures*. Chem. Ing. Tech., 25, 595, 1953.

HENLEY, E. J., SEADER, J. D. *Equilibrium-Stage Separation Operations in Chemical Engineering.* Editora John Wiley & Sons, New York, 1981.

HIGLER, A., CHANDE, R., TAYLOR, R., BAUR, R., KRISHNA, R. *Nonequilibrium modeling of three-phase distillation.* Computers and Chemical Engineering, 28, 2021–2036, 2004.

HOLLAND, C. D., MCMAHON, K. S. *Comparison of vaporization efficiencies with Murphree-type efficiencies in distillation*. I. Chem. Eng. Sci., 25 (3), 431-436, 1970.

HOLLAND, C. D. *Fundamentals of Multicomponent Distillation*. Editora McGraw-Hill, 2.ª ed., New York, 1981.

HUANG, H., RAMASWAMY, S., TSCHIRNER, U. W. E RAMARAO, B. V. *A review of separation technologies in current and future biorefineries*. Separation and Purification Technology, 62(1), 1-21, 2008.

IKEGAMI, T., YANAGISHITA, H., KITAMOTO, D., HARAYA, K., NAKANE, T., MATSUDA, H., KOURA, N., SANO, T. *Production of highly concentrated ethanol in a coupled fermentation/pervaporation process using silicalite membranes.* Biotechnology Techniques, 11 (12), 921-924, 1997.

IPT - Instituto de Pesquisas Tecnológicas do Estado de São Paulo. *Estudo da pré-viabilidade técnica e econômica da hidrólise de biomassa para produção de etanol*. Secretaria de Ciência e Tecnologia do estado de São Paulo, 2000.

ISHIDA, K., SHIMIZU, K. *Novel Repeated Batch Operation for Flash Fermentation System: Experimental Data and Matchematical Modelling*. Journal of Chemical Technology and Biotechnology, 66, 340-346, 1996.

ITO, V. M. *Otimização de colunas de destilação complexas.* Dissertação de Mestrado, Unicamp, Campinas - SP, 2002.

JUNQUEIRA, T. L., DIAS, M. O. S., MACIEL FILHO, R., MACIEL, M. R. W., ROSSELL, C. E. V. *Simulation of the azeotropic distillation for anhydrous bioethanol production: study on the formation of a second liquid phase.* Computer Aided Chemical Engineering, 27, 1143-1148, 2009.

KATO, M. *Vapor-Liquid Equilibrium Measurements for Binary Systems of Acetic Acid with Ethyl Acetate and Vinyl Acetate by the Dew-Bubble Point Temperature Method.* Journal of Chem. and Eng. Data, 33, 499-501, 1988.

KING, C. J. *Separation Processes*. Editora McGraw-Hill, 2.ª ed., New York, 1980.

KOSSACK, S., KRAEMER, K.,GANI, R., MARQUARDT, W. *A systematic synthesis framework for extractive distillation processes.* Proceedings of European Congress of Chemical Engineering (ECCE-6), 2007.

KRISHNAMURTHY, R., TAYLOR, R. *A Nonequilibrium Stage Model of Multicomponent Separation Process – Part I: Model Description and Method of Solution*. AIChE Journal, 31(3), 449-456, 1985.

KWIATKOWSKI, J.R., MCALOON, A.J., TAYLOR, F. JOHNSTON, D.B. *Modeling the Process and Costs of the Production of Fuel Ethanol by the Corn Dry-Grind Process.* Industrial Crops and Products, 23, 288–296, 2006.

LEE, J. H., DUDUKOVIC, M. P. *A comparison of the equilibrium and nonequilibrium models for a multicomponent reactive distillation column*. Computers and Chemical Engineering, 23, 159-172, 1998.

LEE, M.-J., HU, C.-H. *Isothermal vapor-liquid equilibria for mixtures of ethanol, acetone, and diisopropyl ether.* Fluid Phase Equilibria, 109, 83-98, 1995.

LEE, M.-J., CHEN, S.-L., KANG, C.-H., LIN, H. *Simultaneous Chemical and Phase Equilibria for Mixtures of Acetic Acid, Amyl Alcohol, Amyl Acetate, and Water.* Ind. Eng. Chem. Res., 39, 4383-4391, 2000.

LEWIS, W. K. *The efficiency and design of rectifying columns for binary mixtures*. J. Ind. Eng. Chem., 14 (6), 492-497, 1922.

LIMA, U. A., AQUARONE, E., LIMA, W., SCHMIDELL, W. *Biotecnologia Industrial – Processos Fermentativos e Enzimáticos*, Vol. 3, 1° ed., Editora Edgard Blücher LTDA, 2001.

LIPNIZKI, F., FIEL, R.W., TEN, P. *Pervaporation-based hybrid process: a review of process design, applications and economics.* Journal of Membrane Science, 153, 183-210, 1999.

MAIORELLA, B.L., BLANCH, H.W., WILKE, C.R. *Economic evaluation of alternative ethanol fermentation processes*. Biotechnology and Bioengineering, 26, 1003-1025, 1984.

MAPA - Ministério de Agricultura, Pecuária e Abastecimento. Disponível em: www.agricultura.gov.br. Acessado em 12/01/2009.

MEDINA, A. G., ASHTON, N., MCDERMOTT, C. *Murphree and vaporization efficiencies in Multicomponent distillation*. Chem. Eng. Sci., 33 (3), 331-339, 1978.

MEIRELLES, A. J. A. *Expansão da produção de bioetanol e melhoria tecnológica da destilação alcoólica*. In: Workshop “Produção de etanol”. Escola de Engenharia de Lorena, 2006.

MEIRELLES, A., WEISS, S., HERFURTH, H. *Ethanol dehydration by extractive distillation*. Journal of Chemical Technology and Biotechnology, 53, 18-188, 1992.

MINIER, M., GOMA, G. *Production of ethanol by coupling fermentation and solvent extraction.* Biotechnology Letters, 3 (8), 405-408, 1981.

MORTAHEB, H. KOSUGE, H. *Simulation and optimization of heterogeneous azeotropic distillation process with a rate-based model.* Chemical Engineering and Processing, 43, 317-326, 2004

MURPHREE, E. V. *Rectifying column calculations*. Ind. Eng. Chem., 17 (7), 747-750, 1925.

NAVA, J. A. O., KRISHNA, R. *Influence of unequal component efficiencies on trajectories during distillation of a homogeneous azeotropic mixture.* Chemical Engineering and Processing, 43, 305–316, 2004.

NORD, M. *Plate efficiencies of benzeno-tolueno-xylene systems in distillation*. Trans. Inst. Chem. Eng., 42, 741-755, 1946.

NORILER, D. *Modelagem matemática e simulação numérica do escoamento líquido-vapor num prato de destilação*. Dissertação de Mestrado, Unicamp, Campinas - SP, 2003.

NORILER, D. *Modelagem Matemática Multifásica e Simulação Tridimensional e Transiente para Sistemas Gás-Líquido: o Caso do Escoamento Líquido-Vapor em Colunas de Destilação.* Tese de Doutorado, Unicamp, Campinas-SP, 2007.

O'BRIEN, D.J., CRAIG JR., J.C. *Ethanol production in a continuous fermentation/ membrane pervaporation system*. Appl. Microbiol. Biotechnol., 44, 699-704, 1996.

O'CONNELL, H. E. *Plate efficiency of fractionating columns and absorbers*. Trans. AIChE, 42, 741–755, 1946.

OLIVEIRA, M.B., TELES, A.R.R., QUEIMADA, A.J., COUTINHO, J.A.P. *Phase equilibria of glycerol containing systems and their description with the Cubic-Plus-Association (CPA) Equation of State*. Fluid Phase Equilibria 280, 22–29, 2009.

PEREIRO, A.B., RODRÍGUEZ, A. *A study on the liquid–liquid equilibria of 1-alkyl-3-methylimidazolium hexafluorophosphate with ethanol and alkanes.* Fluid Phase Equilibria, 270, 23–29, 2008.

PERES, A.M., MACEDO, E.A. *A Modified UNIFAC Model for the Calculation of Thermodynamic Properties of Aqueous and Non Aqueous Solutions Containing Sugars.* Fluid Phase Equilibria, 139, 47-74, 1997.

PERRY, R.H., GREEN, D.W., MALONEY, J.O. *Perry's Chemical Engineers' Handbook*, McGraw-Hill Companies, Inc., New York, 1997.

PESCARINI, M. H. *Desenvolvimento de um algoritmo para simulação de colunas de destilação multicomponente em estado estacionário utilizando a modelagem de estágio de não equilíbrio*. Dissertação de Mestrado, Unicamp, Campinas -SP, 1996.

PESCARINI, M. H. *Desenvolvimento do modelo dinâmico de estágios de não equilíbrio e simulação de colunas de destilação convencional e extrativa*. Tese de Doutorado, Unicamp, Campinas - SP, 1999.

PESCARINI, M. H., BARROS, A. A. C., MACIEL, M. R. W. *Development of a Software for Simulating Separation Processes Using a Nonequilibrium Stage Model*. In: 6th European Symposium on Computer Aided Process Engineering, 279-284, 1996.

PRADHAN, S., KANNAN, A. *Simulation and analysis of extractive distillation process in a valve tray column using the rate based model*. Korean J. Chem. Eng., 22 (3), 441-451, 2005.

PRESSLY, T.G., NG, K.M. A Break-even analysis of distillation-membrane hybrids, *AIChE Journal*, 44 (1), 93-105, 1998.

RAMALINGHAM, A., FINN, R.K.. *The vacuferm process: A new approach to fermentation alcohol*. Biotechnology and Bioengineering, 19, 583-589, 1977.

REIS, M. H. M., BARROS, A. A. C., MEIRELLES, A. J. A., MACIEL FILHO, R., WOLF-MACIEL, M. R. *Application of plate and component efficiency correlations in homogeneous azeotropic distillation processes*. Ind. Eng. Chem. Res., 45, 5755-5760, 2006.

REPKE, J. U., VILLAIN, O. WOZNY, G. *A nonequilibrium model for three-phase distillation in a packed column: modelling and experiments.* Computers & Chemical Engineering, 28, 775–780, 2004.

REUβ, J., BATHEN, D., SCHMIDT-TRAUB, H. *Desorption by microwaves: mechanisms of multicomponent mixtures.* Chemical Engineering & Technology, 25 (4), 381-384, 2002.

RIVERA, E. C., COSTA, A. C., LUNELI, B. H., WOLF MACIEL, M. R., MACIEL FILHO, R. *Kinetic modeling and parameter estimation in a tower bioreactor for bioethanol production*. Applied Biochemistry and Biotechnology, 148, 163-173, 2008.

RIVERA, E.C., COSTA, A.C., ATALA, D.I.P., MAUGERI, F., MACIEL, M.R.W., MACIEL FILHO, R. *Evaluation of optimization techniques for parameter estimation: Application to ethanol fermentation considering the effect of temperature.* Process Biochemistry, 41, 1682–1687, 2006.

RIVIÈRE, C., MARLAIR, G. *BIOSAFUEL®, a pre-diagnosis tool of risks pertaining to biofuels chains.* Journal of Loss Prevention in the Process Industries, 22, 228–236, 2009.

ROUSSEAU, R. W. *Handbook of Separation Process Technology.* Ed. Wiley. New York, 1987.

SANZ, M.T., GMEHLING, J. *Isothermal vapor–liquid equilibria for different binary mixtures involved in the alcoholic distillation.* Fluid Phase Equilibria, 267, 158–162, 2008.

SATO, M., MATSUURA, K., FUJII, T. *Ethanol separation from ethanol-water solution by ultrasonic atomization and its proposed mechanism based on parametric decay instability of capillary wave.* J. Chem. Phys., 114 (5), 2382-2386, 2001.

SATO, K., AOKI, K., SUGIMOTO, K., IZUMI, K., INOUE, S., SAITO, J., IKEDA, S., NAKANE, T. *Dehydrating performance of commercial LTA zeolite membranes and application to fuel grade bio-ethanol production by hybrid distillation/vapor permeation process.* Microporous and Mesoporous Materials, 115, 184-188, 2008.

SAXENA, R.C., ADHIKARI, D.K., GOYAL, H.B. *Biomass-based energy fuel through biochemical routes: A review.* Renewable and Sustainable Energy Reviews, 13, 167–178, 2009.

SCANDIFFIO, M. I. G. *Análise prospectiva do álcool combustível no Brasil – cenários 2004-2024*. Tese de Doutorado, UNICAMP, Campinas – SP, 2005.

SEILER, M. *Hyperbranched polymers: phase behavior and new applications in the field of chemical engineering*. Fluid phase equilibria, 241, 155-174, 2006.

SEILER, M., JORK, C., KAVARNOU, A., ARLT, W., HIRSCH, R. *Separation of azeotropic mixtures using hyperbranched polymers or ionic liquids. AIChE Journal*, 50 (10), 2439-2454, 2004.

SILVA, F.L.H., RODRIGUES, M.I., MAUGERI, F. *Dynamic modelling, simulation and optimization of an extractive continuous alcoholic fermentation process.* Journal of Chemical Technology and Biotechnology, 74, 176-182, 1999.

SIMO, M., BROWN, C.J., HLAVACEK, V. *Simulation of pressure swing adsorption in fuel ethanol production process*. *Computers and Chemical Engineering*, 32, 1635-1649, 2008.

SOARES, C. *Avaliação experimental dos coeficientes de transferência de massa e calor em uma coluna com pratos perfurados*. Dissertação de Mestrado, Unicamp, Campinas - SP, 2000.

SOBOČAN, G., GLAVIČ, P. *Optimization of ethanol fermentation process design*. Applied Thermal Engineering, 20, 529-543, 2000.

SOUZA, R. R. *Panorama, Oportunidades e Desafios para o Mercado Mundial de Álcool Automotivo.* Dissertação de Mestrado, UFRJ, Rio de Janeiro - RJ, 2006.

SPRINGER, P.A.M., VAN DER MOLEN, S., KRISHNA, R. *The need for using rigorous rate-based models for simulations of ternary azeotropic distillation.* Computers & Chemical Engineering, 26, 1265–1279, 2002.

STANDART, G. *Studies in distillation – V. Generalized definitions of a theoretical plate or stage of contacting equipment*. Chem. Eng. Sci., 20 (6), 611-622, 1965.

SUZUKI, K., KIRPALANI, D. M., MCCRACKEN, T. W. *Experimental Investigation of Ethanol Enrichment Behavior in Batch and Continuous Feed Ultrasonic Atomization Systems*, Chem. Eng. Technol., 29 (1), 44-49, 2006.

SZITKAI, Z., LELKES, Z., REV, E., FONYO, Z. *Optimization of hybrid ethanol dehydration systems.* Chemical Engineering and Processing, 41, 631-646, 2002.

TAYLOR, R., KRISHNA, R. *Multicomponent mass transfer*. Editora Wiley, New York, 1993.

THONGSUKMAK, A., SIRKAR, K.K. *Extractive pervaporation to separate ethanol from its dilute aqueous solutions characteristic of ethanol-producing fermentation processes.* Journal of Membrane Science, 329, 119–129, 2009.

TU, C.-H., WU, Y.-S., LIU, T.-L. *Vapor-liquid equilibria of the binary systems formed by methanol, acetone and methyl vinyl ketone at 100.0 ± 0.2 kPa.* Fluid Phase Equilibria, 129, 129-137, 1997.

VANE, L.M. *A review of pervaporation for product recovery from biomass fermentation processes.* J. Chem. Tech. and Biotech., 80, 603–629, 2005.

VASCONCELOS, C. J. G. *Simulação, otimização e controle de processos para a separação de misturas não ideais*. Dissertação de Mestrado, Unicamp, Campinas - SP, 1999.

WALTER, A., ROSILLO-CALLE, F., DOLZAN, P., PIACENTE, E., CUNHA, K.B. *Perspectives on fuel ethanol consumption and trade*, Biomass and Bioenergy, 32, 730 – 748, 2008.

WEST, R. G., GILBERT, W. D., SHIMIZU, T. *Mechanism of mass transfer on bubble plates: plates efficiencies*. Ind. Eng. Chem., 44 (10), 2470-2478, 1952.

WISNIAK, J., POLISHUK, A. *Analysis of residuals - a useful tool for phase equilibrium data analysis.* Fluid Phase Equilibria 164, 61–82, 1999.

WOLF-MACIEL, M. R., SOARES, C., BARROS, A. A. C. *Validations of the nonequilibrium stage model and a new efficiency correlation for non ideal distillation process through simulated and experimental data*. Computer Aided Chemical Engineering, 9, 321-326, 2001.

YANO, Y. F., MATSUURA, K, FUKAZU, T, ABE, F, WAKISAKA, A, KOBARA, H, KANEKO, K, KUMAGAI, A, KATSUYA, Y, TANAKA, M. *Small-angle x-ray scattering measurement of a mist of ethanol nanodroplets: An approach to understanding ultrasonic separation of ethanol-water mixtures.* J. Chem. Phys., 127 (3), 031101, 2007.

ZALDIVAR, J., NIELSEN, J., OLSSON, L. *Fuel ethanol production from lignocellulose: a challenge for metabolic engineering and process integration*. Applied Microbiology and Biotechnology, 56, 17-34, 2001.

Apêndice

Neste Apêndice são apresentados os diagramas binários dos componentes presentes nas etapas de destilação e desidratação. As curvas y-x apresentam dados da fração molar na fase vapor (y) e da fração molar na fase líquida (x) do componente mais volátil do sistema (indicado pelo índice 1), sob pressão atmosférica (1 atm), utilizando o modelo NRTL para estimativa do coeficiente de atividade na fase líquida e Hayden-O'Connell (HOC) para estimativa do coeficiente de fugacidade na fase vapor.

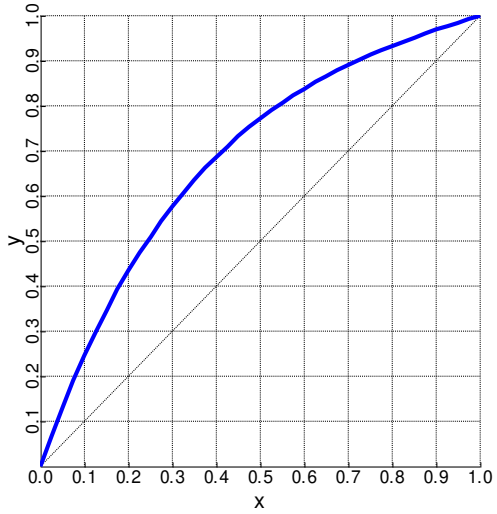

Figura A.1. Diagrama y-x acetaldeído (1) / acetona (2).

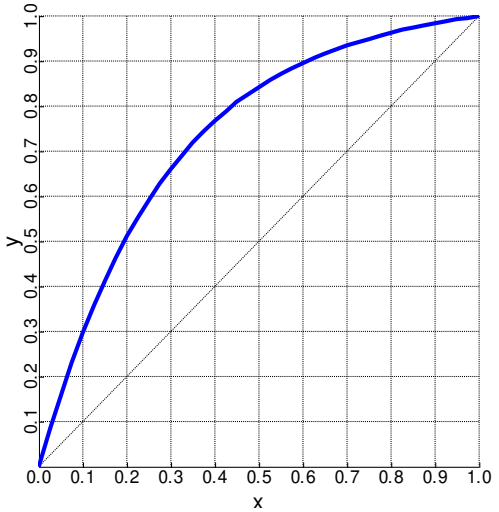

Figura A.2. Diagrama y-x acetaldeído (1) / metanol (2).

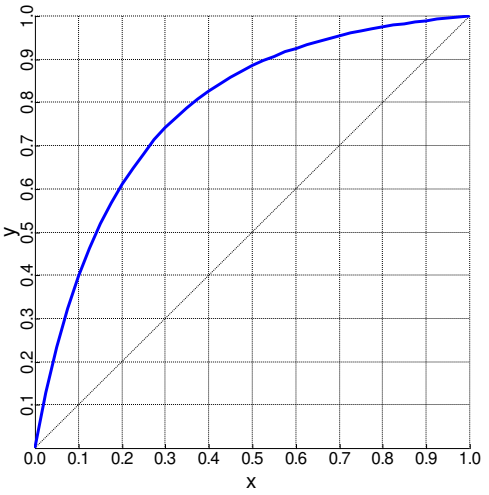

Figura A.3. Diagrama y-x acetaldeído (1) / acetato de etila (2).

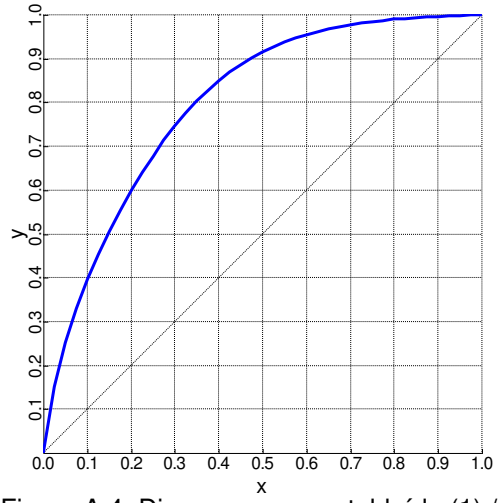

Figura A.4. Diagrama y-x acetaldeído (1) / etanol (2).

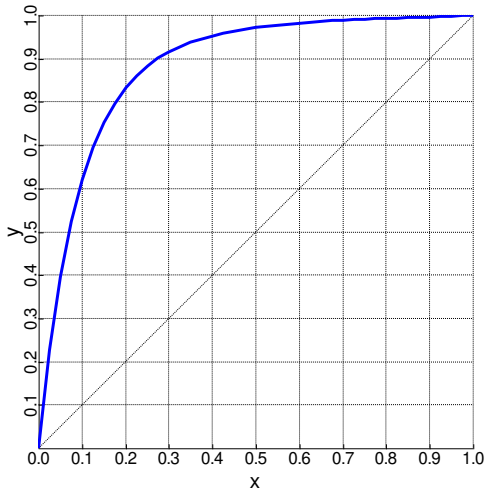

Figura A.5. Diagrama y-x acetaldeído (1) / n-propanol (2).

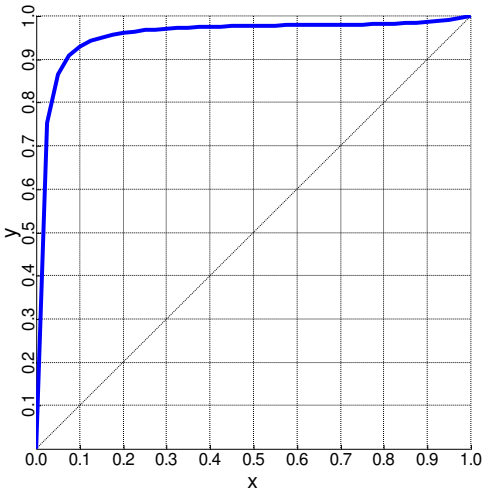

Figura A.6. Diagrama y-x acetaldeído (1) / água (2).

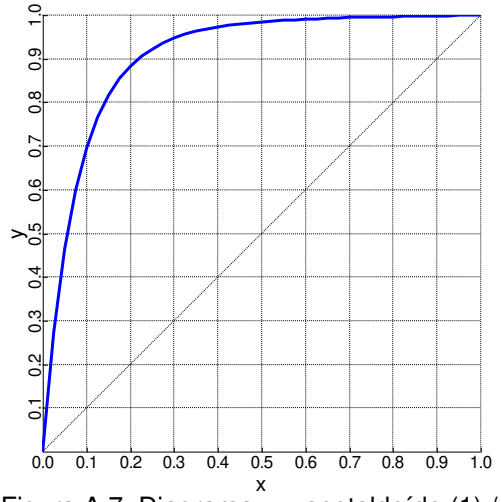

Figura A.7. Diagrama y-x acetaldeído (1) / isobutanol (2).

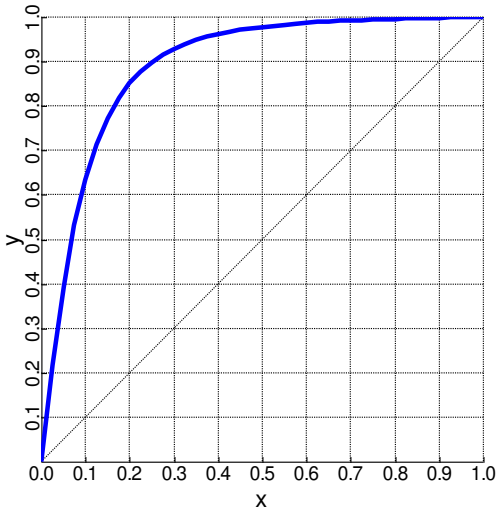

Figura A.8. Diagrama y-x acetaldeído (1) / ácido acético (2).

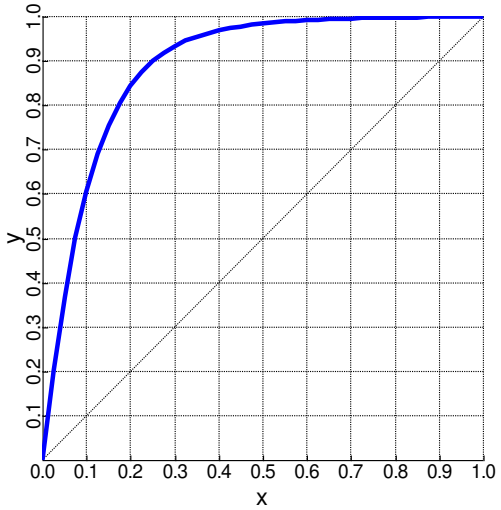

Figura A.9. Diagrama y-x acetaldeído (1) / n-butanol (2).

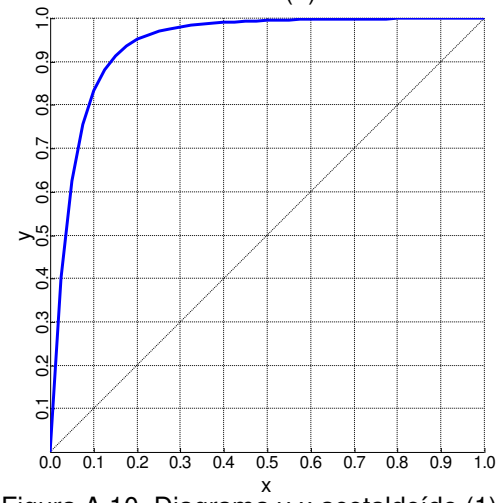

Figura A.10. Diagrama y-x acetaldeído (1) / álcool Isoamílico (2).

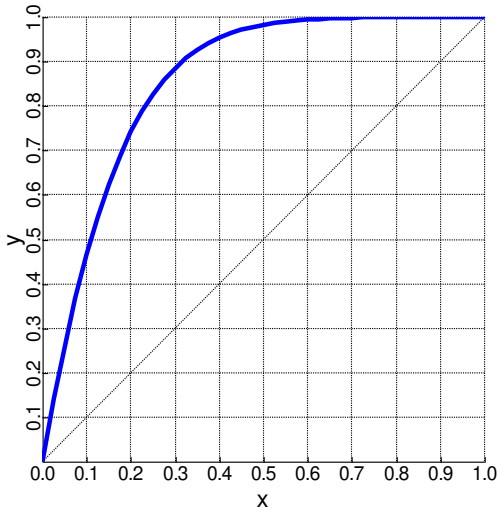

Figura A.11. Diagrama y-x acetaldeído (1) / furfural (2)

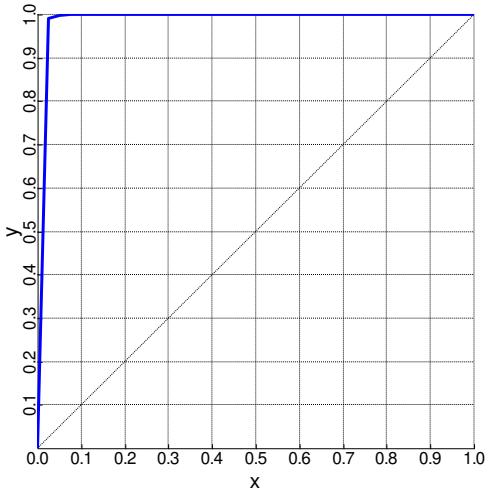

Figura A.12. Diagrama y-x acetaldeído (1) / glicerol (2).

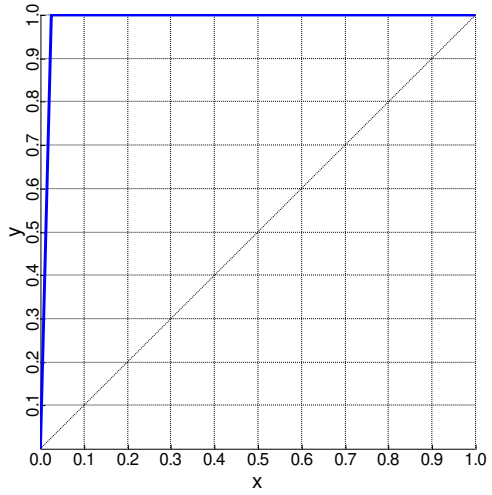

Figura A.13. Diagrama y-x acetaldeído (1) / glicose (2).

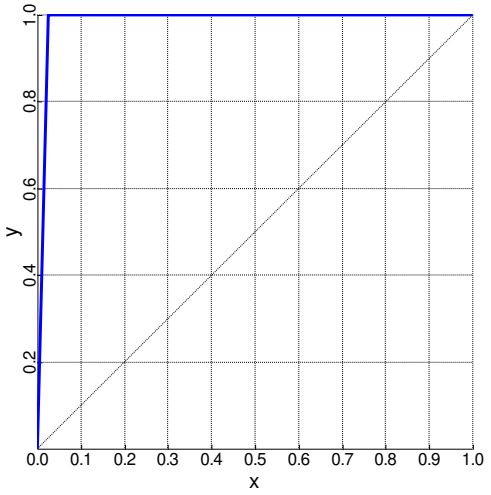

Figura A.14.Diagrama y-x acetaldeído (1) / sacarose (2).

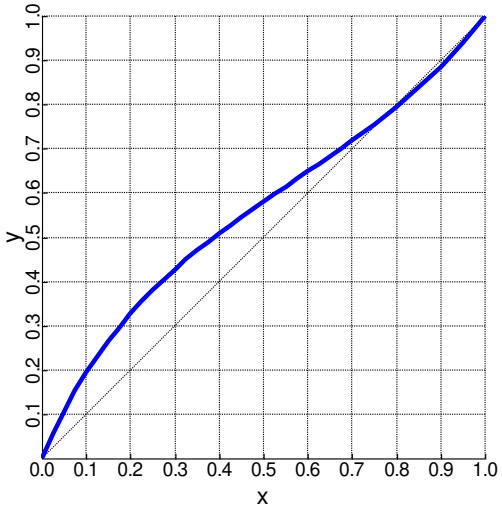

Figura A.15.Diagrama y-x acetona (1)/ metanol (2).

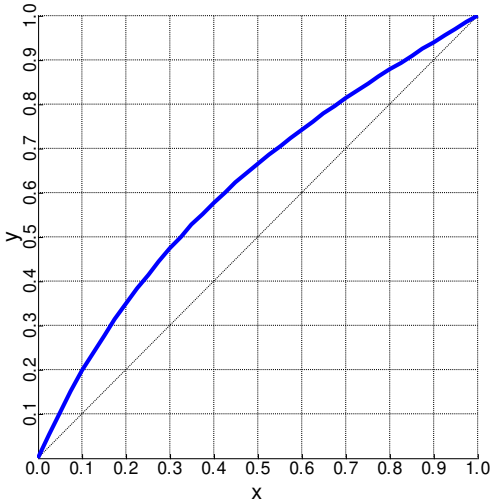

Figura A.16.Diagrama y-x acetona (1) / acetato de etila (2).

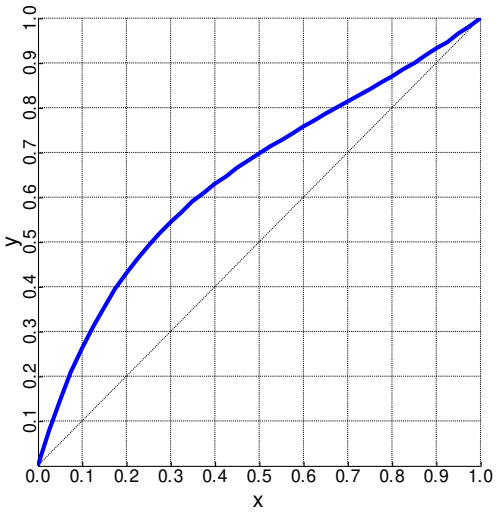

Figura A.17. Diagrama y-x acetona (1) / etanol (2).

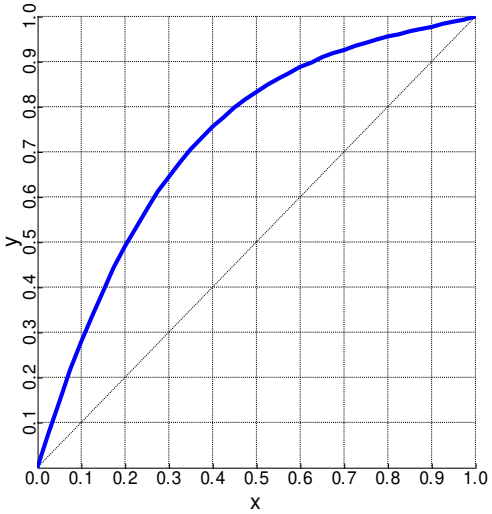

Figura A.18. Diagrama y-x acetona (1) / n-propanol (2).

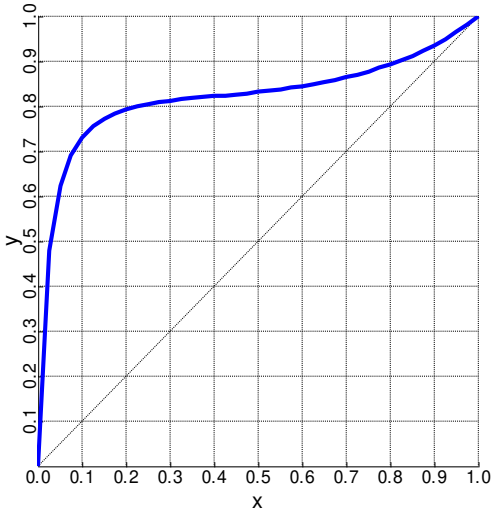

Figura A.19. Diagrama y-x acetona (1) / água (2).

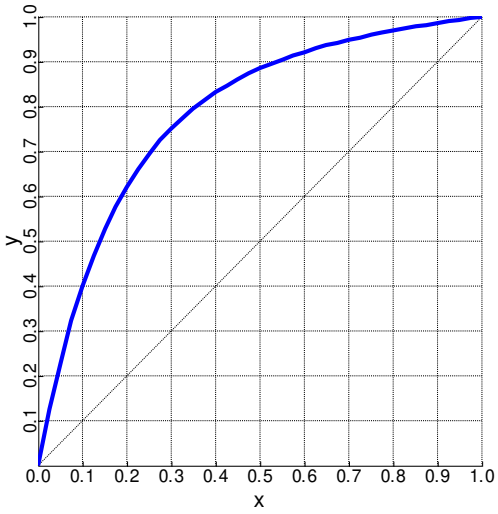

Figura A.20. Diagrama y-x acetona (1) / isobutanol (2).

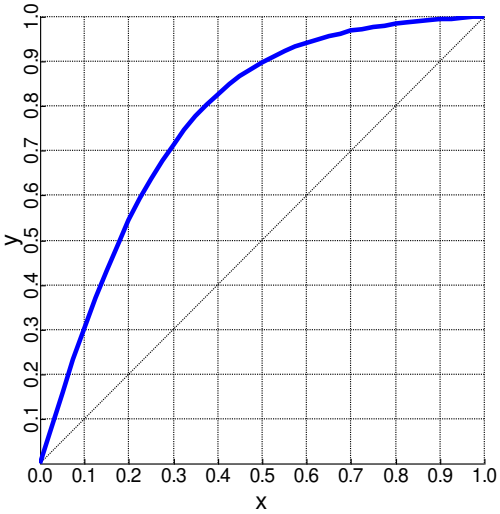

Figura A.21. Diagrama y-x acetona (1) / ácido acético (2).

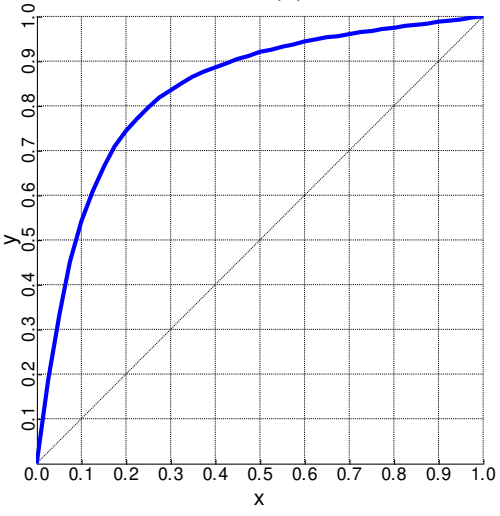

Figura A.22. Diagrama y-x acetona (1) / n-butanol (2).

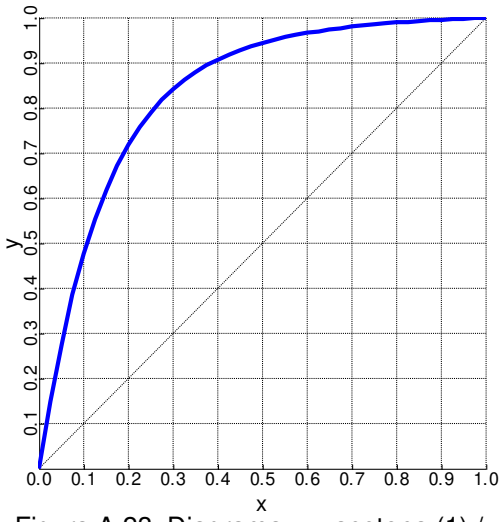

Figura A.23. Diagrama y-x acetona (1) / álcool isoamílico (2).

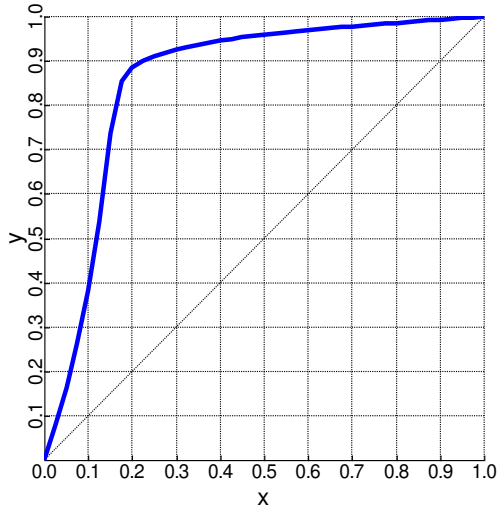

Figura A.24. Diagrama y-x acetona (1) / furfural (2).

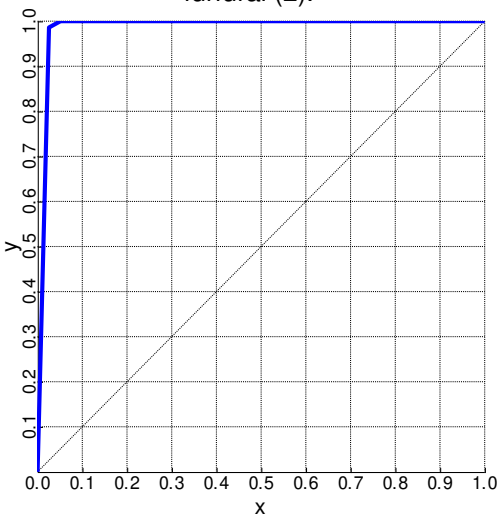

Figura A.25. Diagrama y-x acetona (1) / glicerol (2).

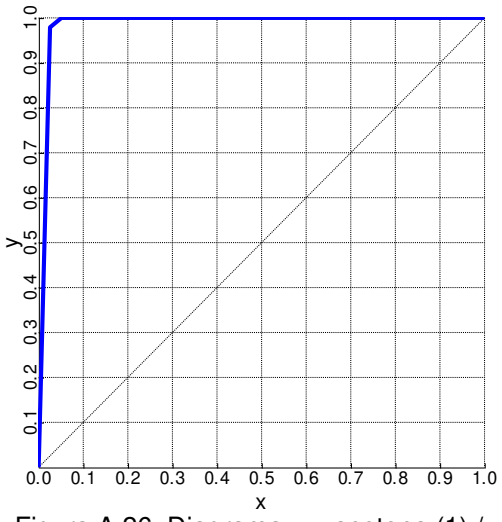

Figura A.26. Diagrama y-x acetona (1) / glicose (2).

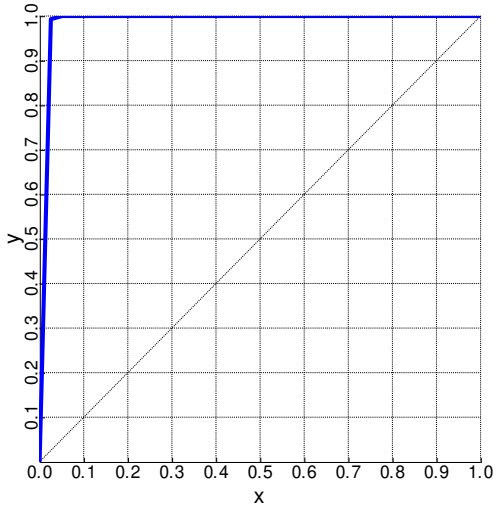

Figura A.27. Diagrama y-x acetona (1) / sacarose (2).

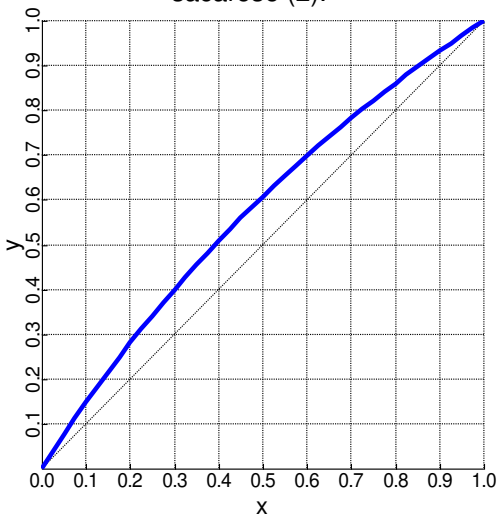

Figura A.28. Diagrama y-x metanol (1) / acetato de etila (2)

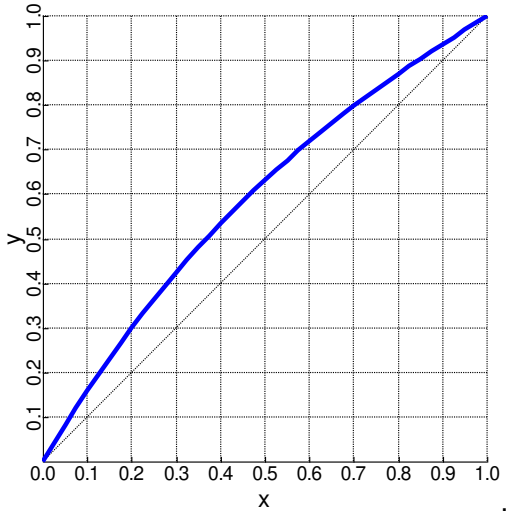

Figura A.29. Diagrama y-x metanol (1) / etanol (2)

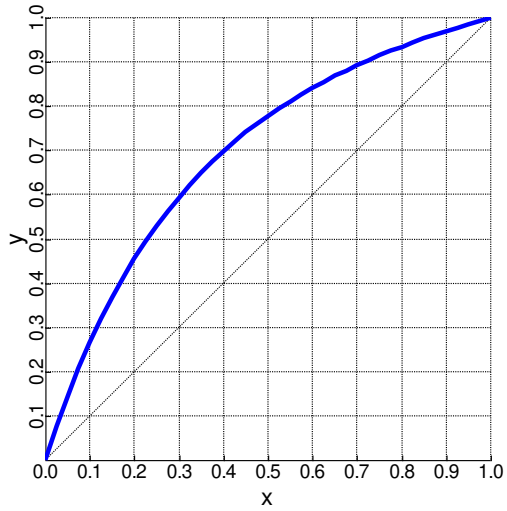

Figura A.30. Diagrama y-x metanol (1) / n-propanol (2).

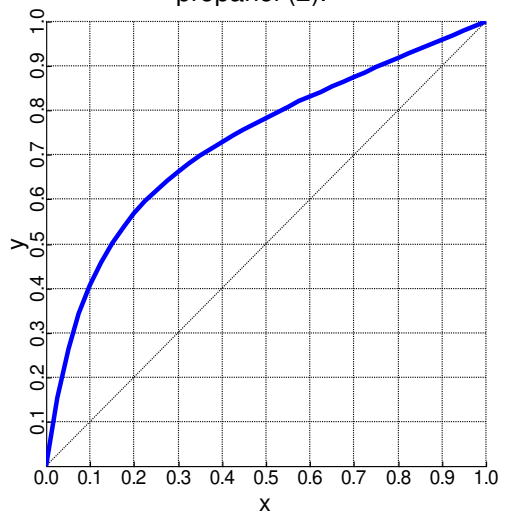

Figura A.31. Diagrama y-x metanol (1) / água (2).

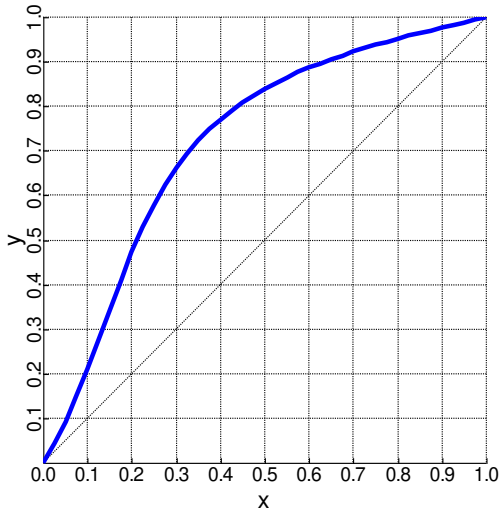

Figura A.32. Diagrama y-x metanol (1) / isobutanol (2).

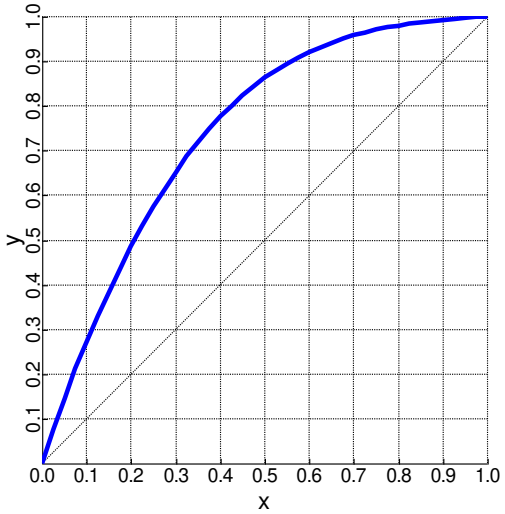

Figura A.33. Diagrama y-x metanol (1) / ácido acético (2).

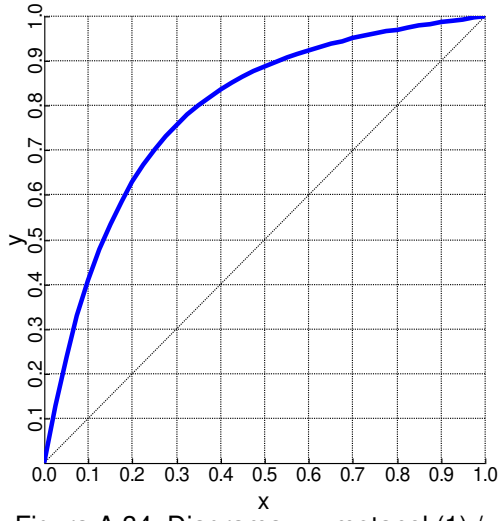

Figura A.34. Diagrama y-x metanol (1) / n-butanol (2).

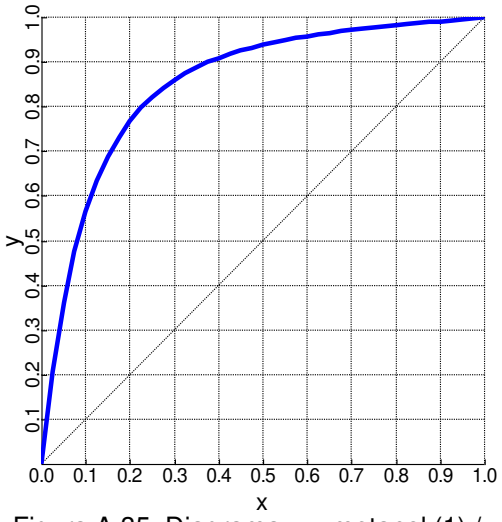

Figura A.35. Diagrama y-x metanol (1) / álcool isoamílico (2).

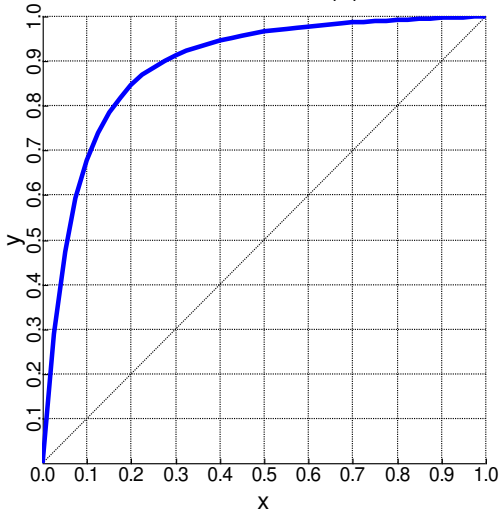

Figura A.36. Diagrama y-x metanol (1) / furfural (2).

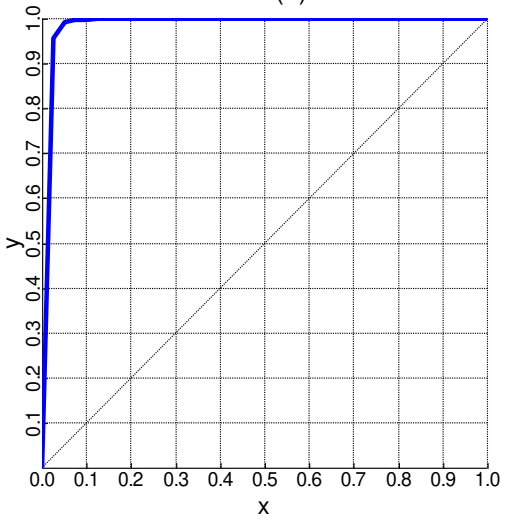

Figura A.37. Diagrama y-x metanol (1) / glicerol (2).

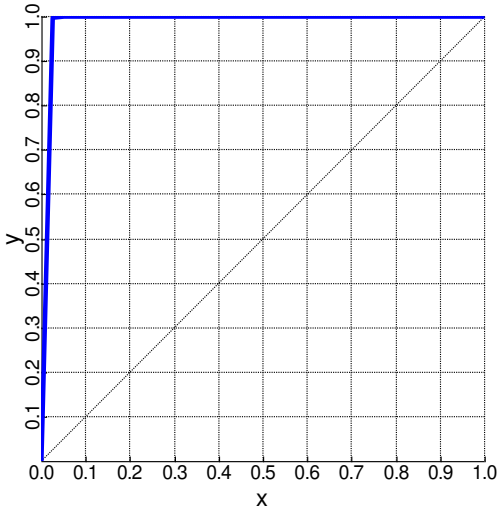

Figura A.38. Diagrama y-x metanol (1) / glicose (2).

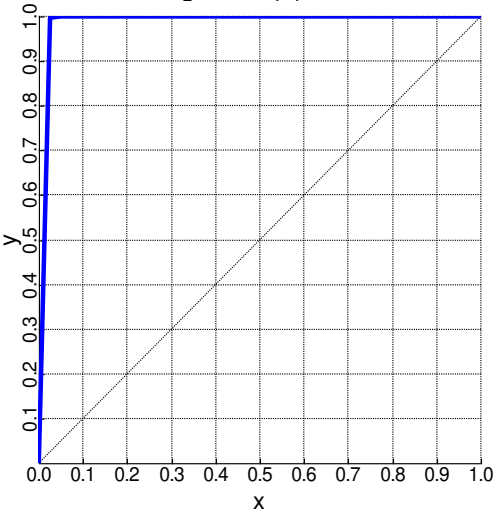

Figura A.39. Diagrama y-x metanol (1) / sacarose (2).

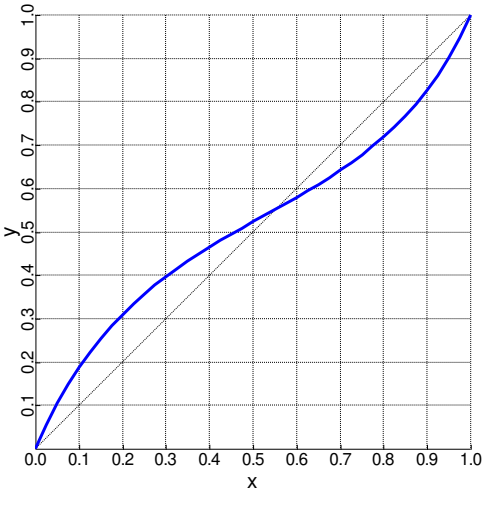

Figura A.40. Diagrama y-x acetato de etila (1) / etanol (2).

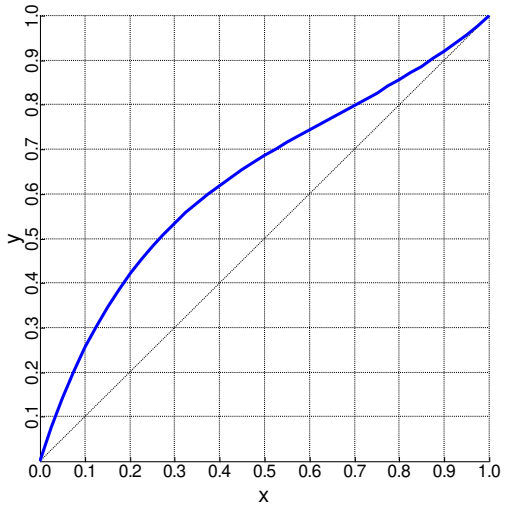

Figura A.41. Diagrama y-x acetato de etila (1) / n-propanol (2).

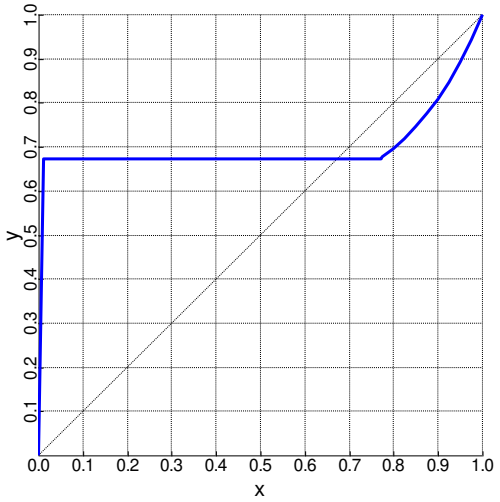

Figura A.42. Diagrama y-x acetato de etila (1) / água (2).

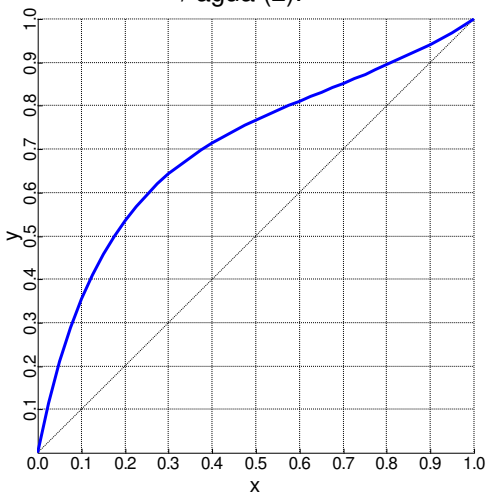

Figura A.43. Diagrama y-x acetato de etila (1) / isobutanol (1).

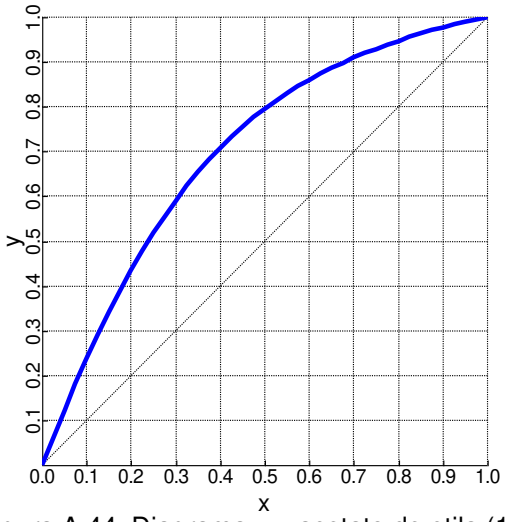

Figura A.44. Diagrama y-x acetato de etila (1) / ácido acético (2).

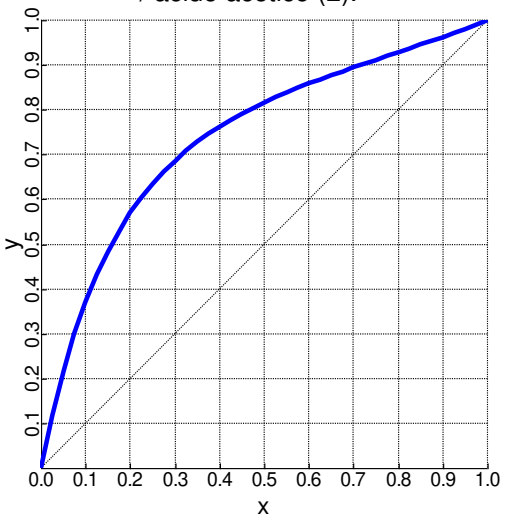

Figura A.45. Diagrama y-x acetato de etila (1) / n-butanol (2).

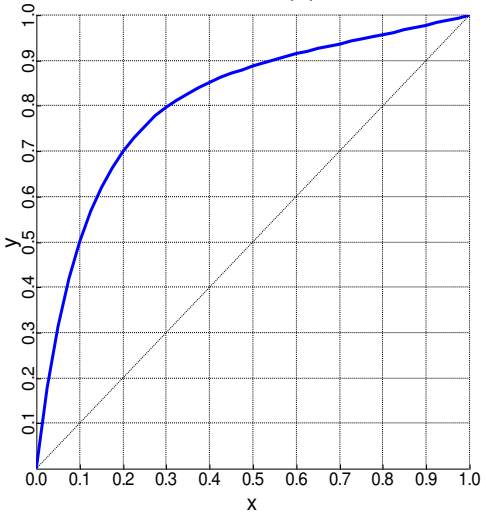

Figura A.46. Diagrama y-x acetato de etila (1) / álcool isoamílico (2).

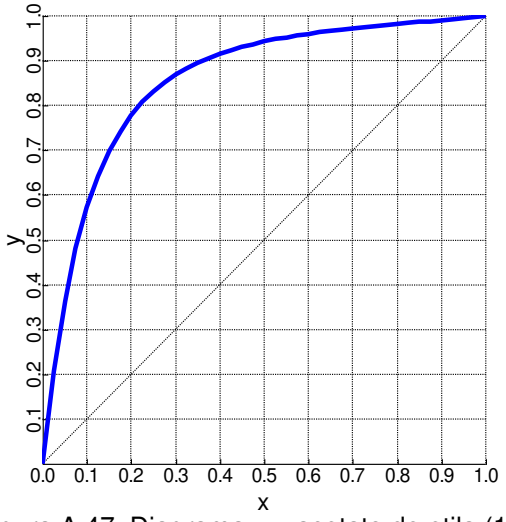

Figura A.47. Diagrama y-x acetato de etila (1) / furfural (2).

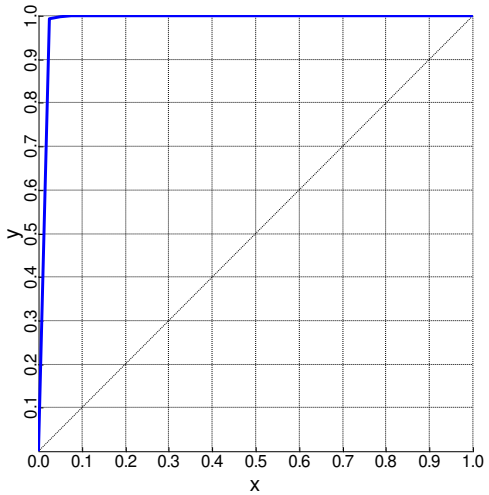

Figura A.48. Diagrama y-x acetato de etila (1) / glicerol (2).

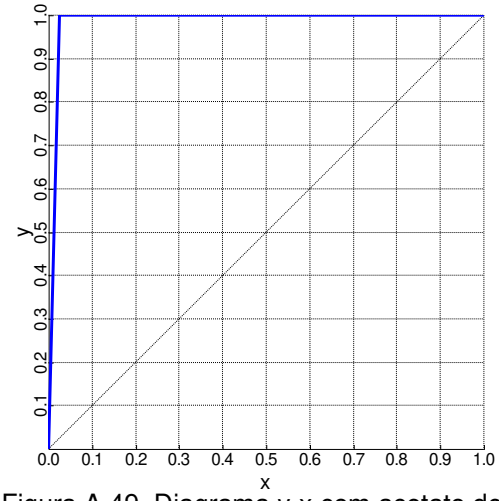

Figura A.49. Diagrama y-x com acetato de etila (1) / glicose (2).

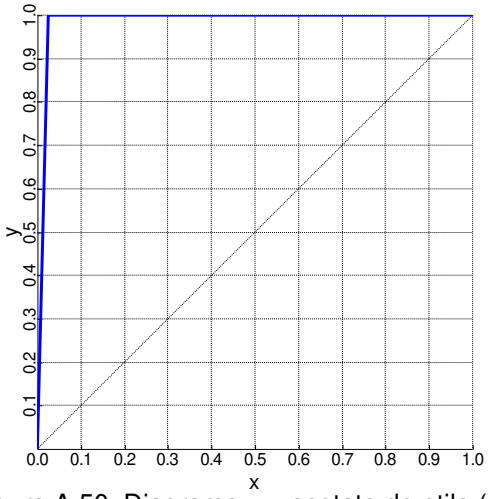

Figura A.50. Diagrama y-x acetato de etila (1) / sacarose (2).

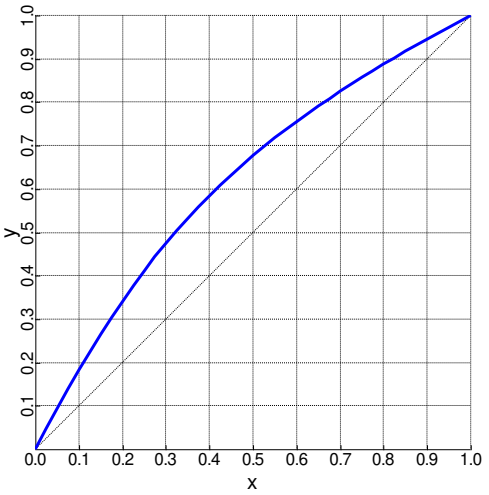

Figura A.51. Diagrama y-x etanol (1) / n-propanol (2).

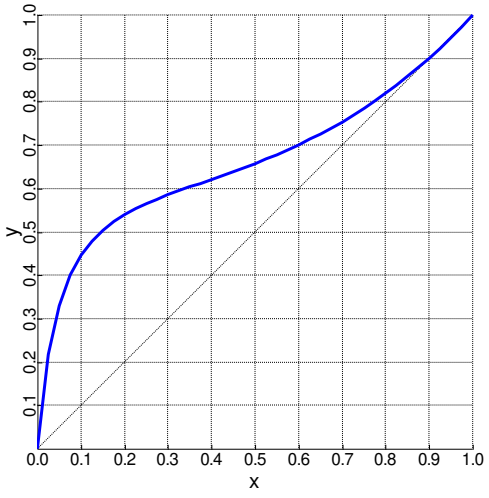

Figura A.52. Diagrama y-x etanol (1) / água (2).

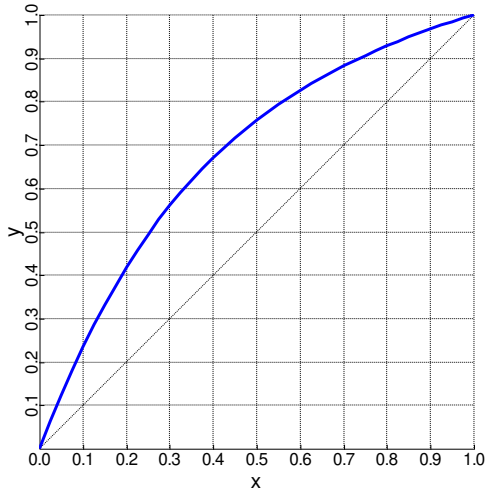

Figura A.53. Diagrama y-x etanol (1) / isobutanol (2).

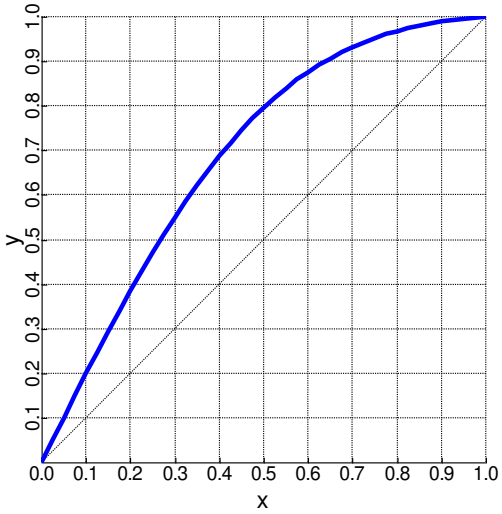

Figura A.54. Diagrama y-x etanol (1) / ácido acético (2).

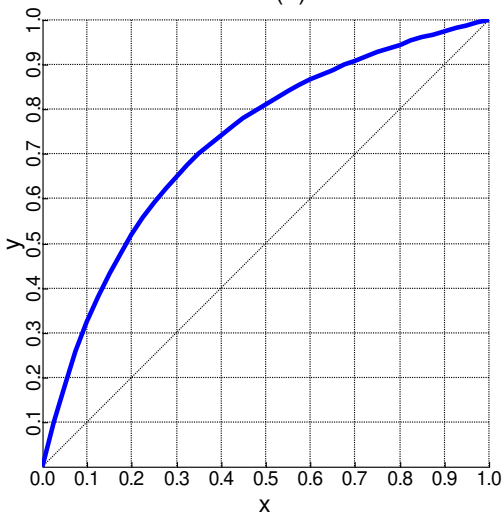

Figura A.55. Diagrama y-x etanol (1) / n-butanol (2).

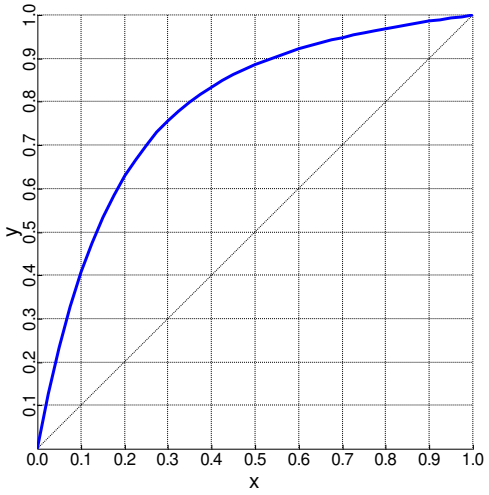

Figura A.56. Diagrama y-x etanol (1) / álcool isoamílico (2).

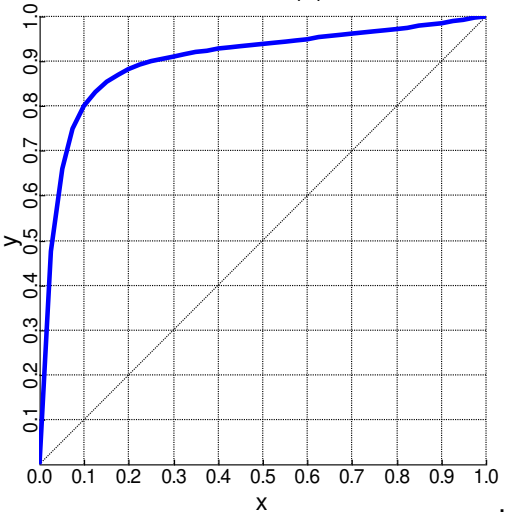

Figura A.57. Diagrama y-x etanol (1) / furfural (2).

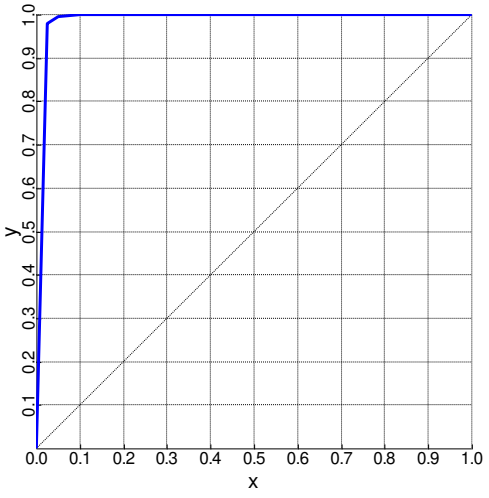

Figura A.58. Diagrama y-x etanol (1) / glicerol (2).

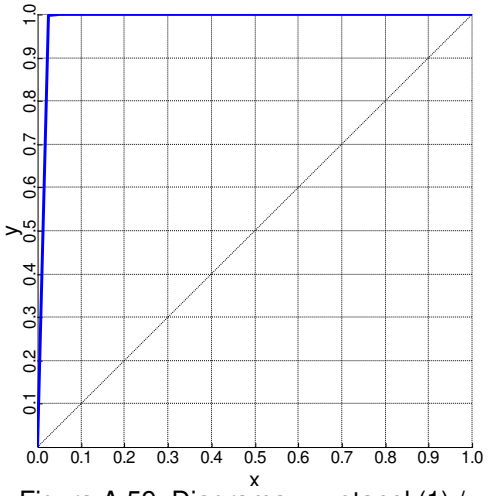

Figura A.59. Diagrama y-x etanol (1) / glicose (2).

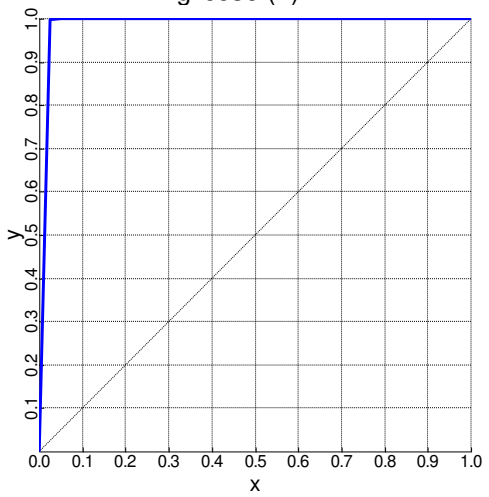

Figura A.60. Diagrama y-x etanol (1) / sacarose (2).

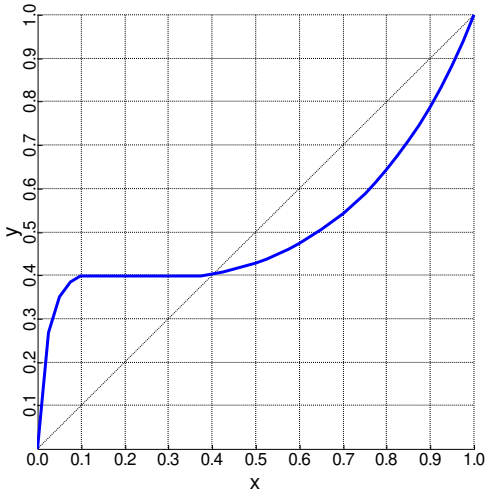

Figura A.61. Diagrama y-x n-propanol (1) / água (2).

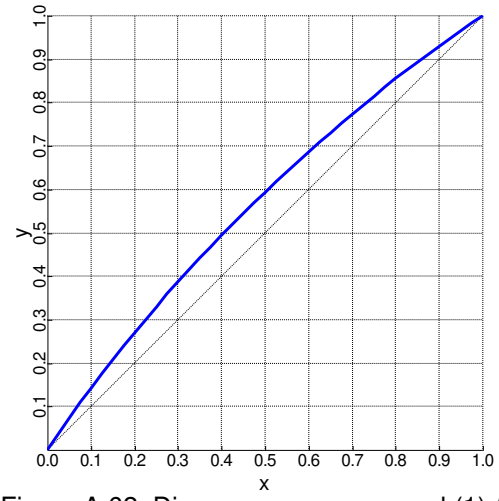

Figura A.62. Diagrama y-x n-propanol (1) / isobutanol (2).

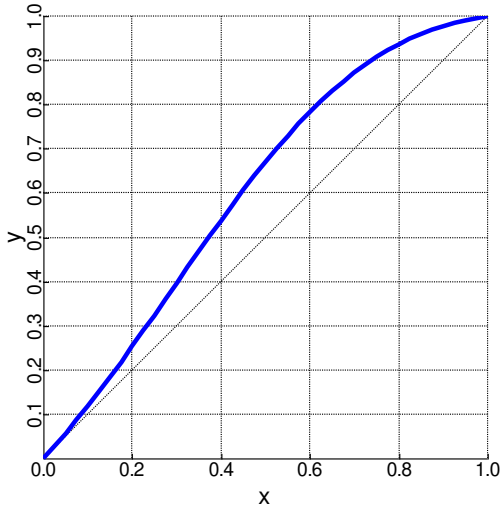

Figura A.63. Diagrama y-x n-propanol (1) / ácido acético (2).

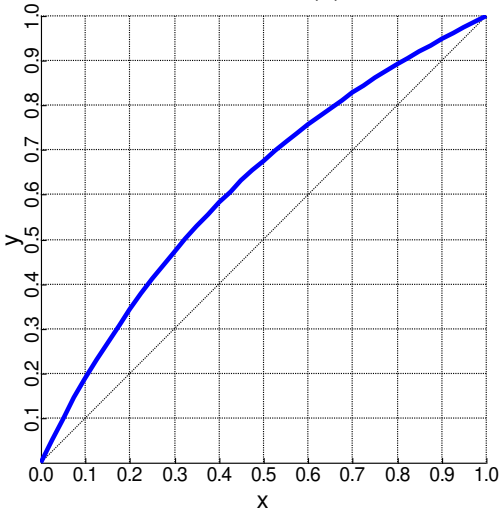

Figura A.64. Diagrama y-x n-propanol (1) / n-butanol (2).

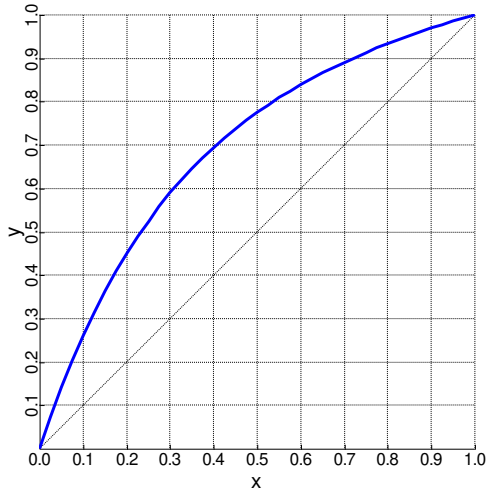

Figura A.65. Diagrama y-x n-propanol (1) / álcool isoamílico (2).

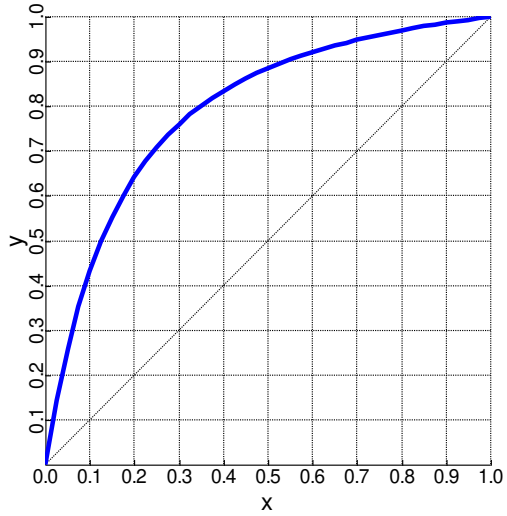

Figura A.66. Diagrama y-x n-propanol (1) / furfural (2).

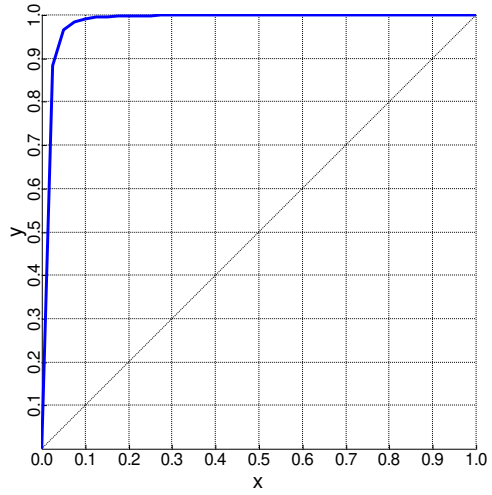

Figura A.67. Diagrama y-x n-propanol (1) / glicerol (2).

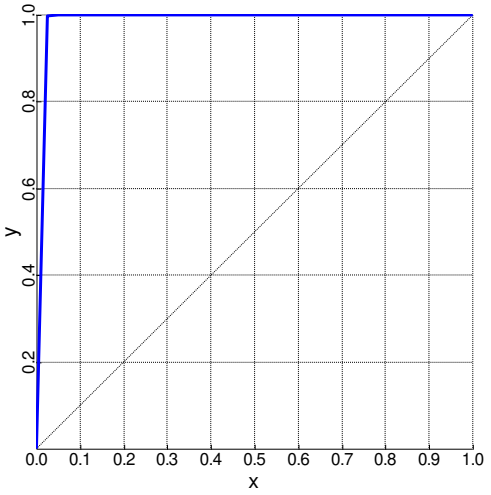

Figura A.68. Diagrama y-x n-propanol (1) / glicose (2).

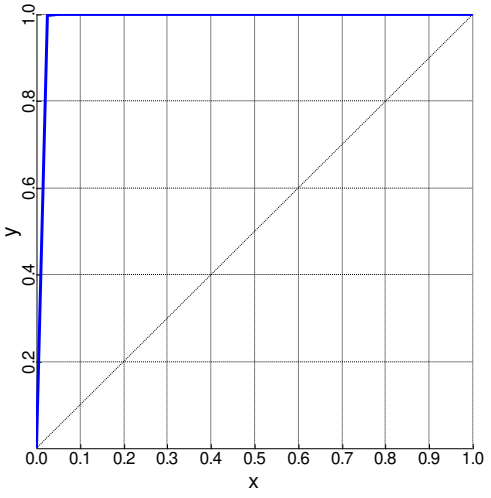

Figura A.69. Diagrama y-x n-propanol (1) / sacarose (1).

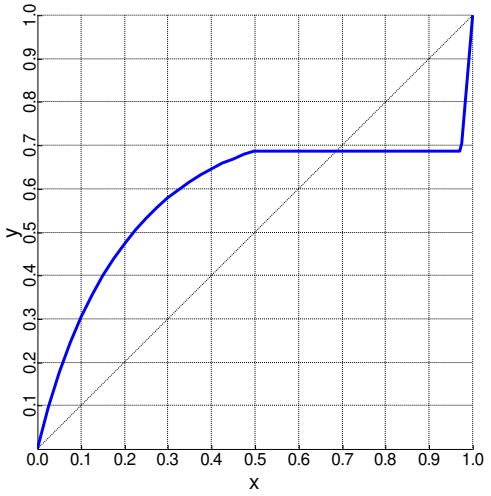

Figura A.70. Diagrama y-x água (1) / isobutanol (2).

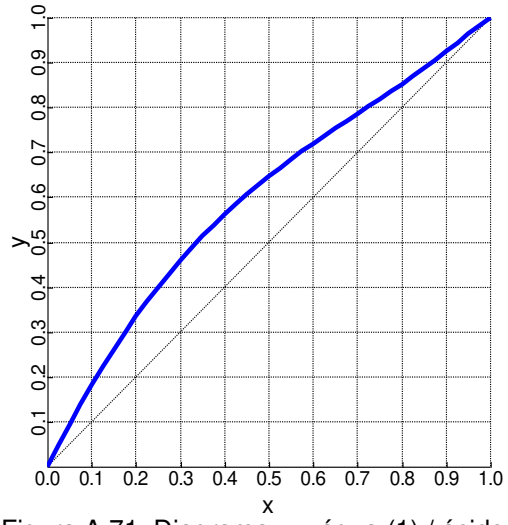

Figura A.71. Diagrama y-x água (1) / ácido acético (2).

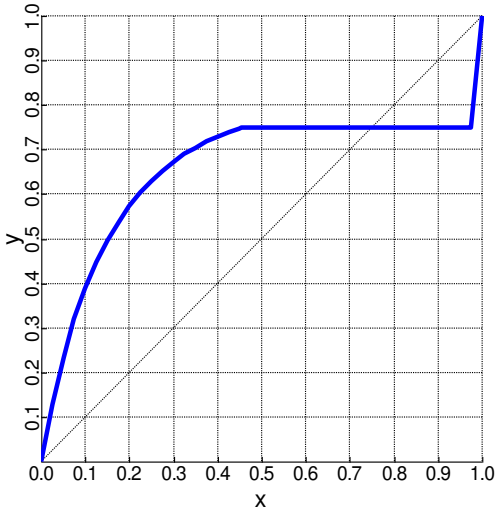

Figura A.72. Diagrama y-x água (1) / n-butanol (2).

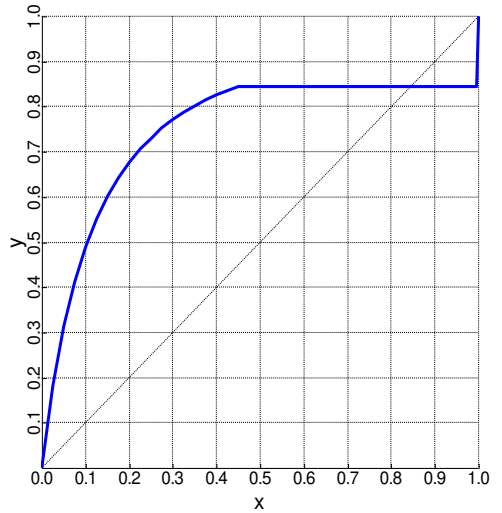

Figura A.73. Diagrama y-x água (1) / álcool isoamílico (2).

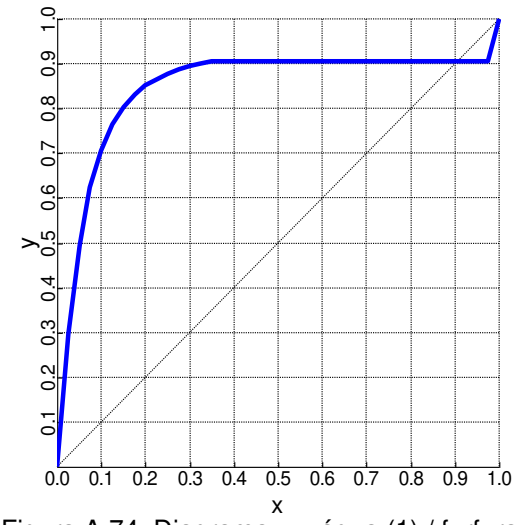

Figura A.74. Diagrama y-x água (1) / furfural (2).

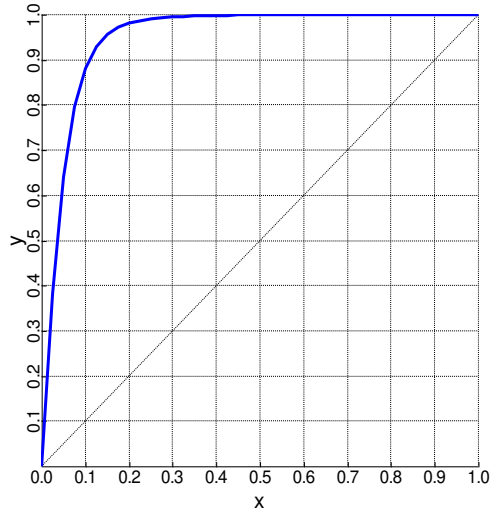

Figura A.75. Diagrama y-x água (1) / glicerol (2).

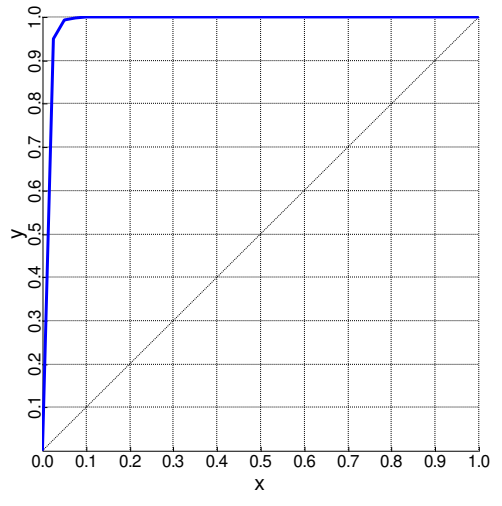

Figura A.76. Diagrama y-x água (1) / glicose (2).

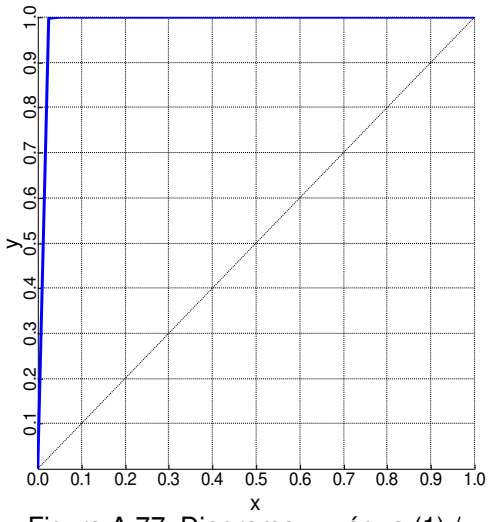

Figura A.77. Diagrama y-x água (1) / sacarose (2).

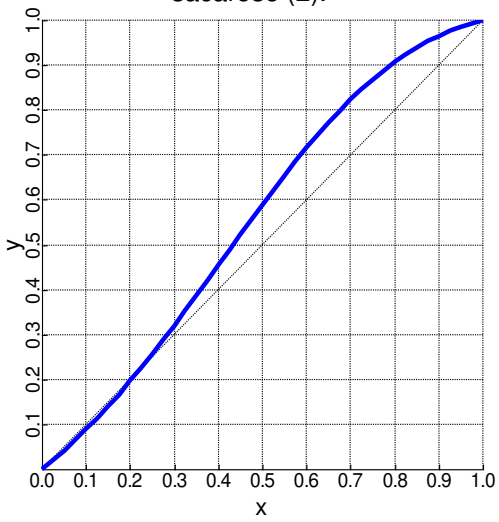

Figura A.78. Diagrama y-x isobutanol (1) / ácido acético (2).

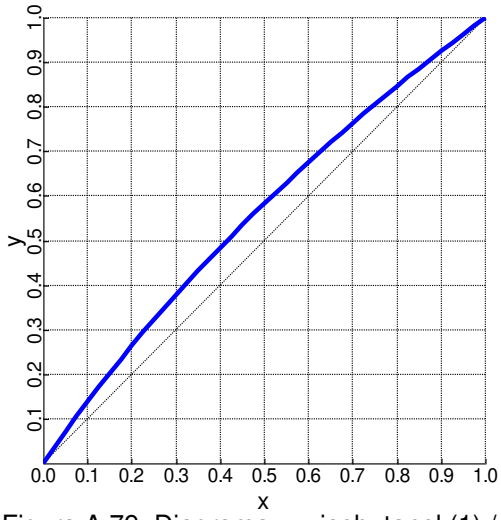

Figura A.79. Diagrama y-x isobutanol (1) / n-butanol (2).

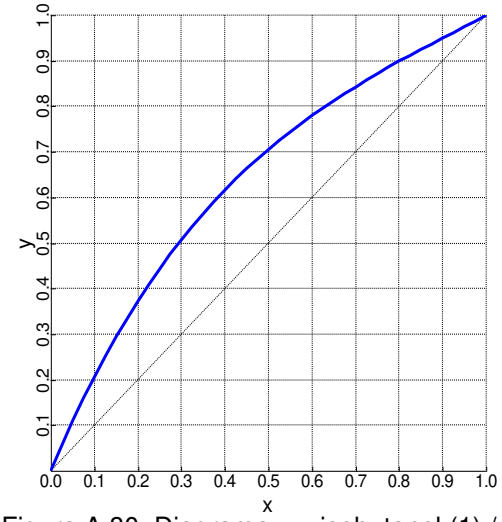

Figura A.80. Diagrama y-x isobutanol (1) / álcool isoamílico (2).

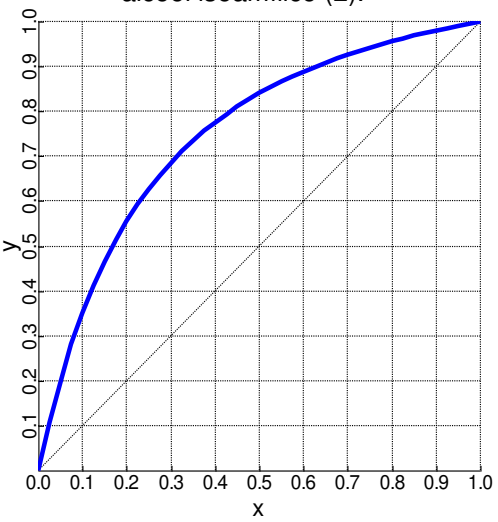

Figura A.81. Diagrama y-x isobutanol (1) / furfural (2).

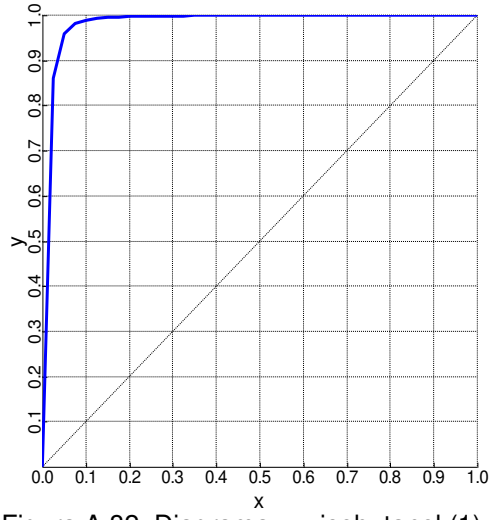

Figura A.82. Diagrama y-x isobutanol (1) / glicerol (2).

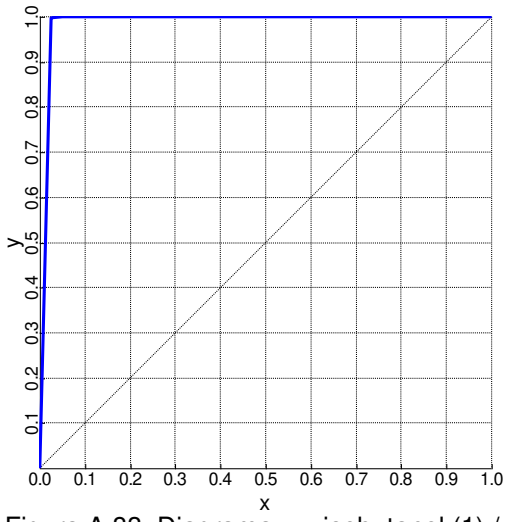

Figura A.83. Diagrama y-x isobutanol (1) / glicose (2).

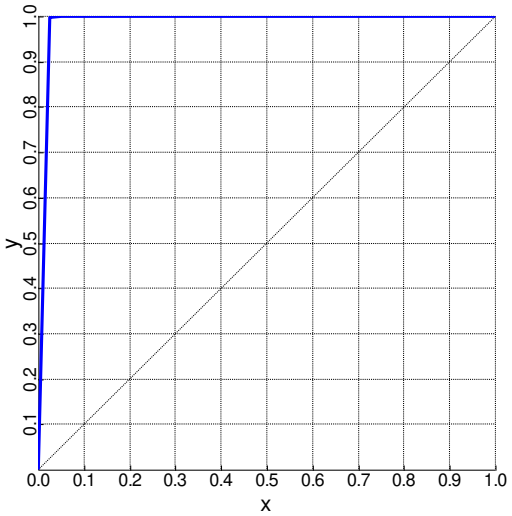

Figura A.84. Diagrama y-x isobutanol (1) / sacarose (2).

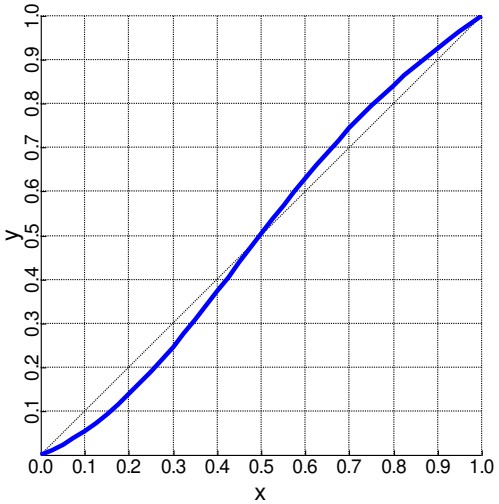

Figura A.85. Diagrama y-x ácido acético (1) / n-butanol (2).

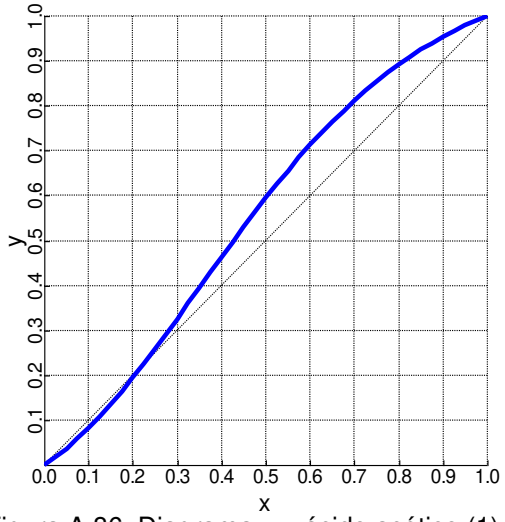

Figura A.86. Diagrama y-x ácido acético (1) / álcool isoamílico (2).

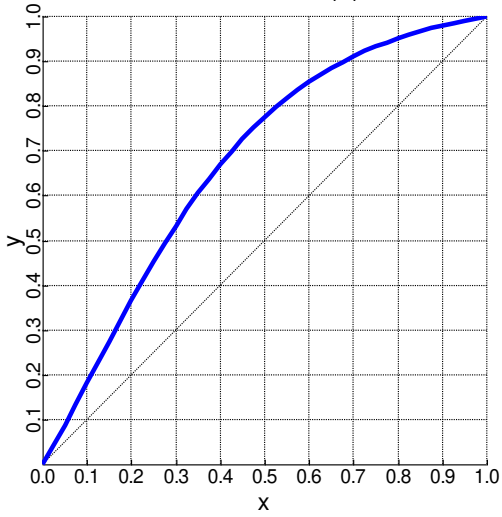

Figura A.87. Diagrama y-x ácido acético (1) / furfural (2).

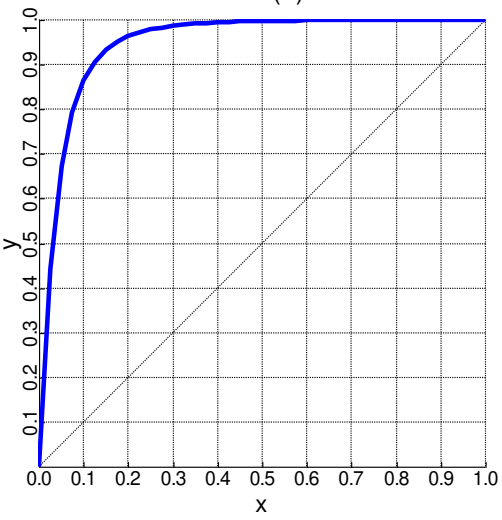

Figura A.88. Diagrama y-x ácido acético (1) / glicerol (2).

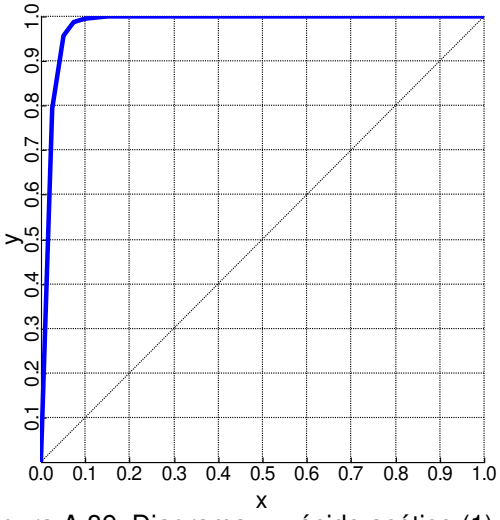

Figura A.89. Diagrama y-x ácido acético (1) / glicose (2).

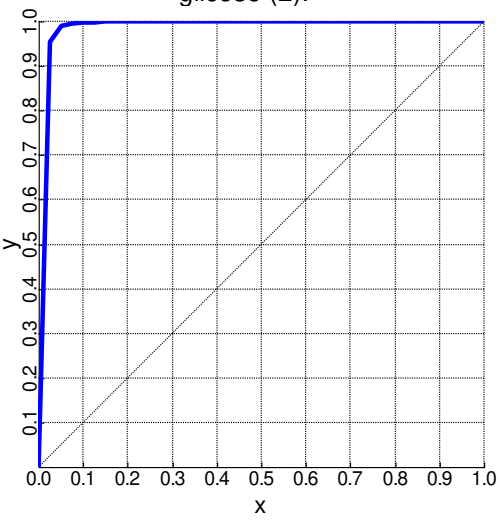

Figura A.90. Diagrama y-x ácido acético (1) / sacarose (2).

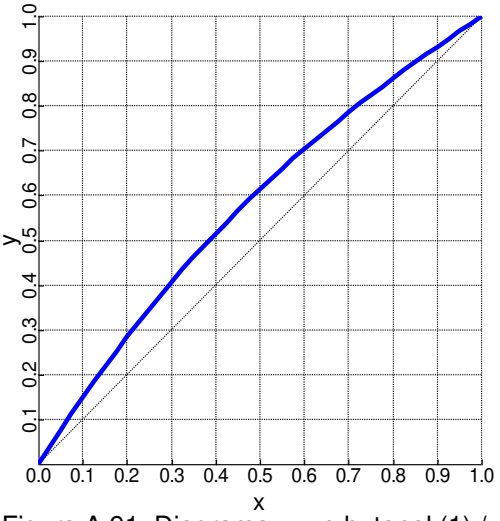

Figura A.91. Diagrama y-x n-butanol (1) / álcool isoamílico (2).

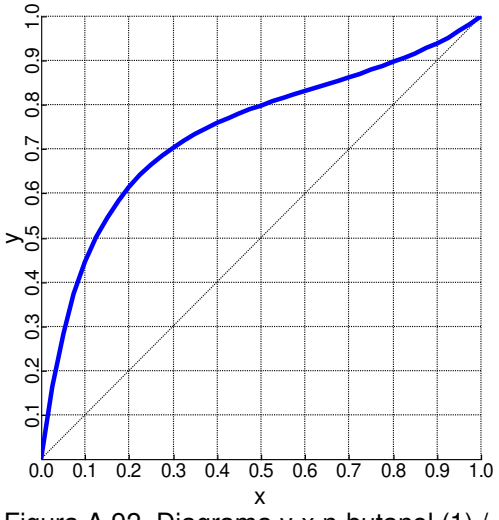

Figura A.92. Diagrama y-x n-butanol (1) / furfural (2).

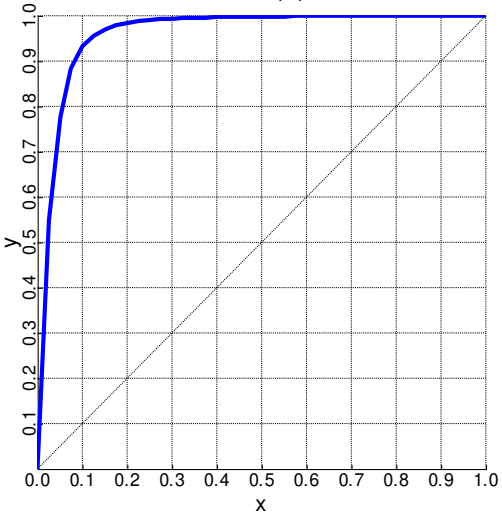

Figura A.93. Diagrama y-x n-butanol (1) / glicerol (2).

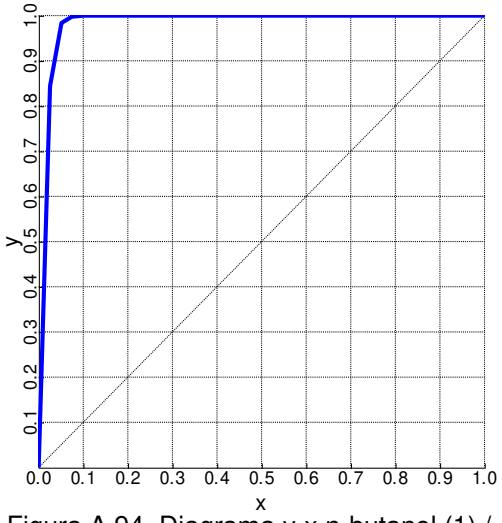

Figura A.94. Diagrama y-x n-butanol (1) / glicose (2).

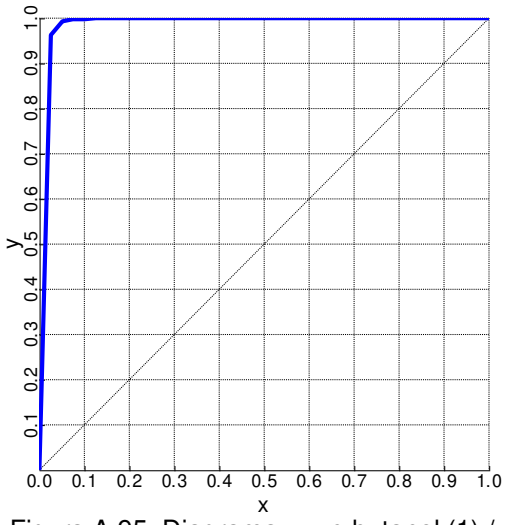

Figura A.95. Diagrama y-x n-butanol (1) / sacarose (2).

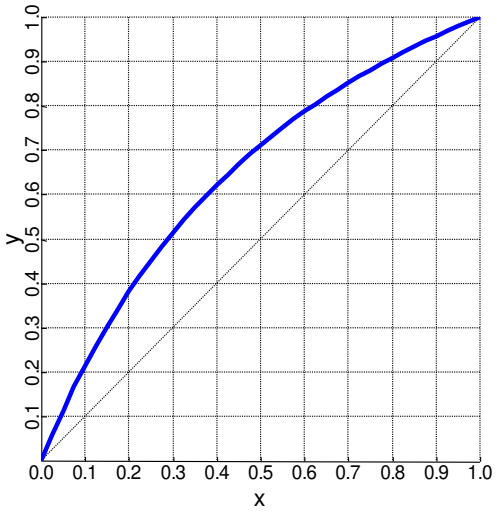

Figura A.96. Diagrama y-x álcool isoamílico (1) / furfural (2).

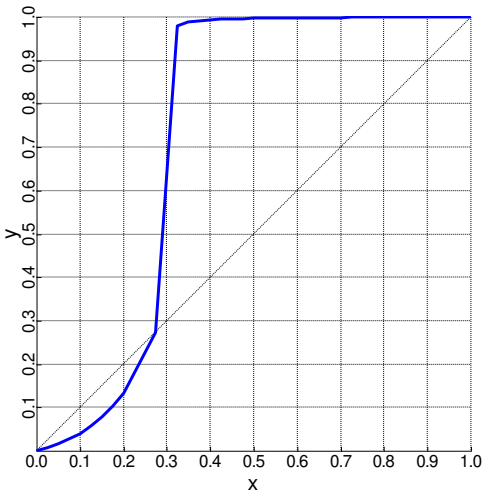

Figura A.97. Diagrama y-x álcool isoamílico (1) / glicerol (2).

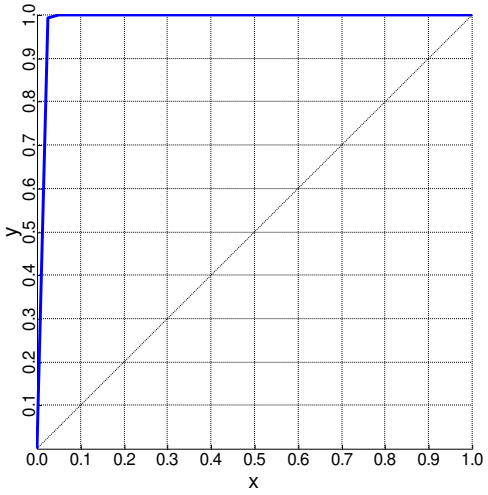

Figura A.98. Diagrama y-x álcool isoamílico (1) / glicose (2).

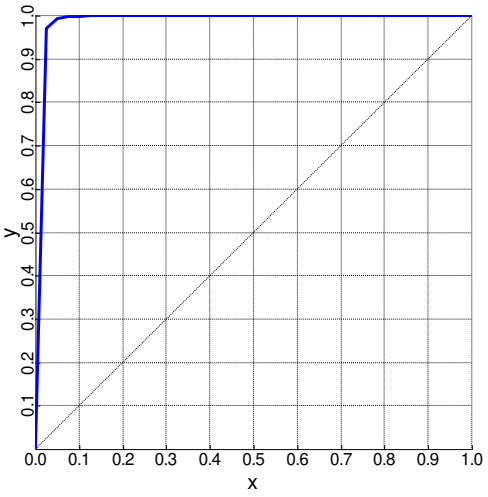

Figura A.99. Diagrama y-x álcool isoamílico (1) / sacarose (2).

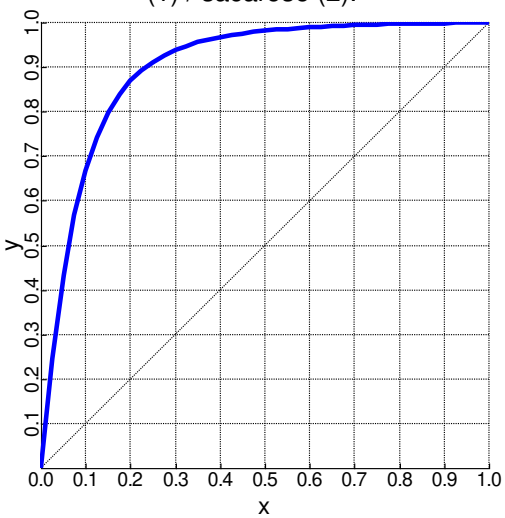

Figura A.100. Diagrama y-x furfural (1) / glicerol (2).

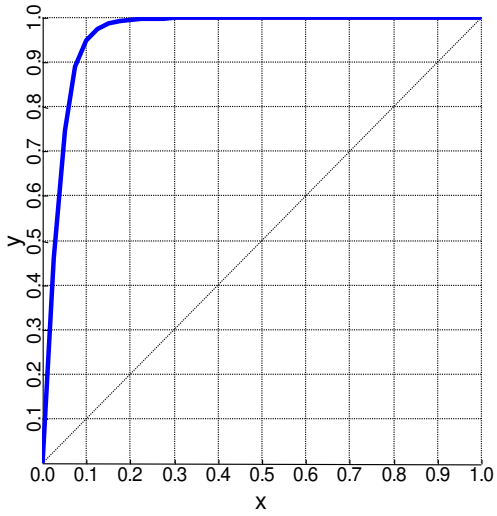

Figura A.101. Diagrama y-x furfural (1) / glicose (2).

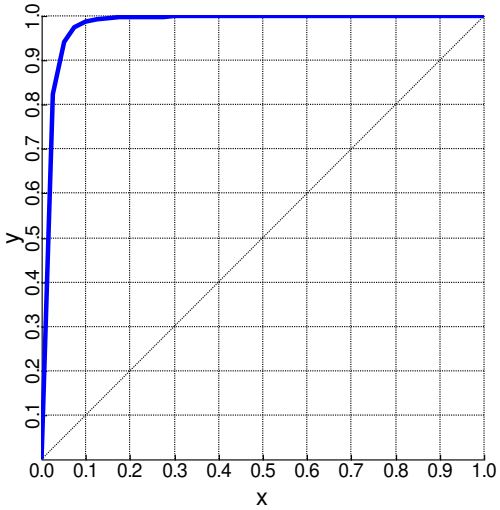

Figura A.102. Diagrama y-x furfural (1) / sacarose (2).

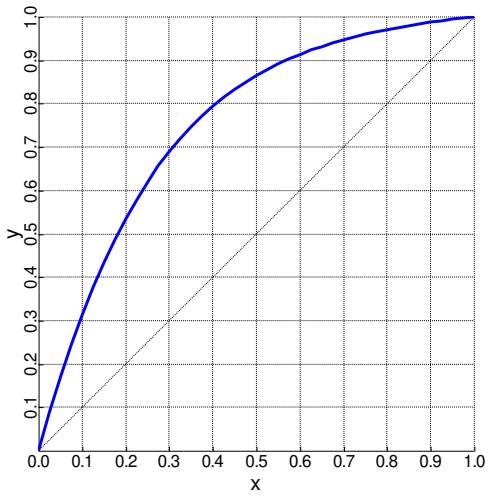

Figura A.103. Diagrama y-x glicerol (1) / glicose (2).

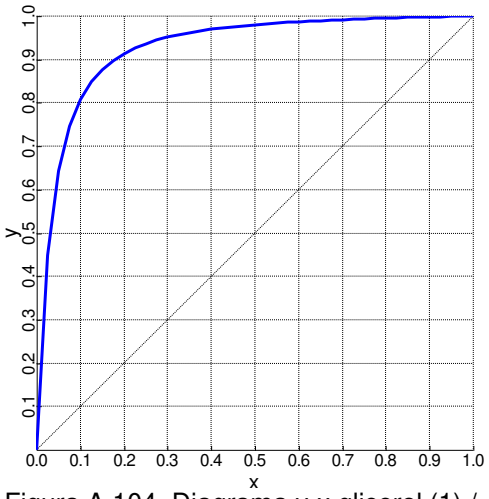

Figura A.104. Diagrama y-x glicerol (1) / sacarose (2).

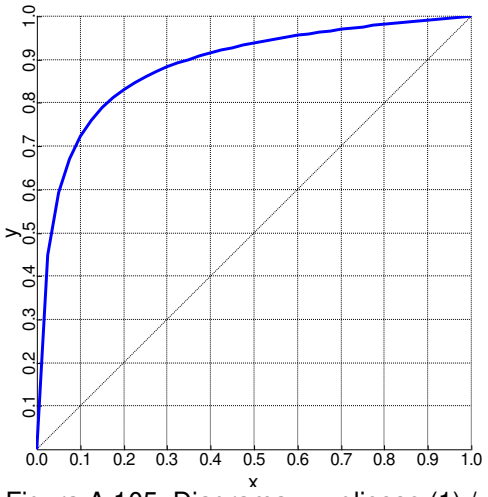

Figura A.105. Diagrama y-x glicose (1) / sacarose (2).

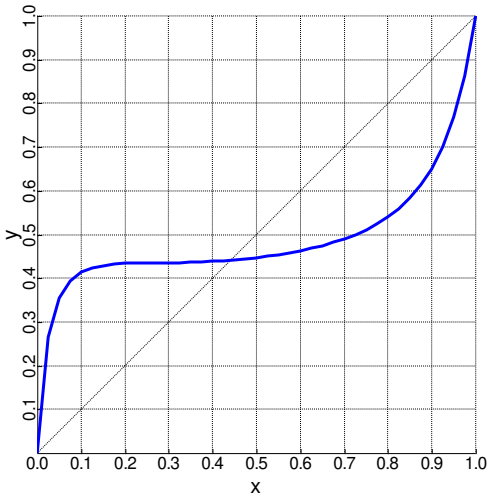

Figura A.106. Diagrama y-x etanol (1) / cicloexano (2).

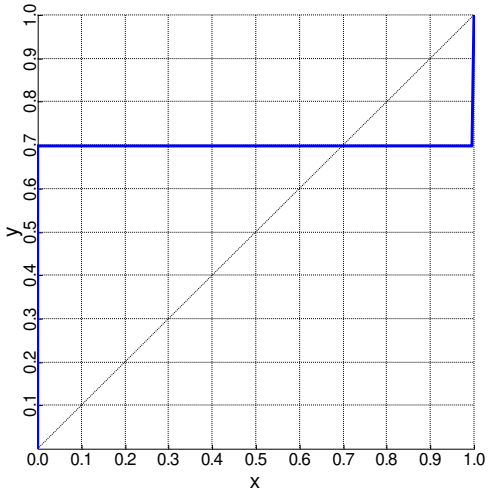

Figura A.107. Diagrama y-x cicloexano (1) / água (2).

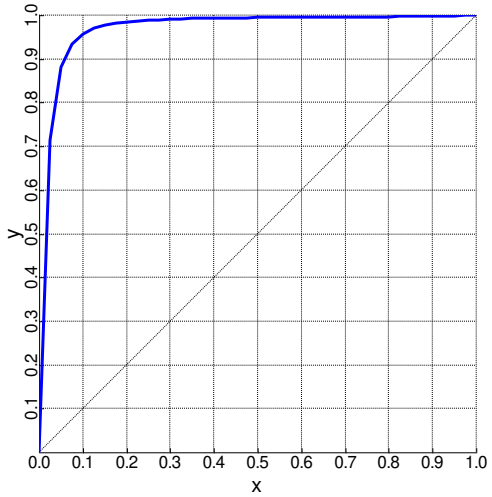

Figura A.108. Diagrama y-x etanol (1) / etilenoglicol (2).

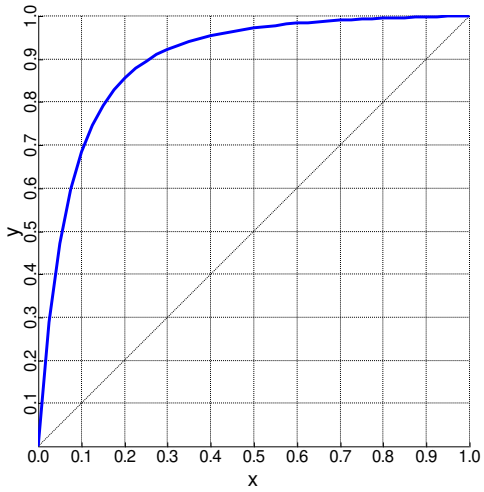

Figura A.109. Diagrama y-x água (1) / etilenoglicol (2).

Os diagramas binários foram analisados de forma a observar as não idealidades presentes no sistema. Os binários foram classificados de acordo com a não idealidade através da Tabela A.1.

Tabela A.1. Não idealidades observadas no sistema.

Não idealidade	Binário	
Azeotropia	Acetona/Metanol Acetato de etila/Etanol Acetato de etila/Água Etanol/Água n-Propanol/Água Água/Isobutanol Água/Furfural Água/n-Butanol	Água/Álcool isoamílico Isobutanol/Ácido acético Ácido acético/n-Butanol Ácido acético/Álcool isoamílico Álcool isoamílico/Glicerol Etanol/Cicloexano Cicloexano/Água
Formação de Duas Fases Líquidas	Acetato de etila/Água n-Propanol/Água Água/Isobutanol Água/Furfural	Água/n-Butanol Água/Álcool isoamílico Álcool isoamílico/Glicerol Cicloexano/Água
Baixa Volatilidade Relativa	Acetona/Metanol Acetona/Acetato de etila Acetona/Etanol Metanol/Acetato de etila Metanol/Etanol Acetato de etila/Etanol Etanol/n-Propanol n-Propanol/Isobutanol	n-Propanol/Ácido acético n-Propanol/n-Butanol Água/Ácido acético Isobutanol/Ácido acético Isobutanol/n-Butanol Ácido acético/n-Butanol Ácido acético/Álcool isoamílico n-Butanol/Álcool Isoamílico
Alta Volatilidade Relativa	Acetaldeído/Água Acetaldeído/Glicerol Acetaldeído/Glicose Acetaldeído/Sacarose Acetona/Glicerol Acetona/Glicose Acetona/Sacarose Metanol/Glicerol Metanol/Glicose Metanol/Sacarose Acetato de etila/Glicerol Acetato de etila /Glicose Acetato de etila /Sacarose Etanol/Glicerol Etanol/Glicose Etanol/Sacarose n-Propanol /Glicerol	n-Propanol /Glicose n-Propanol /Sacarose Água/Glicerol Água /Glicose Água /Sacarose Isobutanol/Glicerol Isobutanol/Glicose Isobutanol/Sacarose Ácido acético/Glicose Ácido acético/Sacarose n-Butanol/Glicose n-Butanol/Sacarose Álcool isoamílico/Glicose Álcool isoamílico/Sacarose Furfural/Glicose Furfural/Sacarose